‘Cartilage Hair Hypoplasia and the *RMRP* gene’

Ph.D. Thesis

to accomplish

Doctorate Degree in Science

at the
Faculty of Biology
Johannes Gutenberg-University of Mainz
in Mainz

Pia Hermanns

Mainz 2005

In memory of my mother

Table of contents

Index of Figures:

Index of Tables:

1 Introduction

1.1 Skeletal development

Cartilage and bone tissue are the main components of the skeleton of vertebrates. They play a major role in movement and support of the body as well as serving as a storage organ for the organism. The different parts of the skeleton derive from different embryonic tissues and are differentiated between the craniofacial, the axial skeleton and the extremities. The craniofacial skeleton results from cells of the neural tube although a few bones originate also from the mesoderm of the cephalon. The axial skeleton including the vertebrae and ribs derive from the sclerotom of the somites. The extremities develop from the lateral mesoderm. Even though the skeleton develops from three different embryonic tissues there are the same cell types responsible for growth and maintanance of the skeleton. These are chondrocytes derived from mesenchymal cells forming the cartilage, osteoblasts derived from the neural tube and mesoderm building the bone and osteoclasts from precursors of the macrophage-monocyte lineage for bone resorption (Karsenty and Wagner, 2002).

The development of the skeleton is a very complex process that can be devided into several phases. The first phase is the patterning, characterized by the activity of genes that determine the general pattern of the early skeleton. The second phase is morphogenesis including organogenesis and histogenesis. These processes are the result of the differentiation of mesenchymal cells to chondrocytes, osteoblasts or osteoclasts to form the cartilage and bone of the developing skeleton. This is followed by the growth phase that determines the length of the bones as well as the proportions of the skeleton. The final stage is the homeostasis. This is a balance between bone formation and bone resorption resulting in a continous renewal of bone substance. These processes are best understood in the development of the extremities. Thus the following paragraphs will focus on the development of the skeleton of the extremities.

Patterning

Patterning defines the position, number, form and the resulting function of all parts of the skeleton (for review see Johnson and Tabin 1997; Schwabe et al., 1998). The development of

the extremities is best understood based on experiments done in chicken studying tissue transplantation and misexpression of genes in living chicken embryos.

The gene cascades including the interactions of transcription factors and signal molecules that are responsible for initiating and maintaining the three developing axes of the extremities are well understood. The three axes are: proximo-distal (shoulder to fingertip), anterior-posterior (thumb to pinky) and the dorso-ventral axis (back of the hand to palm) (Fig. 1).

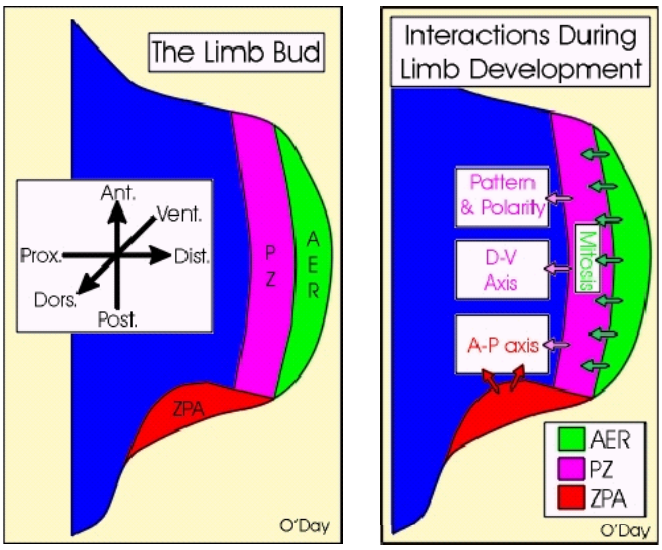

Fig. 1: Schematic of patterning in early limb development.

The development of the extremities starts with the formation of the limb bud that consists of undifferentiated mesenchymal cells. The apical ectodermal ridge (AER) contains fast dividing cells. Underneath the AER is the progress zone (PZ). The zone of polarizing activiy (ZPA) is the posterior organization center. The limb bud grows from proximal to distal.
D-V: dorsal-ventral axis
A-P: anterior-posterior axis.
From:
http://www.erin.utoronto.ca/~w3bio380/lecture/Lect19/L19.htm

The development of the extremities starts with the budding of the limb bud. It consists of undifferentiated mesodermal cells covered by ectoderm. The apical ectodermal ridge (AER) is a thickened part of the ectoderm. Fibroblast growth factor 10 (FGF10) signals that are expressed in the mesenchyme and the epithilial splice form of fibroblast growth factor receptor 2 (FGFR2b) initiate the fomation of the AER (Ornitz and Marie, 2002). The AER in turn is maintained through signals from the underlying mesoderm, the progress zone (PZ) (reviewed by Oberg et al., 2004).

The removal of the AER results in a shortening of the extremities. Depending on the time point of the AER removal, this may cause either a total loss of extremities (when removed early during development) or if removed at a later stage only proximal structures like the humerus, ulna, and radius will develop (Saunders, 1948; Summerbell, 1974). Therefore, the growth and the patterning of the extremities along the proximo-distal axis is AER dependent (Dudley et al., 2002; Sun et al., 2002; Duboule, 2002). These processes are regulated by fibroblast growth factor 4 (FGF4) and fibroblast growth factor 8 (FGF8) signaling in the AER (Cohn and Tickle, 1996). The PZ that consists of undifferentiated proliferating cells remains

unaffected. The growth of the extremities along the anterior-posterior axis is determined by a subpopulation of mesenchymal cells at the posterior end of the PZ that is called the 'zone of polarizing activity' (ZPA) (Saunders and Gasseling, 1968). *Sonic hedgehog* (*Shh*) is a major player in the development of the anterior-posterior axis. Shh is a secretory factor expressed in the ZPA and is also involved in a feedback loop between the ZPA (Shh) and AER (FGF4) (Laufer et al., 1994; Niswander et al., 1994). Experiments in chicken also demonstrate that the maintainance of fibroblast growth factor 9 (Fgf9) and fibroblast growth factor 17 (Fgf17) expression in the AER is Shh dependent (Sun et al., 2000). Misexpression of *Shh* in the anterior axis of the limb bud results in a mirror-like duplication of the distal extremities in mouse and chicken (Riddle et al., 1993), whereas *Shh* knockout mice lack the distal extremeties completely (Chiang et al., 1996). This demonstrates the seminal role of this protein in the development of the extremities along the anterior-posterior axis (Chiang et al., 2001; Kraus et al., 2001). A group of Gli-zinc finger proteins are involved in these processes as well and are activated by *Shh* (Marigo et al., 1996). The dorso-ventral polarity of the extremeities are determined by the secreted glycoprotein Wnt7a in the dorsal extoderm, the homoebox protein Engrailed-1 (En1) with expression in the ventral ectoderm as well as by the transcription factor Lmx1b that is expressed in the dorsal mesoderm (Parr and McMahon, 1995; Loomis et al., 1996; Riddle et al., 1995). *Wnt7a* and *Lmx1b* knockout mice have distally ventralized extremities (Parr and McMahon, 1995; Chen et al., 1998), whereas *En1* knockout mice have dorsalized extremities (Loomis et al., 1996; reviewed by Schwabe and Mundlos, 2004).

The regulation of the temporal and spatial expression of the above mentioned genes is still not completely understood. The characterization of mutations of genes in humans and mouse and their resulting phenotypes have contributed to our understanding of the patterning of the extremities. Besides *Shh*, *Wnt7a*, *En1* and *Lmx1b* the *Pax* genes (*Pax1*, *Pax3*), the retinoic acid receptor, members of the *TGFβ/BMP* gene family and the *Hox* genes play important roles in the development of the extremities as well (Balling et al., 1988; Epstein et al., 1991; Lohnes et al., 1993; Storm et al., 1994; Thomas et al., 1996; Rijli and Chambon, 1997).

Morphogenesis and Growth of Bones

After the patterning of the skeleton cells differentiate into chondrocytes, osteoblasts and osteoclasts. These cells play important roles in bone formation, bone remodeling and bone resorption.

There are two ways to form bone (ossification): the desmal or intramembranous ossification forms most of the skull bones and parts of the claviculae. The enchondral ossification forms the long bones of the skeleton. During intramembraneous ossification mesenchymal cells condense and are invaded by blood vessels. The mesenchymal cells differentiate into osteoblasts and form osteoids consisting of glycoproteins, proteoglycans and collagens. Bone matrix is secreted and the osteoblasts differentiate into osteocytes. More and more layers of

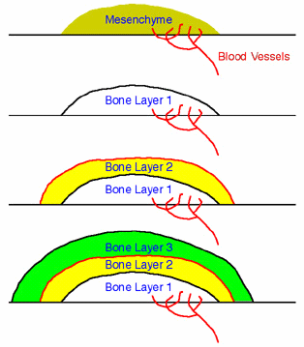

Fig. 2: Schematic of intramembraneous ossification.

Mesenchymal cells condense and differentiate into osteoblasts and later form ostoeids building one bone layer after another.

From:Skulls and Jaws

http://www.auburn.edu/academic/classes/zy/0301/Topic7/Topic7.html

bone material are secreted forming the bone tissue (Fig. 2) (for review see Karsenty and Wagner, 2002). Dermal bones (bone within the dermis of the skin), sesamoid bones (form within tendons like patella and pisiform of the wrist), and perichondral and periosteal bones (formed from connective tisue surounding cartilage and bone) are formed by

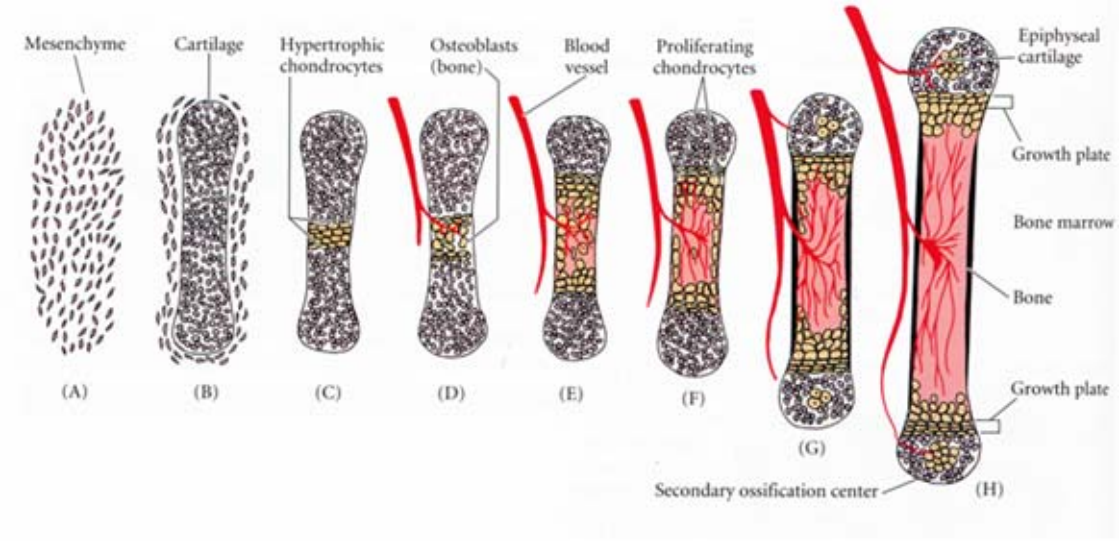

Fig. 3: Schematic of endochondral bone formation Mesenchymal cells condense and differentiate into chondrocytes forming a cartilaginous model of the developing bone. The chondrocytes in the center of the shaft undergo hypertrophy and apoptosis. They mineralize their extracellular matrix and blood vessels invade (primary ossification). Longitudinal growth takes place primarliy through similar processes occurring in the growth plate. Resting chondrocytes differentiate to proliferating and then hypertrophic chondrocytes that undergo apoptosis and are replaced by bone tissue. From: Developmental Biology 5th ed.Gilbert 1997, pg. 354.

intramembranous ossification. In contrast during chondral ossification the whole skeleton is formed as a cartilaginous model that is subsequently replaced by bone tissue. The ossification starts from the diaphysis (middle shaft) by a thickening of bone tissue from the outside (perichondral ossification) and then from the inside (endochondral ossification). Endochondral bone formation starts with the condensation of mesenchymal cells expressing type I collagen that form a cartilaginous model of the developing bone (Fig. 3,4). These cells differentiate during chondrogenesis from resting chondrocytes to proliferating chondrocytes by expressing chondrocyte-specific markers such as type II, type IX and type XI collagens, Gla and other matrix proteins, and finally mature to hypertrophic chondroytes expressing type X collagen (Horton, 1993; Mundlos, 1994; Luo et al., 1995). The transcription factor SOX9 regulates the differentiation of mesenchymal stem cells into chondrocytes as well as the expression of type II collagen (Bi et al., 1999). SOX9 in turn is regulated by NOTCH1. Overexpression of the intracellular domain of NOTCH1 under the control of the type II collagen promoter results in a loss of endochondral bone formation whereas intramembranous ossification seems to remain unaffected (Engin et al., 2005, unpublished data). The different steps of chondrocyte differentiation during endochondral bone formation are temporally and spatially separated (Fig. 4). Factors that influence the differentiation and proliferation of chondrocytes in these processes include hormones, cytokines like IL-8 (Merz et al., 2003), as

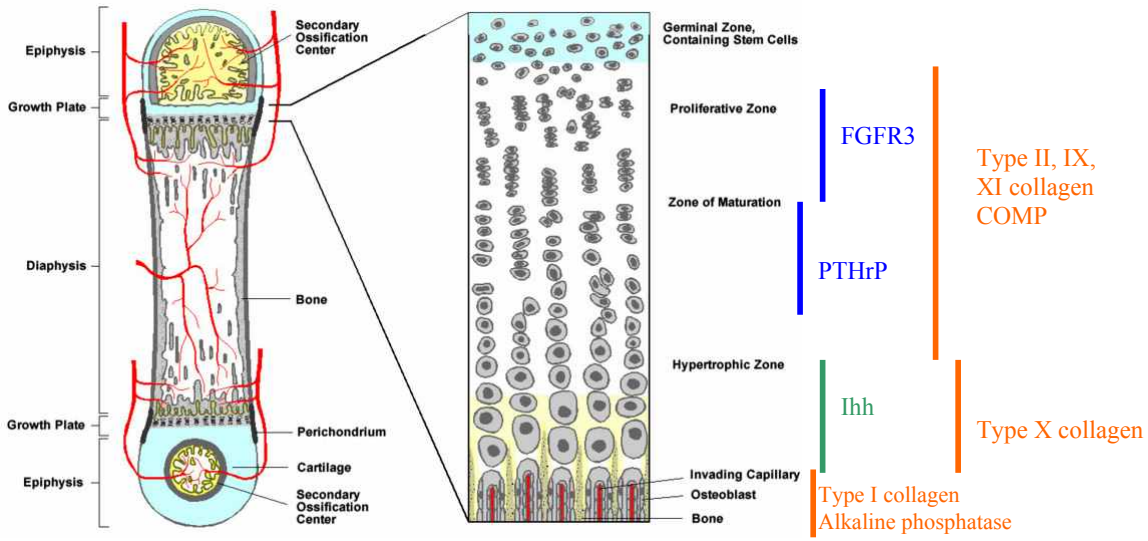

Fig. 4: Schematic of the growth plate

Long bone with epiphysis, growth plate (metaphysis), and diaphysis are shown on the left. The human growth plate is shown in the middle. The expression pattern of some important genes during the endochondral ossification are shown on the right. Receptors (blue), structural proteins (orange) and secreted factors (green) are indicated. Modified from Dreyer et al., 1998; Zabel and Winterpacht, 2000 and; http://www.howe.k12.ok.us/~jimaskew/botzo/ossification.jpg

well as 'fibroblast-growth-factor-receptor-3' (FGFR3) and 'parathyroid hormone related peptide' (PTHrP) and its receptor (PTHrPR) (Colvin et al., 1996; Johnson and Williams, 1993; Amizuka et al., 1994). FGFR3 is a negative regulator of chondrocyte differentiation since *Fgfr3* knockout mice are taller, because of a bigger growth plate caused by an elongated hypertrophic chondrocyte zone compared to wild type littermates. This is based on increased proliferation and maturation of the proliferating chondrocytes (Colvin et al., 1996; Deng et al., 1996). In contrast PTHrPR and PTHrP promote chondrocyte differentiation under the control of 'Indian hedgehog' (Ihh) (Vortkamp et al., 1996; Lanske et al., 1996). Also the group of BMPs (bone morphogenic proteins) induce cartilage and bone formation in mesenchymal cells, thus playing an important role in chondrocyte and osteoblast differentiation during endochondral ossification (Sakou, 1998; Karsenty, 1998). Blood vessels coming from the perichondrium invade during endochondral ossification at the hypertrophic zone where the chondrocytes undergo apoptosis (Fig. 3, 4). Together with the blood vessels osteoblasts form and become part of the ossification process. The expression of type I collagen and alkaline phosphatase is specific for the primary ossification center. This initial ossification process spreads from the diaphysis towards the epiphysis. The same processes are involved in the growth of the long bones and take place in the growth plate. The growth plate is a small zone of cartilage between the diaphysis and epiphysis. In the same temporal and spatial manner resting chondrocytes differentiate to hypertrophic chondrocytes, and then undergo apoptosis (Fig. 4) (reviewed by Kronenberg 2003). A microarray study performed with rat chondrocytes of the proliferative zone compared to chondrocytes of the hypertrophic zone revealed that e.g., cell cycle promoting and transcription activating genes are preferentially expressed in the proliferating zone; whereas differential expressed genes in the hypertrophic zone were involved in extracellular structure, membrane receptor and transporter functions (Wang et al., 2004). At the end of longitudinal growth, usually at the end of puberty, the growth plate closes and is replaced by spongy bone.

The proliferation and differentiation of the chondrocytes are best understood up to now. There are many growth factors and transcription factors described that are involved in the growth of the long bones (for review see Stevens and Williams, 1999). However, there is not much known about the differentiation of osteoblasts (bone formation) and even less about osteoclasts (bone resorption). The *Runx2* (*Cbfa1*) knockout mouse model contributed to our understanding of ostoeblast differentiation. Homozygous *Runx2* knockout mice develop a complete skeleton that consists of only cartilage and no bone tissue at all. This is due to a

lack of osteoblasts (Otto et al., 1997; Komori et al., 1997). This demonstrates that the transciption factor *Runx2* plays an essential role in the differentiation of mesenchymal cells into osteoblasts. The osteoclasts are cells containing multiple nuclei and derive from the fusion of precursor cells of the macrophage lineage (hematopoeitic cell lineage) (Chambers, 2000). After their differentiation the cells build a ruffled membrane through polarization that serves as the site of degradation of the bone matrix. At first the matrix is digested chemically and in a second step by proteins. Mainly the type I collagen is proteolytically cleaved by a protease called 'Cathepsin K'. Mutations in this protease cause pyknodystosis, also called Toulouse-Lautrec disease, a skeletal dysplasia with autosomal recessive inheritance (Motykova et al., 2001, Karsenty, 2001). There are two proteins that play a major role in osteoclast differentiation: Macrophage-colony-stimulating factor (M-CSF) is essential for the maturation of macrophages and osteoclast precursors. Binding of M-CSF to its receptor c-Fos results in the proliferation and maintainance of osteoclasts (Teitelbaum, 2000). The receptor activator of NF-κB ligand (RANKL) is essential for the development of osteoclasts and the differentiation of T-cells. It is also expressed in osteoblast precursors, osteoblasts, and hypertrophic chondrocytes (Han et al., 2005). *Rankl* knockout mice have osteopetrosis because of lack of osteoclasts (reviewed by Karsenty and Wagner, 2002). There is not much known about the factors that regulate the interaction between osteoblasts and osteoclasts during bone formation and bone resorption.

Homeostasis

Even after complete growth of the bone there is still constant remodeling. The bone is constantly resorbed by osteoclasts and newly formed by invading osteoblasts secreting bone matrix. These two processes assure a constant bone mass throughout life, but the regulation of these processes is not completely understood. Oestrogens, calcitonin, vitamin D_3, parathyroid hormone, IL4, IL6, and tumor necrosis factor (TNF) are all thought to be involved in maintaining homeostasis. The generation of mouse models, lacking osteoclasts, has contributed to our understanding of the differentiation of osteoclasts. Two secreted factors and four transcription factors involved in osteoclast differentiation have been isolated (Karsenty, 1999). Disruption of these regulatory networks can lead to a loss of bone mass (**osteoporosis**), due to an increased osteoclast activity, to too much bone (**osteopetrosis**) because of a defect in oseteoclast differentiation, or to **osteosklerosis,** an increased production of bone matrix because of increase activity of osteoblasts (reviewed by Oberg et al., 2004).

1.2 Disorders of the Skeleton

Genetic disorders of the skeleton are usually caused by the disruption of the development of cartilage and bone tissue. The overall incidence of skeletal disorders is around 1:5,000 newborns (Cadle et al., 1996) and there are over 150 different forms of osteochondrodysplasias described so far (Morcuende and Weinstein 2003). The group of skeletal disorders is very heterogeneous. This can be explained by the numerous genes, proteins, interaction of proteins, and different cells that are involved in skeletogenesis. The interruption of any of the individual processes such as patterning, morphogenesis, growth, or homeostasis can result in a different pathogenic phenotype. Many of these disorders present with disproportional growth retardation.

The nomenclature and diagnosis of the bone disorders was mainly based on X-ray features and the clinical presentation of the patients. The identification of genes causing skeletal disorders has facilitated the distinction between diseases with often very similar and overlapping clinical presentations. In addition, the analysis of naturally occurring mouse mutants or mouse models generated by gene targeting have contributed to the understanding of skeletal development in general and the pathogenesis of many skeletal disorders in particular. The disorders of the bone could clinically be divided in 33 groups of osteochondrodysplasias and 3 groups of dysostoses depending on the affected parts of the skeleton (Hall, 2002). Osteochondrodysplasias are disorders of cartilage or bone growth and skeletal development. Dysostoses are malformations of individual bones (single bones or sometimes in combination with others) and are not considered as generalized disorder of the skeleton (Spranger et al., 2002).

Molecularly the skeletal disorders could be divided into 7 groups depending on the underlying pathogenic mechanism of the disease (Superti-Furga et al., 2001). Group 1: Defects in extracellular structural proteins such as the Collagenopathies (for review see Spranger et al., 2002). Group 2: Defects in metabolic pathways (including enzymes, ion channels, and transporters) such as that found in Diastrophic Dysplasia where mutations in the diastrophic dysplasia sulfate transporter gene lead to a defect in the sulfate metabolism (Hästbacka et al., 1994). Group 3: Defects in folding and degradation of macromolecules. An example of this kind of disorder is autosomal recessive Pyknodysostosis arising from mutations in a lysosomal proteinase (Cathepsin K) (Hou et al., 1999). Group 4: Defects in hormones and

signal transduction mechanisms. Some of the best known examples are the activating mutations of PTH/PTHrP causing Jansen Metaphyseal Dysplasia (Schipani et al., 1996) and the lethal Blomstrand Dysplasia caused by inactivating mutations of PTH/PTHrP (Zhang et al., 1998). Group 5: Defects in nuclear proteins and transcription factors like the Nail-Patella Syndrome where mutations in the LIM homeodomain protein (*LMX1B*) have been identified (Dreyer et al., 1998; for review of transcription factors causing skeletal dysplasias see Hermanns and Lee, 2002). Group 6: Defects in oncogenes and tumor suppressor genes. An example for this group would be the Multiple Exostoses Syndrome type 1 and type 2 due to defects of *EXT1* and *EXT2* (Cheung et al., 2001; Duncan et al., 2001). And last but not least Group 7: Defects in RNA and DNA processing and metabolism. This group consists of 3 disorders with autosomal recessive inheritance. Severe combined immuno-deficiency (SCID) caused by mutations in ADA (adenosine deaminase) (Hirschhorn, 1995) and Schminke immuno-osseous dysplasia due to mutations of a chromatin regulator SMARCAL1 (Boerkoel et al., 2002). The latter group also contains the first chondrodysplasia and still one of the few skeletal dysplasias that is not caused by mutations in genes translated into a protein but by a mutation in an RNA gene: the Cartilage Hair Hypoplasia (CHH) (Ridanpää et al., 2001).

1.3 Cartilage Hair Hypoplasia

Cartilage Hair Hypoplasia (CHH) is also known as Metaphyseal Chondrodysplasia McKusick type (OMIM #250250) and was first described in the Amish, an isolated religious group in the USA by Victor McKusick (McKusick et al., 1965). It is an autosomal recessive disorder characterized by short stature, blond fine sparse hair (Fig. 5A), but this may be quite variable, and defective cellular immunity affecting T-cell mediated responses (Mäkitie et al., 1995). Patients may have severe combined immunodeficiency requiring bone marrow transplantation or they may be asymptomatic (Castigli et al., 1995; Mäkitie et al., 1998). Gastrointestinal dysfunctions (Mäkitie and Kaitila 1993) are frequently observed such as malabsorbtion or Hirschsprung's disease (Mäkitie et al., 2001). A predisposition to certain cancers primarily lymphomas has been reported as well (Mäkitie et al., 1995; Mäkitie et al., 1998). The metaphyses of tubular bones are widened, scalloped and irregularly sclerotic (Fig. 5B). Delayed ossification and trabeculation of the long bones are also characteristic findings on X-rays. All long bones are affected. The relative length of the humerus, ulna, radius, tibia and fibula decreases rapidly in early childhood and again at puberty. Relatively short and broad

phalanges of the hands are observed (Fig. 5D). The incidence off CHH in the Amish is 1.5 in 1,000 births; and in Finland is 1 in 18,000 – 23,000 live births. The critical region of the

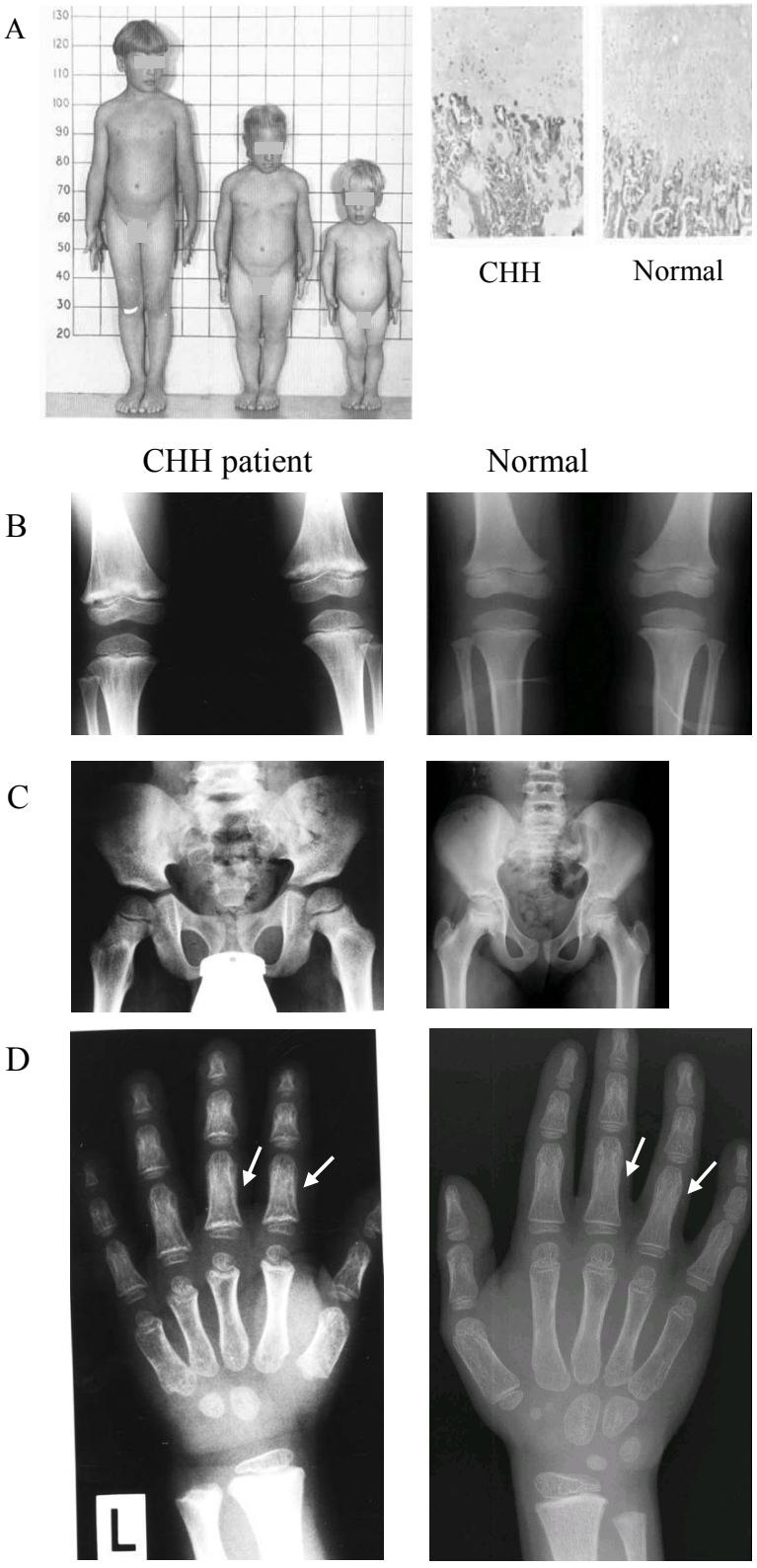

Fig. 5: Characteristic features of CHH.

A: left pannel: short stature in CHH (2 patients on the right) compared to an age matched control on the left. Right pannel: CHH patients have short columns and very few hypertrophic cells in the growth plate.
Pictures provided by Asad Mian, source currently unkown.
B-D: X-rays of a 4 year old CHH patient on the left. X-rays of an approximately 6 year old boy on the right as control for comparison.
B: Characteristic metaphyseal changes in CHH (left) compared to control (right). Flaring and scalloping of the metaphyseal border, delayed ossification and trabeculation of the long bones.
C: X-ray of the pelvis. CHH patient on the left with coxa valga compared to control on the right. No metaphyseal changes at the hip.
D: Characteristic findings in the hands. CHH patient on the left and normal control on the right.
Relatively broad and short phalanges. Delayed ossification and trabeculation of the phalanges.
Metaphyseal cupping starting in the metacarpals and middle and proximal phalanges.

CHH locus was mapped to 9p13 by linkage analysis (Sulisalo et al., 1997.). Ridanpää et al. found that mutations in the *RMRP* (OMIM #157660) gene cause most cases of CHH (Ridanpää et al. 2001). The worldwide emerging mutation spectrum in CHH includes the major 70A>G transition mutation with an ancient founder origin established in Finland, a country where the disorder is uncommonly frequent (Ridanpää et al., 2002; Bonafé et al., 2002; Kuijpers et al., 2003; Nakashima et al., 2003).

1.4 The RMRP gene

RMRP is the RNA component of the RNase MRP (Ribonuclease Mitochondrial RNA Processing) ribonuclease complex. It is an intronless gene transcribed by the DNA dependent RNA polymerase III and not translated into a protein. The human *RMRP* transcript is 267 bp long and the promoter region contains several putative promoter elements; a TATA box, a PSE bining element, a SP1 binding element and an octamer (Fig.6). The functional relevance of these elements *in vivo* however is still unknown. At the 3' end is a RNA Polymerase III stop signal with a run of 5dTs. It is encoded in the nucleus (Chang & Clayton, 1987) but the complex is localized primarily in the nucleolus and to a lesser extend in the mitochondria (Reimer et al., 1988; Li et al., 1994).

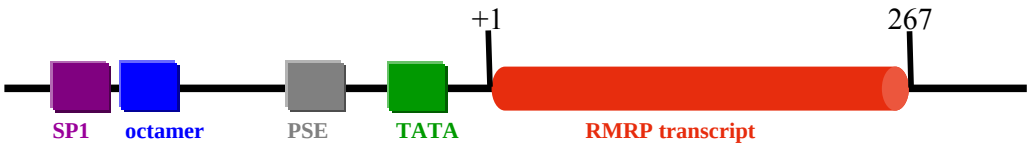

Fig. 6: Schematic of the RMRP gene structure. The RMRP transcript is depicted im red. The transcription start site (+1) and the end of the transcript (267 bp) are indicated. The putative promoter elements are shown; TATA box in green, PSE binding element in grey, octamer in blue, and SP1 binding element in violet.

This complex is highly conserved among a variety of different species, including human, mouse, rat, cow, *Xenopus*, yeast, *Arabidopsis* and tobacco (Schmitt et al., 1992) (Fig. 7). There is no RNase MRP identified in bacteria or *Archaea* yet. However, there has been no *RMRP* orthologe found in *Drosophila* and *C. elegans* yet. The length of the *RMRP* transcript is variable among the different species. The yeast gene consists of 339 bp, the frog gene of 277 bp, in cow of 279 bp, mouse 275 bp or in humans of 267 bp (265 bp are only shown in

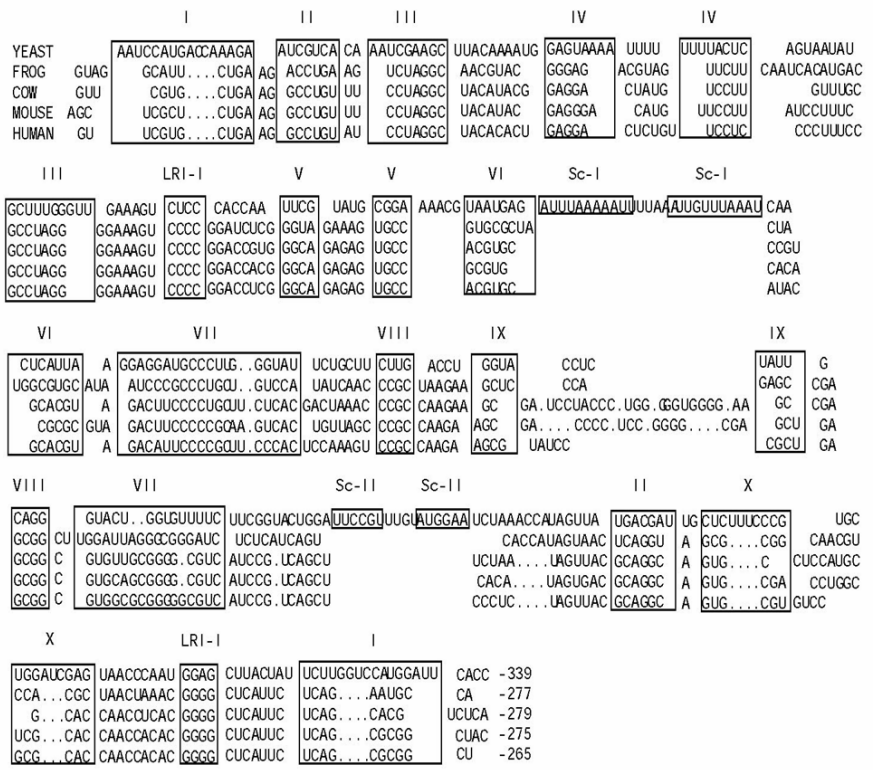

Fig. 7: Sequence comparison of RMRP among different species.

RMRP is highly conserved among a variety of different species. Conserved elements of the secondary structure are boxed.

Schmitt et al., 1992.

Figure 7. The RNA folds to a very complex secondary structure (Fig. 8). Before the RNA is not folded, none of the proteins will bind to the RNA (Walker & Avis 2004). So far ten proteins have been identified that form this ribonucleoprotein complex (summarized by

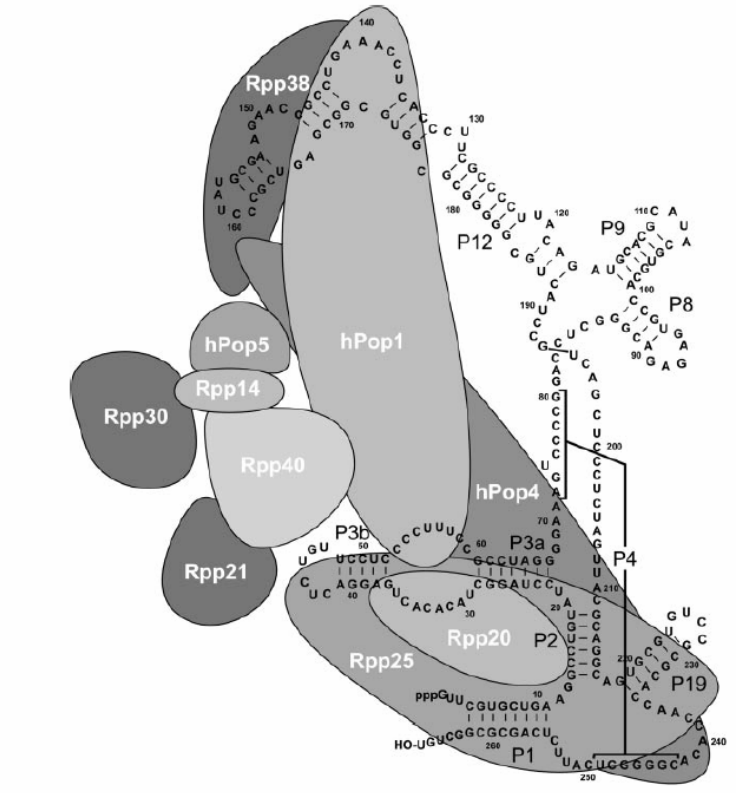

Fig. 8: Schematic of the RNase MRP protein complex.

The complex secondary structure is shown in association to the binding of the proteins to the RNA and each other forming the ribonuclear complex.

Welting et al., 2004

Welting et al., 2004) (Fig. 8). *RMRP* is essential in yeast, since yeast strains deficient for the *RMRP* orthologe, *NME1*, die (Schmitt and Clayton, 1992). *NME1* stands for nuclear mitochondrial endonuclease 1 (Schmitt and Clayton 1992). It has been extensively mutagenized and characterized. Interestingly, if the least conserved part of the *NME1* gene is deleted, no phenotype could be observed. The deletion spanned VIII to VIII (nt 186 – nt 211) (Fig. 7) forming the P8 hairpin (Fig 8). This region of *NME1* is not highly conserved among different species and may lack significance of *NME1* function (Shadel et al., 2000). Studies in yeast have attributed multiple functions to this ribonucleoprotein complex. It is involved in mitochondrial DNA replication. It cleaves the RNA that primes the mitochondrial DNA replication in the RNA/DNA hybrid and is also involved in the RNA primer formation (Chang and Clayton 1987; Lee and Clayton 1997). Some *nme1* mutants exhibit a delay in the progression of the cell cycle at the end of mitosis observed by morphological changes. These mutants arrest in the late cycle of mitosis as large budded cells with dumbbell-shaped nuclei, and extended spindles (Cai et al., 2002). One reason of the cell cycle arrest of these mutants might be the increased level of CLB2. Normally, the 5'UTR of *CLB2* is cleaved by the RNase MRP complex. That in turn causes a rapid degradation of *CLB2* mRNA and leads to a cell cycle progression (Gill et al., 2004). *RMRP* also plays a role in processing of ribosomal RNAs (Chu et al., 1994; Lygerou et al., 1996). In yeast it cuts pre-ribosomal RNA at the A_3 site and helps so to convert the long form of the 5.8S rRNA into the short and active form of the 5.8S rRNA (Fig. 9).

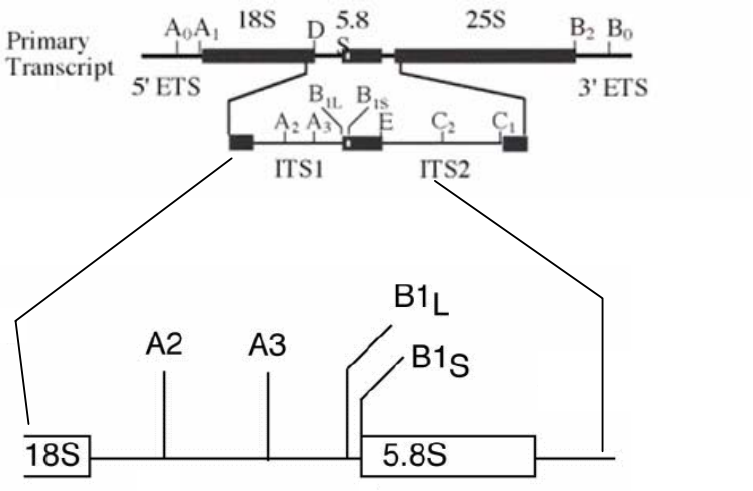

Fig. 9: Schematic of ribosomal RNA processing. The primary transcript is shown on the top and the main cutting sites A_0 to E are shown. The RMRP ribonuclease protein complex cuts at the A_3 site and also controls the maturation of the 5.8 S rRNA that is processed at the $B1_L$ and $B1_S$ sites subsequently. Modified from Fatica 2002 and Gill et al., 2004.

The functional analysis of the RNase MRP endoribonuclease is complicated by the fact, that eight proteins are shared by a related ribonucleoprotein complex, called RNase P. RNase P is also a ribonucleoprtein endoribonuclease and is mainly involved in tRNA precursors maturation (Ref.). The protein RPR2p is unique to the RNase P complex. In yeast two RNase MRP specific proteins have been identified; SNM1 (Schmitt and Clayton 1994) and most recently RMP1 (Salinas et al., 2005).

1.5 Specific Aims

RMRP is the first of the two RNA genes described so far that is not associated with a mitochondrial disease. The second non-mitochondrial disease-causing RNA was the *human telomerase RNA* (*hTR*) when mutated causes the rare autosomal dominant form of congenital dyskeratinosis (CD) (Vulliamy et al., 2001). CD is a progressive bone marrow failure syndrome that is characterized by abnormal skin pigmentation, nail dystrophy, and mucosal leukoplakia. While RNAs can cause disease this has been primarily restricted to mitochondrial disorders. As *RMRP* is not translated into a protein it is not obvious how mutations in the *RMRP* gene might alter its normal function and lead to the pathogenesis of CHH.

Aim of the clinical study of the CHH patients is to delineate CHH from other chondrodysplasias with similar metaphyseal changes such as Metaphyseal Dysplasia type Schmid (MCDS) and maybe to establish a phenotype-genotype correlation linking the critical clinical findings in patients with specific *RMRP* mutations.

Secondly, the effect of the mutations found in the *RMRP* transcript in CHH patients will be analyzed using *Saccharomyces cerevisiae* as a model organism.

Furthermore the promoter of the *RMRP* gene will be characterized and the effect of promoter duplications found in CHH patients on the *RMRP* transcription will be evaluated *in vitro*.

Microarray experiments will be used to identify down-stream targets of *RMRP* that could help to elucidate the pathogenesis of Cartilage Hair Hypoplasia. Candidate genes will be evaluated using transgenic mouse models.

Methods

2.1 DNA isolation methods

2.1.1 Genomic DNA isolation from whole blood (from February 2001 to December 2002)

Blood was stored upon arrival at 4ºC over night. The next day, separation buffer was added at three times the volume of blood and kept on ice for a minimum of one hour. The cells were pelleted by centrifugation at 1000 rpm for 10 minutes at 4ºC. The cell pellet was then resuspended in 700 µl suspension buffer containing 1% SDS and 100 µg/ml proteinase K and incubated at 50ºC overnight. DNA from the proteinase K digest was then extracted with 700 µl saturated phenol followed by phenol:chloroform (1 : 1) and chloroform extractions. To precipitate the genomic DNA 0.7 volumes of isopropanol were added and the DNA precipitate was retrieved with a closed glass Pasteur pipette. The DNA was then washed with 600 µl 70% ethanol and air-dried. The genomic DNA was dissolved in 500 µl of 1 x TE buffer. The concentration of the isolated genomic DNA was determined by measuring the optical density (OD_{260nm}) with a spectrophotometer and the quality by gel electrophoresis. The DNA was stored at 4ºC.

2.1.2 Genomic DNA isolation from whole blood (from January 2003 to present)

To isolate genomic DNA from patient blood, the Purgene™DNA Purification Kit from Gentra (Minneapolis, MN, USA) was used. 10 ml whole blood was poured into a 50 ml centrifuge tube containing 30 ml RBC Lysis Solution. The centrifuge tube was inverted several times to mix the whole blood with the RBC Lysis Solution and incubated at 20ºC for 10 min, then centrifuged at 2,000 x g for 10 min at 20ºC. The supernatant was removed and the white cell pellet resuspended in 10 ml Cell Lysis Solution. 50 µl RNase A Solution was added and incubated for 60 min at 37ºC. The sample was then cooled down to 20ºC and 3.33 ml Protein Precipitation Solution was added to the cell lysate. It was then vortexed for 20 s and centrifuged at 2,000 x g for 10 min at 20ºC. The precipitated proteins formed a tight dark brown pellet. The DNA-containing supernatant was transferred to a new 50 ml centrifuge

tube containing 10 ml 100% isopropanol. The samples were mixed by gently inverting until the white visible threads of DNA formed. The DNA threads were pelleted by centrifugation at 2,000 x g for 3 min at 20ºC. The supernatant was discarded and the tube briefly drained on a clean absorbent paper towel. The DNA was washed with 10 ml 70% EtOH by inverting the tube several times. Centrifugation was carried out at 2,000 x g for 1 min at 20ºC to pellet the DNA. The EtOH was carefully decanted and the tube drained on a clean absorbent paper towel. The DNA was air dried for 20 min and then dissolved in 1 ml DNA Hydration Solution. To rehydrate the DNA the solution was incubated at 20 ºC overnight and then transferred to a 1.5 ml centrifuge tube and stored at 4 ºC. The concentration of the isolated genomic DNA was determined by measuring the optical density (OD_{260nm}) with a spectrophotometer and the quality by gel electrophoresis.

2.1.3 Isolation of genomic DNA from mouse tails for genotyping

Each mouse tail was cut 1 cm from the tip and transferred to a 1.5 ml reaction tube. 700 µl NTES buffer and 100µg/ml proteinase K were added to the reaction tube, which was then incubated overnight in a rocking cylinder at 57ºC. Undigested material was pelleted by centrifugation for 3 min at 13,000 rpm. The clear supernatant was transferred to a 1.5 ml reaction tube and 700 µl of phenol (satured, buffered, pH 8.0) was added. The mixture was rocked for 10 min and then centrifuged for 10 min at 20ºC. A 1000 µl tip, with approximately 1 cm of the end cut off, was used to transfer the aqueous phase into a fresh 1.5 ml reaction tube. Then 700 µl phenol:chloroform: isoamylalcohol (25:24:1) was added, rocked for 10 min and afterwards centrifuged for 10 min at 4000 rpm in a tabletop centrifuge at 20ºC. The aqueous phase was again transferred into a fresh 1.5 ml reaction tube. The genomic DNA was precipitated by adding 700 µl isopropyl alcohol. The DNA was retrieved with a closed end glass Pasteur pipette. The spooled DNA was dipped into 70% Ethanol and the DNA was dried for 5 min at 20ºC. The DNA was dissolved in 200 µl of TE buffer, pH 8.0. The concentration was determined by measuring the optical density (OD_{260nm}) with a spectrophotometer and the quality of the DNA by gel electrophoresis. The genomic DNA was stored at 4ºC.

2.1.4 Isolation of genomic DNA from yeast cells

A single yeast colony was grown to saturation in a 10 ml liquid culture. The cells were pelleted and resuspended in 500 µl sorbitol solution. 50 µl of 30 mg/ml zymolyase and 50 µl of 0.28 M β-mercaptoethanol were added and incubated for 1 hr at 37ºC. The cells were then centrifuged at 14,000 rpm for 5 min, the supernatant decanted and the pellet resuspended in 500 µl Tris/EDTA solution. The cells were lysed with 25 µl 20% SDS and incubated for 30 min at 65ºC. The proteins were precipitated with 200 µl of 5 M potassium acetate and centrifuged at 13,000 rpm for 10 min at RT. The supernatant containing the genomic yeast DNA was treated with RNase A for 1 hr at 37ºC followed by one phenol and one chloroform extraction. Then the genomic DNA was precipitated with 2 volumes of 100% ethanol, centrifuged for 5 min at 12,000 x g. The pellet was washed with 70% ethanol, dried and dissolved in 300 µl TE buffer. The concentration was determined by measuring the optical density (OD_{260nm}) with a spectrophotometer and the quality of the DNA by gel electrophoresis. The genomic DNA was stored at -20ºC.

2.1.5 Isolation of genomic DNA from ES cell clones for Mini-Southern analysis

The ES cells were grown in 96-well U-bottom plates as described in 2.12.1. After they reached confluency the cells were washed twice with PBS. 50 µl Lysis buffer consisting of 10 mM Tris, pH 7.5, 10 mM EDTA pH 8.0, 10 mM NaCl, O.5% sarcosyl, and 1 mg/ml proteinase K was added to each well. The plates were then incubated overnight at 57ºC in a humidified chamber. Then the DNA was precipitated with 100 µl 75 mM NaCl in absolute ethanol and incubated on a plate shaker at RT until a precipitate was visible. The plates were inverted to discard the supernatant and washed three times with 100 µl 70% ethanol. After the last wash the plates were air dried for around 15 min. The DNA was resuspended in 40 µl of the restriction enzyme cocktail mix consisting of 1 x reaction buffer of the enzyme being used, 1 mM spermidine, 100 µg/ml BSA and 10 – 15 U of enzyme. The 96-well plate was then incubated at 37ºC overnight in a humidified chamber

2.1.6 Isolation of plasmid DNA

2.1.6.1 Isolation of plasmid DNA from bacteria for subcloning

For subcloning or to check for correct cloning events the method described by Birnboim and Doly (Birnboim and Doly 1979) was slightly altered. A single colony was picked and grown in 3 ml LB medium overnight at 37ºC, and then centrifuged for 1 min at 12,000 x g at RT. The supernatant was discarded and the pellet resuspended in 200 µl solution I. For alkaline lysis 400 µl solution II was added and the tube was inverted gently 5 times. To neutralize the solution and to precipitate the proteins and bacterial genomic DNA still attached to the cell membrane 300 µl solution III was added and the tube gently inverted 5 times before centrifugation for 10 min at 12,000 x g at 4ºC. The plasmid DNA was precipitated with isopropyl alcohol, and washed with 70% ethanol. The DNA was air dried and dissolved in 50 µl $^1/_4$ x TE buffer.

2.1.6.2 Isolation of plasmid DNA from bacteria for sequencing

The QIAprep® plasmid Miniprep kit (QIAGEN Inc., Valencia, CA, USA) was used to isolated smaller amounts of plasmid DNA for sequencing and cloning. This method is based on the alkaline lysis procedure described by Birnboim and Doly (Birnboim and Doly 1979). The instructions of the manufacturer were slightly altered. A single bacteria colony was picked and inoculated in 3 ml LB medium supplemented with 100 µg/ml ampicillin and grown for not longer than 10 hrs. The cells were harvested by centrifugation at 4,000 x g for 10 min. The bacteria pellet was resuspended in 250 µl cold P1 buffer and transferred to a 1.5 ml centrifuge tube. 250 µl P2 buffer was added to lyse the bacteria cells by inverting the tube until the solution becomes clear. Then 350 µl of P3 buffer was added to precipitate the proteins and the solutions were mixed by inverting the tube several times. The proteins were pelleted by centrifugation at 12,000 x g for 10 min at 4 ºC. The supernatant was decanted into the provided column. The DNA was bound to the column by centrifugation for 1 min at 12,000 x g. The column was washed with 500 µl PB buffer and then with 750 µl PE buffer. The DNA was eluted with 30 µl EB buffer by centrifugation for 2 min. at 12,000 x g. The concentration was determined by measuring the optical density (OD_{260nm}) with a spectrophotometer.

2.1.6.3 Isolation of plasmid DNA from bacteria for transfection

To isolate a larger amount of plasmid DNA, e.g., to transfect adherent cells, the QIAfilter Plasmid Midi prep kit (QIAGEN Inc., Valencia, CA, USA) was used. The instructions of the manufacturer were slightly altered. A single bacteria colony was picked and inoculated in 30 ml LB medium supplemented with 100 µg/ml ampicillin and grown overnight (but not longer than 18 hrs). The bacteria cells were harvested and the resulting pellet was resuspended in 4 ml P1 buffer. 4 ml P2 buffer was added to lyse the bacteria cells, and adding 4 ml P3 buffer precipitated the proteins and genomic DNA. The lysate was centrifuged at 15,000 x g for 30 min at 4ºC and the supernatant was decanted into the barrel of a QIAGEN-tip 100 pre-equilibrated with 4 ml QBT buffer. The column was then washed twice with 10 ml QC buffer and the DNA eluted with 5 ml QF buffer that was pre-warmed to 65ºC. The plasmid DNA was precipitated with 3.5 ml isopropanol and incubated at 20ºC for 10 min and then aliquoted into 2.0 ml tubes, which were then centrifuged at 15,000 x g for 30 min at 4ºC. The pellets were washed with 300 µl 70 % ethanol by centrifugation at 15,000 x g for 10 min at 20ºC. The supernatant was discarded and the pellet air-dried for 30 min and then dissolved in 10 µl of $^1/_4$ x TE buffer. The plasmid DNA was ultimately combined into one tube. The concentration was determined by measuring the optical density (OD_{260nm}) with a spectrophotometer.

2.1.6.4 Isolation of plasmid DNA from yeast cells

The EZ Yeast™ plasmid mini-prep kit (Geno Technology, Inc., St. Lois, MO, USA) was used to recover the plasmid of an over expression genomic yeast library screen. This method is base on the alkaline lysis described by Birnboim and Doly(Birnboim and Doly 1979) with addition of zymolyase. The manufacturer's protocol was followed exactly. 1.5 ml of a saturated yeast cell culture was centrifuged at 600 x g for 2 min. The pellet was resuspended in 150 µl Solution I, 5 µl of LongLife™Zymolyase and 1 µl β-mercaptoethanol was added, vortexed and incubated for 15 min at 37ºC. Then 150 µl RT-pre-warmed Solution II were added and mixed before adding 150 µl Solution III. The precipitated proteins were pelleted by centrifugation at 12,000 x g for 5 min. The supernatant was transferred into a new tube and the plasmid DNA was precipitated by adding 400 µl of isopropanol and pelleted by centrifugation at 12,000 x g for 15 min. The pellet was washed with 70% ethanol, air dried for 10 min and dissolved in 30 µl 1 x TE buffer. 5 µl of plasmid DNA was used for transformation in *E. coli* cells as described in 2.5.

2.2 Total RNA isolation

2.2.1 Isolation of total RNA from mammalian cells

To isolate total RNA from mammalian cells the RNAeasy Midiprep kit (QIAGEN Inc. Valencia, CA, USA) was used. The instructions of the manufacturer were slightly altered. 10^8 cells were harvested and the cell pellet was resuspended in 4 ml RLT buffer and vortexed for 20 s. 70% ethanol was added to the homogenized cell lysate and mixed by shaking vigorously. The sample was then applied to the RNeasy midi column and centrifuged at 3,500 x g for 5 min. The flow-through was discarded. The column was first washed with 4 ml RW1 buffer and then twice more with 2.5 ml RPE buffer. Finally the total RNA was eluted twice with 200µl RNase-free water. The concentration was determined by measuring the optical density (OD_{260nm}) with a spectrophotometer and the quality of the isolated total RNA by gel electrophoresis. The RNA was stored at –80ºC.

2.2.2 Isolation of total RNA from EDTA whole blood

To isolate total RNA from 10 ml EDTA whole blood the RNAeasy Midiprep kit (QIAGEN Inc. Valencia, CA, USA) was used. The instructions of the manufacturer were slightly altered. 1 volume of whole blood was mixed with 5 volumes of EL buffer and incubated for 15 min on ice. During this incubation time the sample was vortexed twice for 20 s and then centrifuged at 400 x g for 10 min at 4ºC. The supernatant was discarded and leucocytes were washed again with 2 volumes of EL buffer. Total RNA was isolated from the leucocytes as described in 2.2.1.

2.2.3 Isolation of total RNA from Saccharomyces cereviseae

To isolate total RNA from *Saccharomyces cerevisiae* the protocol described by Schmitt et al. (Schmitt, Brown and Trumpower 1990) was followed exactly. Yeast cells were grown to an OD_{600nm} around 2.5 to 5.0 in 10 ml of their selective medium and pelleted by centrifugation and then resuspended in 400 µl of AE buffer. 20 µl of 20% SDS and 400 µl phenol were added, vortexed and incubated 4 min at 65ºC. The samples were then immediately chilled on a dry ice/ethanol bath until phenol crystals were visible. After a 2 min centrifugation the

upper aqueous phase was transferred into a new 1.5 ml centrifuge tube. After a phenol/chloroform extraction the RNA was precipitated in 0.3 M Na acetate pH 5.3 and 2.5 volumes of ethanol. The pellet was washed in 80% ethanol, air dried and resuspended in 20 µl of DEPC treated water. The concentration was determined by measuring the optical density (OD_{260nm}) with a spectrophotometer and the quality of the isolated total RNA by gel electrophoresis. The RNA was stored at –80ºC.

2.3. DNA and RNA standard methods

2.3.1 Electrophoresis methods

2.3.1.1 Agarose gel electrophoresis for DNA

Plasmid DNA and PCR products are separated with horizontal agarose gels. 1 x TBE buffer was used as electrophoresis buffer. Dependent upon the size of the expected fragments 0.7% (for longer fragments) to 2% agarose gels containing 100 µg/ml ethidium bromide were used. The gels were run at a maximal voltage of 125 V. The DNA was visualized at 356 nm with the gel imaging system Eagle Sight (Stratagene, La Jolla CA (USA)).
To determine the product size of plasmid DNA and PCR products the 100 bp ladder (NEB, Beverly MA, USA), Marker X or Marker II (Roche, Indianapolis IN, USA) were loaded on the agarose gels.

2.3.1.2 Agarose gel electrophoresis for RNA

Prior to a Northern transfer the RNA was separated on a Glyoxal/DMSO agarose gel. In this procedure denaturation of the RNA was achieved by treating the RNA samples with a combination of glyoxal and DMSO prior to running on an agarose gel made with phosphate buffer. The glyoxal/DMSO method produces sharper bands after northern hybridization when compared to formaldehyde gels. The RNA was mixed 1 : 3 with freshly made glyoxal reaction buffer and incubated at 50ºC for 1 hr, chilled on ice and mixed with $^1/_6$ volume of RNA loading dye. The samples were then loaded on a 1.2% agarose made with 10 mM sodium phosphate buffer, pH 6.8, which contains 0.5 µg/ml ethidium bromide. 10 mM sodium phosphate buffer pH 6.8 containing 0.5 µg/ml Ethidiumbromide was used as

electrophoresis buffer and was constantly recirculated during the 4 hrs run at 80 V. After 2 hrs of electrophoresis the sodium phosphate buffer was replaced with fresh running buffer. The RNA was visualized at 356 nm with the gel imaging system Eagle Sight (Stratagene, La Jolla, CA, USA).

2.3.1.3 PAA gel electrophoresis

Prior to a Northern transfer the RNA was separated on a 7% Polyacrylamide, 6 M urea gel. In this procedure denaturation of the RNA was achieved by treating the RNA samples with a combination of glyoxal and DMSO prior to running on an the PAA gel made with 1 x TBE buffer. The RNA was mixed 1 : 3 with freshly made glyoxal reaction buffer and incubated at 50ºC for 1 hr, chilled on ice and mixed with $^1/_6$ volume of RNA loading dye. The samples were then loaded on a 7% PAA, 6 M urea gel made with 1 x TBE buffer, which contains 0.5 µg/ml ethidium bromide. 1 x TBE buffer containing 0.5 µg/ml Ethidiumbromide was used as electrophoresis buffer and the gel was run for 7 hrs at 80 V. The RNA was visualized at 356 nm with the gel imaging system Eagle Sight (Stratagene, La Jolla, CA, USA).

2.3.2 Purification of DNA fragments from agarose gels

2.3.2.1 Purification of DNA fragments < 10 kb from agarose gels

After electrophoresis the DNA fragments for cloning purposes were cut out from the agarose gel and purified with the QIAquick gel extraction kit (QIAGEN, Valencia, CA, USA) according to the manufacturer's instructions. The DNA used for injection of the transgenic construct was purified with the QIAEX II Gel Extraction kit (QIAGEN, Valencia, CA, USA). The protocol of the manufacturer was slightly altered. After binding the DNA to the glass milk, the complex was washed twice with QG buffer and then three times with PE buffer. The DNA was eluted twice with 15 µl microinjection buffer (10 mM Tris HCl/ 0.1 mM EDTA, pH 7.5). The eluted DNA fractions were combined in one 1.5 ml reaction tube. The yield of the purified DNA was determined by loading 3 µl on an agarose gel.

2.3.2.2 Purification of DNA fragments >10 kb from agarose gels

After restriction enzyme digest and other modifications (generation of blunt ends, treatment with alkaline phosphatase) the DNA was separated on an agarose gel. After electrophoresis the desired DNA fragments were cut out and purified with the QIAEX II Gel Extraction kit (QIAGEN, Valencia CA, USA). The instructions of the manufacturer were slightly altered. The excised gel slice containing the DNA was weighed and 3 volumes of Buffer QX1 plus 2 volumes of H_2O and 30 µl of QIAEX II were added mixed and incubated for 10 min at 50ºC. The samples were then centrifuged for 30 s and washed with 500 µl QX1 buffer and then twice with 500 µl PE buffer. After air-drying the pellet for 30 min the DNA was eluted two times with 20 µl $^1/_4$ x TE buffer. The yield of the recovered DNA was tested by loading 3 µl on an agarose gel.

2.4 PCR techniques

2.4.1 Standard PCR

The polymerase chain reaction was developed by Saiki (Saiki, Gelfand, Stoffel, Scharf, Higuchi, Horn, Mullis and Erlich 1988). The volume of each reaction was 50 µl and contained 50 mM KCl, 10 mM Tris/HCl (pH 8.3), 0.01% gelatin, 1.5 mM $MgCl_2$, 100 nM each of the two primers (sense and antisense), 100 µM each of the four dNTPs and 1 U Taq polymerase (AmpliTaq Gold, Perkin Elmer, Wellesley, MA, USA). 100 ng genomic DNA or 5 ng plasmid DNA were used as a template for the PCR reaction. In the first step the DNA was denatured at 96ºC for 2 min. The following 35 cycles of the PCR consisted of 1 min denaturing at 96ºC for 1 min followed by the annealing of the primers at 56 - 62ºC for 1 min and an elongation step of 1 – 2 min at 72ºC. After the 35 cycles were finished there was a final elongation step at 72ºC for 10 min. Lastly, the samples were cooled down to 4ºC. 5 µl of the PCR reaction was loaded on a 0.7 to 1% agarose gel to control for the specificity and the size of the PCR product.

2.4.2 Long template PCR

To amplify the recombination arms for the *Rmrp* knockout construct from 129SV/EV mouse genomic DNA Accu LA Taq (Sigma, Saint Louis, MO, USA) was used. 500 ng of genomic DNA were used as template in a reaction volume of 50 µl consisting of 50 mM KCl, 10 mM Tris/HCl (pH 8.3), 0.01% gelatin, 1.5 mM $MgCl_2$, 400 nM each of the two primers (sense and antisense), 2% DMSO, 125 µM each of the four dNTPs and 2.5 U Taq polymerase. The DNA was initially denaturated for 30 s at 98ºC. The following 35 cycles consisted of denaturating the DNA at 94 ºC for 1 min followed by the annealing of the primers at 56 - 62ºC for 1 min and an elongation step of 5-10 min at 68ºC. After the 35 cycles were finished there was a final elongation step at 68ºC for 10 min. Lastly the samples were cooled down to 4ºC. 5 µl of the PCR reaction was loaded on a 0.8% agarose gel to control for the specificity and the size of the PCR product.

2.4.3 Site-directed mutagenesis PCR

The nme1 point mutations were introduced via a two-step PCR (Ho, Hunt, Horton, Pullen and Pease 1989)(Higuchi, Krummel and Saiki 1988). To perform the mutagenesis, 2 PCR primers for each mutation and 2 flanking primers were designed as shown in Fig.10. In the first step

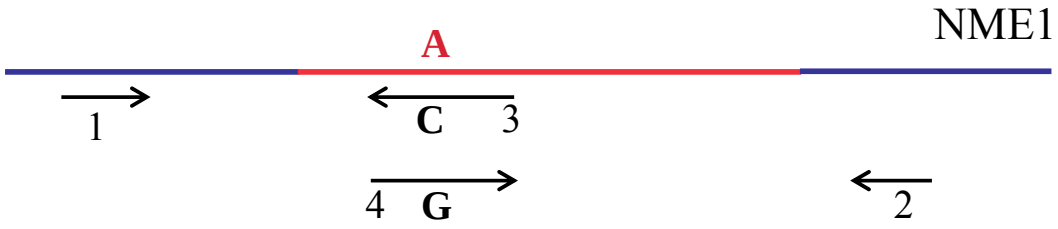

Fig. 10: Schematic of the two-step mutagenesis PCR. In the first step the first product was amplified with primers 1 and 3 and in a second reaction with primers 4 and 2. Primers 3 and 4 awere designed to contain the desired base pair change in the middle of the synthesized oligo nucleotide sequence. The PCR products of the first round were purified and used as templates for the second round of PCR amplification that was done with primers 1 and 2. The RMRP transcript is depicted in red and genomic sequences are in blue.

of the PCR one flanking primer and one primer containing the point mutation were used in two separate PCR reactions primers 1-3 and primers 2-4 (see Fig. 10). Primers 3 and 4 contain the mutation. The PCR products were purified and 5 ng of the templates of the first round were used as substrates for a second PCR step. The flanking primers (1 and 2) were added after the 5^{th} cycle of the PCR reaction. Depending on the product length the PCR was

performed as described in 2.4.1 or 2.4.2. The correct introduction of the mutation was assessed by subcloning of the PCR products (2.4.6) and sequencing of the subclones (2.5.1).

2.4.4 Reverse-Transcriptase

To convert RNA into complementary DNA 4 µg of total RNA isolated as described in 2.2.1 or 2.2.2 was denaturated for 10 min at 70ºC in a maximal volume of 18 µl and directly afterwards chilled on ice. Then 2 µl of random hexamers (c=50 µM), 1.5 µl dNTPs (25 mM each), 1 µl RNase Inhibitor (40 U/µl), 8 µl of 5 x 1st strand synthesis buffer, 4 µl of 0.1 M DTT, and 1.5 µl Reverse Transcriptase (40U/µl) (Invitrogen Corporation, Carlsbad, CA, USA) were added, mixed and incubated at 37ºC for 90 min. The enzyme was inactivated by heating to 94ºC for 10 min. The cDNA was stored at –20ºC until further use.

2.4.5 Quantitative PCR (Real-Time-PCR)

Quantitative PCR was performed to verify the results of the microarray analysis described in 2.11. The LightCycler® 2.0 Instrument and the reagents from Roche Applied Science (Indianapolis, IN, USA) were used for the quantitative PCR and the recommendations of the manufacturer were followed exactly. A fluorescent reporter is used for detecting and quantifying the amount of PCR product in a reaction. The intensity of the fluorescence is proportional to the amount of PCR product generated each PCR cycle which is a function of the quantity of template in each reaction and can be directly monitored. The variation of template among samples is controlled using constitutively expressed gene amplicons that amplify with efficiencies equal to that of the target (gene of interest). Amplicon homogeneity is verified by a melting curve analysis performed subsequent to the last cycle of amplification. Mispriming products and/or primer dimmers, as evidenced by multiple peaks, can sequester flourophore and complicate or even preclude evaluations. Single peak verifications were obtained with each system evaluated in this study. 20 µl reactions are prepared with dNTP concentrations of 1200 mM $MgCl_2$ 4 mM buffer and hotstart enzyme part of proprietary mastermix. cDNA samples were assayed by fluorometry on a BMG Fluostar plate reader (BMG LABTECH GmbH, Offenburg, Germany) using Pico green assay (Molecular Probes, Eugen, OR, USA). Template concentration was ascertained over multiple dilutions and normalized to 40 ng/ul of which a 1:8 dilution was used for Lightcycler amplification. 2 µl of

the 1:8 diltuion (12 ng) was added to each 20 µl reaction and fluorescence monitored for 40 cycles. Crossing points were determined by a second derivative algorithm intrinsic to the Lightcycler software.

2.4.6 Subcloning of PCR products

The PCR products were purified and subcloned into the pGEM-T vector (Promega, Madison, WI, USA) that contained a "T" overhang for direct subcloning of PCR products amplified with Taq-polymerase. 5 µl of 2 x Rapid Ligation Buffer, 1 µl of pGEM-T vector, 3 µl purified PCR product and 1 µl T4 DNA ligase were mixed and incubated either for 3 hrs at RT or at 4ºC over night and then transformed into bacteria cells as described in 2.5. To separate the alleles for the *RMRP* mutation screen of CHH patients 6 colonies were picked after transformation, grown in 5 ml LB-medium supplemented with 100 µg/ml ampicillin overnight at 37ºC and the plasmid DNA was isolated as described in 2.1.6.2 and then sequenced as described in 2.5.1.

2.5 DNA sequencing

2.5.1 Dye terminator reaction

The sequencing of DNA fragments was done as described by Sanger et al. (Sanger, Nicklen and Coulson 1977; Lee, Connell, Woo, Cheng, McArdle, Fuller, Halloran and Wilson 1992). 20 – 50 ng purified PCR product DNA or 200 – 300 ng of plasmid DNA was used as a template for the sequencing reaction in a 10 µl volume. The reaction mix consisted of 0.5 µl of 20 µM primer, and 1 – 2 µl of premix (depending of the size of the PCR products or plasmids). The sequencing reaction was performed in a PTC 200^{TM} (MJ Research, Watertwon, MA, USA) thermocycler as follows: An initial denaturation step for 2 min at 96ºC was followed by an 18 s denaturation step at 94ºC and a subsequent 4 min elongation step at 59ºC repeated for 25 cycles. After the sequencing reaction the volume of the samples was increased to 20 µl total with H_2O and the unincorporated nucleotides were separated with the DyeEx 2.0 purification kit (QIAGEN, Valencia CA, USA) according to the manufacturer's instruction manual. The spin column was gently vortexed to resuspend the resins. The cap of the column was loosened with a quarter turn and the bottom closure of the

column was snapped off, placed into a 2 ml collection tube and centrifuged at 750 x g for 3 min. The spin column was transferred into a 1.5 ml centrifuge tube and the 20 µl sequencing reaction was applied to the center of the resin bed and centrifuged for 3 min at 750 x g. The purified samples were run on an ABI Prism 3700 (PE Applied Biosystems, Foster City, CA, USA).

2.5.2 Dye primer reaction

To each 1.2 µl 'Ready Reaction Premix' (A, C, G, T) 0.5 µl purified PCR product was added, mixed and the standard dye primer sequencing program was run (10 s at 96ºC, 5 s at 55ºC, 1 min at 70ºC repeated for 15 cycles. Then 10 s at 96ºC, 1 min at 70ºC for another 15 cycles). After the sequencing reaction the four samples were combined and the unincorporated nucleotides were separated by precipitation with 35 µl of 100 % ethanol and centrifuged for 30 min at 12,000 x g at 4ºC. The supernatant was discarded and the pellet dried for 3 min in a speed vacuum at high heat. The samples were dissolved in 3 µl deionized formamide/50 mM EDTA and run on an ABI Prism 377 (PE Applied Biosystems, Foster City, CA, USA).

2.6 Competent cells

A single colony of SMR (or an other bacteria strain) cells was picked and incubated in 5 ml LB-medium at 37ºC overnight in a bacteria shaker. 200 µl of this pre-culture was transferred into 200 ml LB-medium and grown to an $OD_{600nm} \sim 0.2 – 0.3$. The cells were then pelleted by centrifugation at 3000 rpm at 4ºC for 10 min and resuspended in 40 ml ice cold 100 mM $CaCl_2$. After incubation for 30 min on ice the cells were again pelleted and resuspended in 2 ml $CaCl_2$ and 350 µl glycerol and stored at –80ºC in 100 µl aliquots.

2.7 Transformation of DNA into bacteria cells

100 µl of competent cells (see 2.6) and 10 – 50 ng of plasmid DNA were mixed and incubated on ice for 20 min followed by a heat shock for 100 s at 42ºC and immediately put on ice for 5 min. Then 400 µl of LB-medium was added and incubated at 37ºC for 60 min in a bacteria shaker. The cells were pelleted by centrifugation for 3 min at 3000 rpm. 400 µl of the supernatant was removed and the bacteria cells were resuspended in the remaining 100 µl and

streaked out on LB-agar plates containing 100 µg/ml Ampicillin and incubated for 12 – 18 hrs at 37ºC. For blue/white selection 40 µl of 20 mg/ml X-gal and 4 µl of 100 mg/ml IPTG were added to the LB-Ampicillin plates.

2.8 Manipulation of yeast cells

2.8.1 High-efficiency transformation of Yeast

Transformation of plasmid DNA into yeast was done according to Adams, Gottschling, Kaiser, Sterns: Methods in Yeast Genetics. A Cold Spring Harbor Laboratory Course Manual. 1997 Edition, which was adapted from Gietz and Schiestl (Gietz, Schiestl, Willems and Woods 1995). A single colony was picked and inoculated in 50 ml of the proper medium and grown at 30ºC until the culture reached an $OD_{600nm} \approx 0.3 – 0.5$. The yeast cells were pelleted by centrifugation at 3500 rpm for 5 min at 20ºC. First the cells were washed with 1 x TE buffer and then with 0.1 M Lithium acetate in 1 x TE. After these two washing steps the cell pellet was resuspended in 500 µl of Lithium acetate/TE buffer and incubated for 30 min at 30ºC. For each DNA sample to be transformed, carrier DNA and transforming DNA were mixed. Generally 5 to 15 µg of carrier DNA and 1 – 5 µg transforming DNA were used. The total volume of the DNA should not be greater than $^1/_{10}$ of the volume of added yeast cells. 150 µl yeast suspension was added to each DNA sample and incubated for 30 min at 30ºC. Then 700 µl PEG solution (10% 10 x TE, 10% 1 M lithium acetate, 80% of a 50% PEG solution) was added and again incubated for 30 min at 30ºC. The heat shock of the yeast cells was performed for 15 min at 42ºC. Afterwards the cells were directly pelleted to remove the PEG solution. The transformed yeast cells were resuspended in 3 ml of the proper selection medium and incubated for 3 hrs at 30ºC. 2 ml of this culture was removed, and the cells were pelleted and streaked on a plate containing the proper selection medium before incubation for 2 – 4 days at 30ºC.

2.8.2 Generation of yeast knockout construct

Exogenous plasmid DNA in the absence of an ARS sequence and containing yeast sequences can integrate at the homologous chromosomal locus when transformed into a yeast strain

(Hinnen, Hicks and Fink 1978). This fact was utilized to generate an *nme1-Δ* strain to elucidate the effect of *nme1* mutations on *NME1* function. The PCR-base strategy is illustrated in Fig. 11. The neomycin cassette was amplified with vector-specific primers containing a 55-bp sequence tail that is homologous to the *NME1* gene locus. The neomycin cassette was amplified using Sc-mut F and Sc-mut R and then transformed into a *Saccharomyces cerevisiae* wild-type strain as described in 2.8.1. Single colonies were sporulated and dissected as described in 2.8.3 to check for the recombination event. To

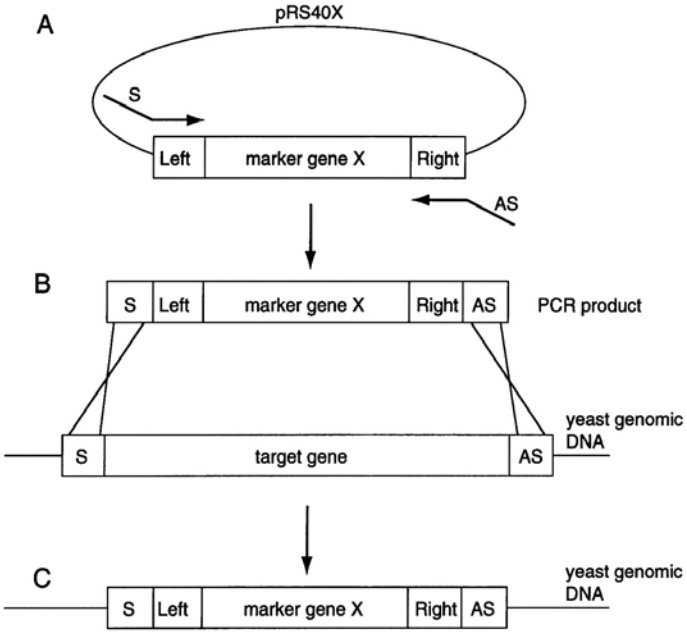

Fig. 11: Cartoon of the design of primers for generating a yeast knock out construct for transformation.

The primer S contains 22 bp of the neomycin gene on it's 3' end. The 5' end of the primer S contains 55 bp of NME1 gene locus specific sequences. The same applies to primer AS that is used as reverse primer. The PCR is performed on plasmid DNA containing the marker gene (neomycin cassette). The purified PCR product was then transformed into a yeast wt strain. With homologous recombination the neomycin cassette replaced the NME1 gene of the yeast genome. From Current Protocols in Molecular Biology, Supplement 39 p. 13.10.5.

rescue the lethal *nme1-Δ* phenotype the NME1 wild type gene that had been cloned into an URA3, CEN plasmid was transformed into the *nme1-Δ* strain. Single colonies were sporulated and dissected as described above. The spores were geno- and phenotyped to determine whether the desired recombination event to replace the endogenous *NME1* gene with a neomycin cassette had occurred.

2.8.3 Sporulation and dissecting of tetrads

A single colony was picked and a patch streak out on an YPD plate was performed prior to incubation for 2 days at 30ºC. A second patch streak out was then carried out on a sporulation plates followed by incubation for 2 days at 30ºC. Cells from the sporulation plates were incubated for 2 – 10 min in zymolyase solution. As shown in Fig. 12 the cells were then dispensed in one single straight line on a YPD-dissecting plate. One tetrad was picked and

the four spores were broken apart and placed separately in one line on the plate and incubated for 2 days at 30ºC. The spores growing on the YPD plate can be picked for further geno- and phenotyping.

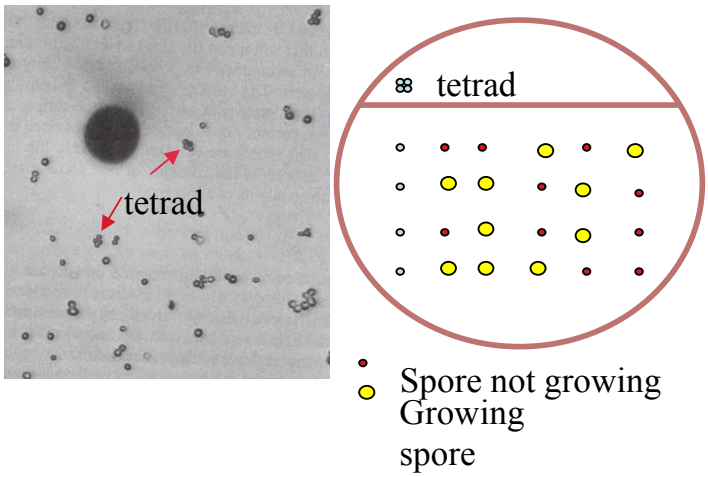

Fig. 12: Schematic of dissecting yeast spores.

Upper panel: Field of a sporulated cultrue. A four-spored cluster (tetrad) is seen to the right of the microneedle tip. The tetrad was picked and transferred to a dissecting plate (from Guide to yeast genetics and Molecular Biology. *Methods in Enzymology*, Vol 194)
Lower panel: Schematic of a dissecting plate. The transferred tetrads were released from the needle in the upper part of the dissecting plate. The four spores building the tetrad were separated in an horizontal line. After incubation at 30 ºC for two days the ratio of growing versus non-growing spores can be determined. If gene is nonessential, 4 spores survive, 2 containing disrupted allele and 2 wt spores. But NME1 is essential, because ko phenotype is lethal.

2.8.4 PI staining of yeast cells for FACS analysis

10^6 yeast cells were centrifuged for 1 min at 10,000 x g at 20ºC. The supernatant was discarded and the cells resuspended in 70% Ethanol and fixed at 4ºC for at least 2 hrs. The cells were then pelleted by centrifugation and resuspended in FACS buffer containing 100 µg/ml RNase A and incubated at 37ºC for 2 hrs. After the RNase A digest the cells were washed with 1 ml 1 x PBS and resuspended in 1 ml PI staining solution for one hour for FACS analysis.

2.8.5 Phloxine B staining of yeast cells for FACS analysis

Yeast cells were grown to logarithmic phase, were diluted 1 : 4, and 20 µg Phloxine B per ml was added. The yeast cells were grown for 4 hrs. 10^6 yeast cells were then centrifuged for 1 min at 10,000 x g at 20ºC. The supernatant was discarded and the cells resuspended in 1 x PBS and directly analyzed with the FACS machine.

2.8.6 Replica plating of yeast cells

To get identical copies of yeast cells growing on plates identical copies of the plates were made by utilizing a replica plating apparatus shown in Figure 13.

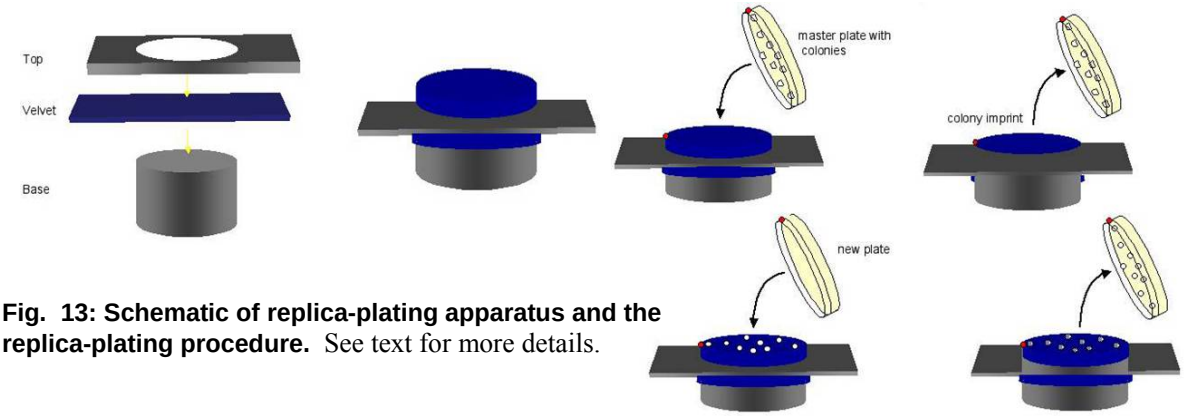

Fig. 13: Schematic of replica-plating apparatus and the replica-plating procedure. See text for more details.

The autoclaved velvet was put on the solid metal block called 'base' and tightened with the top metal plate containing a whole in the middle that has the same size as the base. The master plate with the colonies to be copied was pressed face down on the velvet as illustrated in Fig. 13. A colony imprint was generated on the velvet. A new plate was then pressed face down on the velvet to transfer the colonies to the fresh plate.

2.9 Transfection of adherent cells

Lipofectamine 2000 reagent (Invitrogen Corporation, Carlsbad, CA, USA) was utilized to transfect adherent cells with plasmid DNA. The instructions of the manufactures were slightly altered. The cells to be transfected were grown to a 60 – 70% confluency. Just before transfection the cells were washed with 1 x PBS. For transfection in 6 well plates 800 µl of OPTI-MEM medium (Invitrogen Corporation, Carlsbad, CA, USA) was added to each well and the plates were incubated at 37ºC, 5% CO_2 until the transfection reagents were mixed together. 0.5 to 4 µg of expression plasmid, 0.5 µg reporter plasmid, 0.2 µg CMV-βgal plasmid and 6 µl Plus reagent (Invitrogen Corporation, Carlsbad, CA, USA) for each well were mixed with 100 µl OPTI-MEM medium and incubated at RT for 15 min. Then 4 µl lipofectamine diluted in 100 µl OPTI-MEM were added and incubated at RT for 30 min. After incubation, 200 µl of the transfection mix were added to each well already containing 800 µl OPTI-MEM medium. After 4 hrs of transfection 4 ml of DMEM medium was added

to each well. The cells were harvested 24 to 48 hrs after transfection for luciferase (2.10) and β-gal assays (2.11).

2.10 Firefly luciferase assay in extracts prepared from transfected cells

The luciferase assay described by Wood et al. (Wood, Kao, Gordon and Ridgway 1989) and Brasier et al. (Brasier, Tate and Habener 1989) was slightly altered. 24 to 48 hour after transfection the monolayer of transfected cells was washed twice with 3 ml cold 1 x PBS to obtain a calcium free cell extract, because luciferase is inhibited by only small traces of calcium. 300 µl cold lysis solution (Applied Biosystems, Bedford, MA, USA)/ 50 cm^2 were added and the monolayer scraped with a rubber policeman. The cells were lysed by freezing-thawing three times and vortexing the extracts in between. The remaining cell debris was pelleted by centrifugation at 14,000 rpm for 5 min at 4ºC and the clear supernatant was transferred into a 1.5 ml reaction tube. The cell extract was stored at – 80ºC until the luciferase assay was performed. 300 µl of reaction buffer on ice was added to each assay glass tube. The injector of the luminometer was filled with luciferin solution. Just before the measurement of luciferase activity 50 µl of the cell extract was added to the tube containing the reaction buffer, briefly vortexed and placed into the machine. If the luciferase assay was used to determine the transfection efficiency only 2 µl of the cell extract were mixed with the reaction buffer.

2.11 X-gal assays

2.11.1 X-gal assay from cell extracts prepared from transfected cells.

After the firefly luciferase assay (see 2.10) the β-galactosidase assay was performed. The same cell extract prepared in 2.10 was used for the β-gal assay. 100 µl reaction buffer, 1 µl substrate (Applied Biosystems, Bedford, MA, USA) and 50 µl samples were added to an assay glass tube and briefly vortexed. After a 30 min incubation at 20ºC the samples were measured with a luminometer, whose injector had been filled with accelerator (Applied Biosystems, Bedford, MA, USA).

2.11.2 X-gal staining of lacZ positive newborn mice

The skin of the newborn mice was removed from the body. A little piece of the skin was saved for isolating genomic DNA (see 2.1.3) for genotyping. Then the embryos were rinsed twice with 8 ml 1 x PBS by rotating at 20ºC. After adding 8 ml fixative and rotating for 30 min they were rinsed three times with 8 ml rinse solution for 30 min on a rotator. Then 8 ml staining solution was added and incubation was performed with rotation at 20ºC overnight. After staining the lacZ positive tissues the embryos were washed once with 1 x PBS and then twice with 70% ethanol and stored at –20ºC until sectioning.

2.12 Labeling of DNA and RNA probes with isotopes

2.12.1 Random primed oligo labeling

Feinberg and Vogelstein (Feinberg and Vogelstein 1983) described a method to label double stranded DNA with random primed oligos. The ALL-IN-ONE™ Random Prime DNA Labeling Mix (Sigma, Saint Louis, MO, USA) was used for labeling and the instructions of the manufacturer were followed exactly. 50 ng of purified template DNA in a volume of 10 µl was denatured for 10 min in boiling water. The lyophilized random prime labeling mix was redissolved with 35 µl of $^1/_4$ x TE-buffer. Then the denatured DNA and 5 µl α-^{32}P-dCTP were added, mixed and incubated at 37ºC for 1 hr. Unincorporated nucleotides were separated from the radioactive labeled DNA with G-50 sephadex columns (Roche, Indianapolis, IN, USA) according to the manufacturer's purification procedure. The labeling efficiency was determined by mixing 1 µl of the purified labeled DNA with 3 ml of scintillation liquid and measuring with a Liquid Scintillation Analyzer (Perkin Elmer, Wellesley, MA, USA).

2.12.2 Endlabeling of chemically synthesized oligos

To label the 5' or 3' end of synthezided oligos that have OH groups on either site, the characteristics of the T4 Polynucleotid Kinase (PNK) was utilized. In the presence of γ-^{32}P ATP PNK transfers the isotope labeled phosphate from the ATP to the 5'-OH end of the chemically synthesized oligo. In a total volume of 50 µl 50 pmol oligo, 5 µl PNK buffer

(Roche, Indianapolis, IN, USA) 20 U of PNK (Roche, Indianapolis, IN, USA) and 5 µl γ-^{32}P-ATP were incubated at 37ºC for 1 h. Unincorporated nucleotides were separated from the radioactive labeled DNA with G-25 sephadex columns (Roche, Indianapolis, IN, USA) according to the manufacturer's purification procedure. The labeling efficiency was determined by mixing 1 µl of the purified labeled oligos with 3 ml of scintillation liquid and measuring with a Liquid Scintillation Analyzer (Perkin Elmer, Wellesley, Ma, USA).

2.12.3 Labeling of *in situ* probes with S^{35}

The transcribed part of the mouse *Rmrp* gene was subcloned into the Xho I site of the pBluescript SK$^-$ vector that contains both a T3 and a T7 promoter sequence on the flanking sides. 50 µg of the plasmid DNA was digested with Not I and used as an antisense probe. An additional 50 µg of the same plasmid was linearized with Kpn I and used as sense probe. Then 50 µg/ml proteinase K was added to digest RNases and other proteins. The DNA was purified by a phenol/chloroform extraction and an isopropanol precipitation. The DNA pellet was dissolved in a concentration of 1 µg/µl in DEPC-treated H_2O. For the *in vitro* transcription reaction 1 µg of linearized plasmid, 1.5 µl transcription buffer (BM), 1.5 µl RNTP mix (20 µM each RNTP), 2 U RNase Inhibitor, 3.75 µl 0.1 M DTT, 5 µl ^{35}S UTP and 0.5 µl of either T3 or T7 polymerase were mixed and incubated for 3 hrs at 37 ºC. Adding 1.7 µl 0.3 M $MgCl_2$ and 2 U DNase I in a total volume of 50 µl and an incubation for 15 min at 37ºC digested the template DNA. To precipitate the labeled transcripts 10 µg t-RNA, 250 µl 4 M NH_4OAc and 1 ml 100% ethanol were added and mixed. An aliquot of 30 µl was taken out and mixed with 3 ml counting fluid to use as reference for the calculation of the labeling efficiency after the purification of the labeled transcripts from un-incorporated ^{35}S UTP. The remaining mixture was precipitated for 5 min on ice, and centrifuged for 10 min at 12,000 x g at 4ºC. The supernatant was discarded and followed by a wash with 70% ethanol. After the RNA pellet was air-dried it was resuspended in 100 µl hybridization mix and 2 µl were transferred into a scintillation vial containing 3 ml counting fluid to determine the labeling efficiency. The remaining probes were immediately frozen at – 20ºC until further use.

2.13 Hybridization techniques

2.13.1 Southern Hybridization

This technique was first described by Southern in 1975 and slightly altered (Southern, 1975). Eight to 15 µg of genomic DNA was separated on a 0.8% agarose gel as described in 2.3.1.1 and then directly transferred to a nylon membrane (Amersham Biosciences, Piscataway, NJ, USA) with 0.5 NaOH for 24 to 48 hrs. The DNA was twice UV crosslinked using the Auto-Crosslink program of the Stratalinker (Stratagene, La Jolla, CA, USA). The nylon membrane was pre-hybridized with Church buffer containing 100 µg/ml salmon sperm DNA for 3 hrs. The pre-hybridization solution was then discarded and replaced with fresh Church buffer containing 10^6 cpm/ml radioactive labeled probe (see 2.12.1) and incubated at 65ºC over night. The unbound and unspecific hybridized probe was washed out with increasing stringency of SSC, 0.1% SDS buffer at 65ºC until the remaining activity measured by a Geiger Müller counter indicated around 50 decompositions/s. The membrane was covered with an X-ray film (Kodak) and exposed for 2 hrs - to 3 days at RT or –80ºC.

2.13.2 Northern Hybridization

2.13.2.1 Northern Hybridization with Agarose gels

15 µg total RNA was separated on a 1.2% agarose gel as described in 2.3.1.2 and then directly transferred to a nylon membrane (BioRad, Hercules, CA, USA) with 0.02 N NaOH for 24 hrs. The RNA was UV crosslinked to the membrane with the Stratalinker (Stratagene, La Jolla, CA, USA). The nylon membrane was pre-hybridized with Church buffer containing 100 µg/ml salmon sperm DNA for 3 hrs. The pre-hybridization solution was then discarded and replaced with fresh Church buffer containing 10^6 cpm/ml radioactive labeled probe (see 2.12.1) and incubated at 68ºC over night. The unbound and unspecific hybridized probe was washed out with increasing stringency of SSC, 0.1% SDS buffer at 68ºC until the remaining activity measured by a Geiger Müller counter indicated around 50 decompositions/s. The membrane was covered with an Kodak X-ray film (Eastman Kodak Company, Rochester, NY, USA) and exposed for 2 to 24 hrs at 20ºC or –80ºC.

2.13.2.2 Northern Hybridization with Polacrylamide gels

10 µg total RNA was separated on a 7 % PAA gel as described in 2.3.1.3 and then directly electroblotted to a nylon membrane (BioRad, Hercules, CA, USA) with a semidry Electroblotter (Owl Separation Systems, Portsmouth, NH, USA) for 1 h at 10 V. The RNA was UV crosslinked to the membrane with the Stratalinker (Stratagene, La Jolla, CA, USA). The nylon membrane was pre-hybridized with Church buffer containing 100 µg/ml salmon sperm DNA for 3 hrs. The pre-hybridization solution was then discarded and replaced with fresh Church buffer containing 10^5 cpm/ml radioactive labeled probe (see 2.12.2) and incubated at 42ºC over night. The unbound oligos were removed by washing the membrane twice with 2 x SSC, 0.1% SDS buffer at 42ºC for 20 min each washing step. The membrane was wrapped in a plastic bag and exposed to a phosphoimager sreen from Molecular Dynamics (GE Healthcare, Piscataway, NJ, USA) over night and then scanned with the Storm860 system from Molecular Dynamics (GE Healthcare, Piscataway, NJ, USA) to visualize the bands.

2.13.3 *In situ* Hybridization

Slides for *in situ* hybridization were prepared as described in 2.15.1. Before slides can be used for hybridization, they have to be deparaffinized and sequentially processed in a TissueTek in situ battery. The slides are washed twice with Histoclear for 10 min, then 3 times for 2 min in 100% ethanol followed by 20 sec washes with 95%, 80%, 70%, 50% and 30% ethanol. The hydrated slides are then incubated for 5 min in 0.9% NaCl, then 5 min in 1 x PBS. The tissue section is then fixed for 20 min in 4% PFA/1x PBS. Proteins are digested with a 5 min proteinase K treatment followed by a 5 min wash in 1 x PBS and again an incubation of 20 min in 4% PFA. The tissue is then acetylated for 3 min and a second time for 7 min, washed with 1 x PBS for 5 min followed by an incubation in 0.9% NaCl solution for a further 5 min. The sections were then dehydrated for 20 s in 30% and 50% ethanol, respectively and then 5 min in 70 % ethanol, followed by 20 s incubations in 80%, 95% and 100% ethanol, respectively. After the slides were air-dried in a dust-and RNase-free area, they were pre-hybridized with 90 µl of hybridization solution containing 10 mM DTT and 250 µM α-S-thio-ATP for 1 hr at 65ºC in a 2 x SSC/50% formamide-moistened chamber. The pre-hybridization solution was replace with 60 µl of the labeled probe generated as described in 2.10.2 and incubated overnight at 65ºC in the same chamber used for pre-

hybridization. Unbound probe was removed by washing with 5 x SSC containing 355 µl β-mercaptoethanol at 65 ºC, followed by a 30 min wash in 200 ml of 2 x SSC/50% formamide containing 700 µl β-mercaptoethanol. The formamide was then removed by 3 washes in 200 ml NTE buffer for 10 min at 37ºC each followed by a 30 min RNAse A/RNase T digest at 37ºC. The RNases were washed off by incubating for 15 min at 37ºC in 200 ml NTE buffer followed by a final wash at 65ºC in 200 ml of 2 x SSC/50% formamide containing 700 µl β-mercaptoethanol. The slides were then dehydrated by a series of incubations as follows: 15 min in 2 x SSC, 15 min 0.1 x SSC, 30 s 30% ethanol in 0.3 M NH_4OAc, 30 s 50% ethanol in 0.3 M NH_4OAc, 30 s 70% ethanol in 0.3 M NH_4OAc, 30 s in 95% ethanol and, 30 s in 100% ethanol. The slides were then autoradiographed overnight with a blue X-ray film. The slides were then treated with an emulsion and dried overnight and then exposed for 4 to 6 days at 4ºC. The slides were allowed to warm up to RT for development and were then immersed for 2 min in developer solution, then dipped in water and fixed for 5 min in fixative. After a 10 min wash in water the slides were stained for 2 min with Hoechst dye that stains nucleic acids and other structural cell components, then rinsed with H_2O for 2 min. After air-drying for several hours the slides were then mounted with coverslips using 55 µl Canada balsam. Three days were required for the cement to solidify before they could be viewed.

2.14 Cell culture techniques

2.14.1 Standard cell culture conditions for of adherent cells

Cells were grown in 150 mm Petri dishes with 10 ml D-MEM (Invitrogen, Carlsbad, CA, USA) supplemented with 5% FBS (ATLANTA biologicals®, Norcross, GA, USA), 100 U/ml Penicillin and 100 µg/ml Streptamycin (Invitrogen, Carsbad, CA, USA) (D-MEM full medium) until a confluency of 80%. Cells were then trypsinized for 3 min with Trypsin/EDTA (Invitrogen, Carlsbad, CA, USA) and 10 ml D-MEM full medium was added and the cells transferred into 4 new 150 mm Petri dishes that already contained 10 ml of D-MEM full medium.

2.14.2 Standard cell culture conditions for EBV transformed lymphoblasts

Lymphoblasts isolated from patient blood were EBV transformed in the Cell Culture Core Facility at Baylor College of Medicine in Houston, TX and cultured with RPMI medium supplemented with 5% FBS (ATLANTA biologicals®, Norcross, GA, USA), 100 U/ml Penicillin and 100 µg/ml Streptamycin (Invitrogen, Carsbad, CA, USA). Fresh medium was added to the cells when the pH indicator in the culture medium turned from red to orange/yellow.

2.14.3 Subcloning ES cells for Mini-Southerns after electroporation and neomycin selection:

The neomycin selective media was aspirated and the plates containing the colonies of interest were washed twice with PBS. Colonies of interest were picked and transferred into a 96-well-U-bottom plate containing 25 µl of trypsin/EDTA solution. After all picked colonies are transferred to the 96-well plate, 25 µl per well of M15 media was added and the colonies were disaggregated by pipetting up-and-down and then transferred to a 96-well feeder plate and grown under selection until the medium turns yellow. At this time the cells are ready for further evaluation of construct integration as described in 2.1 DNA isolation of ES cells and Southern hybridization.

2.15 Histology

2.15.1 Tissue embedding in paraffin

Embryos were harvested at E15.5. After fixation in 4 % paraformaldehyde to preserve histological details and to avoid tissue degradation, the embryos were dehydrated in ascending ethanol concentrations (0.9% NaCl, 30% ethanol/0.9% NaCl, 50% ethanol/0.9% NaCl, 70% ethanol in H_2O, 90% ethanol in H_2O and 100% ethanol for 45 min each). The ethanol was replaced stepwise by xylene with an initial incubation in a mixture of 50% ethanol/50% xylene for 30 min at RT on a rocker followed by a 15 min incubation with xylene alone. The tissue was then embedded in paraffin by replacing the xylene with wax. This was done by incubating in a 50% xylene/50% wax mixture at 58ºC for 30 min followed by three exchanges

of wax for 30 min each at 58ºC. The wax and the tissue were decanted into a weighboat at RT and the embryo is placed so that the cut side faced the bottom of the weighboat. The paraffin block was stored at RT until further use. Just before sectioning the paraffin block was incubated at 4ºC overnight for better sectioning.

2.15.2 Sectioning of paraffin embedded tissue

The tissue was embedded in paraffin as described in 2.15.1. The cold paraffin block was mounted on the microtome and 4 µm slices were cut. The sections were flattened by floating on the surface of a 37ºC warm water bath and then carefully transferred to a glass slide. The slides were dried and the sections glued to the glass surface on a 50ºC heating bench over night. The slides were stored in a slide holder at RT until further use.

2.15.3 Haematoxiline-Eosine staining

Sectioned tissue was deparaffinized with three washes in xylene for 3 min each, followed by two 1 min incubations in absolute ethanol, then two 1 min rinses in 90% ethanol and 80% ethanol, respectively, and a final incubation for 1 min in H_2O (Fig. 14). The nuclei were stained red with Mayer's Haematoxylin for 3 min then rinsed in H_2O. For better contrast the slides were incubated in a weakly alkaline $NaHCO_3$ solution to turn the Haematoxylin staining blue. For counterstaining of basic cytoplasmic proteins slides were washed again in H_2O, then dipped ten times into 80% ethanol and stained for 45 s in eosin. Afterwards the slides were dehydrated with successive 1 min incubations in 80% ethanol, 95% ethanol, four times in 100% ethanol and 3 times in xylene. Stained sections were embedded with TissueTek and overlaid with a cover slide.

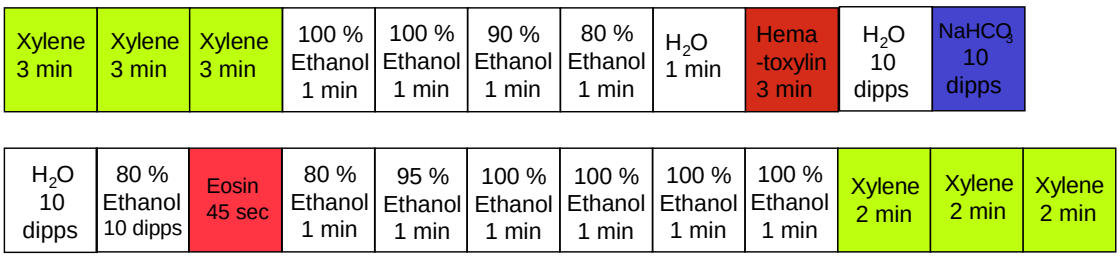

Fig. 14: Schematic of the Haematoxiline-Eosine staining battery.

2.15.4 Nuclear Fast Red staining

Sectioned tissue was deparaffinized with three washes in xylene for 3 min each, followed by two 1 min incubations in absolute ethanol, then two 1 min rinses in 90% ethanol and 80% ethanol, respectively, and a final incubation for 1 min in H_2O (Fig. 15). The nuclei were stained red with Nuclear Fast Red for 3 min then rinsed in H_2O. Afterwards the slides were dehydrated with successive 1 min incubations in 80% ethanol, 95% ethanol, four times in 100% ethanol and 3 times 2 min in xylene. Stained sections were embedded with TissueTek and overlaid with a cover slide.

Xylene 3 min	Xylene 3 min	Xylene 3 min	100 % Ethanol 1 min	100 % Ethanol 1 min	95 % Ethanol 1 min	80 % Ethanol 1 min	Nuclear Fast Red 3 min	H_2O 10 dipps

80 % Ethanol 1 min	95 % Ethanol 1 min	100 % Ethanol 1 min	100 % Ethanol 1 min	100 % Ethanol 1 min	100 % Ethanol 1 min	Xylene 2 min	Xylene 2 min	Xylene 2 min

Fig. 15: Schematic of the Nuclear Fast Red staining battery.

2.16 Microarray Analysis of CHH patient RNA compared to control RNA

To identify genes that are differentially expressed in CHH patients compared to control subjects a microarray analysis was performed. The total RNA from two patients was isolated as described in 2.2.2. The quality and the concentration of the RNA were determined using an Agilent 2100 Bioanalyzer. The HG-U133A and the HG-U133B oligonucleotide arrays from Affymetrix were selected for the microarray analysis. The labeling, hybridization, scanning and the processing of technical replicates of the microarray chips were done in the micro array core facility at Baylor College of Medicine in Houston, TX. The signals of the chips were normalized using RMA (Robust Multi-array Analysis) included as part of the statistical analysis package, Bioconductor
http://128.32.135.2/users/bolstad/ComputeRMAFAQ/ComputeRMAFAQ.html
An appropriate design matrix was created to properly define the samples and their replicates that would be used to fit a linear model for further analysis. An annotated gene or gene ontology list was generated using Affymetrix's web site at

http://www.affymetrix.com/index.affx. The list of up- and down-regulated genes was created with Limma at http://bioinf.wehi.edu.au/l.imma/ and filtered in Excel.

2.17 Establishing a transgenic mouse line

The founders of a transgenic mouse line are mosaic. The degree of mosaicsim depends on the time when the transgene has been integrated into the genome. The earlier it has been integrated the more cells will carry the transgene while the later this event occurs the fewer cells will have the transgene. In order to establish a transgenic mouse line each founder is crossed back to a wild-type mouse of the same strain. The pups resulting from this breeding are called the R1 generation. Each of these pups can differ with respect to transgene expression level. Some pups of the R1 generation might be negative for the transgne. All R1 carrying the transgene are again crossed back to a wild-type mouse of the same strain. The pups from this breeding are the R2 generation. These pups are now equal (only true for each separate mating) in transgene expression levels, so that the R2 mice can be intercrossed. The resulting F1 generation follows Mendelian distribution of the genotypes. The expected genotypes include wild-type mice not carrying a transgene, mice that are heterozygous for the transgene and mice that are homozygous for the transgene. To identify the mice that are homozygous for the transgene the F1 are backcrossed to wild-type mice of the same strain. If the F1 mice are homozygous, all offspring will carry the transgene. The F1 mice whose breeding results in offspring that are positive and negative for the transgene are heterozygous for the transgene. Homozygous F1 mice are intercrossed by brother and sister mating in the following generations to maintain the line (Fig. 16 – see next page).

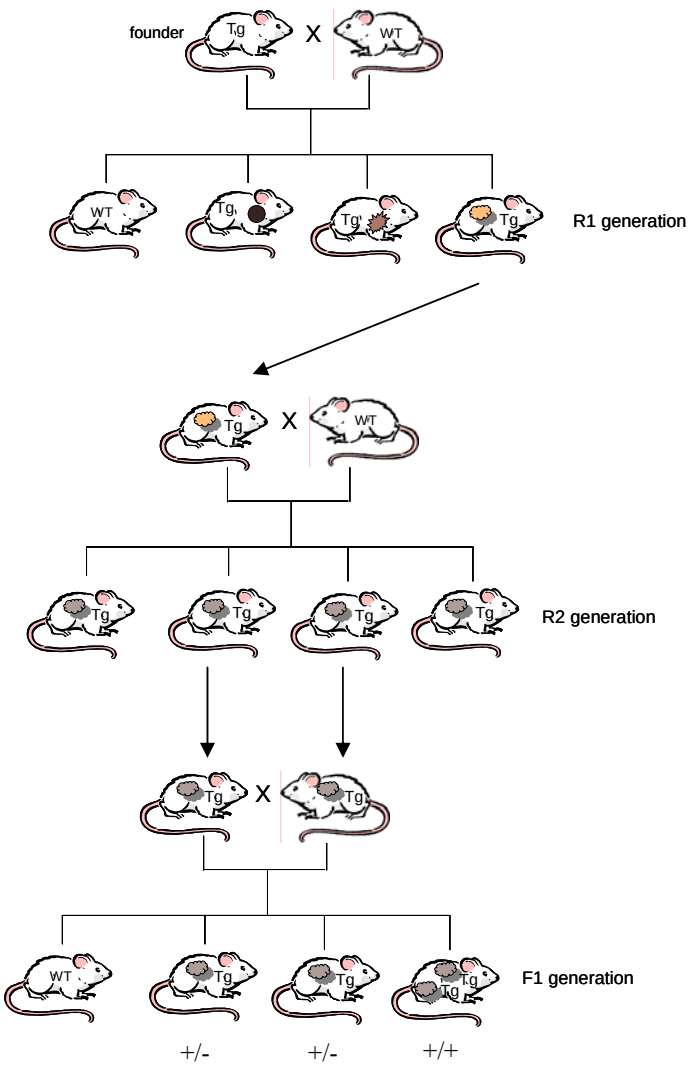

Fig. 16: Schematic of establishing a transgenic mouse line.

A transgenic founder is backcrossed with a WT mouse of the same strain. The pups of the R1 generation are then again backcrossed to a WT mouse of the same strain. The following R2 generation is then intercrossed. The F1 generation follows Mendelian distribution of WT, herterozygous transgenics and homozygous transgenics. The homozygous transgenics are intercrossed to establish and maintain the transgenic mouse line. Tg: transgenic; WT: wild type. The pattern in the different mice illustrates the different distribution of transgene expression levels; +/- heterozygous for transgene; +/+ homozygous for the transgene

Materials

2.18.1 Solutions

5 x 1st strand synthesis buffer	250 mM Tris-Hcl, pH 8.3 375 mM KCl 15 mM $MgCl_2$
AE buffer	50 mM Na acetate, pH5.3 10 mM EDTA, pH 8.0
Agar plates	15 g Agar-Agar in 1000 ml LB-medium
Blue-Dye DNA Loading Buffer	0.25 % bromphenolblue 0.25 % xylene cyanol 40 % sucrose
Church-Buffer	1 mM EDTA, pH 8.0 0.5 M $NaHPO_4$, pH 7.2 7 % SDS 1 % BSA
Dropout liquid media	0.5 % ammonium sulfate 0.17 % yeast nitrogen base 0.13 % drop out powder 2 % glucose
Fixative	0.1 M Na-phosphate buffer, pH 7.3 0.2 % glutaraldehyde 2 % formalin 5mM EGTA, pH 7.3 2 mM $MgCl_2$
2 x FM medium for freezing bacteria	65 % glycerin 0.1 M $MgSO_4$ 25 mM Tris-HCl, pH 8.0
Glyoxal reaction buffer	1 M Glyoxal, pH 7.0 50 % DMSO 10 mM $NaPO_4$ buffer, pH 6.8

In situ hybridization solution	50 % deionized Formamide 0.3 M NaCl 20 mM Tris-HCl, pH 8.0 5 mM EDTA, pH 8.0 10 % dextran sulfate 0.02 % Ficoll 0.02 % BSA 0.02 % Polyvinylprolidone 0.5 mg/ml bakers yeast RNA
LB- medium	1 % tryptone 0.17 M NaCl 0.5 % yeast extract solve in 1000 ml DW, pH 7.5
-leu/5FOA plates	0.17 % yeast nitrogen base 0.5 % ammonium sulfate 2 % glucose 0.13 % -leu/-ura drop out powder 12 mg/l uracil 0.75 mg/l 5-FOA 2 % agar Store plates at 4 ºC
-leu/low ade dropout liquid media	0.5 % ammonium sulfate 0.17 % yeast nitrogen base 0.13 % -leu/-ade dropout powder 2 % glucose 6 mg/l adenine
Luciferin solution	1 mM luciferin in reaction buffer
5 x NTE	0.5 M NaCl 10 mM Tris 25 mM EDTA
Orange G	0.35 % Orange G 30 % sucrose
1 x PBS	120 mM NaCl 2.7 mM KCl 10 mM potassium buffer, pH 7.4
10 x PCR buffer	500 mM KCl 100 mM Tris-Hcl, pH 8.3 0.1 % gelatine 15 mM $MgCl_2$
PI staining solution	50 µg/ml PI in 1 x PBS

Reaction buffer	0.1 M potassium phosphate buffer, pH 7.8 5 mM ATP 15 mM $MgSO_4$
Rinse solution	0.1 M Na-Phosphate buffer, pH 7.3 2 mM $MgCl_2$ 0.1 % Na-deoxycholate 0.2 % NP-40
RNA loading dye	0.15 % Bromphenolblue 0.15 % Xylenecyanol 75 % glycerol
Solution I	50 mM glucose 25 mM Tris-HCl, pH 8.0 10 mM EDTA, pH 8.0 250 µg/ml RNase A lysozyme
Solution II	0.2 N NaOH 1 % SDS
Solution III	1 M Na-acetate, pH 4.8
1 x SSC	0.15 M NaCl 15 mM sodium citrate, pH 7.0
Staining solution	80 mM Na_2PO_4 20 mM NaH_2PO_4 1.3 mM $MgCl_2$ 3mM $K_3Fe(CN)_6$ 3mM$K_4Fe(CN)_6 \bullet 3\ H_2O$ 1 mg X-gal /ml
1 x TAE buffer	0.1 M Tris base 0.1 M acetic acid 1 mM EDTA, pH 8.0
1 x TBE buffer	90 mM Tris base 90 mM boric acid 1.25 mM EDTA, pH 8.3
1 x TE buffer	10 mM Tris-HCl, pH 8.0 1 mM EDTA
Yeast plates	2 % agar in 1 x dropout liquid medium

2.18.2 Kits

x-gal assay	Galacto-Light Plus™ Systems Applied Biosystems, Bedford MA, USA
Plasmid Mini/Midi isolation kit	QIAGEN, Valencia CA, USA
Gel extraction Kit	QIAGEN, Valencia CA, USA
PCR purification Kit	Mo Bio Laboratories Inc., Solana Beach CA, USA
Yeast plasmid isolation kit	GenoTech, St. Louis MO, USA
RNA isolation kit	Gentra, Minneapolis MN, USA
Genomic DNA from blood kit	Gentra, Minneapolis MN, USA

2.18.3 Bacteria strains

SMR4700: recA::Tn10dCAM, sbcC201, hsdrK-, mK+, phoR::Tn10, recA::TN10dCAM, F^-, thi, thr, leu

DH5α: F-, endA1, hsdR17, (r_k^-, m_k^+), supE44, thi-1, Lambda-, recA1, gyrA96, relA1, 80dlacZdeltaM15

XL1-Blue: recA1, endA1, gyrA96, thi-1, hsdR17, supE44, elA1, lac, (F'proAB, $lacI^qZ\Delta M15$, $TN10(tet^r)$

2.18.4 Yeast strains

YPH275: *MAT***a**/*MAT*α, *ura3-52*, *lys2-80*, *ade2-101*, *trp1-Δ1*, *his3-Δ200*, *leu2-Δ1*, CF [TRP1, SUP11, CEN4] (Source: Peter Hieter)

TLG119: Mat a/alpha ade2-1/ade2-1 ura3-52/ura3-52 leu2-3,112/leu2-3,112 LYS2/lys2-1 his3/his3 cce1::HIS3/cce1::HIS3 trp1Δ-1/trp1Δ-1 nme1Δ2::TRP1/nme1Δ2::TRP1 pMES127[URA3 NME1 CEN]

2.18.5 Enzymes, and isotopes

[α^{32}P] dCTP	Valeant, Costa Mesa CA, USA
[γ^{32}P] ATP	Valeant, Costa Mesa CA, USA
[α^{35}S] UTP	Valeant, Costa Mesa CA, USA
Alkaline phosphatase	Roche, Indianapolis IN, USA

Klenow-DNA Polymerase	Roche, Indianapolis IN, USA
Restriction enzymes	Roche, Indianapolis IN, USA, New England Biolabs, Beverly MA, USA
Reverse Transkriptase	Invitrogen, Carlsbad CA, USA
T4-DNA polymerase	Roche, Indianapolis IN, USA
T4-Polynucleotid Kinase	Roche, Indianapolis IN, USA
Taq-DNA Polymerase	Perkin Elmer, Wellesley MA, USA

2.18.6 Molecular Weight Markers

100 bp ladder	New England Biolabs, Beverly MA, USA
λ/Hind III	Roche, Indianapolis IN, USA
Hyperladder II™	Bioline, Canton MA, USA
Huperladder V™	Bioline, Canton MA, USA
Marker X	Roche, Indianapolis IN, USA

2.18.7 Primers

2.18.7.1 Human primer

2.18.7.1.1 RMRP primer

RMRP2	5'-GAAGCGGTCCGGCATTGGCCG-3'
RMRP4	5'-CAACTACTTGGGAGCCTGAGG-3'
RMRP5	5'-GAGCTCGAGGTTCGTGCTGAAGGCCTGTATC-3'
RMRP6	5'-GAACTCGAGACAGCCGCGCTGAGAATGAGCC-3'
RMRP8-Eco RI	5'-GAATTCGATACAGGCCTTCAGCACGAACC-3'
RMRP9-Cla I	5'-ATCGATGTCTTGTTCTTGGTACCCTGG-3'
RMRP14-Cla I	5'-ATCGATCGGTGCCGAAGCGGTCCGG-3'

2.18.7.1.2 RPS19 primer

RPS19-ex1-F3	5'-CCCTGTCACAGTTCCGCCC-3'
RPS19-ex1-R3	5'-CAGGCACGCGCTCTGAGG-3'
RPS19-ex2-F	5'-GGGTACCACGGTTTAGGATG-3'
RPS19-ex2-R	5'-GGGAAAAGCACGATTCAGTC-3'
RPS19-ex3-F	5'-TGGGGACTGAGGTTCAAAAC-3'
RPS19-ex3-R	5'-AGGGTTTCTCTCCCTCTTGG-3'
RPS19-ex4-F	5'-GGAGATGGTCACAGCTAGGC-3'
RPS19-ex4-R	5'-TGGGCTAGTCAGCCAGAGAG-3'
RPS19-ex5-F	5'-ATGCTTGCACAAACAACACC-3'
RPS19-ex5-R	5'-AGCAGCACCAACAGGAAAAG-3'
RPS19-ex6-F	5'-AGACCCAGTTTCCACGTCTG-3'
RPS19-ex6-R	5'-CAGCCATCCTTTCGTTTCTC-3'

2.18.7.1.3 Type X Kollagen (COL10A1) primer

COL10A1-ex1F	5'-CCCGATCTTGTGTGCCTACCC-3'
COL10A1-ex1R	5'-GGACTATCATCCACAGACTGATG-3'
COL10A1-2.2F	5'-ACTGTATAAAGAACTCATCTGTG-3'
COL10A-2.2R	5'-TGGGCTAATTCAGAAGTTGGA-3'
COL10A-3F	5'-ATGTCACTAACCATCCCCTTC-3'
COL10A-3R1	5'-TGTTCCTGGAATCCCTGGCTG-3'
COL10A1-3F1	5'-GGAGAAATGGGACCAATTGGC-3'
COL10A1-3R3	5'-ACCCTCAGGCATGACTGCTTG-3'
GW627	5'-GCTGGCATAGCAACTAAGGGCCTC-3'
GW628	5'-TGTAGGGTGGGGTAGAGTTAGAG-3'

2.18.7.1.4 IL8 primer

NotI-hIL8 Start F	5'-ATAAGAATGCGGCCGCATGACTTCCAAGCTGGCC-3'
End hIL8 Not I R	5'-ATAAGAATGCGGCCGCTTATGAATTCTCAGCCCT-3'
IL8-251-F	5'-GGCTGGCTTATCTTCACC-3'
IL8-251-R	5'-CCTGAGTCATCACACTTCC-3'
IL8-781-F	5'-GGAGAGTCTTAGCTTGCCTAC-3'
IL8-781-R	5'-CAGGCACAGCTCTGCCAGCTAC-3'

2.18.7.1.5 SBDS primer

ex1 F	5'-GCGAGCATCCTGTCAGAGC-3'
ex1 R	5'-GGGCTACTGAGATCTATGACACC-3'
ex2 F	5'-GCAAATGGTAAGGCAAATACG-3'
ex2 R	5'-TCTGATTTCAGGAGGTTTTGG-3'
ex3 F	5'-GGGCAAAGCTCAAACCATTA-3'
ex3 R	5'-CCAGCCTGGGCAATAGAGTA-3'
SDS4F	5'-CCTAAGAAACCATTACCTAATCCAA -3'
SDS4R	5'-GGCAGGAGAATGGCGTGT-3'
ex 5 F	5'-ATTGTGCTTGCCTCAAAGGA-3'
ex 5 R	5'-GGCAGACCACAGACATGAAA-3'

2.18.7.1.6 pre-ribosomal processing

5.8S-mature	5'-CATTAATTCTCGCAGCTAGCGCTGCGTTCTTCATCGACGC-3'
5'-ETS terminal	5'-CTGACACGCTGTCCTCTGGCGA-3'
5'-ETS internal	5'-CCTTGGGGACCGGGTCGGTGGCGC-3'
18S mature	5'-CATGCATGTCTAAGTACGCACG-3'
ITS 1 - 3' end	5'-GTCGTCGGGAGCGCCCTCGCCAAATCGACCT-3'
ITS 2 - 5' end	5'-CCGGGGGTGCCTCCGGGCTCCTCGGGGTGCG-3'
ITS 2 - 3' end	5'-CCCCTCGCCGGGCCCGTCTCCCGACGAGCGTG-3'
28 S mature	5'-TATTAGTCAGCGGAGGAGAAGA-3'

2.18.7.1.7 Quantitative Real-Time PCR primer

IL8-2-F1	5'-ACA GCA GAG CAC ACA AG-3'
IL8-2-R1	5'-CTA CAA CAG ACC CAC ACA A-3'
PBDG-1-F	5'-TGC AAC GGC GGA AGA AAA CA-3'
PBDG-1-R	5'-AGA TGG CTC CGA TGG-3'
HUHPRT-F1	5'-ATT GAC ACT GGC AAA ACA ATG C-3'
HUHPRT-R1	5'-TCC AAC ACT TCG TGG GGT CC-3'
HUCCR3-1F	5'-CTT CCT CGT CAC CCT TC-3'
HUCCR3-2R	5'-ACG ATG CTG GTG ATG AC-3'
HUSTAT1-1F	5'-TAA TCA GGC TCA GTC GGG-3'
HUSTAT1-1R	5'-TCG TGT TCT CTG TTC TGC-3'
HUPF4V1-1F	5'-GAT GCT GTT CTT GGC GTT
HUPF4V1-1R	5'-GGC TAT GAG TTG GGC AGT
HUCD9-1-F	5'-GAT TGC TGT CCT TGC CAT TG-3'
HUCD9-2-R2	5'-TAT CAC CAA GAG GAA GCC GA-3'
HUIER3-1F	5'-CAC TTT CCT CCA GCA ACA-3'
HUIER3-2R	5'-TCT CCG CTG TAG TGT TCT-3'

2.18.7.2 Mouse primer

2.18.7.2.1 Rmrp primer

ASC I-PH2	5'-GAGGGCGCGCCCTGGAGCTCTCTGTCCAGTCCC-3'
Sal I-PH8	5'-CACGTCGACCCCTGAGTTAGTGTCACGGGACCAG-3'
Nhe I-PH9	5'-GCTGCTAGCCTTAGTGTCTGATGTAAGTGGGG-3'
Sac II-PH10	5'-ACTCCGCGGGCCTAGTCACTTGTTGCTAGGGG-3'
5' probe F	5'-GGCTTGCGCTTTTACTGTTC-3'
5' probe R	5'-CCCTCCTTAACCTGGGACTC -3'
3' probe F	5'-ATGCCTCCACAACAAACAGTC-3'
3' probe R	5'-CAGCCAGAACACCTGTACCAT-3'

2.18.7.2.2 G0s2 primer

Not I G0s2 Start F	5'-ATAAGAATGCGGCCGCATGGAAAGTGTGCAGGAG-3'
End G0s2 Not I R	5'-ATAAGAATGCGGCCGCTTAAGAGGCGTGCTGCCG-3'

2.18.7.3 Yeast NME1 primer

NME1-3	5'-CAACTAAAGTTTGAGAGGGC-3'
NME1-5	5'-CTCAGAGCTTGACTCTGTTGC-3'
124C->T-f	5'-CTCATTAAGGAGGATGTCCTTGGGTATTCTGCTTC-3'
124C->T-r	5'-GAAGCAGAATACCCAAGGACATCCTCCTTAATGAG-3'
180g->A-f	5'-CTCTATTGCAGGGTACTAGTGTTTTCTTCGGTAC-3'
180g->A-r	5'-GTACCGAAGAAAACACTAGTACCCTGCAATAGAG-3'
211del-f	5'-GGAATCTAAACCATAGTTGACGATTGCTCTTTCCCG-3'
211del-r	5'-CGGGAAAGAGCAATCGTCAACTATGGTTTAGATTCC-3'
262g->T-f	5'-CTTACTATTCTTGGTCCATTGATTCACCCCTTTTTATTTT-3'
262g->T-r	5'-AAAATAAAAAGGGGTGAATCAATGGACCAAGAATAGTAAG-3'

2.18.7.4 general vector primer

T3A	5'-ATTAACCCTCACTAAAGGG-3'
T7A	5'-AATACGACTCACTATAGGG-3'
SP6	5'-GATTTAGGTGACACTATAG-3'
M13UNI	5'-GTAAAACGACGGCCAGT-3'
M13REV	5'-AACAGCTATGACCATG-3'

2.18.7.5 RNAi Oligos

luc-F	5'-/5Phos/AGCTTGGATTCCAATTCAGCGGGAGCCACCTGATGAAGC TTGATCGGGTGGCTCTCGCTGAGTTGGAATCCATTTTTTG-3'
luc-R	5'-/5Phos/GATCCAAAAAATGGATTCCAACTCAGCGAGAGCCACCCG ATCAAGCTTCATCAGGTGGCTCCCGCTGAATTGGAATCCA-3'

2.18.7.6 Genotyping primer

WPRE-F	5'-TCTCTTTATGAGGAGTTGTGGCCC-3'
WPRE-R	5'-CGACAACACCACGGAATTGTCAGT-3'
Col2a2-F	5'-GGTCCAGCCCGAGCTACTTCTTTAG-3'
Col2-R	5'-AGGGTGACAGAAGGCACAAC-3'
Col10-F	5'-GTAGGACTGTTGTGTGAGTGG-3'
Col10-R	5'-CCAACATGAGGGCAGCAGTTC-3'
Tyr-F	5'-CAAAGACGACTACCACAGCTTGC-3'

2.18.8 Chemicals

Acitic-acid	Fisher Scientific, Fair Lawn NJ, USA
Acrylamide	Biorad, Hercules CA, USA
Agar-agar	USB corporation, Cleveland OH, USA
Agarose	GeneMate, Bioexpress, Kaysville UT, USA
Ecoscint	national diagnostics, Atlanta GO, USA
Ethanol	AAPER Alcohol and Chemical Co, Shelbyville KY, USA
5FOA	Toronto Research Chemicals Inc., North York ON, Canada
Formaldehyde	Fisher Scientific, Fair Lawn NJ, USA
Formamide	Fisher Scientific, Fair Lawn NJ, USA
Hydrochloric acid	J.T. Baker, Phillipsburg NJ, USA
LB Broth	Molecular Biology Laboratories, Solana Beach, CA, USA
Lipofectamine 2000	Invitrogen. Carlsbad CA, USA
D-Luciferin Sodium Salt	BD Biosciences, Franklin Lakes NJ, USA
Methanol	VWR, West Chaster PA, USA
Potassium ferrocyanide	J.T. Baker, Phillipsburg NJ, USA
Sodium pyrophosphate	Fisher Scientific, Fair Lawn NJ, USA
Tryptone	Becton Dickinson and Co, Spraks MD, USA

Xylene	Fisher Scientific, Fair Lawn NJ, USA
Yeast extract	Difco, Becton Dickinson, Sparks MD, USA

All chemicals not listed here were purchased from Amresco, EM Science or Sigma.

2.18.9 Equipment

Bacteria incubator	ORPITAL Incubator Shaker, Gyromax™737 Amerex Instruments Inc., Lafayette CA, USA
Balances	sartorius BP121 S, Goettingen, Germany sartorius LP6200, Goettingen, Germany
Cell culture incubators	CO_2 water jacked incubator series II Thermo Forma Scientific, Woburn MA, USA
Centrifuges	Avanti™ J-25 I, Beckman, Fullerton CA, USA
	eppendorf centrifuge 5415 C Brinkmann Instruments, Hamburg, Germany
	eppendorf centrifuge 5417R Brinkmann Instruments, Hamburg, Germany
	eppendorf centrifuge 5810R Brinkmann Instruments, Hamburg, Germany
	Z233M-2, HERMLE Labortechnik, Wehingen, Germany
	Z233MK-2, HERMLE Labortechnik, Wehingen, Germany
DNA sequencing machine	ABI PRISM™ 377, Applied Biosystems, Foster City CA, USA
Electrophoretic apparatus	Dual Vertical Slab Gel System, cat#DSG-250-02 CBS Scientific Company, Inc., Del Mar CA, USA
Electroblotter	Panther™ Semidry Electroblotter Model HEP-1, #17494 Owl Separation Systems, Portsmouth NH, USA
FACS	Beckman-coulter EPICS XL-MCL, Fullerton CA, USA
Gel imaging system	AlphaImager™2200, Alpha Innotech, San Leandro CA, USA
Hybridization oven	Hybridiser HB-1D, TECHNE, Duxford Cambridge, U.K.
γ-irradiator	Gammacell 1000 Model C with 3 Pencils MDS Nordion, Ottawa ON, Canada
Liquid Scintillation Analyzer	Tri-Carb 2100 TR, Packard Perkin Elmer, Wellesley MA, USA

Luminometer	Lumat LB 9501 EG&G Berthold, Bad Wildbad, Germany
Magnetic stirrer	Corning Stirrer/Hot Plate, Corning Incorporated Life Sciences, Acton MA, USA
Microscopes	Axioplan 2, Zeiss, Jena, Germany
	EXLIPSE TS100, Nikon, Japan
	SMZ150, Nikon, Japan
PCR machine	MJ Research, PTC-200, Watertown MA, USA
pH meter	Corning pH meter 430, Corning Incorporated Life Sciences, Acton MA, USA
Phosphoimager	Molecular Dynamics Storm 860, GE Healthcare Piscataway NJ, USA
Phosphor Screens	Molecular Dynamics, GE Healthcare Piscataway NJ, USA
Power supply	Model PowerPac HC, cat.#164-5052 BioRad, Hercules CA, USA
Safety carbinet	NU-437-400 series 2, class II type A/B3 Nuaire™Plymouth MN, USA
Spectrophometer	GeneQuant II, Pharmacia Biotech, Amersham Biosciences, Piscataway NJ, USA
UV-crosslinker	Stratalinker®2400, Stratagene, La Jolla CA, USA
Waterbath	Isotemp 215, Fisher Scientific, Fair Lawn NJ, USA
	HAAKE B3, Karlsruhe, Germany

2.17.10 Miscellaneous materials

Cell culture material	Costar, Corning Incorporated Life Sciences Acton MA, USA
Coverslips	Fisher Scientific, Fair Lawn NJ, USA
Human tissue Comb A northern blot	RNWAY Laboratories Inc. Kangnam-gu, Seoul, Korea
Nylon membrane (Hybond™-N+)	Amersham Biosciences, Piscataway NJ, USA
Superfrost plus slides	Fisher Scientific, Fair Lawn NJ, USA
X-ray films (Hyperfilm™-MP)	Amersham Biosciences, Piscataway NJ, USA

3 Results

3.1 Clinical Studies

3.1.1 Subjects

All DNAs referred to the lab were assigned a number irrespective of whether it was a patient sample for confirmation of CHH or exclusion of CHH or whether it was a sample of a parent. Thirty-five patients have been recruited to this study; 26 patients for confirmation of CHH and 9 patients for exclusion of CHH. In the 21 males and 14 females the clinical diagnosis had been made or suspected by the referring physician on the basis of significant shortness of stature. In most, deficient growth of scalp hair had been noticed. Radiographs taken at variable times in the patients' natural course had revealed metaphyseal chondrodysplasia. For each patient a sample of peripheral blood was made available for isolation of DNA and molecular confirmation or exclusion of mutations in the *RMRP* gene.

The group of patients was heterogeneous in several respects. The nationality of 12 patients was German, including one pair of sibs and Belgian in another set of sibs as well as 2 more patients from Belgium for exclusion of CHH. Sixteen patients were US citizens, 6 of them being of Hispanic, 10 of Caucasian extraction. Two patients were from Finland (studied by Dr. Outi Mäkitie and therefore excluded from the following clinical study) and 1 patient was from Australia. The age of the patients at the time of the molecular study ranged from 7 months to 32 7/12 years. The exact age at the time of diagnosis could not be determined in several instances. However in nearly all cases CHH was proposed as the diagnosis before or in early childhood.

The clinical and radiographic data were evaluated before the results of the *RMRP* gene mutation screening were available. After reviewing the available clinical data 27 patients of the cohort were included in the clinical study and are further discussed in the following paragraphs. The eight other patients with dwarfism due to skeletal dysplasia, in particular the ones with metaphyseal osteochondrodysplasias other than CHH however were included in the molecular screening study as control subjects.

3.1.2 Clinical Phenotype

All clinical data presented in Table 1 were retrospectively obtained from the clinical records made available with the patients' and/or parents' informed consent or by physical examination of the patients by physicians at Texas Children's Hospital in Houston, TX. Where required and feasible the families were contacted anew by telephone for collection of additional data. To this end a specifically designed questionnaire was used (see appendix 8.2). The referral pattern was different for the European and the American patients. The former had been referred initially by their physicians to colleagues in the regional University Pediatrics Department, with considerable expertise in the nosological diagnosis of osteochondrodysplasias. The blood sample with request for molecular confirmation of the clinical diagnosis was submitted from the latter centers to the laboratory. In contrast, the study samples from most of the US patients were submitted by their local pediatricians.

For systematic gathering of the relevant patient data and presentation in tabular form, the clinical case definition of CHH by Dr. Jürgen Spranger (Spranger et al., 2002) was adopted. These criteria are the result of extensive personal experience with the osteochondrodysplasias in general and CHH in particular. In addition they are based on the clinical data in seminal and original reports on many CHH patients (McKusick et al., 1965; Mäkitie et al., 1992; Mäkitie & Kaitila, 1993; Mäkitie et al., 1995; Mäkitie et al., 1998).

In Table 1 the clinical data for the 27 patients included in this study are tabulated. The radiographic findings in the patients are presented in Table 2. In the body of either table any column represents a single criterium within the CHH definition (Spranger et al., 2002). The results of the mutation screen of the CHH patients are shown in Table 3.

The first and foremost result of this retrospective clinical study is the sobering observation of extensive lack of information regarding some or several criteria in many patients even after repeated and effective new contacts with several of the families involved. There were no data on recumbent length at birth (BL) in as many as 6 of the 27 patients. In 5 patients in the cohort born prematurely, corrections to full term birth were introduced. BL plotted on reference growth curves was below p3 in 9 and near or at p3 in 2 more patients. BL was within normal limits in the remaining 10 subjects (#1, 8-11, 13-16, 26) ranging downward from the high value of p90 (patient # 10) to between p3-P10. It is of interest that, except for

Table 1: Features in Patients with clinical diagnosis of Cartilage-Hair Hypoplasia

Patinets			Growth & Skeletal								Other Systems							
#	S	Age (years)	BL (cm)	Gr.	Sta	J	K	Elb.	H,F	Fi	sH	Inf.	Va.	RBC	Imm		GI	
															Hum	Cel	Hir.	Mal
1	M	7 1/12	49	++	+	()	var	+	+	+	+	+	()	-	Ig	T	-	++
2*	M	8 1/12	43	++	+	-	val	+	+	-	-	-	()	-	-	-	+	+
3	M	32 7/12	44	++	+	+	val	()	+	-	+	-	()	-	()	()	-	-
4	M	6 10/12	44	++	+	()	var	()	()	()	+	()	()	()	()	()	()	()
5	M	()	()	()	()	()	()	()	()	()	()	()	()	()	()	()	()	()
6	M	14 4/12	()	++	+	()	val	+	+	()	+	+/-	()	-	()	()	()	+
7	M	2 10/12	()	()	+	+	()	()	+	()	+	++	()	+	Ig	T	()	+
8	F	14 10/12	48	++	+	-	var	+	+	+	+	_	()	()	-	-	-	-
9	F	5 4/12	45.5 [3]	+	+	+	()	+	+	()	+	+/-	()	()	()	()	-	-
10	M	13 1/12	53	+/-	-	()	()	()	()	()	-	_	()	()	()	()	-	-
11	F	8 3/12	38 [1]	++	+	-	()	+	+	+	+	+	()	-	()	T	+	-
12[s1]	M	29 10/12	()	++	+	+	-	()	+	()	+	+/-	()	-	()	()	-	-
13[s1]	F	25 1/12	47	++	+	+	var	()	+	()	+	+/-	()	-	()	()	-	-
14	M	10 10/12	43 [2]	++	+	()	var	()	+	()	+	-	()	+	()	()	-	-
15	F	1 6/12	49	+/-	+	-	()	-	+/-	()	+	+/-	()	()	()	()	-	-
16	F	11 7/12	48	+	+/-	+	()	-	+	-	+	+/-	-	()	-	-	-	+
17	F	10 8/12	46	++	+	()	()	()	+	()	()	()	-	()	()	T	()	()
18	F	5	41	++	+	()	()	()	()	()	()	()	()	()	()	()	()	()
19	M	26 4/12	()	++	+	+	var	+	+	()	+	+	+	-	()	T	-	-
20	F	9 10/12	35.5 [4]	++	+	()	()	+	+	+	+	+/-	-	+	()	T	++	++
21[s2]	M	5 1/12	40 [2]	++	+	()	()	()	()	()	+	-	-	-	()	()	+	-
22[s2]	F	8 3/12	()	+	+	+	()	()	()	()	+	-	-	-	()	()	-	-
23	F	5 8/12	()	+	+	()	val	()	+	-	-	+/-	()	-	()	()	-	-
24	M	22 1/12	43	++	()	()	()	()	+	()	+	-	-	-	()	()	+	()
25	F	16 6/12	42	++	+	-	()	()	+	()	+	()	+	()	()	()	()	()
26	M	3 7/12	49,5	+/-	+	-	var	+	()	()	-	-	()	()	()	()	-	-
27	M	7/12	41 [5]	++	+		()	-	+	()	+	-	()	++	()	()	-	+

#: patient serial number; *: adopted; [s1] and [s2]: sib pair 1 and sib pair 2;
S: sex; M: male; F: female; Age (years): age on July 1, 2004 in years and months;
(): no information available;
BL (cm): birth length in cm at full term; [1]: at 29 weeks (w) of gestation; [2]: at 34 w; [3]:at 35 w; [4]: at 30 w; [5]: at 41.5 w
Gr: evaluation of growth deficiency (postnatal) derived from measurements of length recorded on age and sex appropriate reference curves (NSG1116-1119) of cumulative increase of longitudinal stature; "++":>8cm below p3; "+": ,8cm below p3; "=/-": initially with in normal limits, from end of infancy growth below but parallel to p3; "-": increase of stature within normal limits
Sta: description of stature: "+": short-limb type dwarfism; "_": proportioned dwarfism
J: large joints; "+" generalized loose jointedness; "-": normal motion range in large joints
Elb: elbow joints: "+": mild limitation of extension; "-": normal range of elbow motion
K: knee: "var": genua vara deformity; "val": genua valga
H,F: "+": hands, fingers and feet, toes significantly shortened; "+/-": milder expression of phenomenon
Fi: fingers and small finger joints: "+":loose small joints, telescoping of distal finger segments into proximal ones, due to loose soft tissue; "-": phenomenon absent
sH: "+": deficient growth and qualify of scalp hair; "-": phenomenon absent
Inf: infections (serious) with incidence significantly above average in age-matched controls
Va: varicella; "+": history of unusually severe clinical varicella; "-": light or average varicella
RBc/WBC" red and white blood cells in peripheral blood sample: "++": overt macrocytic anemia; "+": low red cell count; "++": severe-; "+": mild leucopenia;
IMM; Hum/Cel: results of in vitro humoral or cellular immunity testing; "Ig": low immunoglobulins; "T": low T-cell count
GI: Hir./Mal: gastrointestinal dysfunction: "++": Hirschsprung disease and/or Malabsorption histologically/biochemically proven; "+": significant complaints of either constipation or Hirschsprung-like symptoms or of malabsorption or failure to thrive in infancy or early childhood.
#3, the largest BLs (patients #10, 15 and 26) were recorded in subjects in whom no RMRP mutation has been found.

Stature of the short-limb dwarfism type was confirmed in all patients: by plotting the sequential measurements recorded by the original observers two types of deficient cumulative increase of stature could be discerned among the patients. The first type was seen in patients with BL below the normal range and in the ones with low normal BL. Axial growth was extremely slow in the first subgroup and stature fell below 8cm under the p3 reference curve. These results are recorded by the symbol "++" in the growth (Gr) column in Table 1. In a subgroup of patients with BL within normal limits growth deficiency was less pronounced as their stature remained somewhat closer to but still evolved gradually further below the p3 reference curve. This less severe degree of growth failure is recorded by "+" in the Gr column in Table 1. The second type of failing growth discernable in this study and symbolized by "+" in Table 1, evolved slightly below but remained nearly parallel to p3 as documented by the sequential measurements. It was found in three of the patients (# 10, 23 and 26) either without *RMRP* mutations or with only a single mutant allele detected (# 15). Unfortunately the BL record was not available for patient # 23.

Except for the elbows, the range of motion in the large joints was found to be slightly excessive in 8 of 17 patients. Motion in the large joints was normal in another 6. In the remaining 13 including the 7-months-old infant in whom the range of motion in the large joints can hardly be assessed objectively, information on this feature was not available.

In 15 patients no comment was made on the posture of the lower limbs. In only one subject the legs were described as straight. In the remaining 11 patients the axial deviation in the knee joints was varus in 7 and valgus in 4. Limited elbow extension was confirmed in 9 patients. It was reported absent in only 3, including however the 7-month-old infant. In no less than 15 patients this feature was probably not examined as no comments about it were traceable in the records. In as many as 20 of the 27 patients the hands and feet were described as short and pudgy. The phenomenon of "partial telescoping" of the more distal phalanges by exerting physical pressure distally at the finger tops was found in only 4 patients and noticed as absent also in 4 patients. Lack of cooperation in young children and possibly gradual disappearance of the phenomenon with aging may account for this result. Alternatively the "telescoping" may not have been explored in the 19 remaining patients.

Deficient growth of scalp hair (sH in Table 1) was recorded in 20 of the 27 subjects and not mentioned as a feature in 3 others. Hair growth was judged to be poor in patient # 3 in whom no mutations in the *RMRP* gene were found, and in patient # 15 with only one such mutation detected. However hair growth was described as normal in the three other subjects without

RMRP mutations. Only in patient # 2, a compound heterozygote for two *RMRP* mutant alleles, hair growth was reported as clinically normal.

Other components of the pleiotropic expression in CHH were scarcely recorded in this retrospective study. In 12 patients respiratory or general infections in infancy or early childhood recurred more frequently than in age-matched controls. Infections in infancy or early childhood were of no concern in 10 patients. In 5 other records no relevant data were found. Clinically severe varicella was documented in only 2 patient records. In 6 others the herpes zoster infection was described as within the variable standard range. A similar conclusion had probably been reached, but not recorded in 19 subjects. In the young infant (patient # 27) natural chickenpox had not yet occurred.

In the latter patient severe macrocytic anemia had been diagnosed at 2 months of age. In only patients # 7, 14 and 20 the erythrocyte count in peripheral blood was recorded as low, but MCV was recorded in neither. Low red cell count and/or anemia were absent in 12 cases and not mentioned in the record of 11 others.

In vitro evidence for cellular immunodeficiency was scarcely documented. Low T-cell count was found in only 6 of the patients. In 5 of them also frequent infections had been noticed early in life. In only 3 of the patients in whom frequent infections had not occurred in early life, *in vitro* studies did not show any evidence of cellular immunodeficiency.

Gastrointestinal (GI) dysfunction in CHH may be expressed as malabsorption ("Mal" in Table 1) associated with loose stools or frank diarrhea, signs of celiac disease and/or failure to thrive (FTT). Alternatively the dysfunction may be expressed as constipation, Hirschsprung-like phenomenon or frank Hirschsprung disease. Only in 2 patients in this series both types of GI dysfunction were observed, but in only one of them formally documented. Three patients have had complaints of constipation in early childhood, four more had only temporary problems of malabsorption sometimes associated with signs of FTT.

3.1.3 Radiological Phenotype

The radiographic findings summarized in Table 2 are described either from the radiologist's protocol describing the original radiographs of the skeleton or from the study of the available radiographs. The radiographic features in the 27 patients were evaluated according to the

Table 2: Radiographic Features in Patients with clinical Diagnosis of Cartilage-Hair Hypoplasia at various stages of physical Development

Patients		Infancy			Child- (Adult-)hood			
#	Sex	ShTB	CuFem	RiSt	MetCD	Fib	IntPedic	H, F
1	M	+	( )	( )	+	( )	+	+
2	M	+	( )	( )	+	( )	( )	( )
3	M	( )	( )	( )	+	( )	( )	+
4	M	+	( )	+	+	( )	+	( )
5	M	( )	( )	( )	( )	( )	( )	( )
6	M	+	+	±	+	( )	+	( )
7	M	( )	( )	( )	( )	( )	( )	( )
8	F	+	( )	( )	+	+	+	+
9	F	+	( )	±	+	+	±	+
10	M	( )	( )	( )	+	( )	-	+
11	F	+	( )	±	+	( )	( )	+
12	M	( )	( )	( )	+	+	-	+
13	F	( )	( )	( )	+	+	-	+
14	M	+	+	+	+	( )	( )	+
15	F	( )	( )	( )	( )	( )	( )	( )
16	F	+	( )	( )	+	+	( )	+
17	F	+	( )	( )	+	( )	( )	+
18	F	( )	( )	( )	+	( )	+	+
19	M	+	+	-	+	( )	( )	+
20	F	+	+	+	+	( )	( )	+
21	M	+	+	( )	+	( )	( )	+
22	F	+	+	( )	+	( )	( )	+
23	F	+	( )	( )	+	( )	+	+
24	M	+	( )	( )	+	+	+	( )
25	F	+	( )	( )	+	( )	+	+
26	M	( )	( )	( )	( )	( )	( )	( )
27	M	+	+	( )	( )	( )	( )	( )

( ): no information available; "+": feature described in radiologist report/ or confirmed in radiograph; "±": feature equivocal; "-": feature absent according to own radiographic study or reported absent in radiology report

ShTB: shortened tubular Bones
CuFem: curved Femora with rounded distal metaphyses
RiSt: short Ribs and anterior Angulation of Sternum
MeCD: metaphyseal chondrodysplasia more apparent in Knees than in Hips
Fib: Fibulae distally longer than Tibiae
IntPedic: less than normal craniocaudal Widening of interpediculate Distance in lumbar Spine
H, F: short tubular Bones in Hands, Fingers, Feet, Toes

corresponding standard criteria set forth by Spranger et al (2002) and listed accordingly in Table 2. Although associated with prominent to severe shortness of stature or frank dwarfing the radiographically visible metaphyseal changes usually ranged from subtle or equivocal to moderate. Unfortunately, also in this part of the retrospective study descriptive information or the corresponding informative radiographic documents were too often unavailable. In several instances the radiographs of the skeleton taken in infancy had originally been read as normal. Only three specific features were investigated in the ones available. In 17 of the 27 patients generalized shortening of the large tubular bones had been radiologically confirmed in infancy. Curved femora were documented in 8 infant patients. The distal femoral epiphyses were described as rounded in only few of them. Anterior angulation of the sternum and short ribs were recorded in infancy in only 3 subjects. These features were absent in only one and equivocal in three patients. They had neither been examined nor commented upon in the large majority of the patient group.

In the relevant radiographs taken from childhood to adolescence the metaphyseal chondrodysplasia, more pronounced in the knee than in the hip joints, was most consistently recorded (20/27 patients) as was the case for the significant shortening of the hand and foot bones (18/20 patients). In contrast the proportionally long distal fibulae and the decreased or absent craniocaudal widening of the vertebral interpediculate distances in the lumbar spine had been found each in only 8 patients.

3.2 Mutation Screen of CHH patients

3.2.1 *RMRP* Mutation Screen

Thirty-five patients were recruited to this study for either confirmation or exclusion of CHH. The diagnosis of CHH was made based on the finding of characteristic radiographic features by the referring physician. All referred patients were screened for mutations in the *RMRP* gene (Tab. 3). A 682 bp product was amplified from genomic DNA with the primers RMRP2 and RMRP4 (for primer sequence see 2.18.7.1.1). This product includes 331 bp of the RMRP promoter region, 267 bp of the *RMRP* transcript and 84 bp of sequence 3' of the pol III termination signal. The PCR was performed as described in 2.4.1. The annealing temperature of the primers was 61 ºC and DMSO was added to a final concentration of 2 % in

Fig. 17: M29916 RMRP sequence. The sequence between the primers RMRP2 and RMRP4 (in grey) was amplified for the mutation screen in CHH patients. The RMRP transcript (dark blue) is underlined and the transcription termination signal is shown in green. The published polymorphisms are indicated in purple above the RMRP sequence. Putative promoter elements are shown; TATA box in red, PSE binding element in pink, octamer in yellow and the SP1 binding site in light blue.

the PCR reaction. The mutation analysiswas performed by direct sequencing of the PCR products with dye terminator sequencing (SeqWright). The alleles were separated by subcloning the PCR products in the pGEM T vector (Promega) and variants were confirmed by direct sequencing with the vector-specific primers T7 and SP6. M29916 was used as a reference sequence for the *RMRP* mutation screen and the results of this screen of all referred patients are summarized in table 3. Twenty-two patients have mutations in both alleles, two patients have a mutation in just one allele, and nine patients have no mutations in the *RMRP* gene. Nine alleles with duplication mutations in the promoter region were found. This was primarily between the TATA box and the transcription start site (see Fig. 17). This would be expected to decrease the level of transcription. Two duplications were identified between the TATA box and the PSE (promoter sequence element) element. The TATA box has been found to be located at a fixed distance downstream of the PSE element (Hernandez and Lucito 1899; Mattaj et al., 1988; Kinkel and Pederson 1989; Lobo and Hernandez 1989). Thirty-seven alleles had single base pair substitutions and two alleles showed a deletion of the last

ten bp of the RMRP transcript. The transcription termination signal was not affected by this deletion.

Table 3: Summary of *RMRP* mutation screen in referred patients.

origin	#	Allele 1	Allele 2
German patient	1	**4C>T**	**9T>C**
US patient	2	**124C>T** & +7T>C	**89C>G**
US patient	3	no mutations with RMRP4	no mutation with RMRP2
German patient	4	**-11_-25dupACTACTCTGTGAAGC**	**180G>A** & +7T>C
German patient	5	**-4_-23dupTACTCTGTGAAGCTGAGGAC**	**180G>A**
US patient	6	**194-195insT**	**80G>A** & 156G>C; 177T>C
US patient	7	**-14_-20dupTCTGTGA** & -58 T -> C, -48C->A	**70A>G** & +7T>C
US patient	8	**70A>G** & -282A>G	**70A>G** & -282A>G
US patient	9	**116A>G** & +7T>C; -58T>C; -48C>A	**256_265delCAGCGCGGCT** & -58T>C; -48C>A
German patient	10	+7T>C; -58T>C; -48C>A	+7T>C; -58T>C; -48C>A
US patient	11	**-5_-26dupTACTACTCTGTGAAGCTGAGAA** & -56A>G; -48C>A; -6G>A; 156G>C; 177C>T	**179_180insC**
Belgium patient	12	**-6_-25dupACTACTCTGTGAAGCTGAGA** & -48C>A; -6G>A	**91G>A**, **101C>T** & +7T>C; -58T>C; -48C>A
Belgium patient	13	**-6_-25dupACTACTCTGTGAAGCTGAGA** & -48C>A; -6G>A	**91G>A**, **101C>T** & +7T>C; -58T>C; -48C>A
German patient	14	**70A>G**	**70A>G**
US patient	15	**127G>C** & -56A>G; -48C>A; -6G>A; 156G>C; 177C>T	no mutation or polymorphisms on second allele
US patient	16	**-15_-24dupCTACTCTGTG**	**180G>A**
German patient	17	**70A>G**	**70A>G**
German patient	18	**182G>T**	**213C>G**
German patient	19	**70A>G**	**211 C -> G**
US patient	20	**195C>T** & +7T>C; -58T>C; -48C>A	**256-265delCAGCGCGGCT** & -58T>C; -48C>A
German patient	21	**262G>C**	**70A>G**
German patient	22	**262G>C**	**70A>G**
US patient	23	+7T>C; -58T>C; -48C>A	heterozygous for polymorphisms
US patient	24	**-1_-21dupCTCTGTGAAGCTGAGGACGTG**	**180G>A**
German patient	25	**97G>A** & -58T>C; -48C>A	**14G>T**
US patient	26	+7T>C; -58T>C; -48C>A	-58T>C; -48C>A
US patient	27	**70A>G**	**70A>G**
Belgium patient	28	+7T>C; -48C>A	-58T>C
German patient	29	+7T>C; -58T>C; -48C>A	+7T>C; -48C>A
US patient	30	+7T>C	+7T>C
Belgium patient	31	177C>T	-56A>G; -6G>A
US patient	32	-56A>G; -48C>A; -6G>A; 156G>C; 177C>T	no changes on paternal allele
Australia	33	**-8_-15dupGAAGCTGA** & -58T>C; -48C>A	no mutation or polymorphisms on second allele
Finnland	34	**70A>G**	**70A>G**
Finnland	35	**70A>G**	**70A>G**

Patients #1 to #27 are part of the clinical study. Patients #28 to #35 were excluded from the clinical study, because they did not meet the inclusion criteria and Patients #34 and #35 were originally studied by Dr. Outi Mäkitie. All mutations are in red. Polymorphisms are in black. In dark blue are mutations where it is still unkown whether both changes are pathogenic or only one of them. Neither of these changes have been reported as polymorphisms and were not found in 200 control subjects. Patient # with yellow background indicates that two *RMRP* mutations have been identified (one on each allele). Turquoise background shows patients where only one mutant allele could be found. Patients with no mutations have no background color. The light blue color in the 'origin' column marks patients with reported anemia in their medical charts.

These could be hypothesized to affect the secondary structure of the RMRP complex and perhaps the binding to proteins within the ribonuclear protein complex. However, limited published data at least for two of the subunits (POP1 & POP2) suggest this is not the case (Ridanpää et al., 2001). To date no deletions of the whole gene have been found suggesting that complete loss of function is incompatible with life; and the mutations described here are therefore likely to be hypomorphic alleles.

3.2.2 *COL10A1*

Mutations in the *Type X Collagen* gene (*COL10A1*) have been described in patients with Metaphyseal Chondrodysplasia Schmid type (MCDS) (OMIM #156500) a skeletal disorder with autosomal dominant inheritance. Because the clinical phenotype of the metaphysis in CHH and SMCD patients is very similar, all patients who were negative for *RMRP* mutations have been screened for mutations in the *COL10A1* gene (Chan & Jacenko, 1998). The primer sequences and PCR conditions for the mutation screen were provided by Katja Hilbert from the Children's Hospital of the Johannes Gutenberg-Univerisity of Mainz, Germany (see 2.18.7.1.3 for primer sequences). The *COL10A1* gene consists of three exons. The first two exons are very small (112 bp and 169 bp, respectively). The third very large exon (3019 bp) has been amplified in three overlapping parts for the mutation screen, but only covering the first 1955 bp that includes the entire coding region of exon 3 and a short part of the 3' UTR.

Table 4: PCR condtions for COL10A1 mutation screen

MCDS		**Primers**	**Annealing Temperature**	**Product size**
Exon 1		1 F & 1 R	58ºC	395 bp
Exon 2		2.2 F & 2.2 R	58ºC	380 bp
Exon 3	Part 1	3F & 3R1	58ºC	738 bp
	Part2	3 F 1 & 3 R 3	58ºC	852 bp
	Part3	GW627 & GW628	58ºC	678 bp

The primer combinations to amplify the *COL10A1* gene, the PCR conditions and the expected fragment sizes are shown in Table 4. AL121963 was used as a reference sequence for the mutation screen. Seven of the eight patients with no mutations in the *RMRP* gene have been screened for mutations in the *COL10A1* gene (Tab. 5). Patient #28 could not be screened for the entire COL10A1 coding region, because there was not enough DNA available for further testing. No mutation in *COL10A1* has been found in ten out of the eleven patients screened. Only one patient (#15) had a 935C>T transition resulting in a T279I amino acid change. Interestingly, this is the same patient, who has only one mutant *RMRP* allele (Tab. 3). Fortunately, the parents of this patient were available for screening as well. The *RMRP* mutation was inherited from the father and the *COL10A1* mutant allele is of maternal origin. Seven of the eleven patients have the previously described 176T>C polymorphism that leads to a M27T amino acid change. Since exon 1 of *Col10A1* has never been screened for mutations before, exon 1 was amplified in 20 control DNAs to test, whether - 29G>C might be a mutation affecting *Col10A1* transcription or whether this base pair substitution is a

polymorphism. The analysis of the sequences of the control DNAs revealed that the - 29G>C is a very frequent polymorphism that was found in a heterozygous as well homozygous state in the control population.

Table 5: Summary of COL10A1 mutation screen of RMRP mutation negative patients

CHH #	Exon 1	Exon 2	Exon 3		
			Part 1	Part 2	Part 3
3	No mutation	176T>C, M27T	No mutation	No mutation	No mutation
10	- 29G>C	No mutation	No mutation	No mutation	No mutation
15	-29G>C	176T>C; M27T	No mutation	935C>T, T279I	No mutation
23	- 29G>C	176T>C, M27T	No mutation	No mutation	No mutation
26	No mutation	No mutation	No mutation	No mutation	No mutation
28	-	-	-	-	No mutation
29	- 29G>C	176T>C, M27T	No mutation	No mutation	No mutation
30	- 29G>C	176T>C, M27T	No mutation	No mutation	No mutation
31	- 29G>C	176T>C, M27T	No mutation	No mutation	No mutation
32	- 29G>C	176T>C, M27T	No mutation	No mutation	No mutation
35	No mutation	No mutation	No mutation	No mutation	No mutation

The basepair changes found upstream of exon 1 and in exon 2 are polymorphisms. The basepair substitution in exon 3 of patient #15 is a real mutation, since it has not been found in 30 controls and it has neither been reported as a polymorphism nor a mutation in the literature.

3.2.3 SBDS

Shwachman-Diamond Syndrome (SDS) (OMIM #260400) is an autosomal recessive disorder characterized by exocrine pancreatic insufficiency, hematologic abnormalities and similar changes in the metaphysis as described in CHH and MCDS. Another overlapping feature with CHH is cellular immunodeficiency. Boocock et al (2003) identified mutations in a then uncharacterized gene causing the Shwachman-Bodian-Diamond Syndrome. They named it *SBDS* and it consists of five exons (Boocock et al., 2003). The PCR conditions are summarized in Table 6 and the PCR was performed as described in 2.4.1.

Table 6: PCR conditions for SBDS mutation screen

SBDS	**primers**	**Annealing Temperature**	**Product size**
Exon 1	Ex 1 F & Ex 1 R	66ºC + 1 µl DMSO	566 bp
Exon 2	Ex 2 F & Ex 2 R	66ºC	399 bp
Exon 3	Ex 3 F & Ex 3 R	66ºC	449 bp
Exon 4	SDS4F & SDS 4R	66ºC	489 bp
Exon 5	Ex 5 F & Ex 5 R	66ºC	929 bp

The primer sequences are listed in 2.17.7.1.5. AC073089 was used as a reference sequence for the mutation screen. Patients #3, #10, #23, #26, #29, #30, #31, #32 and, #35 have been screened for mutations in *SBDS*. Patient #32 was diagnosed as a SDS patient. No mutations in the *SBDS* gene have been found. Unfortunately, there has not been enough patient DNA available to test for chromosomal rearrangements (Boocock et al., 2003; Nakashima et al., 2004).

3.3 Search For Modifiers

Interestingly, CHH patients who exhibit the same mutations in the *RMRP* gene present with quite variable clinical phenotypes. Since no clear phenotype-genotype correlation could be established, the question remains as to what causes the quite variable clinical presentation of the CHH patients. One possibility would be that there are modifying genes that could be responsible for the pleiotropic presentation of CHH patients, such as polymorphisms or mutations in other genes.

3.3.1 *IL8* Polymorphisms

Hull et al., showed that two polymorphisms in the *IL8* gene might be responsible for an increased susceptibility to bronchiolitis (Hull et al., 2001). Bronchiolitis is an infection of the upper airways. A number of CHH patients have been reported to have recurrent infections. This might be caused by the presence of the above-mentioned polymorphisms in the *IL8* gene. To test this hypothesis all patients were screened for the presence of the –251 (upstream of exon 1) and 781 (localized in intron 1) SNPs described by Hull et al., 2001. If IL8 is a modifier for increased infections, all patients with immunologic problems or increased infections should have an A at position -251 and a T at position 781, whereas all other patients would be expected to have a T at -251 and a C at position 781. But as shown in Table 7, patients that have no RMRP mutations and have no immunological problems also have an A at position -251 and a T at position 781 like patients #10 and #26. Even patients with recurrent infections (#7, #34) have a T at -251 and a C at 781. This suggests that these *IL8* polymorphisms are most likely not modifiers of the pathogenesis of CHH. This result is not surprising by now, since Hull et al. corrected the bronchiolitis susceptibility locus near *IL8* (Hull et al., 2004).

origin	#	-251	781
German patient	1	A>T het	C>T het
US patient	2	A	T
US patient	3	A>T het	C>T het
German patient	4	T	C
German patient	5	A>T het	C
US patient	6	A>T het	C
US patient	7	T	C
US patient	8	A>T het	C>T het
US patient	9	A>T het	C
German patient	10	A	T
US patient	11	A	T
Belgium patient	12	A	C>T het
Belgium patient	13	A	C>T het
German patient	14	A>T het	C>T het
US patient	15	A>T het	C>T het
US patient	16	A>T het	C
German patient	17	A>T het	C>T het
German patient	18	T	C
German patient	19	A>T het	C
US patient	20	A>T het	C>T het
German patients	21	A	T
German patients	22	A	T
US patient	23	A>T het	C>T het
US patient	24	T	C
German patient	25	T	C
US patient	26	A	T
US patient	27	A>T het	C>T het
Belgium patient	28	no DNA	no DNA
German patient	29	A>T het	C
US patient	30	A>T het	C
Belgium patient	31	A>T het	C>T het
US patient	32	A>T het	C
Australia	33	A>T het	C
Finnland	34	T	C
Finnland	35	A	T
control		T	C

Table 7: IL8 SNP analysis in CHH patient cohort.
All patient numbers with yellow background indicate patients with two *RMRP* mutations. The patients with one *RMRP* mutation have a turquoise back-ground color and all patients with no *RMRP* mutation have no background color. All patients with immuno-logical problems have a light blue background color in the 'origin' column.

3.3.2 *RPS19* Mutation Screen

Mutations in the *RPS19* gene have been found in approximately 25% of patients with the Diamond-Blackfan Anemia (DBA) (OMIM #205900), a rare congenital erythroblastopenia (Willig et al., 1999). Affected patients present with a decreased number or even absence of erythroid precursors in the bone marrow. This is very similar to the severe anemia seen in some CHH patients. Around 30% of the DBA patients exhibit several dysmorphic features such as growth retardation, hand and/or limb malformations, urogenital anomalies and congenital heart defects. RPS19 is one of the 79 ribosomal proteins and is located in the

small 40 S subunit of the ribosome. Rps19 -/- mice die prior to implantation and Rps19 +/- mice exhibit no detectable phenotype (Matsson et al., 2004). A correlation between the severity of anemia and immune deficiency and the height of CHH patients has been reported (Mäkitie et al., 2000). To test whether the anemia and/or immunodeficiency in CHH patients might be caused by mutations in the *RPS19* gene, all patients with reported anemia and immunological problems have been screened for mutations in this gene. *RPS19* consists of 6 exons and the PCR conditions are summarized in Table 8. The PCR was performed as described in 2.4.1 and the primer sequences are listed in 2.18.7.1.5.

Table 8: PCR conditions for RPS19 mutation screen

DBA	Primers	Annealing Temperature	Product size
Exon 1	RPS19 ex1F3 & RPS19 ex1R3	58 ºC	562 bp
Exon 2	RPS19 ex2F & RPS19 ex 3R	58 ºC	659 bp
Exon 3			
Exon 4	RPS19 ex4F & RPS19 ex 4R	58 ºC	688 bp
Exon 5	RPS19 ex5F & RPS19 ex 5R	58 ºC	453 bp
Exon 6	RPS19 ex6F & RPS19 ex 6R	58 ºC	645 bp

For primer sequences see 2.18.7.1.5 of the Material & Methods section. The annealing temperature of all primer pairs is 58°C and expected product sizes are listed in the right column.

The sequence ENSG00000105372 from EMBL was used as a *RPS19* reference sequence for the mutation screen. Sequencing results are given in Table 9. No mutations were found in *RPS19*.

Table 9: Summary of RPS19 mutation screen in CHH patients

origin	#	exon 1	exon 2	exon 3	exon 4	exon 5	exon 6
German patient	1	310insC homo, +36T>C	no mutation	no mutation	no mutation	no mutation	no mutation
US patient	2	no mutation	no mutation	no mutation	no mutation	+70C>T het	no mutation
US patient	7	no mutation	no mutation	no mutation	no mutation	+70C>T het	no mutation
US patient	11	+36T>C homo	+79insC homo, +89G>C homo	no mutation	+14G>A homo	-90C>T homo, +70C>T homo	no mutation
US patient	15	no mutation	+89G>C het	no mutation	+14G>A het	+70C>T het	no mutation
German patient	17	no mutation	no mutation	no mutation	+14G>A het	-90C>T het, +70C>T het	no mutation
German patient	19	insC homo	no mutation	no mutation	+14G>A het	+70C>T het	no mutation
US patient	20	no mutation	+89G>C het	no mutation	no mutation	-90C>T het, +70C>T het	no mutation
US patient	27	no mutation	+89G>C het	no mutation	+14G>A het, +18G>C het	+70C>T het	no mutation
Australia	33	310insC homo	no mutation	no mutation	+14G>A het	-90C>T het, +70C>Thomo	no mutation
Finnland	34	+36T>C homo	+79insC homo, +89G>C homo	no mutation	+14G>A homo	-90C>T homo, +70C>T homo	no mutation
Finnland	35	no mutation	+79insChet, +89G>Chet	no mutation	+14G>A het	-90C>T het, +70C>T het	no mutation

Patient numbers with yellow background indicate patients with two *RMRP* mutations, turquoise background indicates numbers of patients with one *RMRP* mutation. Light blue background in the 'origin' column marks patients with immunological problems.

It seems that the CHH patients have a higher density of polymorphisms than the control population. But all changes were observed in at least one of the five controls and also reported in the NCBI SNP database. The 310insC found in patient #1 and #33 does not affect the ORF of *RPS19*, because the 1st ATG is located at 373-375 bp and therefore in exon 2 of the gene.

3.4 Functional Studies of human RMRP

3.4.1 *RMRP* Expression pattern

To elucidate the expression pattern of the human *RMRP* gene a human multiple Tissue Northern Blot (MTN) (RNWAY Laboratories Inc., Korea) was hybridized with a *RMRP* probe amplified with the primers RMRP5 and RMRP6 at an annealing temperature of 61°C. The PCR reaction was supplemented with 2% DMSO and performed as described in 2.4.1. As template a cDNA generated from total RNA isolated from human whole blood was used. The total RNA was isolated as described in 2.2.2 and transcribed into cDNA as illustrated in 2.4.4. The primer sequence can be found in 2.18.7.1.1. The probe consisted of the entire transcribed part of *RMRP* and was therefore 267 bp long. Before the Northern Hybridization (2.13.2.1) the PCR product was labeled with random hexamers (2.12.1).

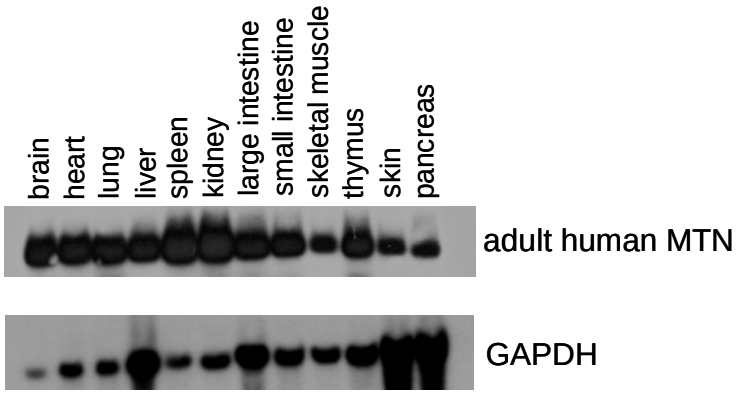

Fig. 18: Human RMRP adult MTN.

The Northern blot was hybridized with the whole *RMRP* transcript (upper panel). In a second hybridization the MTN was probed with *GAPDH* as RNA loading control (lower panel)

As shown in Figure 18 *RMRP* is ubiquitously expressed in all adult tissues tested. It is strongly expressed in most tissues and maybe a little less strongly in skin and pancreas when compared to the *GAPDH* expression pattern that served as a RNA loading control. Interestingly, although *RMRP* is ubiquitously and strongly expressed only a few tissues such as bone, the hematopoetic system and hair are affected in CHH patients.

3.4.2 *RMRP* Promoter Studies

To elucidate the effect of the RMRP promoter duplication found in CHH patients on *RMRP* transcription the RMRP promoter had to be characterized. Different upstream sequences of the RMRP promoter region were amplified. The promoters of genes that are transcribed by polymerase III are usually very short, e.g. the human U6 promoter is 265 bp (Chen et al., 2003) and the mouse U6 promoter 355 bp (Ref.) long. Therefore two putative RMRP promoter sequences differing in length were amplified (Fig. 19). The putative minimal

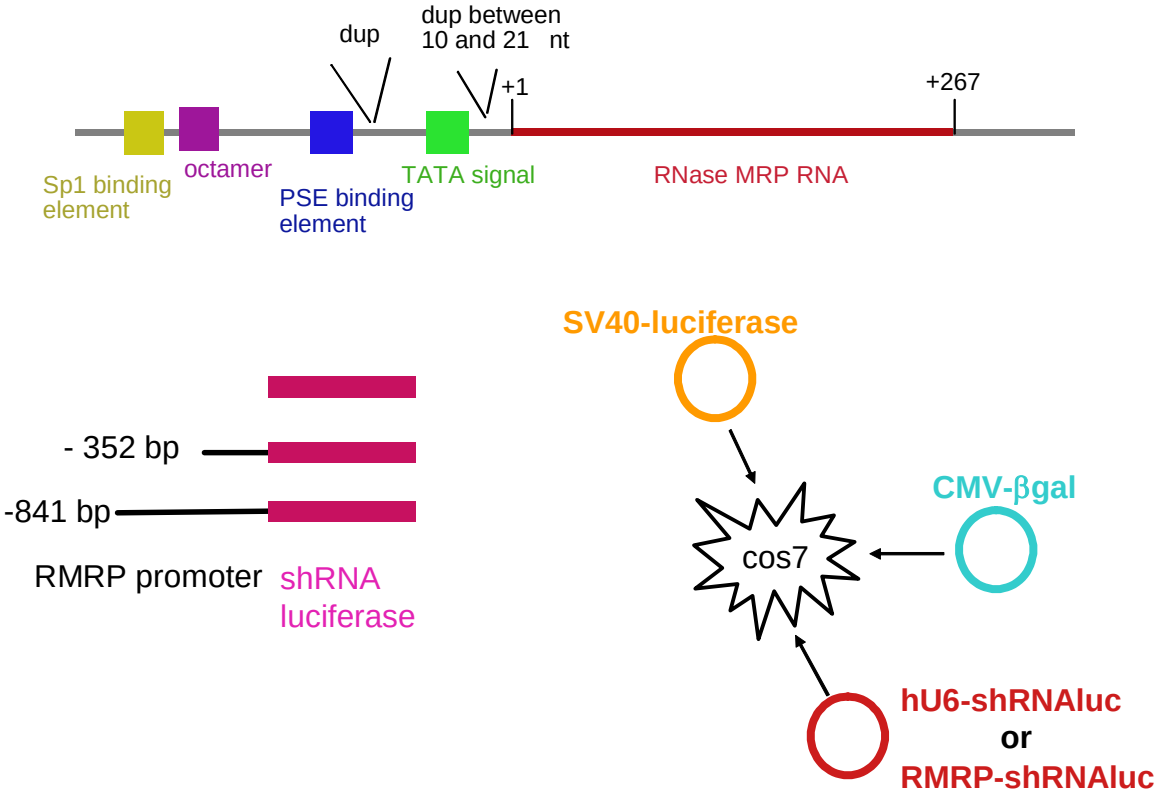

Fig. 19: Schematic diagram of the transfection constructs.

The upper panel shows a cartoon of the RMRP gene structure. The lower panel on the left shows the promoter constructs tested. The 352 bp RMRP promoter contains the 4 putative promoter elements TATA signal, PSE binding element, octamer and SP1 binding element. The 841 bp promoter includes the 352 bp sequence plus 489 bp of 5' upstream sequences. Both promoters were cloned in front of a short hairpin RNA that targets the luciferase reporter gene (shRNAluc) of the pGL3 Control reporter vector (Promega) that is a SV40-luciferase vector. The short hairpin RNA (shRNA) without promoter serves as negative control. The right cartoon shows the co-transfection of the plasmids used in this assay. SV40-luciferase (=pGL3 control) is the reporter plasmid (orange). CMV-βgal serves as control for transfection efficiency and the human U6 promoter (hU6) driving shRNAluc is the positive control for this assay. The RMRP-shRNAluc is the construct to be tested.

promoter was 352 bp long and contained the TATA signal, the PSE binding element, the octamer and the SP1 binding site. It was amplified from human genomic DNA with the primers RMRP8-Eco RI and RMRP14-Cla I (for sequences see 2.18.7.1.1) as described in 2.4.1. The second promoter included an additional 500 bp of upstream sequence, was 841 bp in length, and was amplified with the primers RMRP8-Eco RI and RMRP9-Cla I (for sequence see 2.18.7.1.1) as described in 2.4.1. The annealing temperature for the PCR reaction was 61°C for both primer pairs. The PCR products were subcloned into the *EcoRI* and *ClaI* sites of the vector pSilencer U6 (Ambion) containing an RNAi oligo targeted against the luciferase reporter gene of the vector pGL3 Control (Promega). The U6 promoter of this vector was removed with a *KpnI* and *ApaI* digest. The remaining vector was then religated. The sequence for the RNAi oligo was provided by Michael Schlabach (Steve Elledge's laboratory at Baylor College of Medicine in Houston, TX). The short hairpin RNA (shRNA) was cloned into the *EcoRI* and *HindIII* sites of the vector. The transfection was done in triplicates and as described in 2.9. Twenty-four hours after the transfection was stopped the cells were split 1:2 and then grown for a further 24 hrs (Fig. 20). The cells were then harvested and assayed for luciferase (2.10) and β-galactosidase activity (2.11.1).

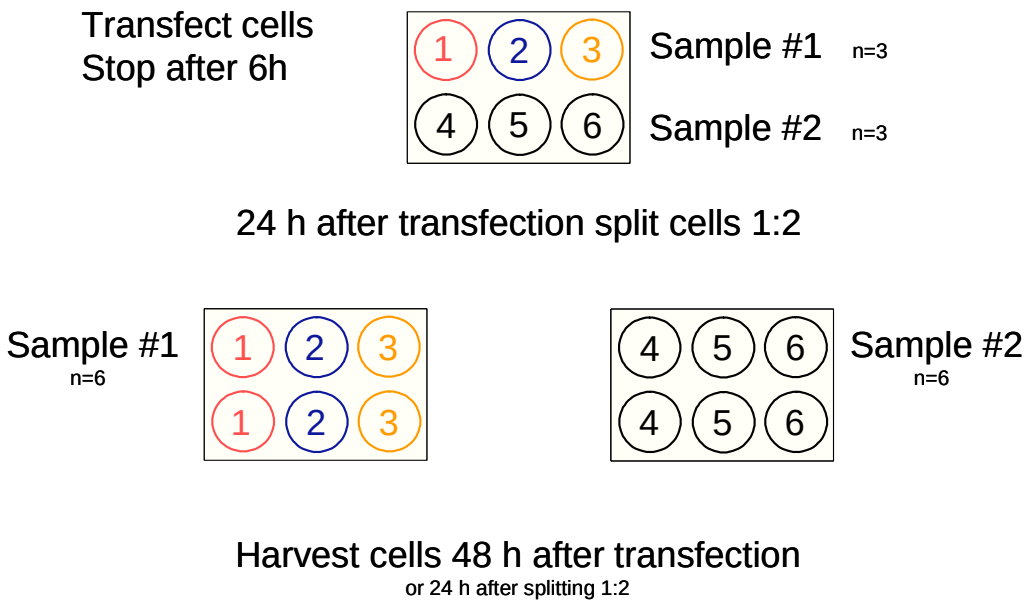

Fig. 20: Cartoon of the transfection assay.

The transfections were done in triplicates (3 wells for one test sample). 24 hrs after the transfection was stopped the cells were split 1:2 and grown for further 24 hrs. Then the cells were harvested for luciferase and β-galactosidase assays.

If the promoter is active and the shRNA transcribed it will act as a short interfering RNA (siRNA). This will in turn interfere with the protein production of the co-transfected reporter plasmid pGL3 Control that is a luciferase expressing reporter plasmid under the control of a constitutively active SV40 promoter. This will lead to a decrease in the measured luciferase activity. In short, if the RMRP promoter is active a decreased luciferase activity will be seen when compared to the negative controls. The first negative control is a vector containing just the U6 promoter without the shRNA targeted against luciferase (U6). The second negative control is a vector with just the shRNA and without any promoter (luc). The U6 promoter driving the shRNAluc serves as a positive control for this assay (U6luc). The transfection results are shown in Fig. 21.

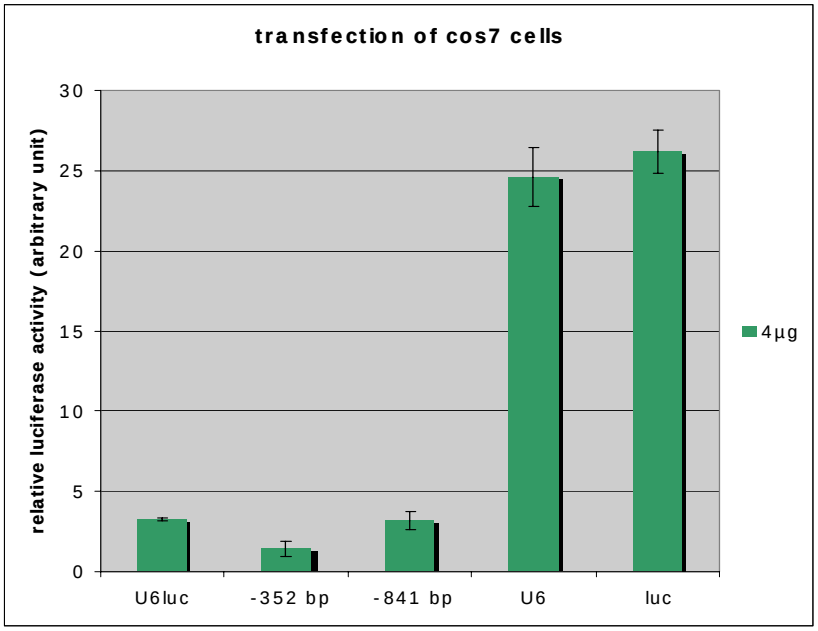

Fig. 21: Transfection result of the characterization of the RMRP promoter.

The U6luc construct serves as positive control for this assy. The U6 promoter without the shRNA and the shRNA without any promoter are negative controls in this assay. The latter two show the basic luciferase activity of the pGL3 control vector if there is no interference in the assay.

As shown in Figure 20 both RMRP promoters tested downregulate the luciferase gene expression that results in a decrease of luciferase activity when compared to U6 and luc alone. The 352 bp promoter seems to be stronger than the 841 bp because the luciferase activity is even more decreased than that of the positive control with the U6 promoter driving the shRNA targeted against the luciferase gene (U6luc). This result suggests that the 352 bp sequence upstream of the RMRP transcription start site is sufficient as a promoter sequence. To elucidate the effect of the promoter duplications found in CHH patients three of the mutated sequences were amplified with the primers RMRP8-Eco RI and RMRP14-Cla I, sequenced and subcloned into the expression vector as described above. These mutant promoter constructs were also transfected into cos7 cells. The same strategy as described

above was followed. The amount of promoter plasmids transfected was reduced from 4 µg plasmid DNA to 2 µg and 1 µg plasmid DNA, respectively. The DNA amount was reduced to test the promoter activity in a linear range of the assay to get an approximately dose dependent response. Four µg of promoter plasmid DNA saturates the assay. The promoter duplications of CHH patients #4, #12, and #16 (Tab. 3) were tested.

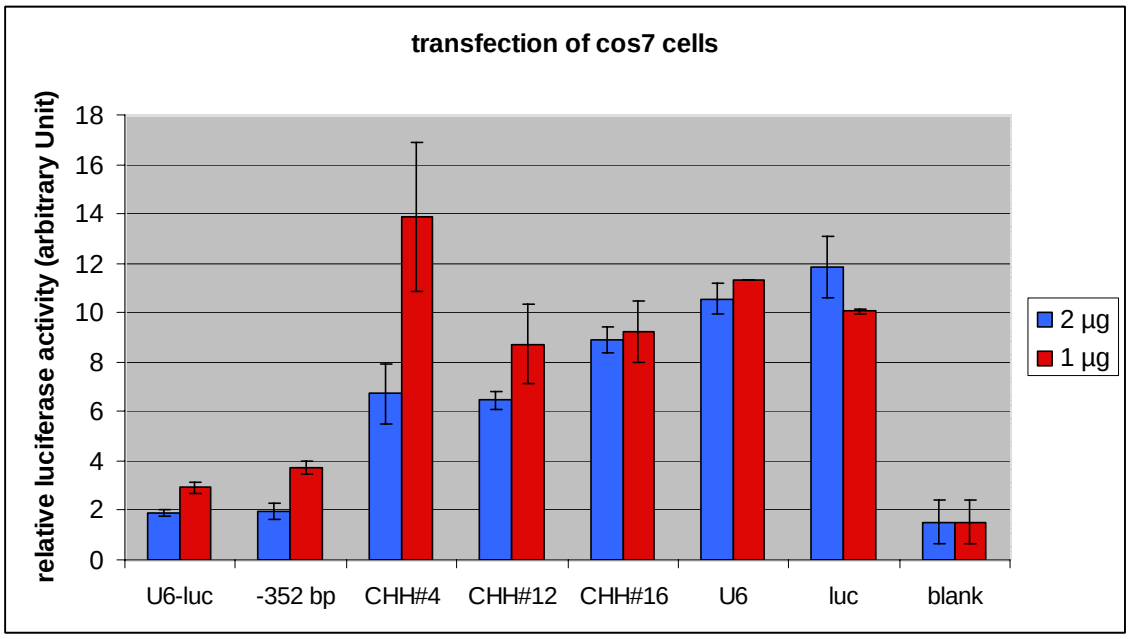

Fig. 22: Test of promoter activity of promoter duplications found in CHH patients. The U6-luc and wt RMRP (-352 bp) promoters reduce the luciferase activity significantly (close to background level when using 2 µg plasmid DNA shown in blue bars). All the mutant RMRP promoters show a higher luciferase activity when compared to the controls (U6-luc, -352 bp). But the promoter activity does not seem to be completely abolished, since the luciferase activity is slightly lower than the activity measured in the negative controls (U6, luc).

As shown in Figure 22 the activity of the mutant RMRP promoters is reduced compared to the wt promoter *in vitro*. The lower activity of the mutant promoters results in a higher luciferase activity when compared to the positive controls U6-luc and the wt RMRP promoter (-352 bp). But the promoter activity does not seem to be completely abolished, since the measured luciferase activity is still a little less than in the negative controls (U6, luc). This suggests that the promoter duplications found in CHH patients lead to a decrease of RMRP transcription *in vitro*.

3.4.3 Mitochondria in CHH patients

Because of the involvement of the *RMRP* yeast orthologe, *NME1*, in mitochondrial replication (Chang and Clyton 1987; Lee and Clayton 1997) the mitochondria of a CHH patient fibroblast cell line were analyzed via electron microscopy and compared to a wt control fibroblast cell line. The fibroblasts were provided by Dr. Andrea Superti-Furga (Lousanne, Switzerland). The patient was compound heterozygous for a base pair substitution. This patient was not part of the clinical study. The electron microscopy was performed by Prof. Dr. Hans-Anton Lehr in the Pathology at the Johannes-Gutenberg University Clinics of Mainz (Mainz, Germany). No morphological differences could be observed comparing the mitochondria of the CHH patient cell line to the wt control.

The same cell lines were also analyzed for mitochondrial depletion (number of mitochondria in a cell) via real time quantitative PCR by Dr. Lee-Jun C. Wong in the Molecular Diagnostic Laboratory in the Department of Molecular and Human Genetics at Georgetown University Medical Center (Washington, DC, USA). This analysis did not reveal any increased mitochondria depletion in the CHH patient cell line compared to the wt control. These two analyses suggest that the mitochondria function is not affected in CHH patients.

3.4.4 Ribosomal RNA Processing

Studies in yeast have shown that *RMRP* plays a critical role in the processing of ribosomal RNA. In yeast it cleaves at the A_3 site that leads to the maturation of the 5.8S rRNA (Chu et al., 1994). Therefore the ribosomal RNA processing was analyzed in CHH patient cell lines. For this experiment total RNA was isolated from EBV transformed lymphoblast cell lines from six CHH patients, one SBDS (#32), and one MCDS (#15) patient as well as three control cell lines. The RNA was separated on an agarose gel (2.3.1.2) or a polyacrylamide gel (2.3.2.2), respectively, blotted on nylon membranes and then hybridized (2.13.2.1; 2.13.2.2) with probes labeled with [γ^{32}P] dCTP (2.12.2) specific for the different rRNA species (mature and immature) (for sequences see 2.18.7.1.6). The six CHH patients represent almost the whole spectrum of mutations found. One patient is compound heterozygous for a base pair substitution (#2), two patients are homozygous for the most common 70A>G transition (#8 and #27), and three patients are compound heterozygous for a promoter duplication and a base pair substitution (#11, #16, #24).

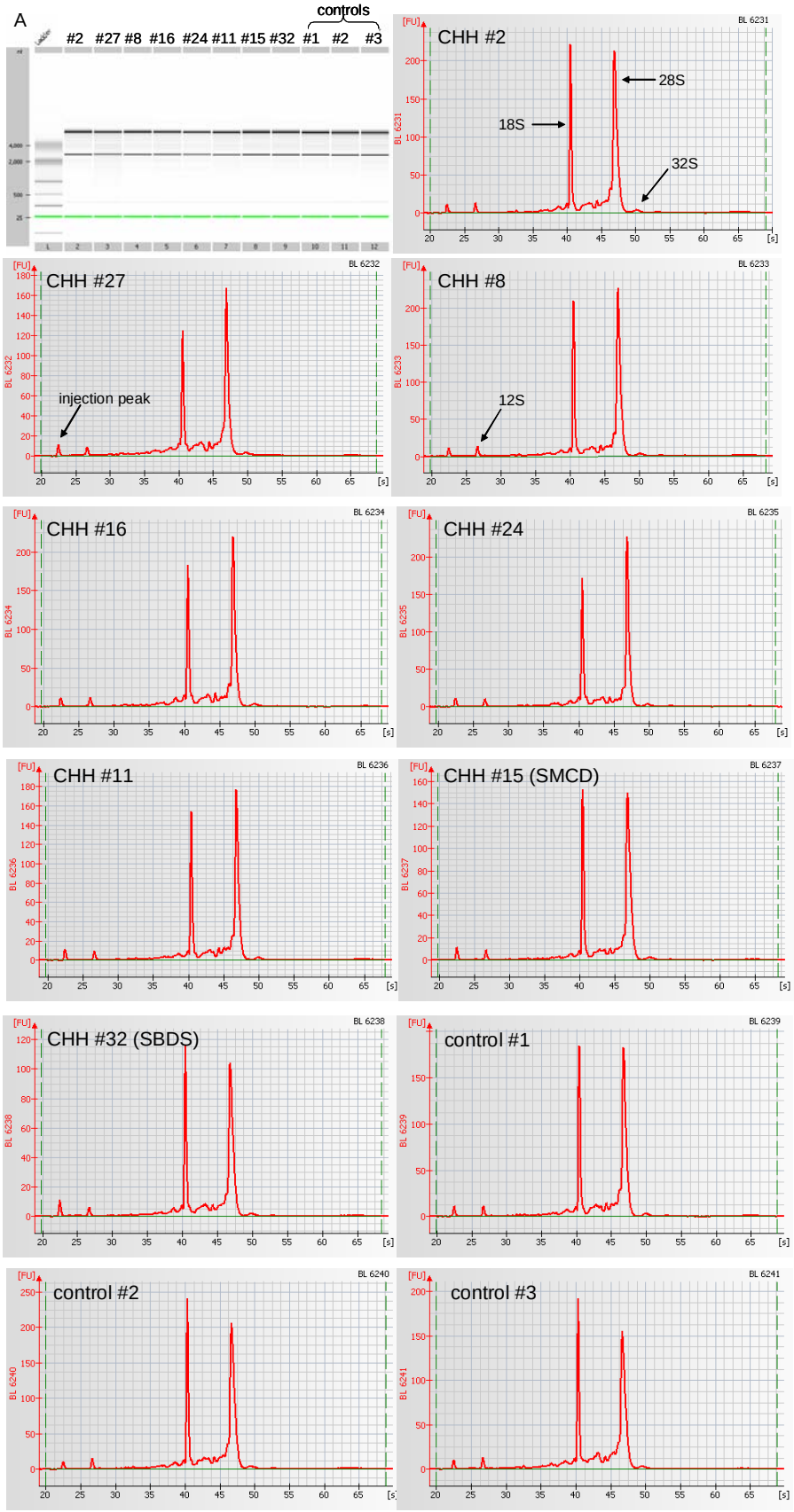

Fig. 23: Standard Quality Assurance of CHH patient total RNA.

The outputs of the Agilent Bioanalyzer 2100 are shown. The 32S, 28S, 18S and 12S rRNAs could be separated nicely. A: shows virtual gel figure generated by the Agilent software.

As shown in Figure 23 there was no difference in the ribosomal RNA processing observed. The quality assurance with Agilent Bioanalyzer 2100 also demonstrated the high quality of the RNA. The resolution of this instrument however is not high enough to look for changes in the small RNAs such as the 5.8S rRNA. To elucidate whether there might be an alteration in the processing of the 5.8S rRNA as observed in many *nme1* mutants in yeast (Chu et al., 1994; Lygerou et al., 1996) the total RNA was separated on a 2% agarose or a

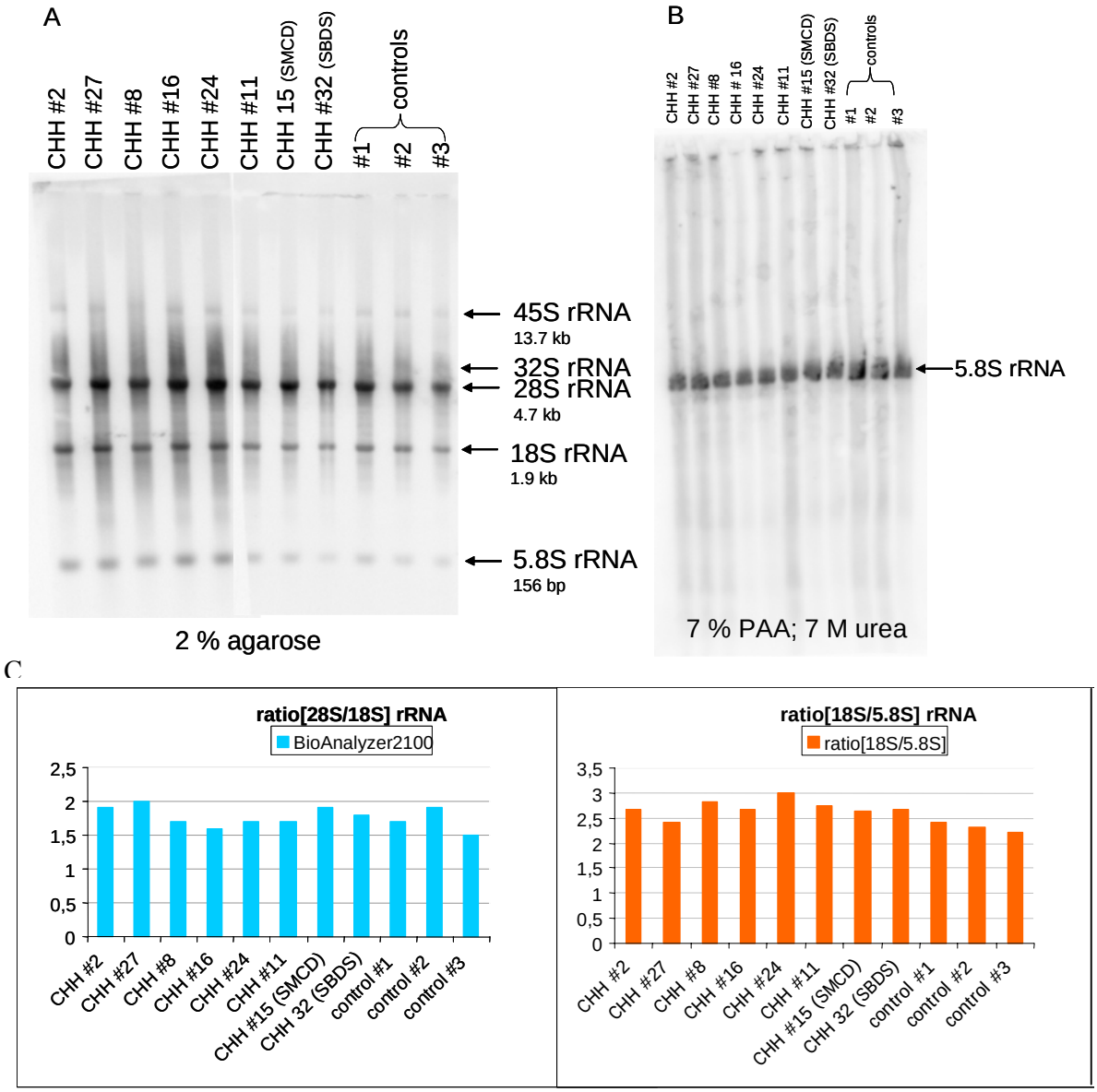

Fig. 24: Pre-ribosomal processing in CHH patient cell lines. Total rRNA has been isolated from EBV transformed lymphoblastoid cell lines of CHH patients and separated on (A) 2% agarose gel (B) 7% PAA;7M urea gel. A: hybridization with rRNA probes specific for the various species of pro-cessing (45S, 32S, 28S, 18S, and 5.8S rRNAs). B: shows specificity of the mature 5.8S rRNA probe. No shift of the 5.8S rRNA is seen in either the patients or the controls. C: Quantification of the ratios of different rRNA species with the Bio Analyzer 2100 (left) or the Storm ImageQuant software (right). No significant difference of the ratios in CHH patients vs. controls could be observed.

a 7% polyacrylamid gel, respectively (Fig. 24). The ratios of the different species was determined by the Agilent software for the ratio of the [28S/18S] rRNA and with the Image Quant software of the Storm phosphoimager system for the [18S/5.8S] rRNA ratio. As shown in Figure 24C there is no significant difference of the two ratios in CHH patients when compared to wt controls. This result suggests that the rRNA processing in the B-cells of the CHH patients tested is not affected. This is expected since CHH patients have a T-cell defect, if affected. T-cells among other blood cell types get destroyed during the EBV transformation procedure.

3.5 Microarray Analysis

Total RNA was isolated from two CHH patients (#2 and #8) and two sex and ethnicity matched controls with the RNeasy Midi Kit from Qiagen. Patient #2 was compound heterozygous for a 89C>G transversion and a 124C>T transition. Patient #8 was homozygous for the most frequently found 70A>G transition. The concentration and the quality of the total RNA was determined with the BioAgilent System in the Microarray Core Facility at Baylor College of Medicine, Houston, TX. The Mircoarray Core Facility at Baylor also performed the labeling of the total RNA as well as the hybridization of the microarray chips U133A and U133B from Affymetrix. These experiments were done in technical replicates with independent labeling and hybridization procedures. The data were then normalized with the R software. Genes that are up-regulated in CHH patients when compared to normal controls are listed in Table 10 and the down-regulated genes are shown in Table 11.

Table 10: Up-regulated in CHH patients

Affymetrix ID	gene name	gene symbol	Fold Change	Function
206637_at	G protein-coupled receptor 105	GPR105	4.9	G-protein coupled receptor protein signalling pathway; rhodopsin-like receptor activity
213524_s_at	putative lymphocyte G0/G1 switch gene	G0S2	4.2	regulation of cell cycle
203153_at	interferon-induced protein with tetratricopeptide repeats 1	IFIT1	3.2	immune response
206025_s_at	tumor necrosis factor, alpha-induced protein 6	TNFAIP6	3.2	signal transduction; inflammatory response
220532_s_at	LR8 protein	LR8	3.1	histogenesis and organogenesis

Affymetrix ID	gene name	gene symbol	Fold Change	Function
207815_at	platelet factor 4 variant 1	PF4V1	3.1	immune response; chemokine activity
201005_at	CD9 antigen (p24)	CD9	3.0	integral to plasma membrane
211506_s_at	Interleukin-8	IL8	3.0	G-protein coupled receptor protein signaling pathway; immune response; cell cycle arrest; neutrophil chemotaxis
208304_at	chemokine (C-C motif) receptor 3	CCR3	2.6	G-protein coupled receptor protein signaling pathway; rhodopsin-like receptor activity
211990_at	major histocompatibility complex, class II, DP alpha 1	HLA-DPA1	2.6	MHC class II receptor activity; antigen presentation; immune response
206207_at	Charot-Leyden crystal protein	CLC	2.6	antimicrobial humoral response; phospholipid metabolism; development
201563_at	sorbitol dehydrogenase	SORD	2.5	sorbitol metabolism, vision, zinc ion binding oxidoreductase activity
209189_at	v-fos FBJ murine osteosarcoma viral oncogene homolog	FOS	2.4	cell growth and/or maintenance; inflammatory response; regulation of transcription from Pol II promoter
206111_at	ribonuclease, RNase A family, 2 (liver, eosinophil-derived neurotoxin)	RNASE2	2.4	chemotaxis; RNA catabolism
206361_at	G protein-coupled receptor 44	GPR44	2.2	protein coupled receptor protein signaling pathway; rhodopsin-like receptor activity
203290_at	major histocompatibility complex, class II, DQ alpha 1	HLA-DQA1	2.2	MHC class II receptor activity; antigen presentation; immune response
205041_s_at	orosomucoid 1	ORM1	2.2	acute-phase response; transporter activity (extracellular space)
207111_at	egf-like module containing, mucin-like, hormone receptor-like sequence 1	EMR1	2.2	neuropeptide signalling pathway; cell adhesion receptor activity; calcium ion binding; G-protein coupled receptor activity
200986_at	serine (or cysteine) proteinase inhibitor, clade G (C1 inhibitor), member 1, (angioedema, hereditary)	SERPING 1	2.1	complement activation, classical pathway; serine protease inhibitor activity
206851_at	ribonuclease, RNase A family, 3	RNASE3	2.1	xenobiotic metabolism, RNA catabolism
219863_at	cyclin-E binding protein 1	CEB1	2.1	regulation of CDK activity; ubiquitin-protein ligase activity
202086_at	myxovirus (influenza virus) resistance 1, interferon-inducible protein p78 (mouse)	MX1	2.0	signal transduction; immune response; induction of apoptosis

Affymetrix ID	gene name	gene symbol	Fold Change	Function
211922_s_at	catalase	CAT	2.0	response to oxidative stress, electron transport
210029_at	indoleamine-pyrrole 2,3 dioxygenase	INDO	2.0	immune response; tryptophan catabolism; oxidoreductase activity; pregnancy
201631_s_at	immediate early response 3	IER3	2.0	cell growth and/or maintenance; apoptosis inhibitor activity
207328_at	arachidonate 15-lipoxygenase	ALOX15	2.0	electron transport; inflammatory response
208253_at	sialic acid binding Ig-like lectin 8	SIGLEC8	2.0	heterophilic cell adhesion; signal transduction; sugar binding transmembrane receptor activity
204415_at	interferon, alpha-inducible protein (clone IFI-6-16)	G1P3	2.0	immune response
201801_s_at	solute carrier family 29 (nucleoside transporters), member 1	SLC29A1	2.0	nucleoside transporter activity
205483_s_at	interferon, alpha-inducible protein (clone IFI-15K)	G1P2	2.0	immune response
209043_at	3'-phosphoadenosine 5'-phosphosulfate synthase 1	PAPSS1	2.0	adenylylsulfate kinase activity; sulfate adenylyltransferase (ATP) activity; ATP binding
209969_s_at	signal transducer and activator of transcription 1	STAT1	2.0	regulation of transcription; intracellular signaling; cytokine receptor signal transducer activity; regulation of cell cycle

Table 11: Down-regulated genes in CHH patients

Affymetrix ID	gene name	gene symbol	Fold Change	function
219759_at	leukocyte-derived arginine aminopeptidase	LRAP	-4.7	Peptidase_M1;membrane alanyl aminopeptidase activity
210873_x_at	apolipoprotein B mRNA editing enzyme, catalytic polypeptide-like 3A	APOBEC3A	-2.4	mRNA processing; zinc binding; hydrolase activity
205033_s_at	defensin, alpha 1, myeloid-related sequence	DEFA1	-2.3	xenobiotic metabolism; immune response
217753_s_at	ribosomal protein S26	RPS26	-2.2	structural constituent of ribosome
206488_s_at	CD36 antigen (collagen type I receptor, thrombospondin receptor)	CD36	-2.1	blood coagulation; cell adhesion; receptor activity; fatty acid metabolism
210321_at	granzyme H (cathepsin G-like 2, protein h-CCPX)	GZMH	-2.0	apoptosis; trypsin proteolysis and peptidolysis; chymotrypsin hydrolase
211734_s_at	Peptidase_M1;membrane alanyl aminopeptidase activity	FCER1A	-2.0	immune response; integral plasma protein; receptor signaling protein, IgE binding

The genes that are up-regulated in CHH patients are mainly genes that play a role in the immune response, cell cycle regulation and metabolism. The list of down-regulated genes in this microarray analysis is relatively short and more heterogeneous. The genes are involved in the immune response, RNA processing and some genes have enzyme activities.

3.5.1 *RMRP* expression level in CHH patients

Since ribosomal RNAs and genes that are not translated into proteins are not represented on the Affymetrix microarray chips quantitative real-time-PCR was performed to analyze the expression level of *RMRP* of three CHH patients when compared to six normal controls. Total rRNA isolated from whole blood (see 2.2.2) served as template for the reverse transcription that was performed as described in 2.4.4. An equal amount of cDNA for all samples was used for the quantitative PCR (see 2.4.5). Blood from CHH patients #2 (compound heterozygous for 89C>G; 124C>T), #8 (homozygous for 70A>G), and #16 (with a 10 bp promoter duplication -23_-14dup; 180G>A) as well as from their sex and ethnicity matched controls was available. The rRNA of patients #2, #8 and their corresponding controls has already been used in the Affymetrix chip assay (3.5). In addition three more

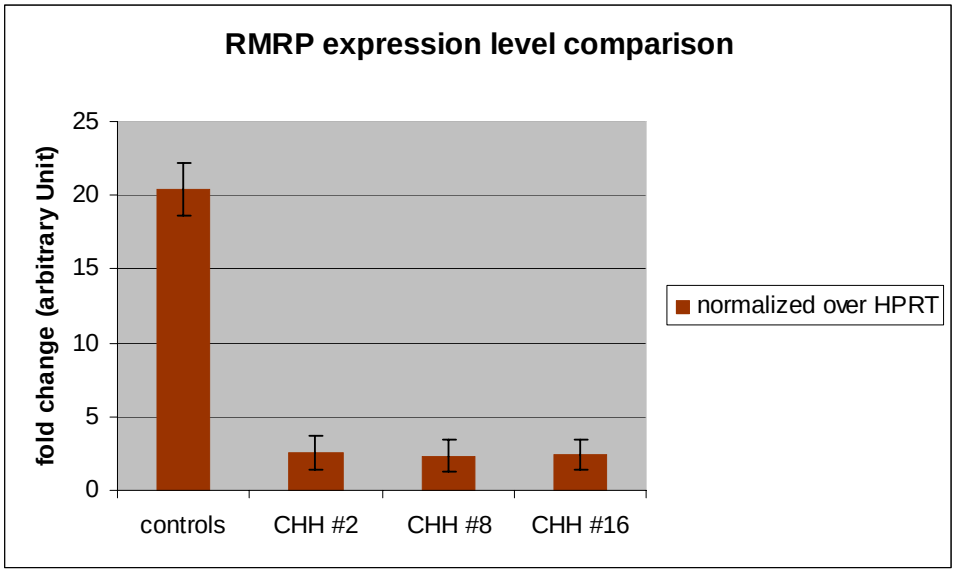

Fig. 25: Quantitative Real-Time PCR analysis of RMRP in CHH patients.

The RMRP expression level of three CHH patients was compared to six normal controls. RNA level of the RMRP transcript is approximately 6 – 7 fold downregulated compared to the controls. The expression level is normalized over the expression of the housekeeping gene HPRT.

rRNA samples from one control were added to the analysis. The blood samples from this person were taken at three different time points over a course of almost three years. The latter samples serve as a control of variability of gene expression over time in one healthy person. The RMRP expression level seems to be decreased in all three patients tested irrespective of the kind of mutation detected in these patients. Patient #2 is compound heterozygous for 89C>G and 124C>T, patient #8 is homozygous for 70A>G, and patient #16 is compound heterozygous for -23_-14dup and 180G>A. The expression levels were normalized using the housekeeping gene HPRT as a reference gene (Fig. 25).

3.6 Mouse Studies

3.6.1 In Situ Hybridization

The *Rmrp in situ* probes were generated as described in 2.12.3 and the *in situ* hybridization was performed as illustrated in 2.13.3. Pictures from the slides were taken under darkfield with the Axioplan 2 microscope from Zeiss (Germany) using the Axiovision software (Zeiss,

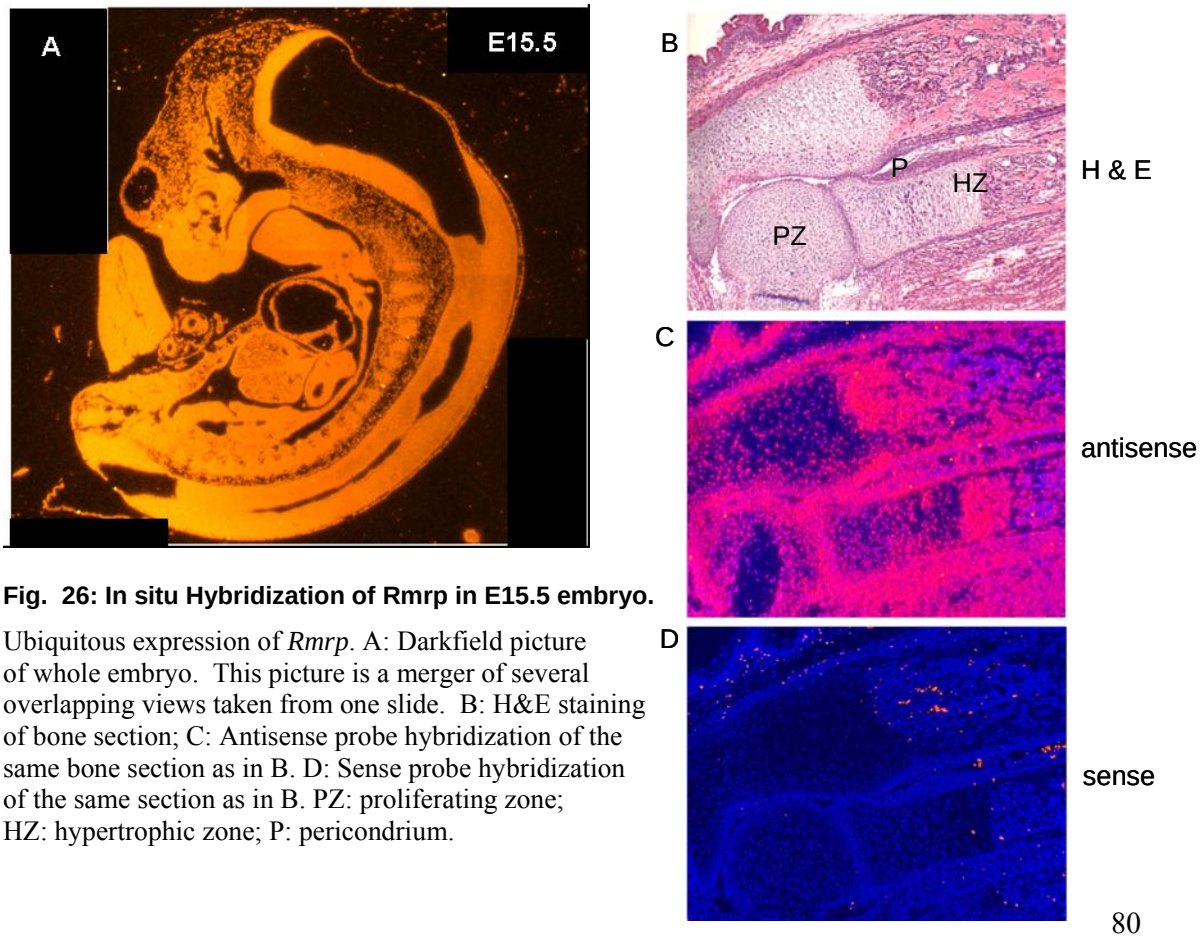

Fig. 26: In situ Hybridization of Rmrp in E15.5 embryo.

Ubiquitous expression of *Rmrp*. A: Darkfield picture of whole embryo. This picture is a merger of several overlapping views taken from one slide. B: H&E staining of bone section; C: Antisense probe hybridization of the same bone section as in B. D: Sense probe hybridization of the same section as in B. PZ: proliferating zone; HZ: hypertrophic zone; P: pericondrium.

Germany). As shown in figure 26 *Rmrp* is ubiquitously expressed at E15.5. E10.5, E11.5, E12.5, E13.5, E14.5, and E17.5 have been tested as well and strong and ubiquitous expression was also observed. It seems that *Rmrp* might be more strongly expressed in the hypertrophic chondrocytes and pericondrium than in the zone of proliferating chondrocytes. There is also very strong expression in the epiphysis.

3.6.2 *Rmrp* KnockOut Construct

To identify downstream targets of *Rmrp* a knockout construct has been generated. With this construct and through homologous recombination the endogenous *Rmrp* gene will be replaced by a neomycin cassette that is flanked by loxP sites that originate from *Drosophila melanogaster*. In the presence of *cre recombinese*, the sequence between two loxP sites aligned in the same direction is deleted (Fig. 27). The left recombination arm was amplified

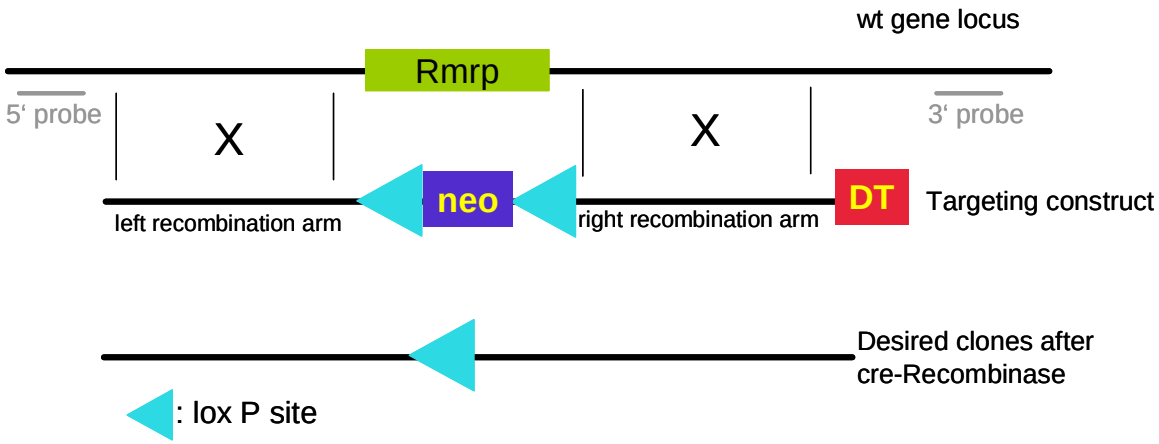

Fig. 27: Schematic of the strategy to generate an Rmrp knockout mouse model.

The wt gene locus is depicted at the top. Underneath is the targeting construct shown. The horizontal lines indicate the boundaries of the homologous sequences between the wt gene locus and the targeting construct. The 'X' marks the recombination events. DT stands for diphtheria toxin and serves as negative selection marker. Neo stands for neomycin that is used for positive selection.

with the primers 'Sal I-PH8' and 'Nhe I-PH9' (2.18.7.2.1) and replaced so the lacZ gene of the vector (Fig. 28). The right recombination arm was amplified with the primers 'Asc I-PH2' and 'Sac II-PH10' (2.18.7.2.1) as described in 2.4.2 with an annealing temperature of 61°C. The PCR-buffer was supplemented with 2% DMSO. The two arms were then cloned in a directional manner into the targeting vector that already contained the neo-loxP and the

DT cassettes, respectively (gift from Dr. Cornelius Boerkoel, Baylor College of Medicine, Houston, TX) (Fig. 28). The construct has been verified by sequencing of the junction

Fig. 28: Schematic of the knockout vector. The universal vector for generating knockout mice already contains a lacZ gene (blue),a neo cassette flanked by loxP sites (yellow), and a diphterin toxin gene (DT) (black). There are two multibple cloning sites. One before the lacZ gene and the second between the neo cassette and the DT gene. Restriction sites, that were used to generate the Rmrp knockout construct are boxed in green.

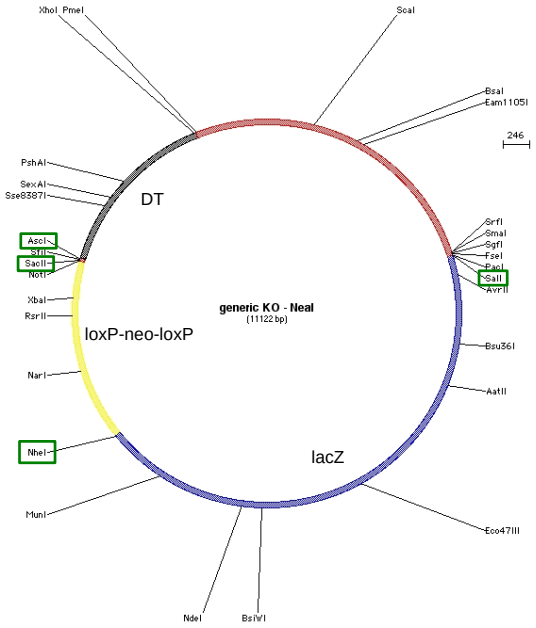

fragments and restriction digests with 3 different enzymes. The plasmid DNA (40 µg) containing the *Rmrp* knockout construct was linearized with *PmeI*. The DNA was purified by phenol/chloroform extraction followed by an ethanol precipitation. The concentration and

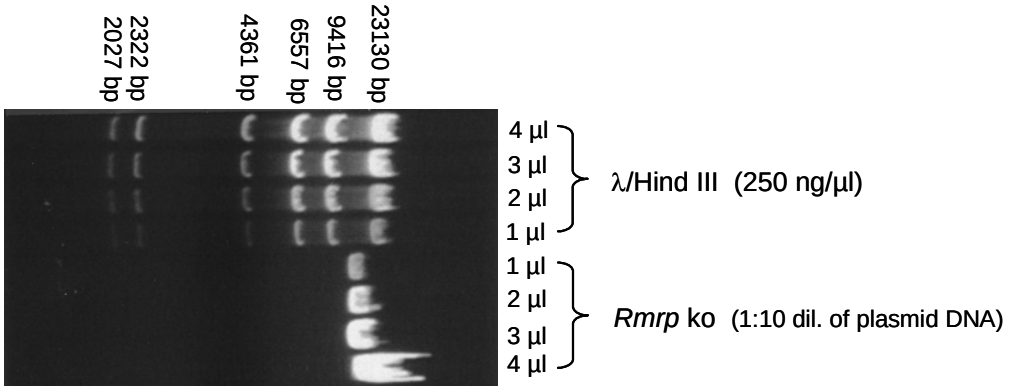

Fig. 29: Quantification of Rmrp knockout construct before electroporation.

The plasmid DNA containing the *Rmrp* knockout construct was linearized with Pme I and phenol/chloroform purified and then ethanol precipitated. 1 µl, 2 µl, 3 µl, 4 µl of a 1:10 dilution of the plasmid DNA was loaded on an agarose gel. To determine the DNA concentration of the construct the DNA standard marker (λ/Hind III from Roche) was loaded in different amounts on the same gel. The concentration can be estimated by comparing the intensity of the bands. The concentration of each band of the marker is supplied by the manufacturer).

purity of the DNA was determined by agarose gel electrophoresis (2.3.1.1) (Fig. 29). The electroporation of the construct into ES cells, the cell culture work, and the picking of 300 ES cell clones for DNA analysis was done by Yuqing Chen in the laboratory. The ES cell clones were grown in 96 well plates to saturation. Then genomic DNA was isolated (2.1.5) and digested with *KpnI*. To analyze the ES cells for the correct recombination event the DNA was transferred to a Nylon membrane and hybridized with the 5' probe and the 3' probe (Fig. 27) (2.13.1). The probes were amplified with the primers "5'probe F" and "5' probe R" and "3' probe F" and "3' probe R" respectively (2.18.7.2.1) with mouse genomic DNA as template as described in 2.4.1. The 5' probe spanned 892 bp and the 3' probe was 944 bp long. Both were labeled with [α32P] dCTP using random hexamers (2.12.1). The schematic view of the restriction pattern of the wt gene locus and the expected restriction pattern if the targeting construct has been integrated into the genome with homologous recombination is seen in Figure 30. Also the expected hybridization pattern is shown on the right. If no

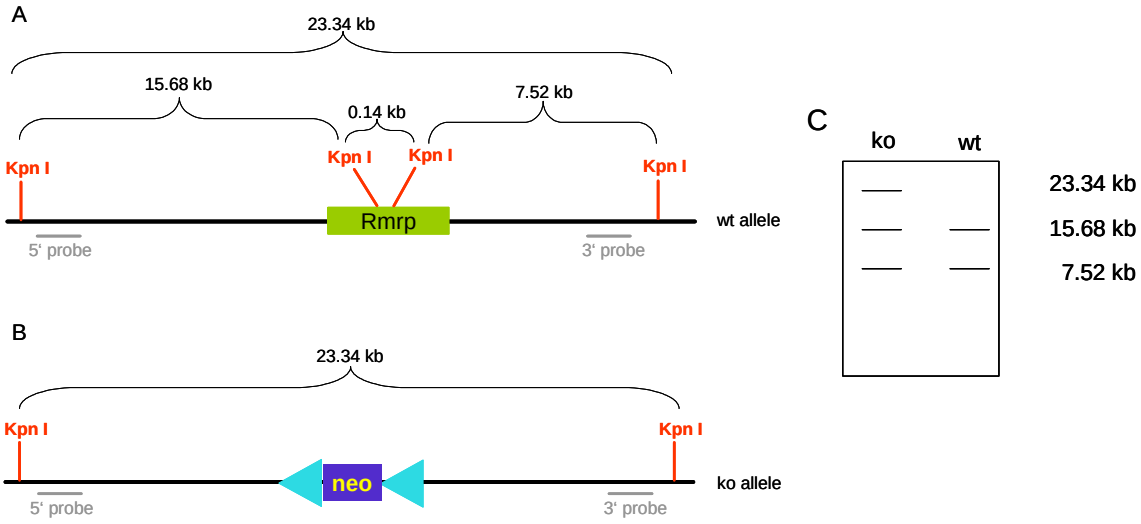

Fig. 30: Schematic of the expected Mini-Southern result.

A: The restriction map of the wt gene locus is shown when digested with Kpn I. B: The restriction map if the targeting construct has replaced the wt Rmrp gene through homologous recombination. C: shows the expected hybridization pattern when Mini-Southern is hybridized with the 5' and the 3' probe at the same time. On the right are the expected sizes in kb. ko: knockout; wt: wild type

homologous recombination takes place in the ES cells the Southern would show two bands (15.68 kb and 7.52 kb, respectively). If homologous recombination takes place in the ES cells three bands would be expected on the Southern (23.34 kb for the recombinant, 15.68 kb and 7.52 kb for the wt alleles, respectively). Unfortunately, none of the 300 ES cell clones screened was positive for the knockout allele. All clones showed the wt allele pattern (data

not shown. The signals were pretty weak and therefore the X-ray film did not scan very well.).

The *Rmrp* knockout construct was not further pursued, because the loss of function of *Rmrp* might be lethal. The very strong ubiquitous expression of *Rmrp* (Fig. 26) supports this hypothesis as well as the fact that there are no deletions of the whole *RMRP* gene described in CHH patients so far.

3.6.3 Transgenic Mouse Studies

The microarray studies showed a significant up-regulation of several cytokines and cell cycle regulatory genes. To test whether the overexpression of these genes might be responsible for the metaphyseal changes observed in CHH patients transgenic mice were generated. To overexpress the genes of interest in proliferating and hypertrophic chondrocytes the target genes were cloned under the control of the 6 kb Col2a1 promoter (Zhou et al., 1998) and the 10 kb *Col10a1* promoter (Zheng et al., 2003) respectively. The focus at this point was on the following two genes: *G0s2* and *IL8*.

3.6.3.1 G0s2

The study of the T-cell function of CHH patients suggests that T-cells of CHH patients have a defect in the G0 to G1 transition of the cell cycle (Kooijman et al., 1997). Therefore *G0s2* is a very good candidate for transgenic mouse studies, because it is a putative lymphocyte cell cycle switch gene that can promote the transition from the G0 to the G1 phase of the cell cycle or vice versa depending upon the stimulus (Cristillo et al., 1997).). It is approximately 4.2 fold up-regulated in an Affymetrix microarray experiment in two CHH patients when compared to two normal controls (Tab. 10). To study the effect of an overexpression of *G0s2* in proliferating and hypertrophic chondrocytes it was cloned under the control of the Type II collagen and the type X collagen promoters, respectively.

Figure 31 shows a cartoon of the G0s2 transgenic constructs and the cloning strategy. The mouse *G0s2* gene was amplified with the primers G0s2-F and G0s2-R flanked by *NotI* linkers

(2.18.7.2.2). Total RNA from an E18.5 mouse embryo was used as template in the RT-PCR reaction (2.4.4) and cloned under the control of the Col2a1 and Col10a1 promoter respectively. These two plasmids already contained a lacZ reporter gene and were generated by Dr. Guang Zhou in the laboratory. The Col2a1-G0s2-lacZ and Col10a1-G0s2-lacZ constructs were then released with Pme I and subcloned into the tyrosinase coat color vector obtained as a gift from Ting Fen Tsai (Hsiao et al., 2004) that also contained two chicken insulators. The whole transgene was released with Pac I (Fig. 31), gelpurified (2.3.2.2) and injected into pronuclei derived from the FVB/N mouse strain. The pronuclei injections were done by Yuqing Chen in the laboratory.

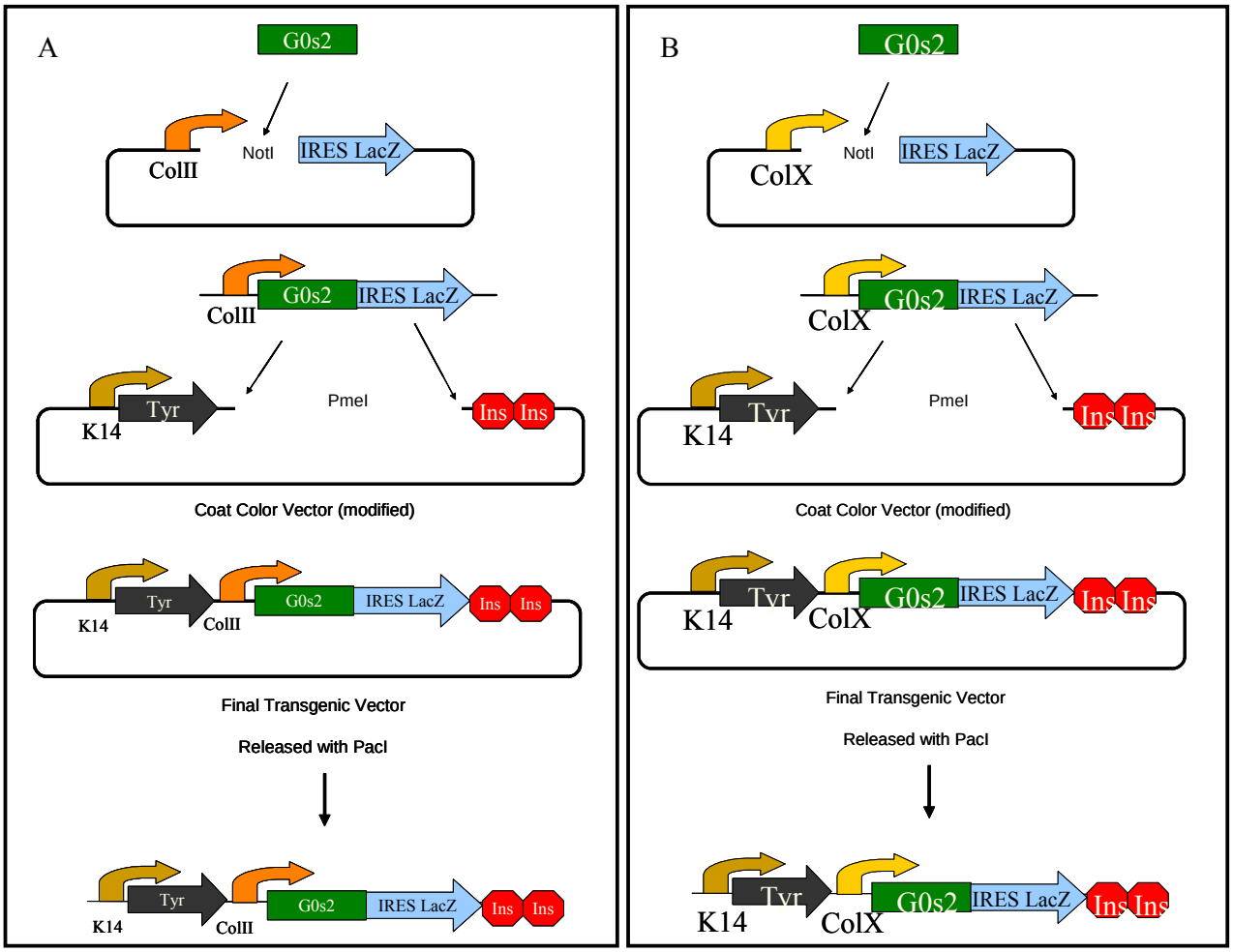

Fig. 31: Cloning strategy of *G0s2* transgenic mouse constructs.
The *G0s2* gene was amplified using E17.5 whole embryo total RNA as template for the RT-PCR and with Not I flanked primers. The PCR product was cloned in to the Not I site of the Col2a1-lacZ (A) and the Col10a1-lacZ (B) plasmid vectors, respectively. Both fragments were released with Pme I and cloned into the Pme I site of the coat color vector, between the tyrosinase gene driven by the K14 promoter and the two chicken insulators. The transgenic constructs were released with Pac I and injected into pronuclei. Tyr: tyrosinase; Ins: chicken insulators; ColII: Col2a1 promoter; ColX: Col10a1 promoter; K14: K14 (keratinocyte) promoter; IRES: internal ribosomal entry site.

3.6.3.1.1 Tyr-Col2a1-G0s2-lacZ

In order to evaluate the severity of the phenotype that might be caused by the expression of the transgene skeletal preparations of embryos at 18.5 dpc were performed and stained for β-galactosidase expression. In addition genomic DNA derived from the skin of all embryos was isolated and tested for the integration of the transgene into the mouse genome. The genotyping was done by PCR using Col2-F and G0s2-R as primers in the PCR reaction to amplify genomic DNA isolated from the tip of the tail or a piece of the skin from mouse embryos (2.1.3). All embryos whose skeleton stains blue were also positive in the genotyping PCR reaction. From two surrogate mothers 14 embryos could be isolated. Five of those showed a strong blue staining and 1 only a very weak staining for X-gal. Just by visually observing the embryos there was no obvious phenotype detectable. Three transgenic embryos and two wt littermates were then embedded into paraffin, sectioned and counterstained with Nuclear Fast Red. Since no obvious phenotype could be observed in the transgenic founders a transgenic mouse line has been established (2.17). The F1s of these lines have been collected at P1 (birth), stained with X-gal (2.11.2), genotyped by PCR (2.4.1), embedded into paraffin (2.15.1), sectioned (2.15.2), and the sections have been counter stained with Nuclear Fast Red (2.15.4) (Fig. 32).

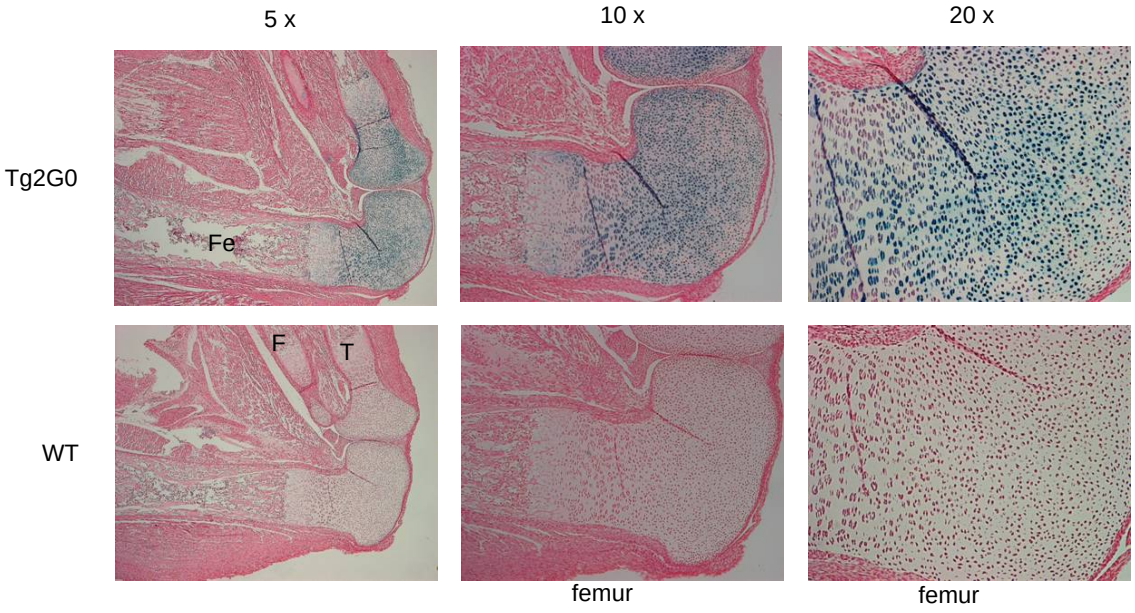

Fig. 32: Hind limb section of the Col2a1-G0s2-IRESLacZ transgenic mouse.

Hind limb paraffin sections after X-gal staining and counterstaining with Nuclear Fast Red. Fe: femur; T: tibia; F: fibula; WT: wild type; Tg2G0: Col2a1-G0s2-IRESLacZ transgenic.

No phenotype in the growth plate of all bones and transgenic mouse lines examined could be observed by microscopy. It might be that G0s2 does not play a role in the CHH phenotype, or does not play a role in the proliferating chondrocyte zone. It also might be that the transgene expression was not high enough to observe a phenotype, because none of the founders of the transgenic mouse lines had black eyes or any change in the coat color (color of the fur). The X-gal staining of the sections shows very nicely the tissue specific expression of the transgene.

3.6.3.1.2 Tyr-Col10a1-G0s2-lacZ

In order to evaluate the severity of the phenotype that might be cause by the expression of the transgene skeletal preparations of embryos at 18.5 dpc were performed and stained for β-galactosidase expression. In addition genomic DNA of the skin of all embryos was isolated and tested for the integration of the transgene into the mouse genome. The genotyping was done by PCR using Col10-F and G0s2-R as primers in the PCR reaction. From three surrogate mothers eleven embryos at 19.5 dpc could be isolated. One of these embryos stained blue for β-galactosidase expression even though three embryos were positive in the genotyping PCR reaction. Just by visually observing the embryos there was no obvious phenotype detectable. Two transgenic embryos and two wt littermates were then embedded into paraffin, sectioned and counterstained with Nuclear Fast Red.

Since no obvious phenotype could be observed in the transgenic founders a transgenic mouse line has been established (2.17). The F1s of these lines have been collected at P1 (birth), stained with X-gal (2.11.2), genotyped by PCR (2.4.1), embedded into paraffin (2.15.1), sectioned (2.15.2), and the sections have been counter stained with Nuclear Fast Red (2.15.4) (Fig. 33).

No phenotype in the growth plate of all bones and transgenic mouse lines examined could be observed by microscopy. It might be that G0s2 does not play a role in the CHH phenotype, or does not play a role in the hypertrophic chondrocyte zone. It also might be that the transgene expression was not high enough to observe a phenotype, because none of the founders of the transgenic mouse lines had black eyes or any change in the coat color (color of the fur). The

X-gal staining of the sections shows very nicely the tissue specific expression of the transgene in the zone of hypertrophy.

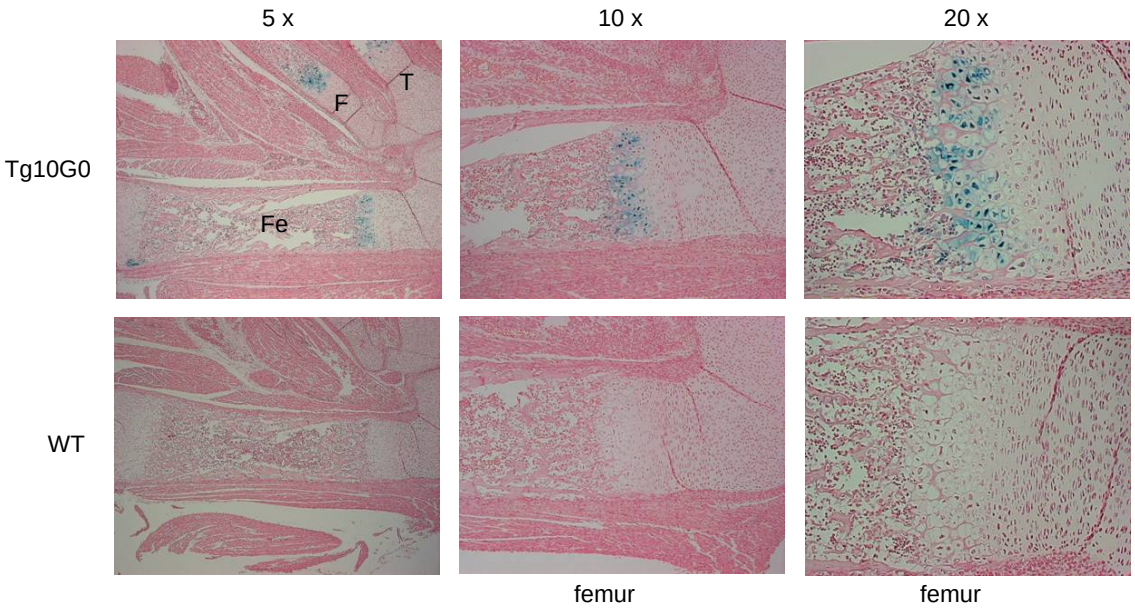

Fig. 33: Hind limb section of the Col10a1-G0s2-IRESLacZ transgenic mouse.

Hind limb paraffin sections after X-gal staining and counterstaining with Nuclear Fast Red. Fe: femur; T: tibia; F: fibula; WT: wild type; Tg10G0: Col10a1-G0s2-IRESLacZ transgenic.

3.6.3.2 hIL8

Besides the very well known function of *IL8* in the immune system and homeostasis, *IL8* and *GROα* induce articular chondrocyte hypertrophy and calcification through p38 and MAPK. P38 MAPK pathway activation also promotes hypertrophic chondrocyte differentiation and apoptosis. In addition transglutaminase 2 (TG2) is stimulated. TG2 among other transglutaminases modulates differentiation and calcification of chondrocytes and is a mediator of tissue repair (Merz et al., 2003). *IL8* is approximately 3 fold up-regulated in an Affymetrix microarray experiment in two CHH patients when compared to two normal controls (Tab. 10). To study the effect of an overexpression of *IL8* in proliferating and hypertrophic chondrocytes it was cloned under the control of the Type II collagen and the type X collagen promoters, respectively.

The lacZ reporter gene in a transgenic construct might inhibit the expression of the transgene of interest (Dr. Guang Zhou, Baylor College of Medicine, personal communication). To increase the transcription efficiency of the transgene the lacZ gene utilized in the previous transgenic mouse studies was replaced with a woodchuck hepatitis virus posttranscriptional regulatory element (WPRE). WPRE is thought to posttranscriptionally stimulate the expression of heterologous cDNA up to 10 fold in a variety of vector systems (Donello et al., 1998; Zufferey et al., 1999). This WPRE element followed by the human growth hormone polyadenylation signal (hGHpA) was also used in transgenic mouse studies by Dr. Asad Mian

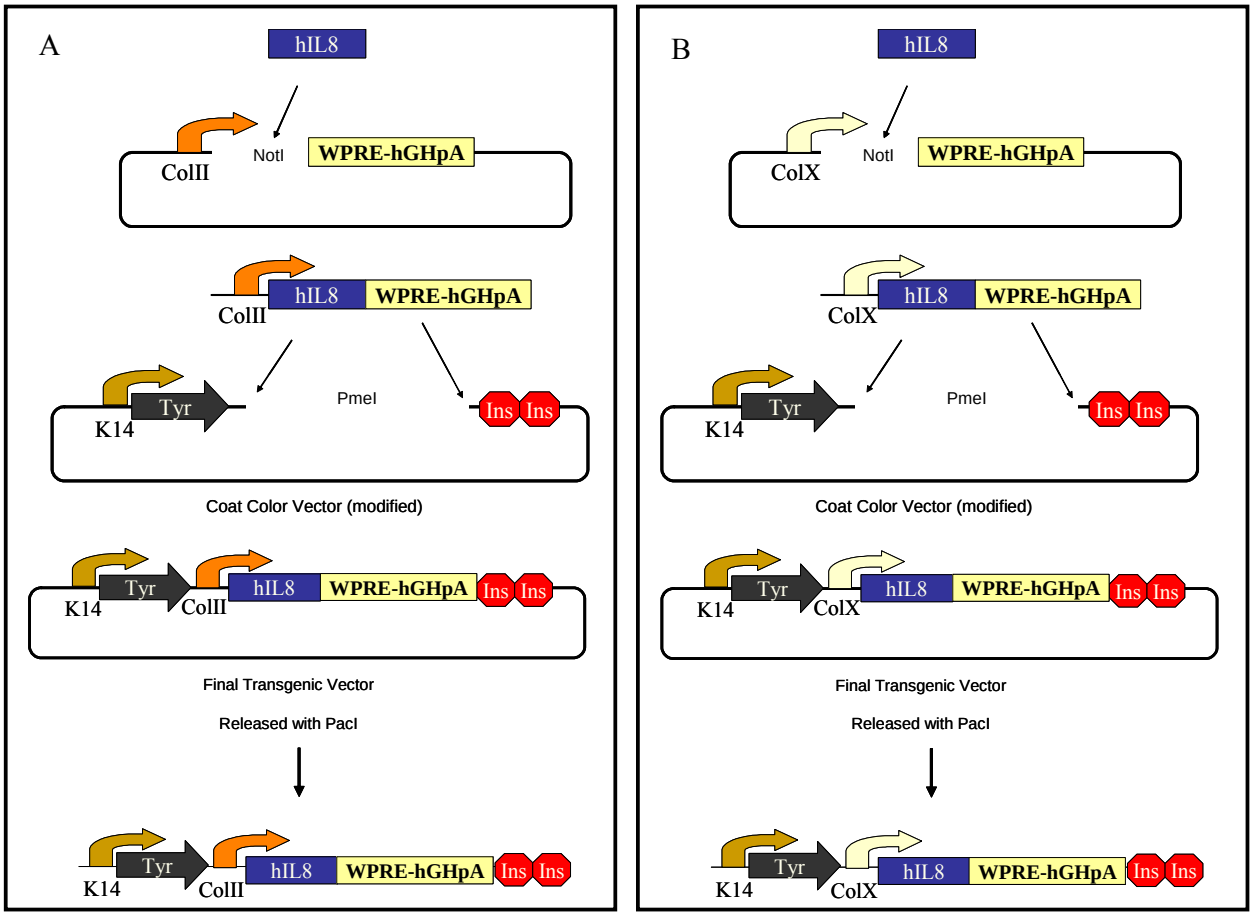

Fig. 34: Cloning strategy of hIL8 transgenic mouse constructs.

The *hIL8* gene was amplified using E17.5 whole embryo total RNA as template for the RT-PCR and with Not I flanked primers. The PCR product was cloned in to the Not I site of the Col2a1-WPRE (A) and the Col10a1-WPRE (B) plasmid vectors, respectively. Both fragments were released with Pme I and cloned into the Pme I site of the coat color vector, between the tyrosinase gene driven by the K14 promoter and the two chicken insulators. The transgenic constructs were release with Pac I and injected into pronuclei. Tyr: tyrosinase; Ins: chicken insulators; ColII: Col2a1 promoter; ColX: Col10a1 promoter; K14: K14 (keratinocyte) promoter; WPRE: woodchuck hepatitis virus posttranscriptional regulatory element; hGHpA: human growth hormone polyadenylation signal.

in the laboratory and he showed that the WPRE element indeed upregulates the transgene expression (Mian et al., 2005). So far there have been 4 different IL8 transgenic mice generated. Since there is no real mouse homolog to *IL8* the human *IL8* gene has been successfully used in these studies.

An overview of the *hIL8* transgenic constructs is depicted in figure 34. The human *IL8* gene was amplified with the primers IL8-F and IL8-R flanked by *NotI* linkers (2.18.7.1.4). Total RNA isolated from human blood (2.1.2) was used as template in the RT-PCR reaction (2.4.4) and cloned under the control of the *Col2a1* and *Col10a1* promoter respectively. A WPRE element was already inserted into the two collagen vectors by Feyza Engin in the laboratory. The Col2a1-hIL8-WPRE and Col10a1-hIL8-WPRE constructs were released with *PmeI* and subcloned into the tyrosinase coat color vector obtained as a gift from Ting-Fen Tsai (Hsiao et al., 2004). The transgene was then released with Pac I, gelpurified (2.3.2.2) and injected into pronuclei derived from the FVB/N mouse strain. The pronuclei injections were done by Yuqing Chen.

3.6.3.2.1 Tyr-Col2a1-hIL8-WPRE

Since there was no lethality phenotype reported in previous transgenic mouse studies no lethal phenotype was expected in this study either. Just by visually observing the embryos there was no obvious phenotype detectable. Since no obvious phenotype could be observed in the transgenic founders a transgenic mouse line has been established (2.17). The F1s of these lines have been collected at P1 (birth), genotyped by PCR (2.4.1), embedded into paraffin (2.15.1), sectioned (2.15.2), and the sections were stained with H&E (2.15.3) (Fig. 35).

No phenotype in the growth plate of all bones and transgenic mouse lines examined could be observed by microscopy. It might be that IL8 does not play a role in the CHH phenotype, or does not play a role in the proliferating chondrocyte zone. It also might be that the transgene expression was not high enough to observe a phenotype, because none of the founders of the transgenic mouse lines had any change in the coat color (color of the fur). Only one founder had black eyes and was used to generate the Col2a1-hIL8-WPRE transgenic mouse line. However, this founder and none of the following generations had any change in the color of their fur.

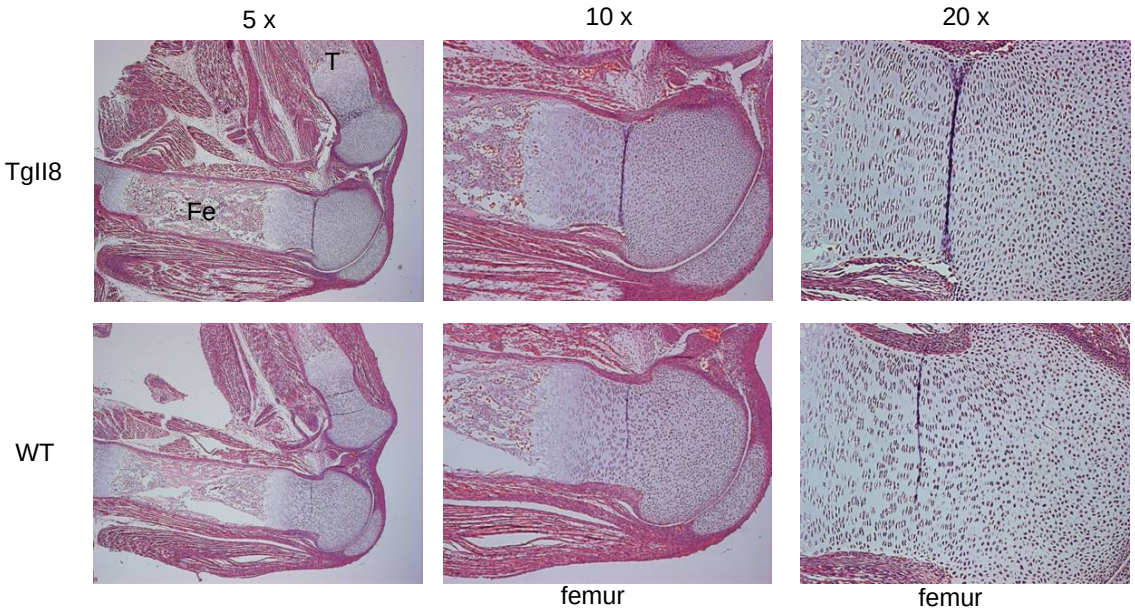

Fig. 35: Hind limb section of the Col2a1-hIL8-WPRE transgenic mouse.

Hind limb paraffin sections after H&E staining of a P1 mouse embryo. Fe: femur; T: tibia; WT: wild type; TgII8: Col2a1-hIL8-WPRE transgenic.

3.6.3.2.1 Tyr-Col10a1-hIL8-WPRE

Although this construct has been injected three times into pronuclei, but none of the recipient mothers have gotten pregnant up to now. This might be due to the construction work that has been going on at the same time. This construct is on hold right now, because it might be that IL8 does not play an important role in the pathogenesis of CHH as previously thought (see discussion).

3.7 Yeast Studies

Because *RMRP* is not encoded into a protein, it is hard to predict how a mutation in this gene might alter its function. *RMRP* is highly conserved among a variety of different species including *Arabidopsis thaliana* and *Saccharomyces cerevisiea* (1.4; Fig. 7). To study the effect of mutations of *RMRP* on its function, mutations that have been found in CHH patients and that were conserved between human and yeast were introduced into the yeast ortholog *NME1* (*nuclear mitochondrial endonuclease 1*).

3.7.1 Nme1 Knock Out

Before the effect of *nme1* mutations can be studied, an *nme1* deficient strain had to be generated. The endogenous *NME1* gene was replaced with a neomycin resistance gene amplified from the pFA6a.kanMX2 plasmid. The forward and reverse primer contained 18 bp of vector specific sequence with the addition of 50 bp homologous to the 5' and 3' NME1 flanking regions, respectively (2.8.2; Fig.11). The resulting PCR product was transformed into a wt yeast strain as described in 2.8.1 and positive transformants were selected on YPD plates containing G418. A single colony was picked and streaked out on a second G418 plate to obtain single colonies. To test for the correct recombination event, a single colony was picked and patched on a YPD plate to grow the yeast strains to logarithmic phase. The colonies were then patched on a sporulation plate and grown overnight at 30ºC. Tetrads were picked and dissected (Fig. 12 and Fig. 36.). If the correct recombination event took place, a two to two distribution of growing versus non-growing tetrads would be expected, since loss of *NME1* function results in lethality (Schmitt & Clayton 1992). As expected a two to two distribution of colonies was observed (Fig. 36). PCR with a neo-specific primer and one primer specific for the *NME1* gene locus that was designed outside the recombination arm was also performed (2.8.2). As shown in Figure 36 the correct yeast strains were obtained. To rescue the lethality of the loss-of-function of *NME1* an episomal plasmid containing the wt *NME1* gene was transformed into the G418-resistant strain described above. Again,

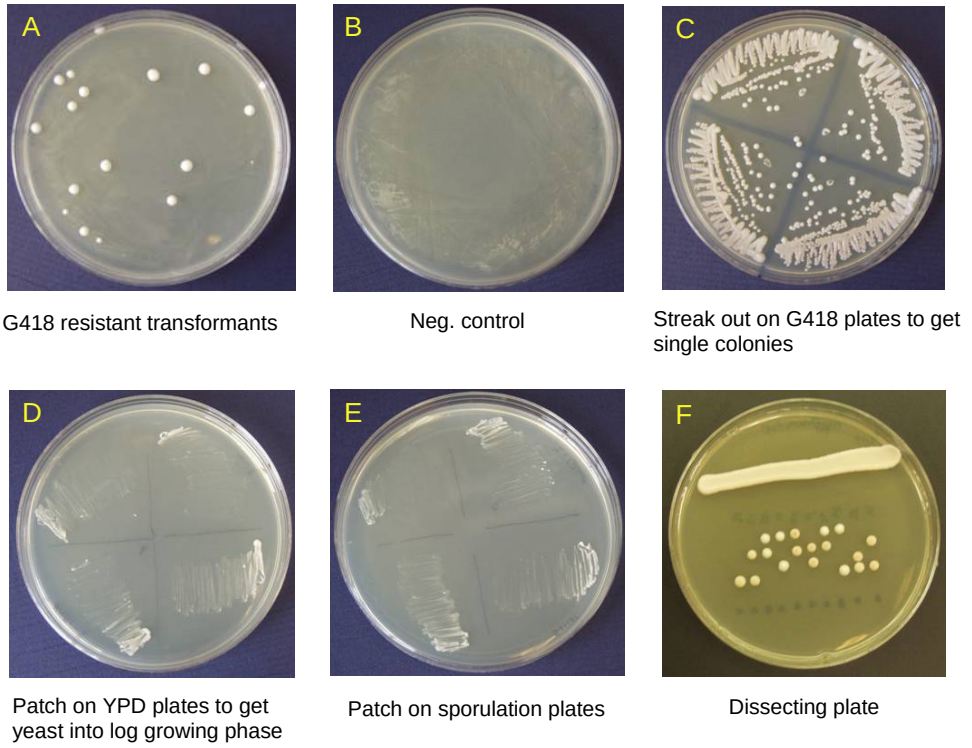

Fig. 36: Generation and test of nme1Δ.

A: The PCR product containing a neomycin expression cassette flanked by 50 bp of homologous sequence to the *NME1* wt locus was transformed into the YPH275 (2.17.4) yeast strain and selected for G418 resistant clones. B: negative control of the transformation. C: Streak out for single colonies. D: Patch on YPD plates to grow G418 resistant colonies to a logarithmic growth phase. E: The cells obtained in step D were patched on sporulation plates and grown over night at 30°C. F: Spores from E were dissected and a two to two growth of the tetrads can be observed, confirming that loss of *NME1* function is lethal and that a nme1Δ strain has been generated.

transformants were selected for G418 resistance. Colonies were picked and re-streaked on G418 plates to obtain single colonies. Single colonies were picked and subsequently patched on YPD plates, following an overnight incubation at 30ºC, then patched on sporulation plates and grown for one day before tetrads were picked and dissected as described above. The resulting colonies were then pheno- and genotyped (Fig. 37) by replica-plating on different selective plates. The growth on YPD-low ade plates tests for cell viability and the maintenance of an episomal fragment containing a suppressor gene, which gives rise to white colonies. Colonies that have lost the episomal fragment produce a red pigment. The growth on –ura plates shows the ability of the wt *NME1* gene on the episomal plasmid to rescue the lethal phenotype associated with the loss-of-function of the endogenous *NME1* gene. The growth on G418 plates indicates the occurrence of the recombination that resulted

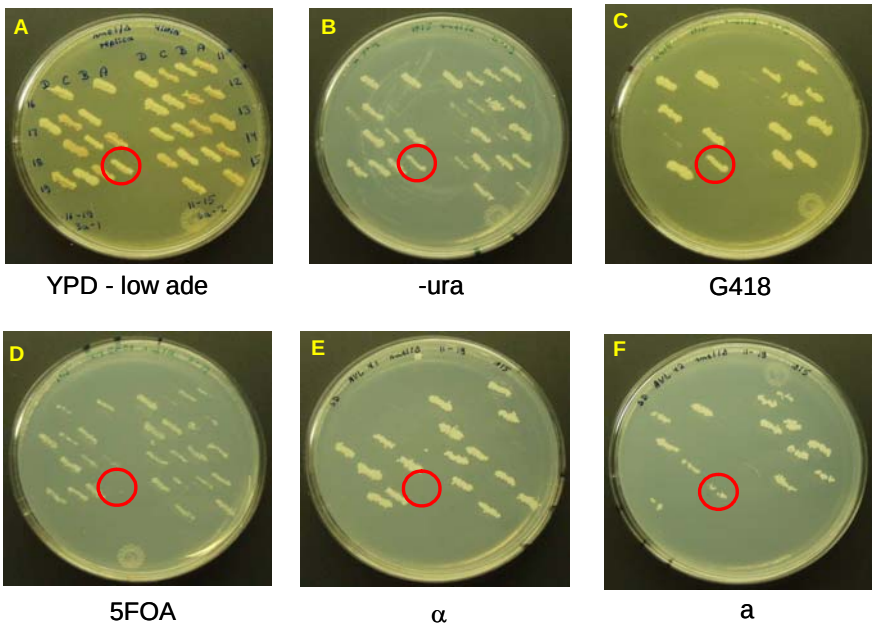

Fig. 37: Pheno- and Genotyping of the correct nme1Δ strain.

A: Dissected tetrads were grown on YPD/low ade medium to test for growth and maintenance of the episomal chromosome. B: Selection for the wt *NME1* gene on an episomal URA3 plasmid. C: Selection for the neomycin cassette integration. D: All yeast cells containing the URA3 plasmid should not grow on 5FOA. E and F: Mating test of tetrads. Only haploid yeast cells can mate and should only grow on either the α mating test plate or the a mating test plate. The red circle indicates the strain that has the correct pheno- and genotype.

in the integration of the neomycin resistance gene into the yeast genome. The replica plating on 5FOA plates tests for the tetrad containing the neomycin resistant gene, because 5FOA is used for negative selection of strains containing the URA3 plasmid. That means the episome with the WT gene is shuffled out and results in lethality because of the loss of function of the *NME1* gene. The mating test reveals the real haploid strains, because only haploid strains are able to mate. In summary a strain that grows as a white colony on a YPD/low ade plate, also exhibits growth on –ura, G418, and α or a mating tester plates, but does not grow on 5 FOA plates is the strain with the intended pheno- and genotype. This strain was selected and used for all further experiments. The following studies were performed with colonies 4C and 19A. Figure 37 shows the pheno- and genotyping of the correct yeast strain for the following experiments.

3.7.2 Functional tests of first *Nme1* Mutant Strains

3.7.2.1 Viability Test Of nme1 Mutant Strains

To study the effect of the human mutations, the point mutations were introduced into an episomal Nme1 construct via a 2-Step-PCR (2.4.3). The mutations were cloned into a CEN vector containing the LEU2 gene as a positive selection marker. At the beginning of this work we concentrated on the so-called 'Main Finnish' mutation – a 70A→G base pair substitution – because of the lack of our own CHH patient cohort at that time. In order to make it easier in the future to study the effect of human mutations, the ability of the human *RMRP* transcript under the control of the ADH promoter that is constitutively active in yeast to rescue the lethality was tested. As a control the *NME1* transcript was also cloned under the control of the ADH promoter. These constructs were all cloned on a LEU2, CEN plasmid and transformed into the nme1-Δ/pNME1 URA3, CEN strain (3.8.1, Fig. 37). As experimental controls the *NME1* wt gene was also cloned into a LEU2, CEN plasmid and an empty vector served as a negative control.

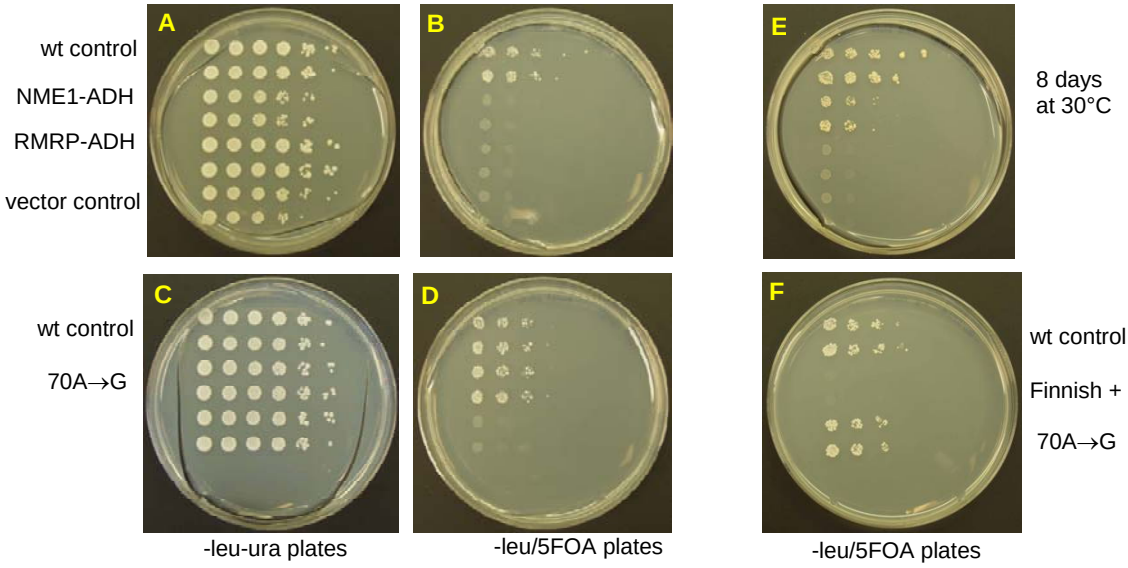

Fig. 38: Viability test of the first nme1 mutant strains.

All experiments were done in duplicates. On each plate a 1:10 dilution from the left to the right was performed. A and C: control for cell number. B, D, F: viability test of different yeast strains when the wt plasmid was shuffled out by growth on 5FOA plates. The wt control and the $nme1^{70A>G}$ mutant sustain growth. All other strains are lethal. E: After 8 days of incubation at 30°C the NME1 wt gene under the control of the ADH promoter seems to grow very slowly.

70A>G plasmid was able to rescue the lethality and growth was indistinguishable from the wt plasmid whereas neither the pNME1 nor the pRMRP under the control of the ADH promoter plasmids were able to complement the growth defect. After 8 days of incubation the appearance of colonies containing pNME1 under the control of the ADH promoter were observed. These results indicate that although the ADH promoter is a very strong and a constitutive active promoter, it is not sufficient to rescue the lethal phenotype. It is possible that *NME1* is not processed correctly after transcription, because the ADH promoter is usually recognized by the Pol II promoter machinery and *NME1* is normally transcribed by Pol III. Interestingly, when a second plasmid containing a mutation in addition to the 70A>G base pair substitution was introduced, because of a PCR artifact, lethality was observed as well (Fig. 38F).

3.7.2.2 Chromosomal Stability Test

RMRP is also thought to be involved in maintaining or stabilizing chromosomes during cell division (Cai et al., 2002). Because human patients are susceptible to cancer, the most common human mutation 70A>G was tested for its ability to affect chromosomal stability during mitosis. In this assay, the maintenance of a chromosomal fragment containing a suppressor gene that will give white colonies was followed. With serial passage and loss of this fragment early in cell division, colonies will appear red. For this experiment the nme1-Δ/pNME1 LEU2, CEN and the nme1-Δ/pnme170A>G LEU2, CEN were transformed with a plasmid containing the ade suppressor gene and a tryptophan gene for positive selection. Both strains were grown until the logarithmic phase and plated for single colonies on –leu plates. The cells were diluted so that around 150 cells could be expected to grow on each plate. The calculation was based on the assumption that a culture in logarithmic phase contains approximately 3x106 cells/ml at an $OD_{600nm} = 0.1$.

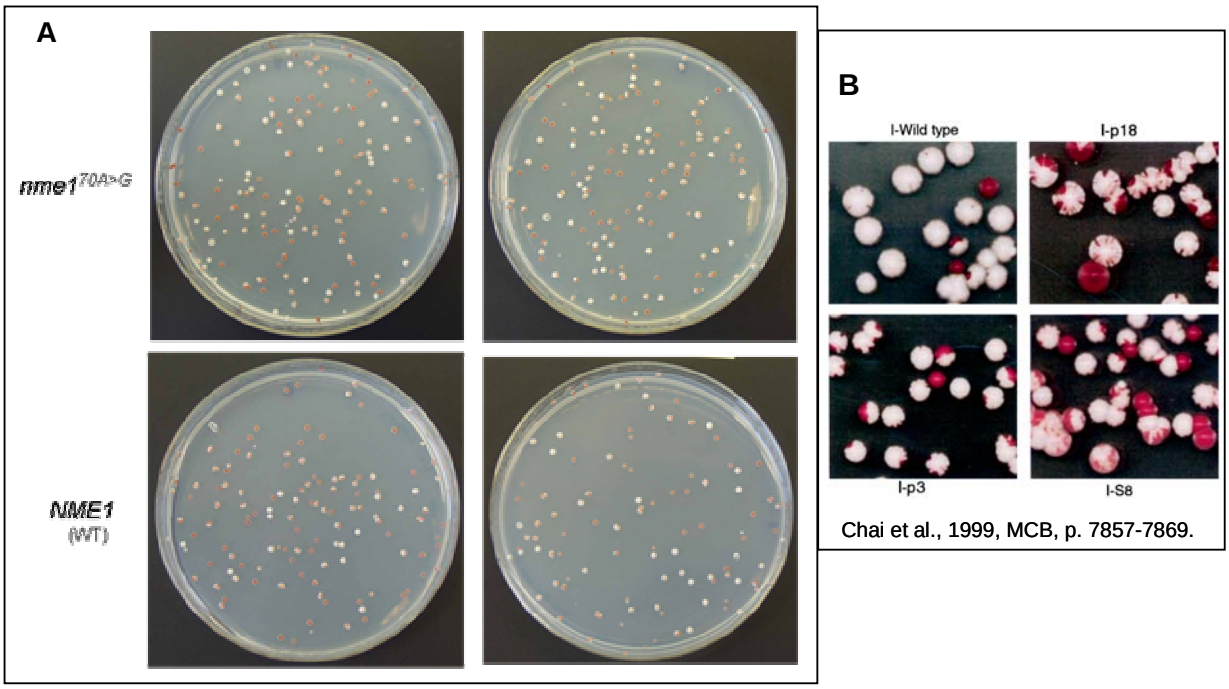

Fig. 39: Chromosomal stability test of nme170A>G mutant.

A shows the comparison of the chromosomal segregation of an episomal chromosomal plasmid in WT and mutant strains. There is no difference in the red/white sectoring between the mutant and the wt strain. B: shows an example what to expect, if there would have been decreased chromosomal stability during mitosis. In the upper left corner a wt strain is depicted. All other panels show mutant strains with loss of chromosomal stability in various degrees from Cai et al., 1999.

The colonies shown on the plates in Figure 39 were counted and grouped in different categories. White colonies contain the episomal chromosomal fragment. Red colonies have lost the chromosomal fragment early during the first cell divisions and red/white sectored colonies have lost this fragment later during the cell divisions. The earlier the chromosomal fragment is lost the redder the colony will grow (Fig. 39 B right panel).

Table 12: Colony count of chromosomal stability test of nme170A>G mutant

Strain	White colonies	Red colonies	Sectored colonies	White small colonies	total
4C wt	6 (4.8 %)	54 (43.5 %)	62 (50.0 %)	2 (1.6 %)	124
19A wt	14 (13.6 %)	31 (30.1 %)	56 (54.4 %)	2 (1.9 %)	103
4C 70A>G	13 (8.8 %)	51 (34.5 %)	77 (52.0 %)	6 (4.1 %)	148
19A 70A>G	14 (8.8 %)	53 (33.3 %)	86 (54.1 %)	6 (3.7 %)	159

Two nme1-Δ/pNME1 strains (4C WT, 19A WT) were tested as well as two nme1-Δ/pnme1$^{70A<G}$ (4C 70A>G, 19A 70A>G). White colonies contain the episomal chromosomal fragment. Red colonies have lost the chromosomal fragment early during the first cell divisions and red/white sectored colonies have lost this fragment later during the cell divisions. White small colonies indicate loss of mitochondria.

On either the WT or the *nme1*$^{70A>G}$ mutant background, no differences were observed in the percentage of red versus white colonies. This suggests that the most common mutation does not alter proper chromosome segregation during mitosis.

3.7.2.3 Mitochondrial Function Test

In Table 12 a slight increase in the number of cells that grow as white small colonies on low ade plates indicated a possible increase in mitochondrial depletion. The difference was most likely not statistically significant, but because *RMRP* has been implicated in mitochondrial DNA replication (Chang and Clayton 1987) the mitochondrial activity of *nme1* mutant strains was studied. In this experiment, the ability of the 70A>G allele to grow using only glycerol as a carbon source at different temperatures was tested (Fig. 40). Yeast mutations affecting mitochondrial function will often give a growth or lethality phenotype. This experiment was

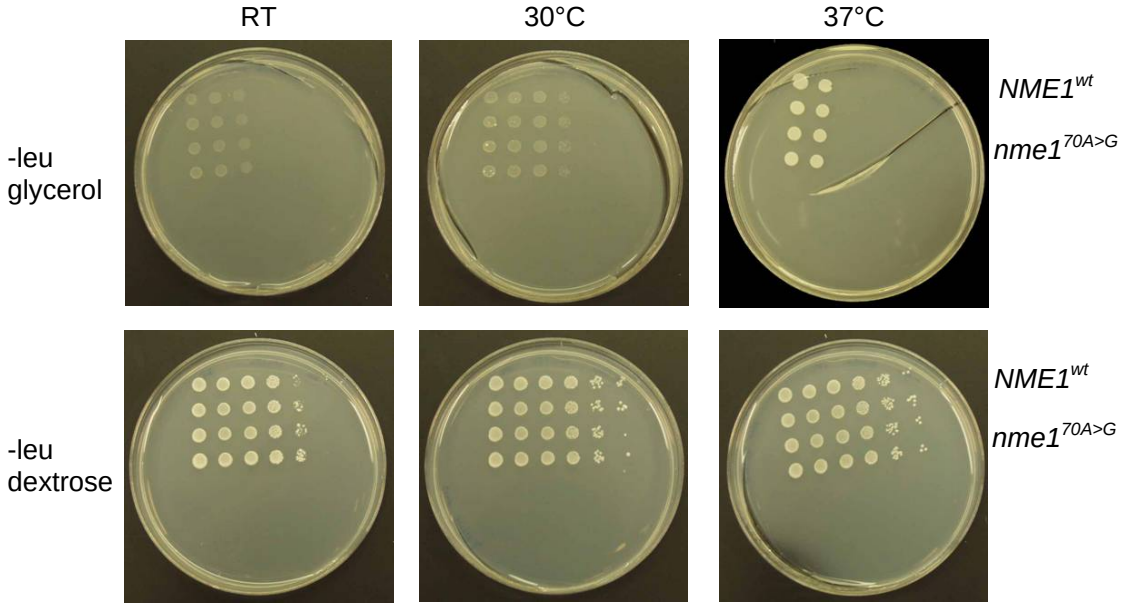

Fig. 40: Mitochondrial function test of nme170A>G mutant.

On each plate from the left to the right is a 1:10 dilution of the yeast cells. The first two rows are *NME1* wt strains. The third and forth row are *nme1*$^{70A>G}$ mutant strains. The plates were incubated at different temperatures; RT, 30°C, and 37°C. Upper panel: test plates for mitochondrial function of *nme1*$^{70A>G}$ mutant strains by growth on glycerol as carbon source. Lower panel: Control plates for cell number and normal growth with dextrose as carbon source. RT: room temperature; WT: wild type

done in duplicates. On each plate from the left to the right is a 1:10 dilution of the yeast cells. The first two rows are *NME1* wt strains. The third and forth row are *nme1*$^{70A>G}$ mutant strains. These strains were replica plated on –leu plates containing dextrose as a carbon source (Fig. 40 lower panel) that serves as a control for cell numbers and on –leu plates

containing glycerol as the only carbon source (Fig. 40 upper panel). All plates were then incubated at different temperatures; room temperature, 30°C and 37°C. As shown in Figure 40 there is no growth difference between the mutant and the wild type strains.

In a more general assay for mitochondrial function or depletion the ability to produce a red pigment was tested. Deficient mitochondrial function will cause small white colonies while normal colonies will appear red. This experiment (Fig. 41) was done in duplicates. Yeast cells were grown to logarithmic phase and spread out for single colonies so that around 200 cells could be expected on each plate. The cells were then categorized into red colonies and

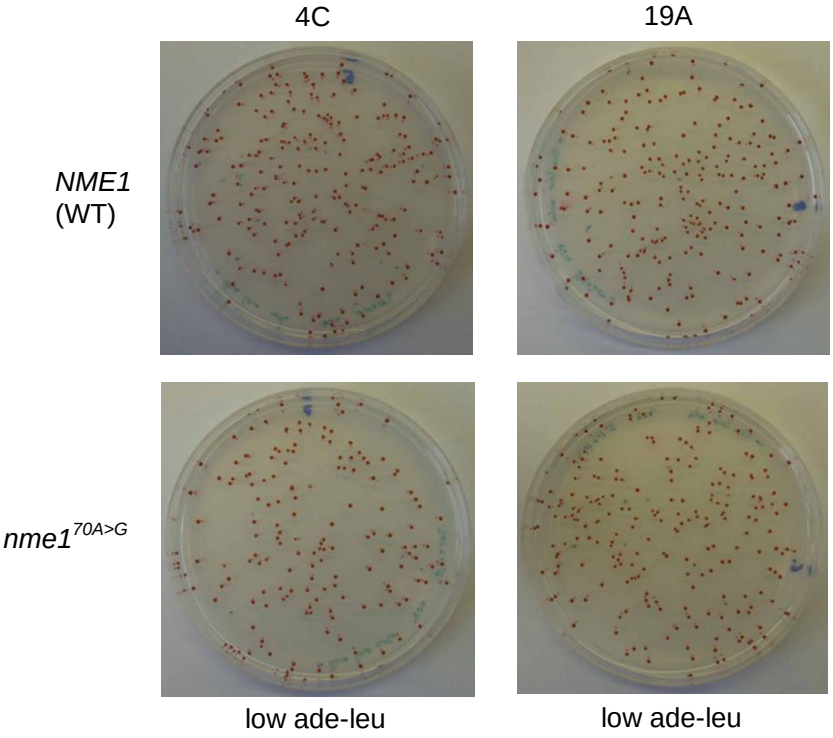

Fig. 41: Mitochondrial depletion test of the nme170A>G mutant. Normal yeast cells will grow as a red colony. Yeast cells with increased mitochondrial depletion will grow as white colonies. Upper panel WT control, lower panel: nme170A>G mutant strain. No white colonies could be observed on either plate indicating that mitochondrial function is normal in the mutant strains.

Table 13: Quantification of mitochondrial depletion test

Strain	Red colonies	White colonies	Small red colonies	Total
4C wt	203 (91.4 %)	0	19 (8.6 %)	222
19A wt	132 (97.8 %)	0	3 (2.2 %)	135
4C 70A→G	165 (96.5 %)	0	6 (3.5 %)	171
19A 70A→G	224 (96.6 %)	0	8 (3.4 %)	232

white colonies and counted (Tab. 13). No white colonies were observed on the WT plate as well as on the plate containing the mutant strain.

Again using this independent assay, there was no difference between the wt and the nme1$^{70A>G}$ allele. Hence, the most frequently found mutation does not seem to affect mitochondrial function in yeast.

3.7.3 Functional tests of second set of *nme1* mutant strains

Since the human RMRP gene does not rescue the lethality four more mutations were introduced into the *NME1* gene via 2-Step-PCR (2.4.3). These mutations were found in CHH patients referred to the laboratory at a later time point of this study and were conserved between human and yeast (Fig. 42). The 2-bp deletion mutant was introduced, because it has been shown that only deletion mutants show a phenotype (Shadel et al., 2000). This deletion

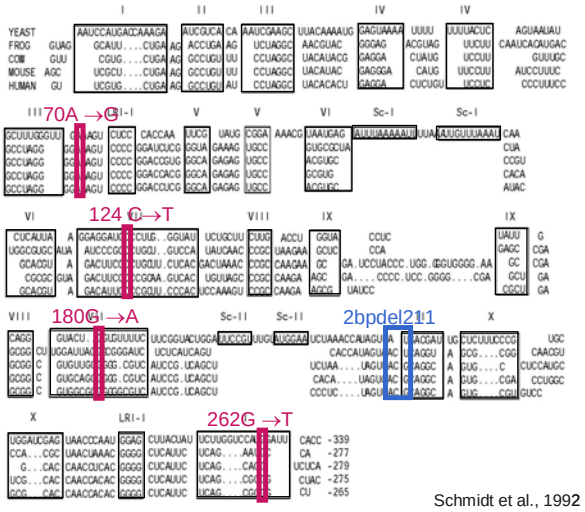

Schmidt et al., 1992

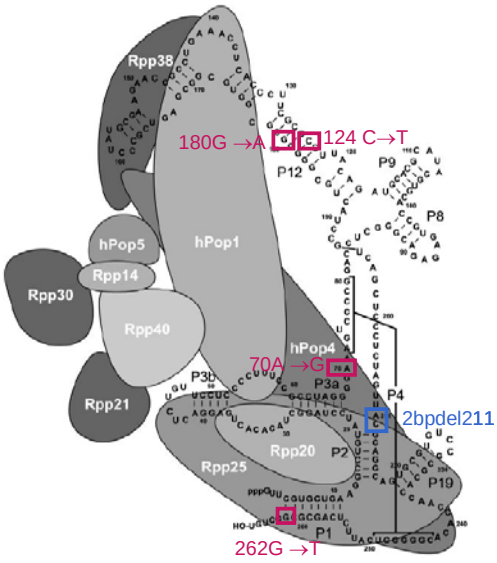

human *RMRP* secondary structure

Welting et al., 2004

Fig. 42: The four new nme1 mutations.

The mutations highlighted in red were found in CHH patients and were conserved between human and yeast. The mutation in blue has not been found in a CHH patient, but the deletion spans the region of a human mutation (211C>G; Tab. 3). On the left is the secondary structure of RMRP is depicted and the position of the mutations are indicated. The three new point mutations might affect a stem loop structure whereas the 70A>G and the 2bpdel might affect the P4 helicase structure. (Schmitt et al., 1992; Welting et al., 2004)

might affect the helicase P4 structure in the RNase MRP ribonucleotide complex. Interestingly, all 'new' mutations shown in red in Figure 42 might be involved in building a stem loop structure of the *RMRP* gene (Fig. 42).

To make the direct comparison to the human mutations easier, the bp numbering of the human positions was kept. Since the yeast *NME1* gene is 72 bp longer, the bp position of the mutations introduced into the yeast gene are therefore slightly different. Table 14 gives a summary of the actual positions of the mutations in the yeast *NME1* gene compared to the human mutations found in CHH patients and that are conserved among all species.

Table 14: Nomenclature of the yeast mutant strains

Human *RMRP*	Yeast *NME1*	Name of yeast mutant strain
70A>G	84A>G	*nme1*$^{70A>G}$
124C>T	168C>T	*nme1*$^{124C>T}$
180G>A	216G>A	*nme1*$^{180G>A}$
211C>G	267_268delAT	*nme1*^{2bpdel}
262G>T	331G>T	*nme1*$^{262G>T}$

The positions of the human mutations are compared with the position of the conserved base pair in the yeast gene. The right column summarizes the name of the respective yeast mutant strain. For easier direct comparison the human base pair positions are kept.

The above listed mutations were introduced into the NME1 gene via a 2-Step-PCR (2.4.3). Yeast genomic DNA (2.1.6.4) was used as template for the first PCR reaction (Fig. 43A). The annealing temperature was 58°C and the primer sequences are listed in 2.18.7.3.

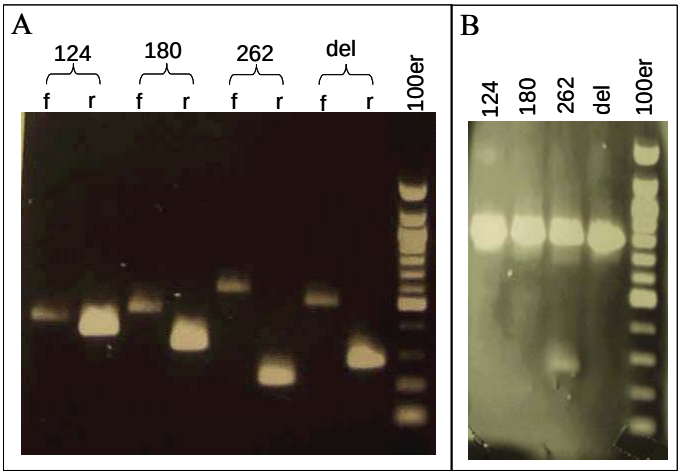

Fig. 43: Gel pictures of the Two-Step-PCR of the site directed mutagenesis on the NME1 gene.

A: First step of the PCR reaction.
B: Second step of the PCR reaction.
The numbers represent the introduced mutations (see Tab. 14).
f: forward primer contains mutation;
r: reverse primer contains mutation.
100er : 100 bp ladder from New England Biolabs (Beverly, MA)

The PCR products were purified and subcloned into the pGEM T vector and checked for the correct introduction of the intended point mutation via direct sequencing (2.5.1) of the plasmid DNA (2.1.6.2). The mutated *nme1* gene was then cloned into YCplac111 that is a LEU2, CEN vector.

3.7.3.1 Viability test of second set of nme1 mutant strains

As already described in 3.7.2.1 multiple episomal plasmids with different mutations as listed in Table 14 were generated, transformed in the *nme1Δ* strain, and tested for viability (Fig. 44).

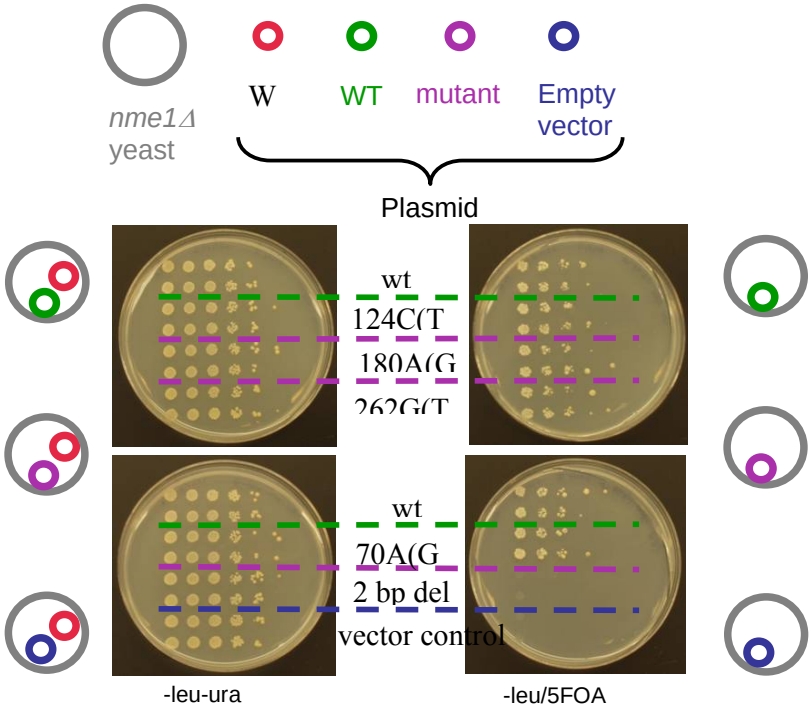

Fig. 44: Viability test of the second set of nme1 mutant strains.

All experiments were done in duplicates. On each plate a 1:10 dilution from the left to the right was performed. The plates on the left side control for cell number. The plates on the right side test for viability of the mutant *nme1* strains. The circles on the left and the right side of the Petri dishes respectively illustrate the genotype of the yeast strains in each row. All, but one mutant strain, are able to sustain growth. The *nme1*^{2bpdel} mutant is lethal.

Figure 44 shows the result of the viability test of the new mutant strains. The control for this experiment is on the left. The assay is depicted on the right side. When a wild type NME1 is present on one episomal plasmid (red circle) the yeast grew equally well irrespective of the nature of the *NME1* gene on the other plasmid. This was equally true if the NME1 gene was

another wild type NME1 (green circle), any of the RMRP human mutations (violet circle), or an empty plasmid (blue circle). Interestingly, when the WT episomal plasmid (red circle) was shuffled out the other plasmids containing the point mutations were able to sustain growth again, but the strain with the 2-bp deletion does not grow without the WT episome. In summary, the human RMRP point mutations that were introduced into the NME1 gene do not abolish its essential function in yeast, while the 2-bp deletion did so.

3.7.3.2 Cell Cycle Analysis via FACS

Cai et al. (Cai et al., 2002) demonstrate that RMRP plays a critical role in the cell cycle progression at the end of mitosis. A cell cycle arrest or a very severe cell cycle delay could be observed by visual examination of yeast colonies with a light microscope. Yeast can morphologically be distinguished in the different stages of the cell cycle. A very slight cell cycle delay can also be detected by FACS analysis.

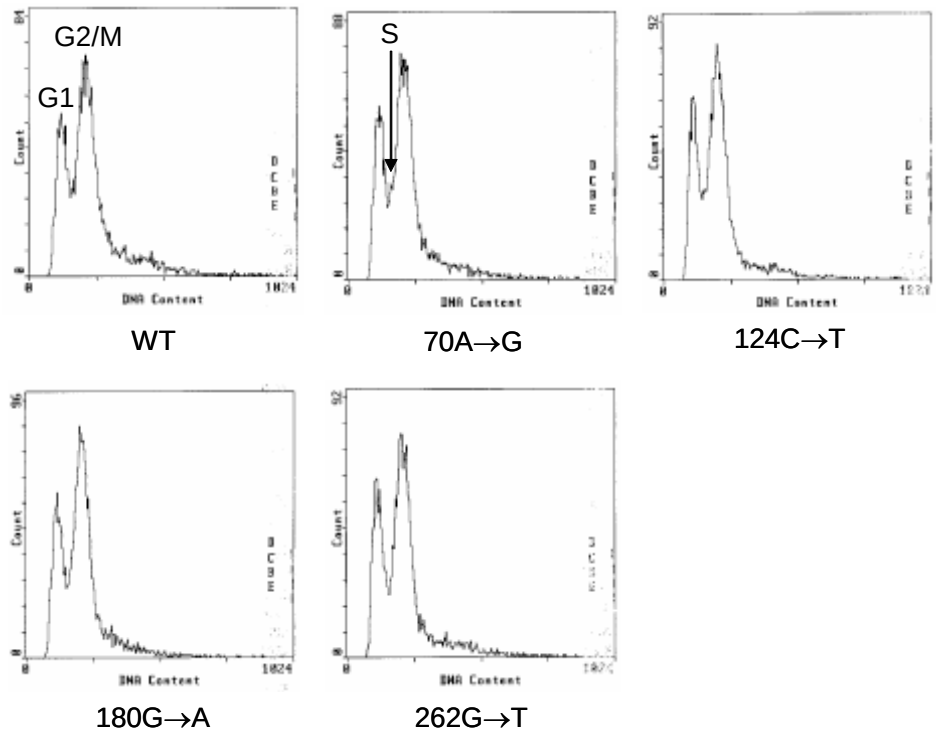

Fig. 45: Flow cytometry of nme1mutant strains.

Yeast strains were grown to logarithmic phase, 10^6 cells were fixed in 70% ethanol, stained with Propidium Iodide and sorted by flow cytometry. G1, S, and G2/M phase of the cell cycle can be separated. The point mutations do not affect the cell cycle of the mutant strains. WT: wild type

The yeast strains that were viable in 3.7.3.1 were again grown until logarithmic phase, 10^6 cells were fixed in 70% ethanol, stained with PI (2.8.4) and sorted by flow cytometry. The G1, S and G2/M phases of the cell cycle can be distinguished by this method (Fig. 45). The point mutations do not seem to delay the cell cycle progression. A cell cycle defect would cause a change in the DNA content (x-axis) of either the G1 or the G2/M phase. But as shown in Figure 44 there is not shift in the DNA content in either mutant strain when compared to the WT strain.

3.7.3.3 Telomere Blot

Another potential mechanism that could affect the timing of cell differentiation would be accelerated senescence. Therefore the lengths of the telomeres of the mutants have been tested. Southern blot analysis (2.13.1) was performed using yeast genomic DNA (2.1.4) digested with *XhoI*, separated on an agarose gel (2.3.1.1) and hybridized with a telomere specific fragment (2.12.1). Use of this probe reveals a characteristic 1.4 kb band representing the telomere ends of 2/3 of the yeast chromosomes (Fig. 46). If the telomere is shortened a shorter sized fragment would be expected. Similarly, if the telomere is lengthened a longer sized fragment would be visible.

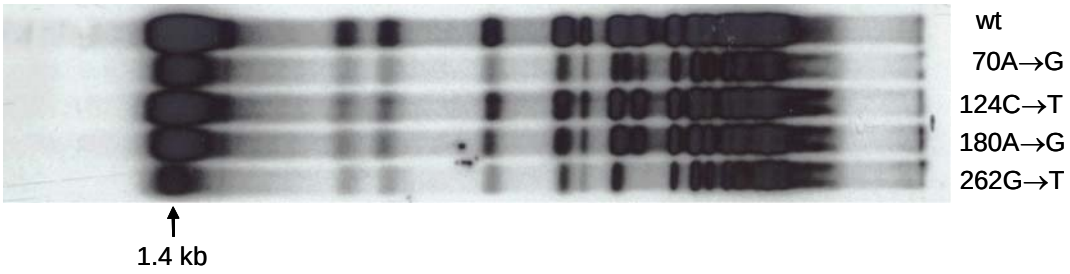

Fig. 46: Telomere blot of the nme1mutant strains.

Yeast genomic DNA was digested with *XhoI*, separated on an agarose gel, transferred to a nylon membrane, and hybridized with a telomere specific probe. This procedure revealed a characteristic band of 1.4 kb. There is no difference in the telomere length of the mutant strains when compared to the WT strain. The missing band of the *nme1*$^{262G>T}$ is a natural alteration observed in this kind of experiments.

The telomere length of the mutant nme1 strains are comparable to the wild type strain. The 'missing' band of the *nme1*$^{262G>T}$ is a natural alteration observed in this kind of experiments (Alison Bertuch, personal communication).

3.7.3.4 γ Irradiation Test

Under normal conditions the *nme1*^{mutant} strains do not seem to alter any of the vital functions of NME1 in yeast that have been looked at so far. The question now remains how the mutant cells respond to stress. One possible way to introduce stress is ionizing radiation that is a type of ionizing radiation. This type of radiation produces free radicals such as reactive oxygen that can damage DNA (Riley 1994). Nme1Δ/pNME1 cells were grown to logarithmic phase, 10^6 cells were stained with Phloxine B (2.8.5) to control whether putative changes in the cell cycle are due to the mutation introduced into the yeast strains or are just simply an effect of the γ irradiation (Fig. 47). Phloxine B stains the nucleus of dead or dying cells red and cannot penetrate into healthy/living cells. As demonstrated in Figure 47 the yeast cells seemed to

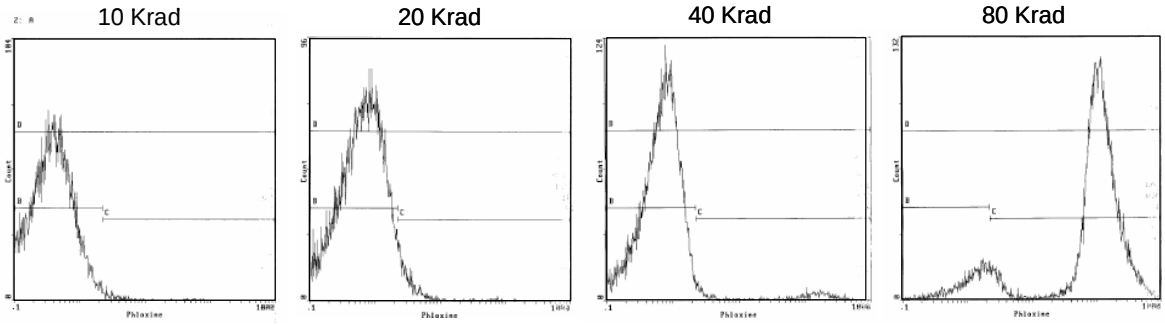

Fig. 47: Test γ irradiation experiment with nme1Δ/pNME1.

Cells were grown to logarithmic phase and then irradiated with different doses (10, 20, 40, 80 Krad respectively), stained with Phloxine B and sorted vie FACS analysis. 40 Krad is already a very damaging dose, since the first dead cells appear (tiny peak on the right). 80 Krad seemed to be a lethal dose since most of the cells are dead and therefore stain with Phloxine B (shift of the peak to the right).

tolerate up to 40 Krad of γ irradiation very well. At 80 Krad most of the yeast cells seemed to be dead, because of the shift of the peak to the right indicating that Phloxine B penetrates into the nucleus. To test the stress induced response, the *nme1*^{mutant} strains were grown until logarithmic phase, γ irradiated with different amounts of radiation, diluted 1: 10 and then grown up to 48 hrs after irradiation. An aliquot of each mutant that was not irradiated served as a control. After 4, 8, 12, 24 and 48 hrs 10^6 cells were taken out of the culture for a cell cycle assay. The cells were fixed in 70 % ethanol, then stained with PI as described in 2.8.4 and sorted via FACS analysis (see Fig. 48). Ionizing radiation such as γ irradiation is known to cause an intra-G_1 cell cycle arrest (Nilssen et al., 2003). Therefore, it is not surprising to

Fig. 48

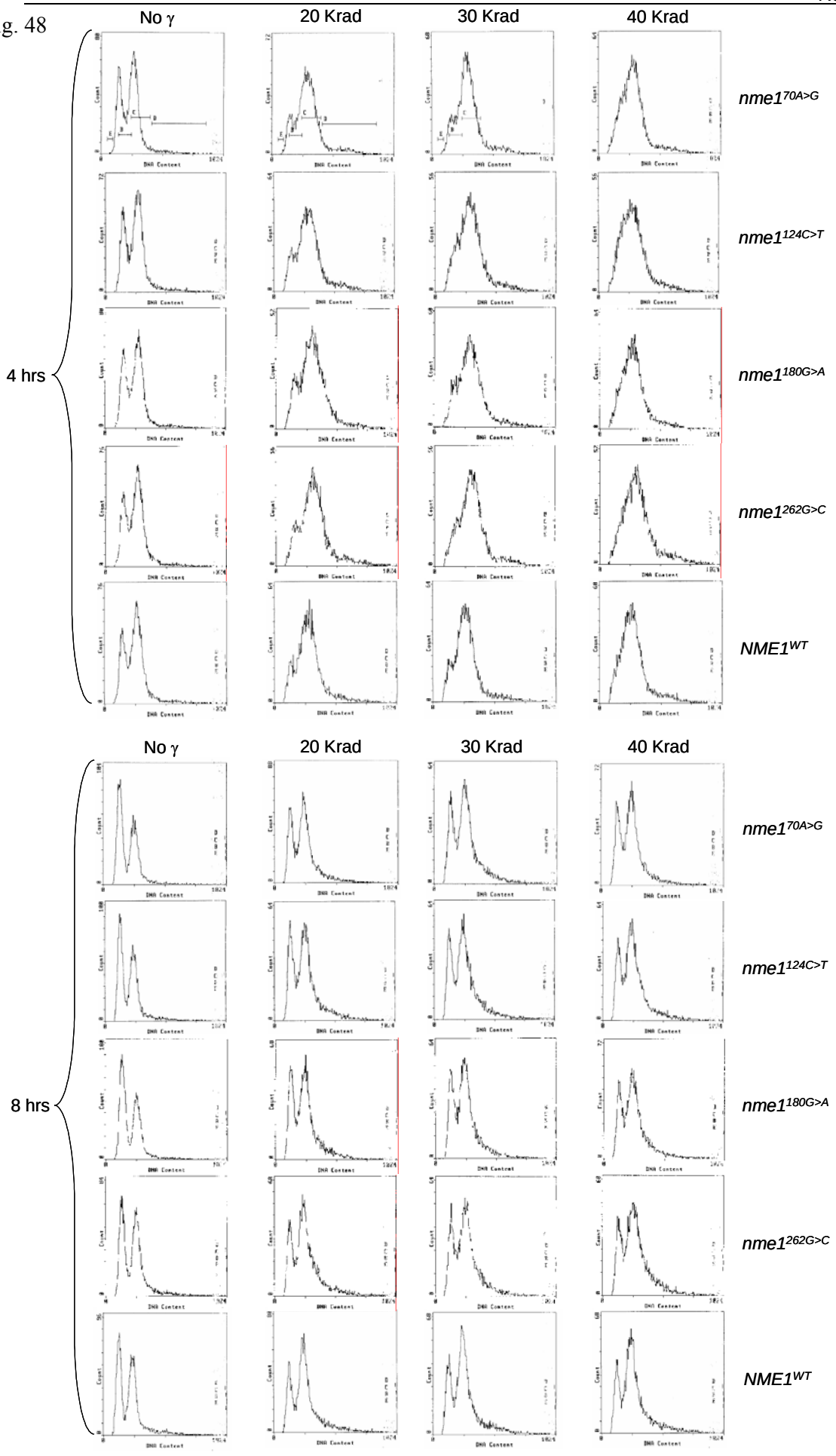
No γ
20 Krad
30 Krad
40 Krad
4 hrs
nme1^70A>G
nme1^124C>T
nme1^180G>A
nme1^262G>C
NME1^WT
No γ
20 Krad
30 Krad
40 Krad
8 hrs
nme1^70A>G
nme1^124C>T
nme1^180G>A
nme1^262G>C
NME1^WT

Fig. 48: FACS analysis of γ irradiated nme1mutant yeast cells.

The yeast cells were grown to logarithmic phase, irradiated with various doses, then diluted 1:10. After 4 and 8 hrs 10^6 cells were fixed in 70% ethanol, stained with PI and sorted via FACS. After 4 hrs all cells are arrested in G_1 phase of the cell cycle, but after 8 hrs all cells have returned to the normal cell cycle.

observe a G_1 cell cycle arrest 4 hrs after exposure to the γ irradiation (Fig. 48). Eight hrs after irradiation the cells had recovered completely and all *nme1*^{mutant} strains grew equally well as the WT control. Therefore the DNA damage response might not be affected in these cells.

3.7.3.5 Ratio Of The Long And Short Form Of The 5.8 S rRNA

The best-described function of *NME1* is the processing of the pre-rRNA (Chu et al., 1994; Lygerou et al., 1996). Total RNA was isolated (2.2.3) from the mutant yeast strains and separated on a polyacrylamide gel (2.3.1.3). The gel was stained with ethidium bromide. The 5S rRNA and the tRNAs served as loading controls. In wild type cells there is a higher concentration of the $5.8S_S$ rRNA (short form of the 5.8S rRNA), which is part of the ribosome

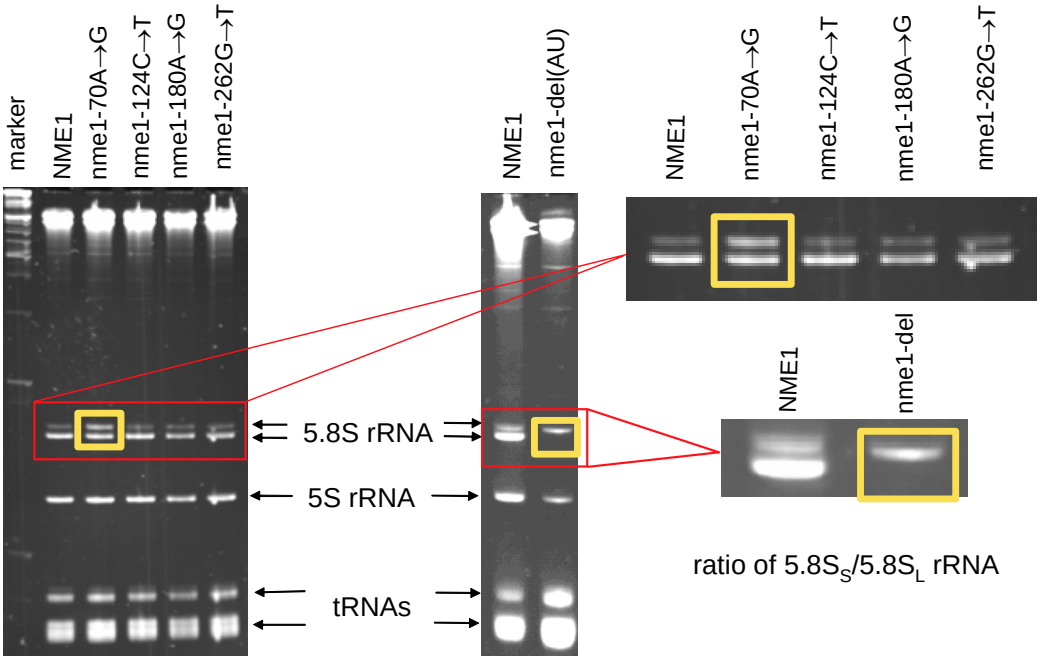

Fig. 49: Pre-ribosomal processing of nme1mutant strains.

Total RNA was isolated from each strain and separated on a 7% polyacrylamid, 7 M urea gel. The 5S rRNA and the tRNAs serve as loading controls (right side of the figure). The *nme1*^{2bpdel} only grows on a plate at RT and only in diploid yeast cells. On the left a blow up of the right side illustrates the alterations in the processing of the 5.8S rRNA. Normally, the ratio of the short (lower band) versus the long (upper band) is 1:10. The nme1$^{70A>G}$ mutant has approximately a ratio of 1:3 whereas the *nme1*^{2bpdel} lacks the $5.8S_S$ form completely.

than the 5.8 S_L rRNA (long form of the 5.8S rRNA). Two of the five *nme1* mutants exhibit an alteration in this ratio. The *nme1*$^{70A>G}$ mutant strain has an ratio of approximately 2:3 of the short and the long form of the 5.8S rRNA whereas the 2-bp deletion mutant lacks the short form of the 5.8S rRNA completely. The latter one showed only minimal growth, indicating that most of its function is abolished (Fig. 49).

3.7.4 Yeast Genomic Overexrpession Library Screen

As shown in 3.7.3.1 the *nme1*^{2bpdel} mutant is lethal. In order to identify genes, which might be able to rescue the lethality of this mutant strain a yeast genomic overexpression library was screened (gift from Dr. Alison Bertuch) (Engebrecht et al., 1990). Since the library was generated with LEU2, CEN plasmids the 2-bp deletion as well as the *NME1* WT gene used as a control had to be subcloned into a HIS, CEN plasmid. The titer of the genomic overexpression library was determined in a pilot transformation to determine the transformation efficiency. Based on the test transformation it could be calculated how many plates would be necessary to screen 100,000 colonies. 120 –leu-ura-his plates have been replica plated as described in 2.8.6 on 120 5FOA-leu-his plates to shuffle out the WT *NME1* gene on the URA3, CEN plasmid and to test for genes that might rescue the lethal phenotype of the *nme1*^{2bpdel} mutant strain. A schematic of this assay is depicted in Figure 50. The nme1Δ strain generated in 3.7.1 containing the *NME1* wt gene on a URA3, CEN plasmid and the *nme1*^{2bpdel} on a His, CEN plasmid was used. This strain was grown to logarithmic phase and transformed with a yeast genomic overexpressing library. As a positive control instead of the library a pNME1, LEU2, 2 µm vector was transformed as well as an empty 2 µm vector used as a negative control. Colonies growing on both –leu-ura-his and 5FOA-leu-his plates contain the desired plasmids bearing sequences that confer the ability to rescue the lethality. In order to isolate the rescuing plasmids positive colonies were picked and a dilution streak out was performed. Four colonies for each streak out were picked and the plasmids were isolated using the GenoTech yeast plasmid isolation kit (2.1.6.4). The so purified DNA was then re-transformed into the original strain used at the beginning of this experiment. A single colony was picked after the transformation and grown overnight in 3 ml –ura-leu-his medium. A 1:10 serial dilution was then performed and replica-plated on a –ura-leu-his plate and a 5FOA-leu-his plate (Fig. 50).

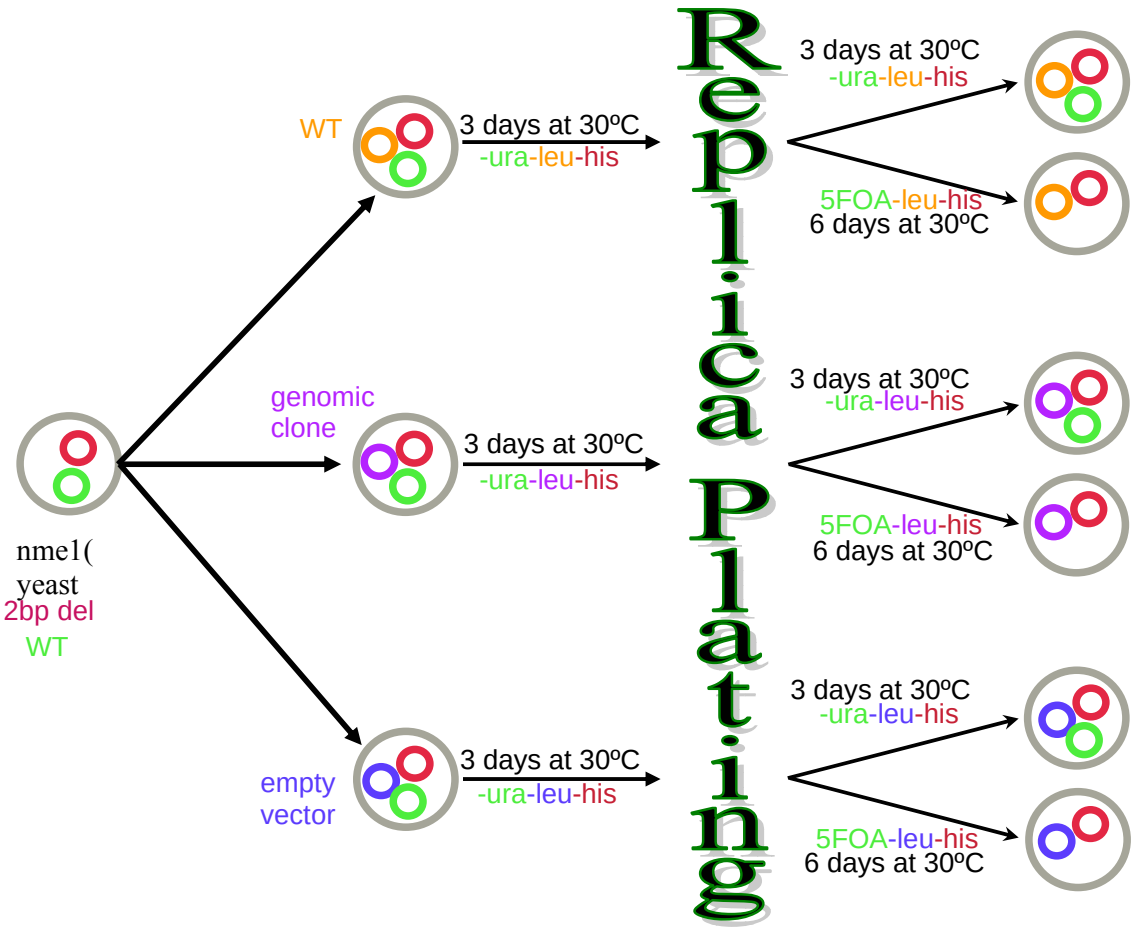

Fig. 50: Cartoon of the yeast genomic overexpression library screen.

The starting yeast strain was the nme1Δ/pnme1^{2bpdel}pNME1 strain. As a positive control for this experiment an other pNME1, as a negative control an empty vector, and as assay a yeast overexpression genomic library were transformed into this strain. After 3 days the plates were replica-plated on 5FOA-leu-his plates. The first plates (-ura-leu-his) were incubated for 3 more days and the latter ones were grown for 6 days at 30°C. The clones that grew on –ura-leu-his and on 5FOA-leu-his rescue the lethality of nme1^{2pbdel}.

As shown in Figure 51 only clone #22.1 rescued the lethal phenotype of the *nme1*^{2bpdel} mutant strain. The other clones might be false positives from the primary screen. The plasmid from clone #22.1 was isolated with the GenoTech yeast plasmid isolation kit (2.1.6.4) and then transformed into bacteria (2.7). Ten individual bacteria colonies were inoculated in 5 ml of LB medium supplemented with 100 µg/ml ampicillin and grown overnight at 37°C. Plasmid DNA was isolated (2.1.6.2) and sequenced as described in 2.5.2. Figure 52 shows a schematic of the 'rescuing' genomic yeast clone.

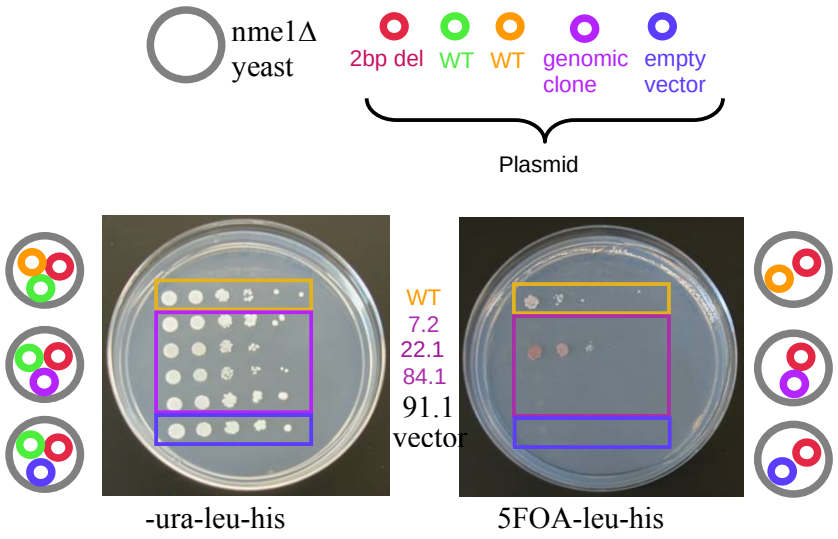

Fig. 51: Re-testing of the putative rescuing clones of the yeast genomic overexpression library screen.

From the left to the right of each plate a 1:10 dilution of the yeast cells was performed. The right side controls for the cell numbers. The left side depicts the assay of the ability of the genomic clones to rescue the lethality of the *nme1*^{2bpdel} mutant strain. The cartoon on either side of the Petri dishes illustrates the genotype of the different yeast strains. Only one clone (#22.1) seems to rescue the lethality of the *nme1*^{2bpdel} mutant strain. The other clones seemed to be false positives from the primary screen. WT: wild type

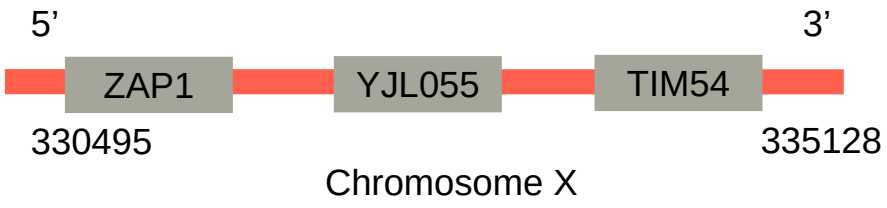

Fig. 52: Schematic of the rescuing clone of the overexpression library screen.

The genomic clone contains three genes. ZAP1 is a zinc regulated transcription factor. YJL055 is an uncharacterized ORF without any known function. TIM54 belongs to the mitochondrial transmembrane transporter proteins.

Seven of the plasmid DNAs sequenced contained the rescuing clone shown in Figure 52. ZAP1 is a zinc-regulated transcription factor that binds to zinc-responsive promoter elements to induce transcription of target genes. It regulates its own transcription and the protein contains seven zinc-finger domains. YJL055W is an uncharacterized open reading frame. It might be a member of the lysine decarboxylase family, because it shares a characteristic and highly conserved protein motif: PGGXGTXXE. This motif might be functionally important,

but there is no experimental evidence yet. TIM54 stands for Transclocase Inner Membrane, 54 kDa and is a translocase for the insertion of proteins into the inner membrane of mitochondria. Two of the plasmids contained the 2-bp deletion of the NME1 gene and one clone contained a WT NME1 genomic clone. This suggests that the 'rescuing' clone was a mixed colony and the rescuing effect was caused by the NME1 WT locus and likely not by the genomic clone shown in Figure 52.

4 Discussion

4.1 Clinical Studies

This study also confirms and extends the most important clinical findings previously reported in other series (McKusick et al., 1965; Mäkitie & Kaitila 1993) which had served here as the reference for phenotype definition (Spranger et al., 2002). In addition to being retrospective this study was multicentric as well, because patient samples for molecular confirmation of CHH and the accompanying clinical information were referred from various locations in two continents.

This study also confirms that the McKusick type of metaphyseal osteochondrodysplasia is radiologically only mild to moderate. Nevertheless it interferes significantly with normal growth at least from birth and results already in early childhood in short-limbed type of disproportionate dwarfism. The failing growth had apparently a prenatal onset in eight of the patients because the birth length (BL, either measured at term or extrapolated to term in case of premature birth) was already below p3. In the remaining patients in this cohort BL was within normal limits but growth failure was manifest from early infancy. The average BL in 21 patients in whom *RMRP* mutations were subsequently found was 45.9cm being 45.5cm in boys (N = 11) and 46.3cm in girls (N = 10) in this cohort. In all subjects small stature and slowing growth became progressively evident with age. Too few measurements were available in most patients, but plotting them revealed quantitative variability. Already in early childhood the stature was as much as more than 6 SDs in some and between 4 and 6 SDs below the average in age-matched controls in other subjects. The most severely dwarfed were the patients with BL below p3. Although no upper segment measurements were available from the records, the dwarfism described or photographically documented was indeed of the short-limbed type in all. No report of final or adult height can be reported in this cohort of CHH patients as the measurements in the older patients were performed too early in adolescence. The remaining patients were too young at the time of study.

The growth pattern in patient # 3 was congruent to that in all patients with *RMRP* mutations. It was however qualitatively different in the four other patients without such mutations or with only a single mutation detected. In these subjects linear growth proceeded alongside but

slightly below p3 throughout the observation period. The BL was unknown in one of them, but average or even large in the other three. This different growth pattern has been discerned before the results of the mutation screening were available. Because in none of these patients any mutation in the *COL10A1* gene (Table 5) encoding the type X short non-fibrillar collagen of cartilage has been detected, the alternate diagnosis of Schmid type metaphyseal dysplasia (MCDS) (MIM # 120110) radiologically related to CHH (Spranger et al., 2002) had to be dropped as well. Hence it can be concluded that patients # 10, 15, 23 and 26 have a metaphyseal dysplasia different from CHH as well as from MCDS. This small subgroup may represent more than one chondrodysplasia. A similar conclusion has been reached following the study of 20 MCDS patients without *COL10A1* mutation, among whom only two were subsequently shown to be homozygous for the 70A>G major mutation and to have CHH (Ridanpää et al., 2003). The clinical description of the latter two patients shows the clinical and radiological phenotype to be entirely congruent to the definition of CHH adopted here and to the average phenotypes described in past reports (Mäkitie & Kaitila 1993; Spranger et al., 2002)

Other skeletal and connective tissue malfunctions and clinical abnormalities reported by Mäkitie and Kaitila (1993) are confirmed in comparable proportions in this study. Insignificant differences are not only due to statistics in this smaller cohort of patients. Due to the entirely retrospective and multicenter nature of the present study, an unfortunately large number of "no information" scores had been obtained from the original clinical records rendering the patient base even smaller. Most criteria used for phenotype definition in this "meta-analysis" were not known and hence not applied by most of the US referring physicians. In the European and in some US patients the clinical diagnosis had been reached by recognition of the physical and radiological "Gestalt " of CHH by the referring experts. As this type of diagnosis is based on the phenotype as a whole rather than on tabulating the separate components, often the separate features figuring in the definition were not recorded. It is of interest that by either approach for the clinical diagnosis of CHH, in a nearly equal number of patients (N = 2 and N = 3 respectively) no *RMRP* mutations were detected.

Marked ligamentous and joint laxity (J column in Table 1) was found in 8/14 subjects but reported absent in 6/14. Information about this feature was unavailable in the remaining 13 patients. Limited extension of the elbows was noticed in 9/13 and absent in 4/13 patients but no data were recorded in 14 others. Significant chest deformity, lumbar hyperlordosis and

severe scoliosis had not been recorded in any of the patients. Information about knee posture and function when standing or walking was lacking in over half (14/27) of these patients. Some subjects were obviously too young for evaluation of this feature. In seven instances moderate genua vara, in 4 others mild genua valga were recorded. The knee joints and lower limbs were described as straight in only two patients (# 10 without *RMRP* mutation and # 16). Short hands, fingers, feet and toes were a consistent component in the phenotype, although not recorded in 7 of the 27 subjects. The "telescoping" phenomenon in the distal and middle interphalangeal finger joints was present in 4/9 patients, but not commented upon in 18 other patient records. Lack of cooperation in the very young patient and probably gradual disappearance of this feature from adolescence may account for the inconsistency of this finding.

Only few of the patients in this cohort had associated extra-skeletal abnormalities or dysfunctions except for deficient growth of scalp hair found in the large majority (21/25). In 4/25 the hair was considered normal. Three patients in the latter subgroup were subsequently shown to bear no *RMRP* mutation. In one true CHH patient the hair was reported to be clinically normal. It was however not studied microscopically. Microscopically hair can be a valuable tool for diagnostic purposes (Silengo et al., 2002). Lack of deficient scalp hair and some other extra-skeletal features associated with the CHH phenotype has been viewed in support of the diagnosis of "variant CHH" when associated with *RMRP* mutations (Bonafé et al., 2002). One may wonder about the clinical merit of the notion of variant CHH. In the largest cohort reported 7% of patients had no hair hypoplasia (Mäkitie & Kaitila 1993). True CHH patients may have normal hair growth and no or almost no other extra-osseous dysfunction. At the time of closure of the study there had been no mention of any malignancy in any of the patients. Evidence of increased incidence of malignancies in CHH has been reported in other cohorts (Mäkitie & Kaitila 1993; Mäkitie et al., 1998).

The *in vivo* and *in vitro* evidence of immune deficiency was either not or not systematically investigated or reported, especially in patients without any clinical evidence of unusually frequent infections. Abnormally frequent recurrence of severe and generalized infections was recorded in 5/23. In 8/23 less morbid infections were noticed. The proportion corresponds well with that of 43% in a previous report (Mäkitie et al., 1998). The occurrence of infections not considered abnormally frequent in early childhood was reported in 10/23 patient records. Clinical varicella was in the normal range of severity in 6/27 and abnormally severe and

generalized in only 2 subjects (# 20 and 21). In one of the latter intensive care hospitalization was required. No conclusion on the frequency of low white blood cell count below reference values may be reached from the available data. Phenotyping of WBCs with immunofluorescent monoclonal antibodies had either not been performed or not or incompletely reported in the patient records. In only two patients (# 7 and 20) belonging to the subgroup with severe clinical infections, lymphocyte proliferative responses to several mitogens had been shown to be subnormal. In these two patients, referred from different centers, severe growth failure was recorded confirming the correlation found elsewhere (Mäkitie et al., 1998) between severity of growth failure, increased tendency of clinical infections in the previous year and the lymphocyte stimulation index. In both patients the tests were performed in early childhood when infections were a significant problem. However in most of the patients in this cohort, including some other subjects with severe growth failure, there was no clinical indication of immune deficiency and apparently no need for *in vitro* immunology studies. Failure to confirm the findings by others calls for the need for prospective and comparable investigation of the immune function, in all CHH patients. In the larger study from Finland (Mäkitie et al., 1998) 84% of patients presented with impaired lymphocyte proliferative response to mitogen stimulation although less than half of them had a history of proneness to infections.

Macrocytic anemia was not investigated systematically in several of the patients as too few records (14/27) contain results in this regard. It was severe in infant patient # 27 of Amish extraction and required treatment with packed cells (Williams et al., 2005). As in 4/24 other affected in the cohort the anemia subsided gradually.

The findings at hand confirm the observation that gastrointestinal complications in young CHH patients are of at least two types: firstly, Hirschsprung-type constipation or frank Hirschsprung disease and secondly, malabsorption type ‘failure to thrive’ (FTT) and/or diarrhea (Mäkitie & Kaitila 1993). Hirschsprung disease had been proved histologically in 2 of the patients and significant constipation recorded in 4/20 subjects of this study. In 15/20 patients there was no gastrointestinal dysfunction. There were two instances of histologically and immunologically proved coeliac disease and 5 other cases with infantile episodes of severe malabsorption, diarrhea and/or FTT. Also the latter complications had become less frequent and less morbid with increasing age.

From the contents of Table 1 the conclusion emerges that in this series, the CHH patients with the most severe growth failure are the ones with clinically expressed immune deficiency and gastrointestinal complications, both being most significant in late infancy and early childhood.

Patient # 3 had a clinical phenotype quite congruent with CHH, but no *RMRP* mutations were found. But this patient was not tested for a uniparental disomy (UPD) for chromosome 9. There are two CHH patients reported with a maternal UPD (Sulisalo et al., 1997). The four patients without *RMRP* mutations are different from CHH, although they are obvious examples of short limb-type dwarfism. Radiologically they have a mild metaphyseal chondrodysplasia different from CHH: the growth pattern differs from birth; they have no extra-skeletal features. No investigations of the immune and/or the gastrointestinal system were performed, as they were clinically not indicated. In each of the patients (#10, #23, #26) Schmid type Metaphyseal Chondrodysplasia has been ruled out formally. Patient #10 was also negative for *FGFR3* mutations. The existence of still one or more alternate, as yet undelineated metaphyseal chondrodysplasias of which these patients are examples can be proposed.

The latter conclusion represents the most obvious genotype-phenotype correlation detected by this study. In contrast no correlation between the type of *RMRP* mutation and either the occurrence or severity of any phenotypic feature of CHH was found in this study. Severe growth deficiency is observed in compound heterozygotes for two base pair substitutions (patient # 2) as well as in a patient heterozygous for a single nucleotide substitution and any type of molecular structural aneuploidy mutation such as a duplication of the promoter region (patient # 4, 5, and 7), insertion (patient # 6), deletion (patient # 20). It cannot be ruled out that in prospective studies with more uniform and detailed investigational approach to the patients' phenotypic features, more refined aspects of the correlation between the CHH genotype and phenotype may still be detected. To this end generating a specific questionnaire based on the features in the CHH case definition, guideline of this retrospective study, for the purpose of qualitatively improving the clinical information made available to the molecular biology laboratories may be a useful first step (8.2).

In the absence of understanding the physiologic role of the *RMRP* gene it seems quite impossible to assess the meaning of the many genetic polymorphisms within and about this region of interest.

Short stature was as expected to be a major feature in the CHH subjects; yet it was found to be quite variable, as it ranged from mildly below the normal range to rather severe dwarfism. Most probably this osteochondrodysplasia has its onset in the last trimester of pregnancy. At the time its features are insufficiently distinct in order to be consistently discernable by ultrasonographic study.

4.2 Mutation Screen of CHH patients

35 patients were recruited to this study. The referring physician made the diagnosis of CHH on the finding of characteristic radiographic features. All referred patients were screened for mutations in the *RMRP* gene (see Tab. 3). In the cohort of 35 patients 9 alleles with duplication mutations in the promoter region were found. This was primarily between the TATA box and the transcription start (see Figures 6, 16). This would be expected to decrease the level of transcription. The TATA box has also a fixed distance downstream to the PSE (proximal sequence element) (Hernandez and Lucito 1899; Mattaj et al., 1988; Kinkel and Pederson 1989; Lobo and Hernandez 1989). The PSE is recognized by the snRNA activating protein complex ($SNAP_c$). The TATA box is recognized by the TATA box binding proteins (TBP) like TFIIIB (Waldschmidt et al., 1991; Murphy et al., 1992; Sadowski et al., 1993; Yoon et al., 1995; Schramm et al., 2000; Teichmann et al., 2000). The RNA polymerase III is recruited by $SNAP_c$ and mainly by TBP (Sepehri Chong et al., 2001). If the distance between the PSE and the TATA box is greater because of the sequence duplication, transcription of *RMRP* could be inhibited, because $SNAP_c$ and TBP might not be able to interact and therefore unable to recruit the RNA polymerase III. 37 alleles had single base pair substitutions, 2 alleles with an insertion of a single base pair and also 2 alleles with a deletion of the last ten base pairs of the transcript. These could be hypothesized to affect the secondary structure of *RMRP* and perhaps the binding to proteins within the ribonuclear complex. However, limited published data at least for two of the subunits suggest this might not be the case (Ridanpää et al., 2001). And 20 alleles exhibit no mutations in the *RMRP* gene. To date no deletions of

the whole gene have been found suggesting that complete loss of function is incompatible with life and likely these are all hypomorphic alleles.

Interestingly, the pathogenic mutations (boxed in red and green in Fig. 53) seem to fall in highly conserved regions of the *RMRP* gene whereas the polymorphisms (boxed in blue in Fig. 53) seem to be mostly located in less conserved regions.

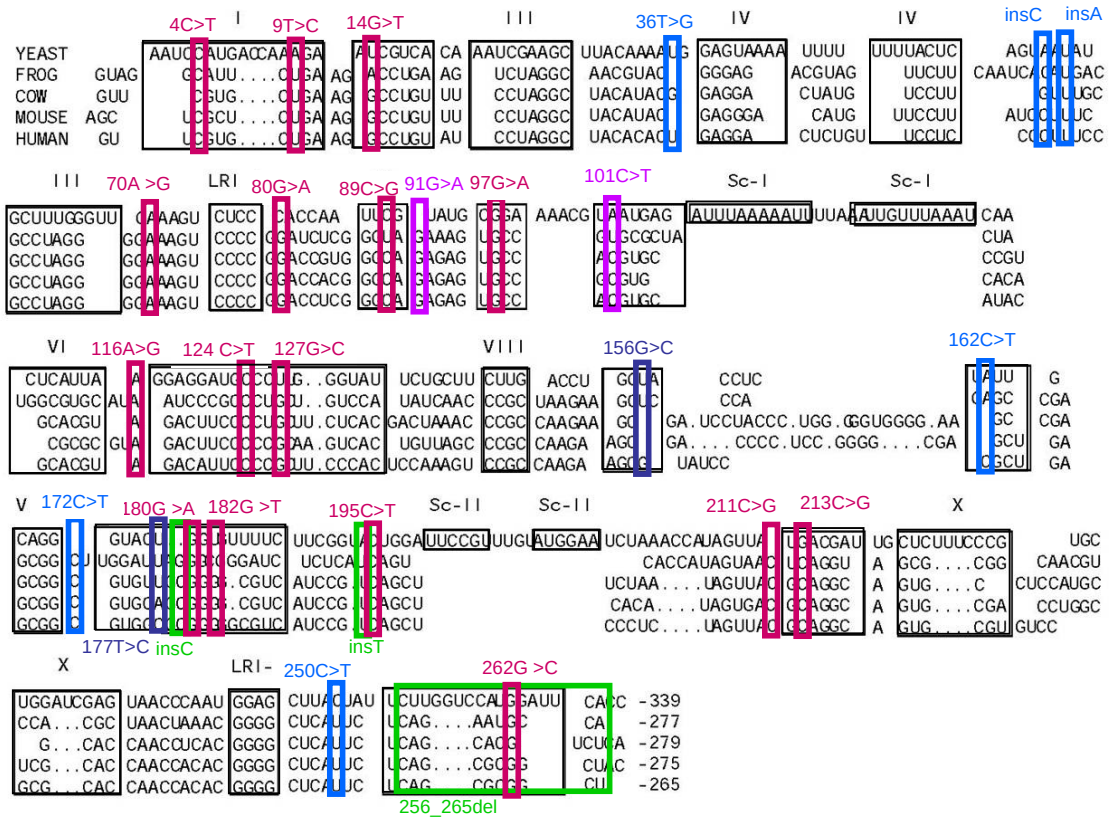

Fig. 53: Schematic view concerning the status of conservation of human RMRP mutations.

Pathogenic *RMRP* mutations seem to cluster in highly conserved regions. They are always conserved among the mammals. The polymorphisms seem to fall into regions that are not conserved among species. Exceptions would be three polymorphisms described in the literature that were not found in the patient and control cohort of this study. Pathogenic RMRP base pair substitutions are boxed in red; the pathogenic insertions and deletions are boxed in green. The two base pair substitutions found on one allele of the CHH siblings #12 and #13 are boxed in purple. The two polymorphisms found in this study are boxed in dark blue whereas the published polymorphisms that have not been found in this study are boxed in light blue.

When looking at the structural model for the human RNAse MRP complex (Welting et al., 2004), the same phenomena can be seen. The pathogenic mutations (shown in red in Fig. 54) seem to cluster in hairpin structures whereas the polymorphisms (depicted in blue in Fig. 54) are mostly located in loops. This suggests that the conserved regions might be functionally

important and mutations in those regions might affect proper function of the RNase MRP complex.

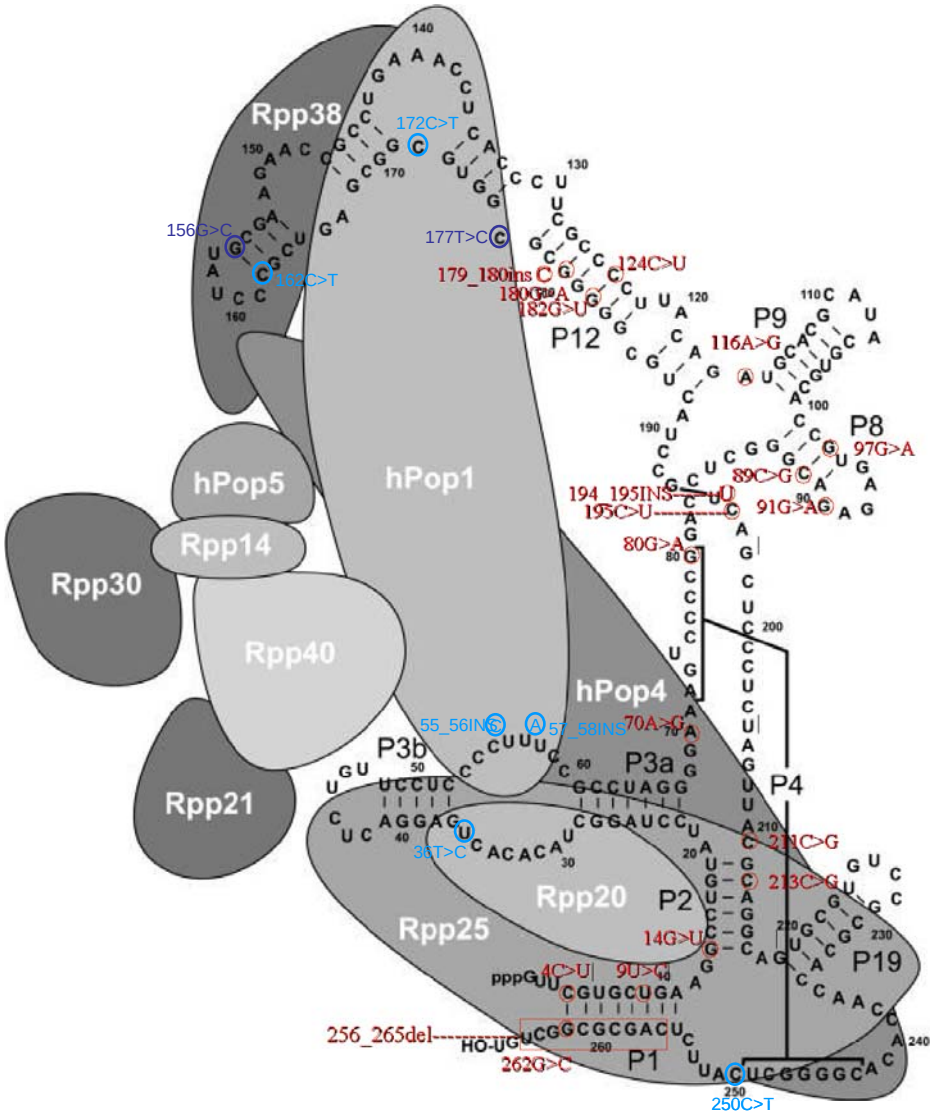

Fig. 54: RMRP mutations and polymorphisms and their position in the RNase MRP complex.

Pathogenic *RMRP* mutations are depicted in red. The two polymorphisms found in this study are shown in dark blue. The other published polymorphisms are indicated in light blue. Modified from Welting et al., 2004.

So far forty-one pathogenic single base pair substitutions have been published. In this study fourteen new mutations in the *RMRP* transcript could be identified (Tab. 15). Previously fifteen promoter duplications have been described and five new duplications of the promoter region have been found in this cohort of CHH patients (Tab. 16). Interestingly, all promoter mutations seem to fall between the TATA signal and the transcription start site of the *RMRP* transcript. *RMRP* seems to be highly polymorphic despite of its conservation throughout a

Table 15: Pathogenic RMRP base pair substitutions

mutation	Reference(s)
4C>T	Ridanpää et al., 2002, *Eur J Hum Genet* **10**:439-447; Ammann et al., 2004, J *Pediatr Hematol Oncol* **26**(6):379-381.
5G>A	Loeys et al., 2002; Clinical Genetics Meeting
9T>C	This study
14G>T	This study
40G>A	Superti-Furga et al., 2002 ASHG Meeting
56_57insTTCCGCCT	Ridanpää et al., 2002, *Eur J Hum Genet* **10**:439-447
63C>T	Ridanpää et al., 2002, *Eur J Hum Genet* **10**:439-447, Kuijppers et al., 2003, *J Med Genet* **40**:761-766
64T>C	Superti-Furga et al., 2002 ASHG Meeting
65delA	Casas et al., 2003; Clinical Genetics Meeting
70A>G	Ridanpää et al., 2001, *Cell* **104**;195-203
79G>A	Ridanpää et al., 2002, *Eur J Hum Genet* **10**:439-447
80A>G	This study
89C>G	This study
91G>A, 101C>T	This study
94_95delAG	Ridanpää et al., 2002, *Eur J Hum Genet* **10**:439-447
97G>A	This study
96_97dupTG	Ridanpää et al., 2001, *Cell* **104:**195-203; Ridanpää et al., 2002, *Eur J Hum Genet* **10**:439-447
99C>T	Ridanpää et al., unpublished
116A>G	This study
118A>G	Ridanpää et al., 2002, *Eur J Hum Genet* **10**:439-447
124C>T	This study
126C>T	Ridanpää et al., 2002, *Eur J Hum Genet* **10**:439-447
127G>A	Superti-Furga et al., 2002 ASHG Meeting
127G>C	This study
146C>A	Ridanpää et al., 2002, *Eur J Hum Genet* **10**:439-447
152A>G	Ridanpää et al., 2002, *Eur J Hum Genet* **10**:439-447
154G>T	Ridanpää et al., 2002, *Eur J Hum Genet* **10**:439-447
179_180insC	This study
180G>A	Ridanpää et al., 2002, *Eur J Hum Genet* **10**:439-447, #8, #21, #15
182G>C	Ridanpää et al., 2002, *Eur J Hum Genet* **10**:439-447
182G>A	Nakashima et al., 2003, *Am J Med Genet* **123**A:253-256
182G>T	This study
193G>A	Ridanpää et al., 2001, *Cell* **104:**195-203; Ridanpää et al., 2002, *Eur J Hum Genet* **10**:439-447
195C>T	Bonafé et al., 2002, *Clin Genet* **61**:146-151; Ridanpää et al., 2002, *Eur J Hum Genet* **10**:439-447
194-195insT	Kuijppers et al., 2003, *J Med Genet* **40**:761-766, #12
195C>T	Ridanpää et al., 2002, *Eur J Hum Genet* **10**:439-447, #18
211C>G	Ridanpää et al., 2002, *Eur J Hum Genet* **10**:439-447
213C>G	This study
214A>G	Ridanpää et al., unpublished
214A>T	Ridanpää et al., 2002, *Eur J Hum Genet* **10**:439-447
218A>G	Nakashima et al., 2003, *Am J Med Genet* **123A**:253-256, Harada et al., 2005, *Bone* **36**:317-322
230C>T	Ridanpää et al., 2002, *Eur J Hum Genet* **10**:439-447
236A>G	Ridanpää et al., 2002, *Eur J Hum Genet* **10**:439-447
238C>T	Bonafé et al., 2002, *Clin Genet* **61**:146-151; Ridanpää et al., 2002, *Eur J Hum Genet* **10**:439-447
242A>G	Ridanpää et al., 2002, *Eur J Hum Genet* **10**:439-447
243C>T	Ridanpää et al., 2002, *Eur J Hum Genet* **10**:439-447
244G>A	Superti-Furga et al., 2002 ASHG Meeting
252T>G	Ridanpää et al., unpublished
256-265delCAGCGCGGCT	This study
260C>G	Superti-Furga et al., 2002 ASHG Meeting
261C>T	Ridanpää et al., 2002, *Eur J Hum Genet* **10**:439-447
262G>C	This study
262G>T	Ridanpää et al., 2001, *Cell* **104**;195-203
264C>A	Ridanpää et al., 2002, *Eur J Hum Genet* **10**:439-447
indel	Loeys et al., 2002; Clinical Genetics Meeting

All mutations that have not been described in the literature have a turquoise background color.

Table 16: Pathogenic RMRP promoter duplications

promoter duplications	Reference(s)
-7_3dupGGACGTGGTT	Ridanpää et al., 2002, *Eur J Hum Genet* **10**:439-447
-8_-1dupAGGACGTG	Superti-Furga et al., 2002 ASHG Meeting
-14_-1dupAAGCTGAGGACGTG	Ridanpää et al., 2002, *Eur J Hum Genet* **10**:439-447
-21_-1dupCTCTGTGAAGCTGAGGACGTG	This study
-14_-3dupAAGCTGAGGACG	Bonafé et al., 2002, *Clin Genet* **61**:146-151
-20_-4dupTCTGTGAAGCTGAGGAC	Ridanpää et al., 2001, *Cell* **104:**195-203; Ridanpää et al., 2002, *Eur J Hum Genet* **10**:439-447
-20_-4dupTCTGTGAAGCTGGGGAC	Nakashima et al., 2003, *Am J Med Genet* **123A**:253-256
-23_-4dupTACTCTGTGAAGCTGAGGAC	Harada et al., 2005, *Bone* **36**:317-322
-25_-5dupACTACTCTGTGAAGCTGAGGA	Superti-Furga et al., 2002 ASHG Meeting
-26_-5dupTACTACTCTGTGAAGCTGAGAA	This study
-7_-6insCCTGAG	Ridanpää et al., 2001, *Cell* **104**;195-203, Ridanpää et al., 2002, *Eur J Hum Genet* **10**:439-447
-7_-6insAACGAAGCTGAG	Ridanpää et al., unpublished
-25_-6dupACTACTCTGTGAAGCTGAGA	This study
-14_-7dupAAGCTGAG	Ridanpää et al., 2002, *Eur J Hum Genet* **10**:439-447
-16_-7dupTGAAGCTGAG	Ridanpää et al., 2002, *Eur J Hum Genet* **10**:439-447
-15_-8dupGAAGCTGA	This study
-25_-11tripACTACTCTGTGAAGC	Ridanpää et al., 2001, *Cell* **104:**195-203, #21
-23_-14dupTACTCTGTGA	Ridanpää et al., 2001, *Cell* **104**;195-203, Ridanpää et al., 2002, *Eur J Hum Genet* **10**:439-447
-20_-14dupTCTGTGA	Ridanpää et al., 2002, *Eur J Hum Genet* **10**:439-447
-24_-15dupCTACTCTGTG	This study

All promoter duplications that have not been described in the literature previously have a turquoise background color.

Table 17: RMRP Polymorphisms

polymorphisms	Reference(s)
-282A>G	This study
-149T>A	Ridanpää et al., 2002, *Eur J Hum Genet* 10:439-447
-58T>C	Bonafé et al., 2002, *Clin Genet* 61:146-151, Ridanpää et al., 2002, *Eur J Hum Genet* 10:439-447
-56A>G	Bonafé et al., 2002, *Clin Genet* 61:146-151, Ridanpää et al., 2002, *Eur J Hum Genet* 10:439-447
-48C>A	Bonafé et al., 2002, *Clin Genet* 61:146-151, Ridanpää et al., 2002, *Eur J Hum Genet* 10:439-447
-24C>G	Bonafé et al., 2002, *Clin Genet.* 61:146-151
-6G>A	Bonafé et al., 2002, *Clin Genet* 61:146-151
36T>G	Nakashima et al., 2003, *Am J Med Genet* 123A:253-256
55_56insC	Nakashima et al., 2003, *Am J Med Genet* 123A:253-256
57_58insA	Bonafé et al., 2002, *Clin Genet* 61:146-151
156G>C	Bonafé et al., 2002, *Clin Genet* 61:146-151
162C>T	Nakashima et al., 2003, *Am J Med Genet* 123A:253-256
172C>T	Nakashima et al., 2003, *Am J Med Genet* 123A:253-256
177C>T	Bonafé et al., 2002, *Clin Genet* 61:146-151
250C>T	Bonafé et al., 2002, *Clin Genet* 61:146-151
+5T>C	Bonafé et al., 2002, *Clin Genet* 61:146-151
+7T>C	Bonafé et al., 2002, *Clin Genet* 61:146-151

The polymorphism that has not been described earlier in the literature has a turquoise background color.

variety of species. Maybe this might be due to a failure of repair mechanisms, relaxed selective pressure or a local hot spot for a high mutation rate. Of the sixteen reported polymorphism eight could also be seen in this study (Tab. 17).

Interestingly, all promoter duplications were found to be compound heterozygous with a single nucleotide substitution and never together with a second mutation affecting the promoter region. In addition the nucleolar localization signal (NLS) (nt 23-62) seems to be unaffected with mutations. This suggests that mutations in the NLS as well as a reduced *RMRP* level caused by promoter duplications increasing the critical distance of the TATA box to the transcription start site might be lethal. In the future when more CHH patients have been screened or identified mutations in the NLS might be detected as well.

Typical radiographic changes (Spranger et al., 2002) were most consistent among the CHH patient cohort and might be features to distinguish CHH from metaphyseal chondrodysplasias like MCDS, and other metaphyseal skeletal dysplasias. In addition to the radiographic features normal to low birth length, a growth curve in childhood at or below -3SDs and subjective abnormalities like poor hair growth were correlated with the detection of *RMRP* mutations. *RMRP* seems to be highly polymorphic despite of its conservation throughout a variety of species. Reasons for this might be failure of repair mechanisms, relaxed selective pressure or a local hot spot for a high mutation rate. Whether the polymorphisms in the *RMRP* gene contribute to the pleiotropic and variable phenotype of CHH remains unclear. Abundant mutations in the promoter region were detected. These may cause a hypomorphic state that decreases the level of *RMRP* transcription. The point mutations do not seem to alter the essential functions of the yeast orthologue of RMRP, but they might decrease RNA stability in humans as shown in the quantitative Real-Time PCR analysis (Fig. 24).

4.3 Search for Modifiers

CHH presents with a very pleiotropic and variable phenotypes. Even patients with the same pathogenic mutations can clinically present differently. The *RMRP* gene is very polymorphic but no geno- and phenotype correlation could be shown and therefore it is still unclear

whether the polymorphisms act as modifiers in CHH. More population studies might be necessary to clarify this point.

Alternatively, epigenetic factors, polymorphisms or mutations in other genes might act as modifiers resulting in the pleiotropic presentation of CHH. For example the severe anemia seen in CHH presents very similar to the anemia in Diamond-Blackfan Anemia. 25% of these patients have mutations in the *RPS19* gene (Willig et al., 1999). Therefore all CHH patients with reported anemia and other immunological problems were screened for mutations in the *RPS19* gene. But no mutations could be identified. But it seemed that CHH patients are more polymorphic than the five controls tested. Whether the *RPS19* polymorphisms might act as modifiers remains still unclear. Further population studies would be necessary, but this was outside of the scope of this work.

In the literature there is an increasing number of reports of the association of a single nucleotide polymorphism and a disease. For example a polymorphism in the tumor necrosis factor (TNF) increased the risk of gastric cancer after *Helicobacter pylori* infection in a Chinese population (Li et al., 2005). Or a polymorphism in the urokinase-type plasminogen activator gene results in an elevation of amyloid beta protein 42 and late onset Alzheimer's disease (Ertekin-Taner et al., 2005). Also polymorphisms in a promoter region might be pathogenic. For instance a polymorphism in the thymidylate synthase promoter enhancer region increases the risk of colorectal adenomas and may modify the survival chance after the disease (Chen et al., 2004). A whole-genome SNP genotyping and haplotype-based analysis might be of interest in clinical genetic testing (Craig and Stephan, 2005; Lee et al., 2005).

There are two patients (#15, #33) having only one mutant *RMRP* allele. Patient #33 was originally screened for mutations in the *COL10A1* gene suspecting MCDS, but no mutations were found. In contrast, patient #15 has one mutant *RMRP* allele inherited from the father and one mutation in the *COL10A1* gene inherited from the mother. Interestingly, the mother also carries a *RMRP* mutant allele (Fig. 55). In this family the *RMRP* mutation might act as a modifier. The height of the family members varies quite a bit. It would be interesting to study this family in more depth. Maybe the family members, who are very short, might carry the *COL10A1* mutation in addition to a *RMRP* mutation. The siblings exhibiting a height in the middle range might carry only the *COL10A1* mutation whereas the tall people might carry no mutant allele or one *RMRP* mutant allele (Fig. 56).

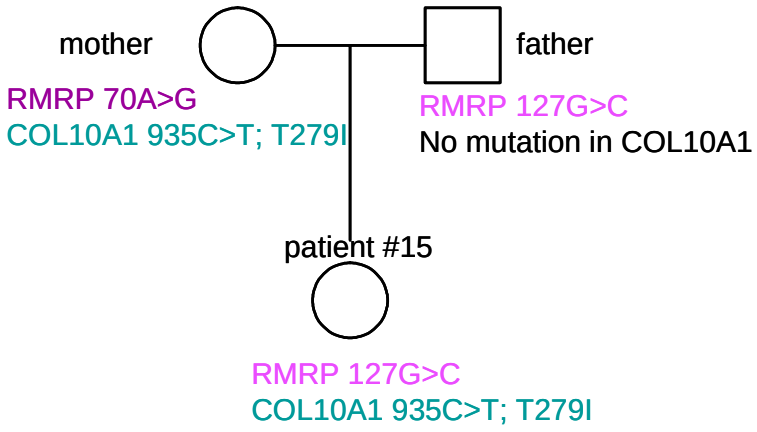

Fig. 55: Complex mutations found in patient #15.

The mother of patient #15 carries a mutant *RMRP* allele (lilac) and a *COL10A1* mutation (green). The latter mutation was inherited by the affected daughter who also carries a mutant *RMRP* allele that was inherited from the father (pink).

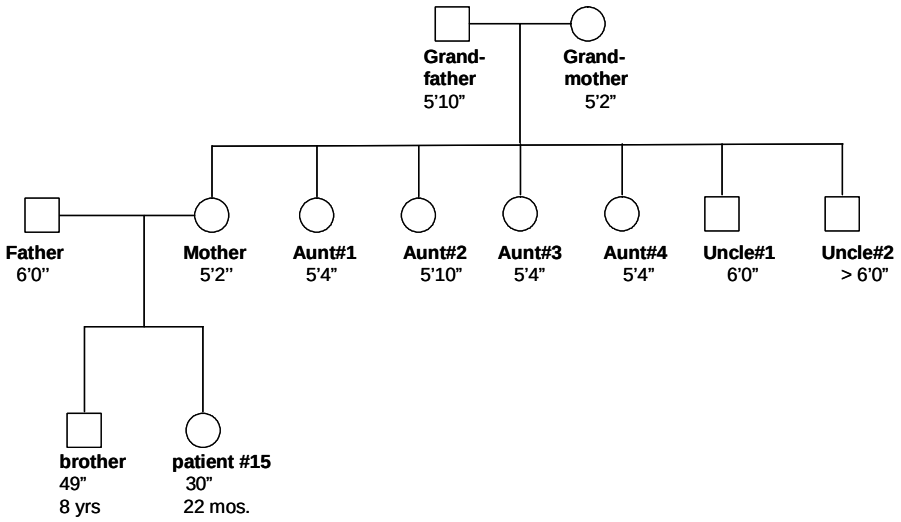

Fig. 56: Family pedigree of patient #15.

All family members are indicated in relation to the patient. The height is shown underneath each relative.

MCDS and CHH have radiological overlapping features such as short stature and similar metaphyseal changes of the long bones. But the onset of the growth failure is different. CHH has a neonatal onset whereas MCDS's short stature presents usually after the first year of life. The metaphyses in CHH patients are more severely affected than in MCDS. The metacarpals and phalanges are short in CHH patients but the hand radiographs of MCDS patients are usually normal. The MCDS radiographic changes are most severe at the hips (reviewed by

Ridanpää et al., 2005). Recently, a MCDS patient with radiographic changes in the hands has been reported (Elliott et al., 2005). Only one of the fifteen patients of this study was screened for mutations in the *COL10A1* gene but none for *RMRP* mutations. The diagnosis of MCDS was made just based on the radiographic presentation of the patients. It could well be that one mutant *RMRP* allele might be responsible for the hand alterations in MCDS cases similar to patient #15 in this study. Some other interesting aspect is presented in a paper reporting an effective treatment of a CHH patient with growth hormones (GH) (Harada et al., 2005). This is the first report of an effective GH treatment since CHH was first described in 1965 (McKusick et al., 1965). Previously, it was thought that GH treatment does not improve the height of CHH patients (reviewed by Bocca et al., 2004), but the final adult height of this patient (currently a teenager) is still speculative. These latter two studies also suggest that modifiers that could be responsible for the pleiotropic presentation of CHH might exist.

4.4 RMRP promoter studies

In eukaryotes the transcription of the genes is performed by three highly related RNA polymerases. Each polymerase transcribes a certain set of genes and is dependent on transcription factors to recognize the promoter sequences. RNA polymerase I transcribes the ribosomal RNA genes that are organized in tandem repeats. Thus, this RNA polymerase needs to recognize just one promoter structure. The RNA polymerase II transcribes genes that code for proteins and some small nuclear RNA (snRNA) genes. The regulatory region of the RNA polymerase II promoter is very variable in its structure reflecting the very complex regulation of gene expression during development. The RNA polymerase III transcribes structural or catalytic RNAs that are usually shorter than 400 bp. The transcription termination signal of the latter RNA polymerase is a simple run of four or more T residues (Paule and White, 2000).

There are three different types of RNA polymerase III promoters. The type 1 promoter contains an intragenic internal control region consisting of an A box, intermediate element and a C box. The 5S rRNA gene is the only example of a type 1 promoter and this internal control region is highly conserved among a variety of different species (Bogenhagen, 1985). The type 2 promoter is also intragenic and consists of an A box and a B box. The Adenovirus 2 VAI gene and tRNAs have typical type 2 promoters (Galli et al., 1981; Hofstetter et al.,

1981; Sharp et al., 1981; Allison et al., 1983). The type 3 RNA polymerase III promoter is external and the core promoter consists of a proximal sequence element (PSE) and a TATA box that is located at a fixed distance downstream of the PSE element (Hernandez and Lucito 1988; Mattaj et al., 1988). The PSE element on its own is sufficient for transcription of snRNA transcription by RNA polymerase II (Kunkel and Pederson 1989; Lobo and Hernandez, 1989).

The *RMRP* gene is transcribed by RNA polymerase III and sequence elements of a type 3 promoter are present (Topper and Clayton, 1990). The core sequence elements such as the PSE element and a TATA box can be found upstream of the transcription initiation site of the *RMRP* gene. In addition, transcription factor binding sites like a SP1 binding element and an octamer (recruits the transcription factor Oct-1) sequence could serve as distal sequence elements (DSE) to enhance the transcription of *RMRP* similar to the DSE element of the human U6 snRNA gene (reviewed by Schramm and Hernandez, 2002) (Fig. 57). *In vitro* studies showed that 352 bp upstream of the transcription start site of the RMRP gene are sufficient for activating transcription. The promoter duplications identified in CHH patients decrease the transcription activity *in vitro*. It still remains unclear whether the promoter

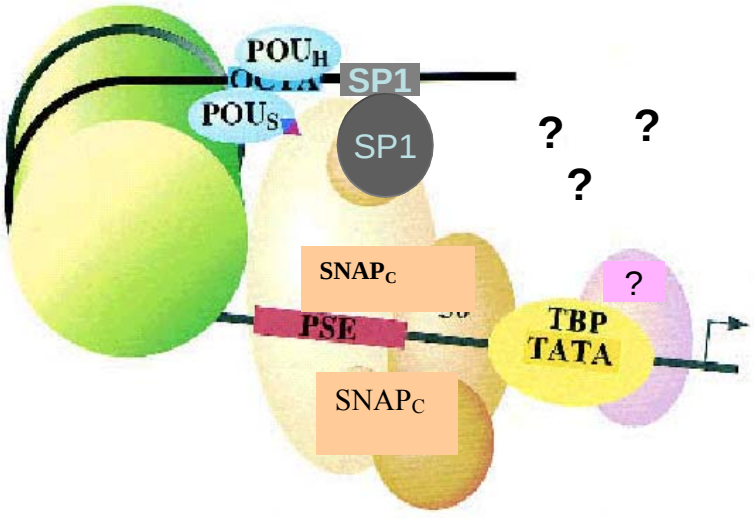

Fig. 57: Schematic depicting the putative activation of the RMRP promoter.

TBP might bind to the TATA box and together with the binding of SNAP$_c$ to the PSE element the RNA polymerase III could be recruited to the promoter. With the help of binding to a nucleosome the putative DSE elements (octamer and SP1 binding site) could act as promoter enhancer. Maybe there are other transcription factors or proteins involved in mediating *RMRP* transcription that are indicated with questionmarks. TBP: TATA box binding protein; SNAP$_c$: snRNA activating protein complex; DSE: distal sequence element. Modified from Zhao et al, 2001 and Schramm and Hernandez, 2002.

duplications abolish transcription completely *in vivo*. Previous reports suggest a complete loss of promoter activity (Nakashima et al., 2003), but even a four fold or more reduction in transcription activity could have been missed in the study of Nakashima et al, since they isolated total RNA from EBV transformed patient lymphoblasts, performed an RT-PCR and sequenced these products directly. Whether the octamer and the SP1 binding site function as transcription enhancer remains unclear, but this could be tested by the promoter activity in transfection studies when these elements are deleted compared to the activity when these elements are present in the promoter construct.

Lobo and Hernandez (1989) reported that the specificity of the RNA polymerase III promoter can be converted to a RNA polymerase II promoter and vice versa just by altering the distance of the TATA box to the transcription start site or by generating a TATA box (Lobo & Hernandez, 1989). In addition $SNAP_c$ is involved in the transcription of snRNA transcribed by RNA polymerase II and RNA polymerase III. To test whether the promoter duplications found in the CHH cohort might convert the polymerase III promoter to a polymerase II promoter, different parts of RMRP upstream sequences were amplified and subcloned in front of a luciferase reporter gene and co-transfected with a CMV-βgal plasmid into different cell lines. The putative minimal promoter contains the SP1 and PSE binding elements as well as the TATA signal and is 352 bp long. The second putative promoter sequence contains the latter promoter + 500 bp upstream of the 'minimal' promoter, but very preliminary data suggest that the promoter duplications found in CHH patients might not convert the polymerase III promoter into a polymerase II promoter.

These data suggest that the *RMRP* promoter might function similar to the human U6 transcription initiation complex. The TBP can bind to the TATA box and a $SNAP_c$ complex to the PSE element. The distance between the PSE element and the octamer of the *RMRP* promoter is 141 bp long and might be enough to position the octamer sequence just above of the $SNAP_c$ complex bound to the PSE element through a nucleosome mediated conformation change of the DNA at the *RMRP* gene locus. The OCT-1 transcription factor belongs to the POU-domain protein family. Together with the SP1 transcription factor and maybe additional proteins the *RMRP* transcription could be regulated (Fig. 57) (Mittal et al., 1999; Ma and Hernandez, 2002). The promoter duplications identified in some CHH patients increase the critical distance of the TATA box to the transcription initiation site, which is usually 25 to 30 bp downstream of the TATA element. This will most likely abolish proper transcription

initiation that in turn will lead to a decrease of *RMRP* transcript level as shown in the *in vitro* studies (Fig. 21). Whether the transcription of the *RMRP* gene is completely abolished *in vivo*, as previously suggested (Nakashima et al., 2003), remains still uncertain.

4.5 Pre-Ribosomal Processing

In humans the major ribosomal RNA genes are organized in tandem repeats on chromosomes 13, 14, 15, 21 and 22. They are present in around 250 copies and transcribed by RNA polymerase I as a primary transcript of 13.7 kb containing the 28S, 18S and 5.8S rRNA. This primary transcript undergoes a very complex processing by many different protein and protein complexes that results in the maturation of the 28S, 18S and 5.8S rRNAs. Figure 58 gives an overview of the rRNA processing in yeast. But this pathway is conserved in mammals as well (reviewed by Fatica, 2002). The 5S rRNA gene is located on chromosome 1 also with multiple copies.

The analysis of the ribosomal RNA processing of EBV transformed lymphoblastoid cell lines of six CHH patients with two mutant *RMRP* alleles did not show any alterations in the concentration of the different rRNA species. This is most likely due to the material used in this experiment. During the EBV transformation T-cells among other cells get destroyed and the immortalized cell lines mainly consist of B-cells. Since the cellular immune responses are affected in CHH that are mediated by T-cells, B-cells might not be affected in CHH patients. Unfortunately, there was no other tissue available for total RNA isolation to perform this experiment, ut it shows very nicely the specificity of the probes used and this method can easily be repeated when proper material of CHH patients will become available. The Standard Quality Assurance offered by the microarray core facility at Baylor College of Medicine can serve as a control for the phosphoimager analysis when comparing the signal intensities of the different rRNA species.

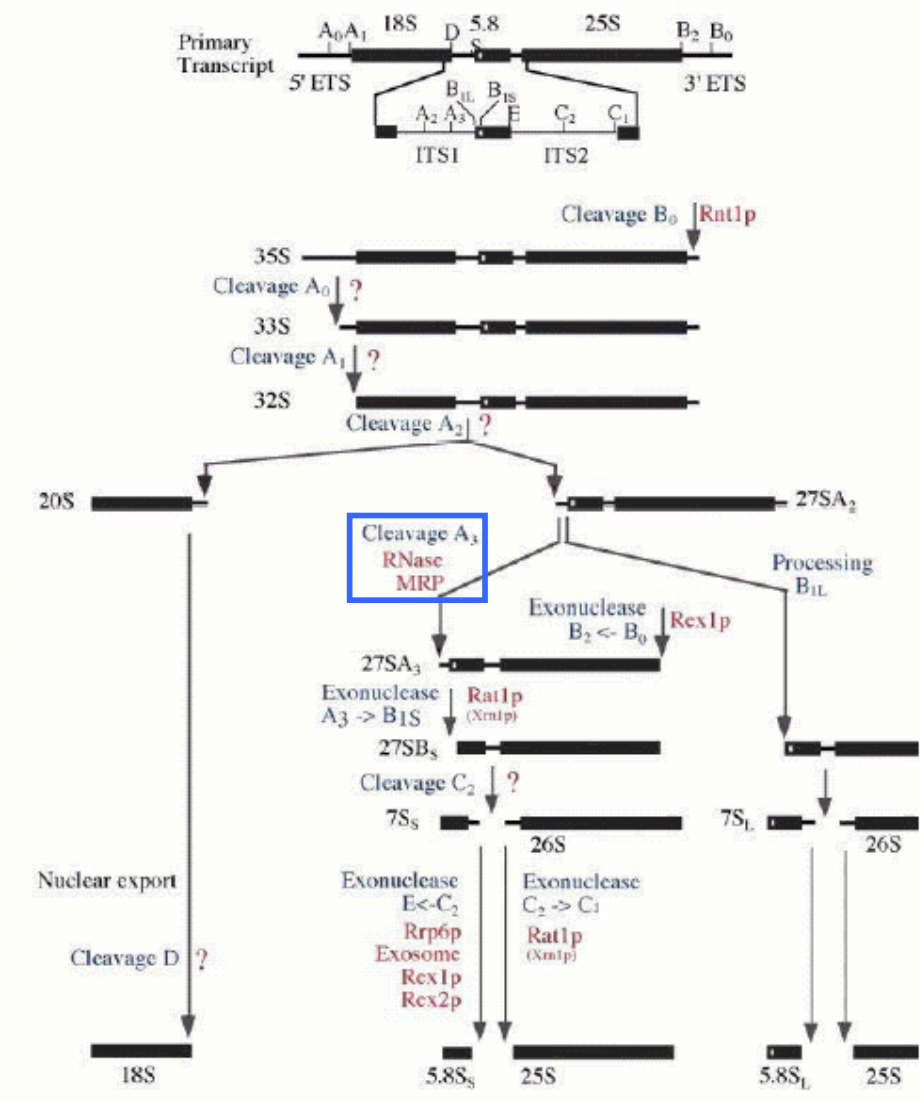

Fig. 58: Schematic of the ribosomal RNA processing in yeast.

The rRNAs are transcribed as a polycistronic primary transcript. Many different enzymes are involved in the maturation of the rRNA species. This very complicated and complex process is relatively conserved. From Fatica, 2002.

4.6 Microarray analysis

DNA microarrays are a powerful tool to study differences in expression levels of two specimens. This technique was first applied to the identification of differences in expression patterns of benign and malignant tissue (Golub et al., 1999). The identification of differences in expression patterns in various breast cancers can predict important clinical properties like

the probability to relapse (van't Veer et al., 2002) or the survival chance of a patient with breast cancer (SØrlie et al., 2001).

To identify downstream targets of RMRP an Affymetrix microarray experiment was performed using the human genome chips U133A and U133B. Both chips contain 39,000 genes. Two patient RNA samples were available for this assay (CHH#2 and CHH#8). Both patients had single base pair substitutions. CHH#2 was compound heterozygous for 89C>G and 124C>T and CHH#8 was homozygous for 70A>G. The two control samples were sex and ethnicity matched. The two patients were children at the time of this study, but the control samples were obtained from young adults. The microarray experiment was done in technical replicates. Technical as well as biological replicates are important, depending on the starting material being used. Replicate experiments generally reduce errors caused by different concentrations of spotted DNA, mRNA and total RNA, different batches of slides, different efficiency of the RNA labeling (Luo et al., 2003).

The great potential of microarray analysis is limited by the lack of good data analysis tools (Nadon and Shoemaker, 2002; Eckel et al., 2005). Currently, most statistical analysis of microarray data depends on the assumption that the data is normally distributed with the variances not dependent on the mean of the data (Pan, 2002). More and more studies suggest that microarray data violate these assumptions rather dramatically. Several alternative models have been proposed for the measurement of errors in microarray data (Chen et al., 1997; Ideker, 2001; Rocke and Durbin, 2001; Tarca et al., 2005).

Figure 59 shows the actual images of the chips after hybridization that were used in the microarray experiment. This was one of the first experiments done in the microarray core facility at Baylor College of Medicine. There are some intensity differences detectable when comparing the technical replicates with the first run of the experiment. These intensity variances add some challenges to the analysis algorithm, because of the variation caused by technical issues rather than actual change in gene expression levels (for summary and overview see box 1 below). This problem also exists when using a dual-dye microarry experiment (Dobbin et al., 2005).

In addition the variance is even bigger when using heterogenous samples like total RNA isolated from human blood. At the end of the thesis total RNA of a third patient (CHH#16) could be obtained. This patient was compound heterozygous for a promoter duplication

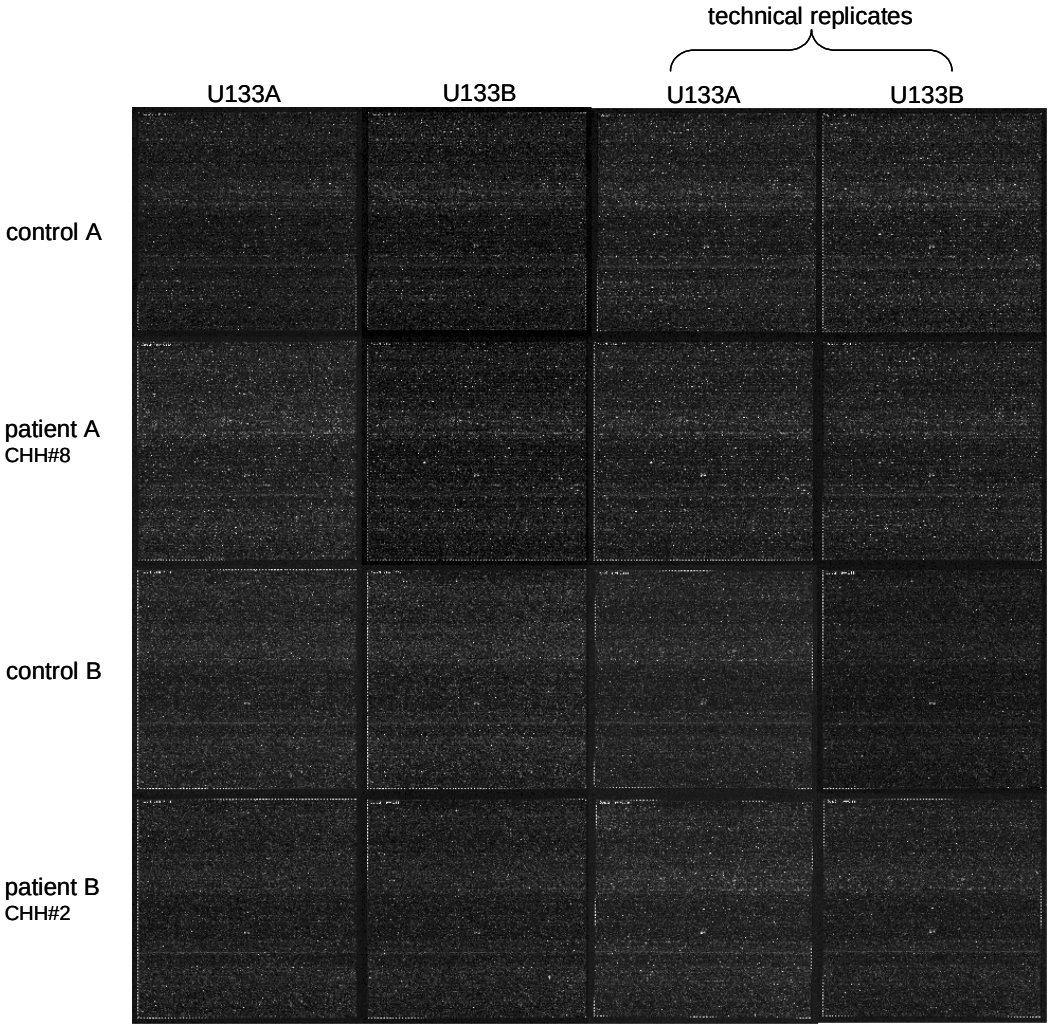

Fig. 59: Microarray chip images.

The actual chip images of the microarray experiment are shown. The first row contains the slides hybridized with the RNA of control A. The second row shows the slides of patient A, the third row illustrates the images of the slides used for control B and the last row depicts the images of the slides of patient B. The first column represents the U133A and the third column the technical replicates of U133A. The second column shows the U133B chips and the fourth column the technical replicates of the U133B chip. Images provided by Brian Dawson.

(-15_-24dup) and a single base pair change (180G>A). Again, a sex and ethnicity matched control was abailable as well, but the age could not be matched in this case either. To verify the findings of the microarray analysis quantitative Real-Time PCR was performed on three

genes that were up-regulated in the Affymetrix experiment (CCR3, PF4V1, IL8 and STAT1 respectively) (Fig. 60).

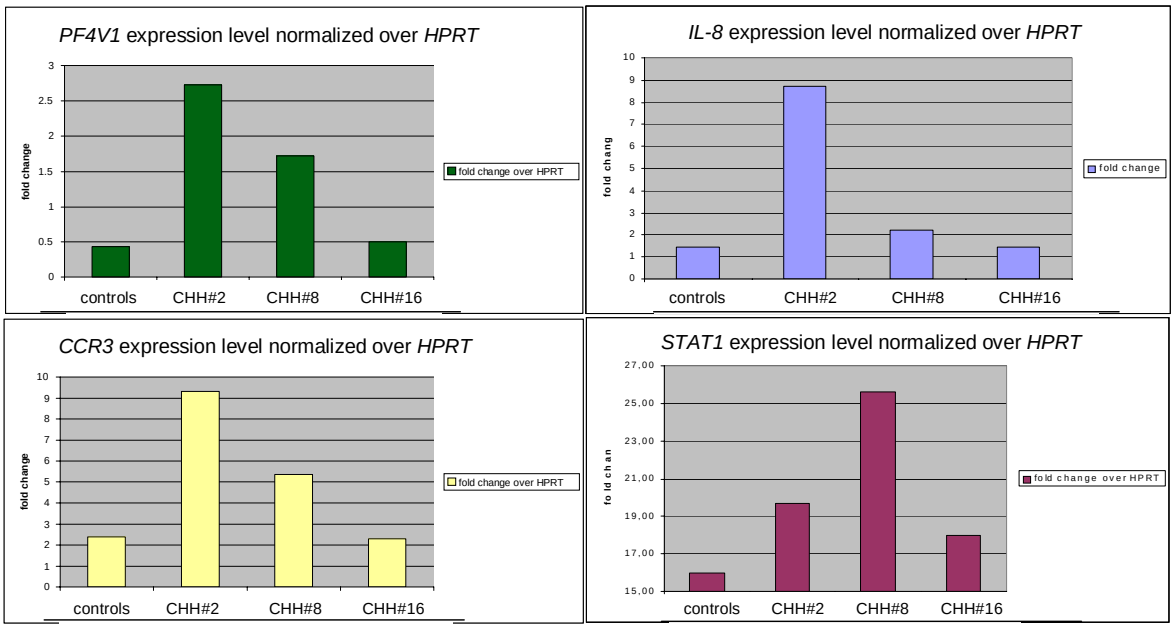

Fig. 60: Quantitative Real-Time PCR for verification of the Affymetrix microarray analysis

Three genes that were upregulated in the microarray experiment were tested with quantitative Real-Time PCR. The expression level of these genes of the two patients used for the chip experiment and a third patient that was recruited at the end of this study were tested. The results show, that CHH#2 and CHH#8 correlate with the findings of the microarray, but the third patient does not seem to be too different when compared to the controls. Only *STAT1* seems to be up-regulated in the latter patient as well.

The results show, that CHH#2 and CHH#8 correlate with the findings of the microarray. The gene expression level of *CCR3*, *IL8* and *PF4V1* in patient CHH#16 seems to be normal when compared to the controls. Only *STAT1* seems to be up-regulated in the latter patient as well. The consistency of patients #2 and #8 between the microarray experiment and the quantitative Real-Time PCR suggests that the correct statistical analysis tool for this set of experiment was used. The housekeeping gene that served as reference was *HPRT* in this study, because the expression level of this gene was most consistent among the controls and in between runs. The choice of a proper reference gene is very important, since even housekeeping genes can be differently expressed among different samples (Wang et al., 2004).

In other disciplines, the true power of the chips has been demonstrated when they have been used to characterize large samples sets of homogenous cell populations. An example of such success is the use of microarrays to predict treatment response in patients with B cell

lymphomas. In those studies, characterization of gene expression patterns by microarray techniques allowed the segregation of lymphomas into two broad categories with differences in response to therapy (Alizadeh et al., 2000).

A good experimental design is very important. It will facilitate the data analysis and the results will be more robust and reliable. That includes:

- Matched samples
  - Ethnic background,
  - Age
  - Body mass index
  - And any other critically important clinical parameter
- Matched samples will reduce
  - Variations of expression due to unique genetic and environmentally related profiles for each individual in the study

Systematic biases of microarray data

- Different sources of RNA
  - RNA degradation, stability of transcripts
- Different time points of analysis (Tu et al., 2004)
  - Prospective sample collection
  - Comparison of one set of microarrays with a second set
- Different production lots of microarrays (Tu et al., 2004)
  - Variation from spot to spot due to unevenness in slide surface properties
  - Dust contamination
  - Incomplete washing
- Different microarray platforms

Analysis biases:

- Statistical method used to analyze microarray data
  - Lack of understanding of the distribution and error structure of microarray data
  - Gene expression data depart rather dramatically from the assumptions required by traditional statistical methods
    - Poor performance of these methods (Wang and Eithier, 2004)
- Small number of samples relative to large number of genes
  - Tends to cause low sensitivity and low specificity (Wang and Eithier, 2004)

Box 1: Summary of microarray biases that might influence the data analysis.

4.7 Mouse Studies

4.7.1 *RMRP* Knock-Out Mouse Model

To study the effect of loss of RMRP function a construct for a knockout mouse model was generated. After electroporation of this construct 100 ES cell clones were screened for the correct recombination event, but unfortunately, no positive ES cell clone could be identified. The probe used for the hybridization of the Mini-Southern needs to be optimized to get a stronger signal. In addition, a different diagnostic enzyme might decrease the false positive clones due to incomplete enzymatic digestion with Kpn I of the genomic DNA isolated from ES cell clones. It also might be that much more ES cell clones needed to be screened in order to isolate one or two positive ES cells. For example, for the *Brca1* knockout mouse 900 ES cell clones had to be screened to get one positive clone for the targeting construct (Allan Bradley personal communication).

But on the other hand loss of *RMRP* might be lethal. The very strong ubiquitous expression of *Rmrp* (Fig. 26) supports this hypothesis as well as there are no deletions of the whole *RMRP* gene described in CHH patients so far. Recently, *RPS19* has been knocked out. RPS19 is one of the 79 ribosomal proteins and is located in the small 40S subunit. Rps19-/- mice are lethal prior to implantation (Matsson et al., 2004). Since *RMRP* is also involved in rRNA processing loss of *RMRP* might therefore also be very early lethal during development.

To circumvent a possible lethality of the *RMRP* classic knockout mouse model two different approaches might be taken. Firstly, a knock-in construct that introduces the 70A>G base pair substitution into the *RMRP* wt locus might give rise to a CHH mouse model. This mutation is found in the majority of CHH patients and is actually the only mutation found among the Old Order Amish. In addition this position is highly conserved among a variety of species (Fig. 53). Secondly, a conditional targeting allele could help to understand the function of *RMRP* in specific tissues or at certain time points during development.

To elucidate *RMRP*'s function during bone development several cre-expressing transgenic mice could be utilized. To study early stages of the limb development a $Rmrp^{flox/flox}$ mouse line could be crossed with *Prx1-cre* transgenic mice. *Prx1* stands for *paired-related homeobox gene-1* and is expressed in the limb bud mesenchyme (Cserjesi et al., 1992) and

acts through a BMP mediated signaling pathway (Lu et al., 1999). This would knock-out *RMRP* in the mesenchymal cells of the limb bud as early as E9.5 (Logan et al., 2002). If *RMRP* might be involved in patterning events of the developing limb this mouse breeding could reveal this function.

When studying the function of *RMRP* in osteoblasts a *Col1a1-cre* expressing mouse line (Dacquin et al., 2002) could be crossed with an $Rmrp^{flox/flox}$ line. Type I collagen is expressed in osteoblasts, odontoblasts, fibroblasts and mesenchymal cells. The identification of an osteoblast specific enhancer element of the mouse *Col1a1* gene restricted *Col1a1* expression to osteoblasts (bone forming cells) and odontoblasts (dentin-forming cells) in teeth. Very low activity of *Col1a1* was seen in tendons but in no other tissues (Rossert et al., 1995). Alternatively, if this should result in a lethal phenotype an inducible *Col1a1-cre* transgenic line could be utilized like the *Col1a1-CreERT2* line. The Cre recombinase is fused to a mutated ligand-binding domain of the estrogen receptor. The cre-recombinase gets only activated in the presence of a synthetic estrogen antagonist 4-hydroxytamoxifen that is injected intraperitoneally into the transgenic mice (Kim et al., 2004). These studies could unravel *RMRP*'s function in bone formation.

More importantly, regarding the *RMRP* gene and CHH the study of the growth plate of the developing bone might help to understand the pathogenesis of this disorder. For this purpose the $Rmrp^{flox/flox}$ line could be crossed with Col2a1-cre (Zhou et al., 1998) and Col10a1-cre (Keller et al., unpublished data) to study the function of *RMRP* in proliferating chondrocytes or hypertrophic chondrocytes, respectively. If *RMRP* plays a role during bone growth a shortening of the long bones similar to the radiographic findings in CHH patients would be expected as well as a shortening of the hypertrophic zone with less hypertrophic chondrocytes as seen in the histology of the growth plate of a CHH patient (1.3).

Similarly, the hair growth is affected in CHH. Most patients have blond, brittle and sparse scalp hair. To elucidate the function of RMRP in hair growth it would be important to perform an *in situ* hybridization using *RMRP* as a probe on mouse skin sections at different stages of development. In addition it might be helpful to look at the hair of CHH patients more closely. Do CHH patients have less hair follicles or do they loose hair more easily? If a skin biopsy of a CHH patient would be available, the skin could be analyzed looking at any alterations in the thickness of different skin layers. Depending on the expression pattern of

the *in situ* hybridization and the observations of the analysis of CHH patient hair and skin a suitable promoter for cre expression could be chosen. K14-cre would be a great transgenic mouse line to study hair follicle development. K14 is expressed in the basal layer of skin cells and the outer layer of hair follicles that are the skin progenitor cells. K1, K5 and loricorin promoters could be used to study more differentiated cell layers (Hanakawa et al., 2002; Merritt et al., 2002).

It might be easier to study the function of *RMRP* in T-cells directly on CHH patient cells isolated from peripheral blood since it is very easy to obtain them in sufficient quantities. The T-cells of CHH patients have been studied extensively in the past (Mäkitie et al., 2000a; Mäkitie et al., 2000b; Mäkitie et al., 2001; Bocca et al., 2004). All these studies come to the same conclusion that the T-cells of CHH patients show a proliferation defect *in vitro* rather than increase apoptosis. More precisely, the patient's T-cells have a defect in the transition of the G0 to the G1 phase of the cell cycle (Yel et al., 1999).

It might be of great interest to study the role of *RMRP* during bone and hair follicle development as well as in T-cell differentiation, since these are the tissues that are most consistently affected in CHH patients. These few examples might give a glimpse of possibilities to elucidate the function of *RMRP* in a variety of different tissues or at different time points during development.

4.7.2 Transgenic Mouse Studies

The Affymetrix microarray experiment performed with two CHH patient samples compared to two control samples showed upregulation of several cytokines and cell cycle control genes (Tab. 10). Two of these genes were selected for transgenic mouse studies, because of their biological function.

The first gene was *IL8*, because of its fundamental roles in development, homeostasis and in the immune system. IL8 is secreted by several cell types in response to inflammatory stimuli. The 3' UTR of *IL8* is essential for posttranscriptional suppression of *IL8* gene expression. In osteoarthritis (OA) IL8, GROα and their receptors are upregulated and the p38 MAPK

pathway gets activated. This results in a stimulation of transglutaminases (TG2) that in turn leads to hypertrophy and calcification of articular chondrocytes (Fig. 61) (Merz et al., 2003). Since there is no mouse orthologue of the human *IL8* identified yet and the human *IL8* gene has successfully been used in previous transgenic mouse studies (Simonet et al., 1994; Horiguchi et al., 2000; Wen and Wu 2001; Kucharzik and Williams 2003), the human *IL8* gene was also chosen for this transgenic mouse study and cloned under the control of the

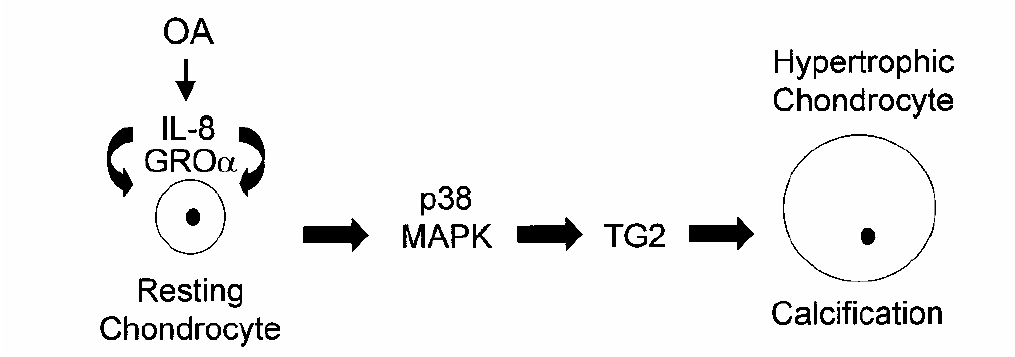

Fig. 61: Function of IL8 in OA cartilage.

In OA cartilage IL8, GROα and their receptors expression are upregulated. Through p38 MAPK pathway and transglutaminases (TG2) they promote hypertrophic differentiation and calcification of chondrocytes. From: Merz et al., 2003.

Col2a1 and *Col10a1*, respectively to study whether upregulation of *IL8* in proliferating and hypertrophic chondrocyte will result in a similar bone phenotype as seen in CHH patients. Unfortunately, only mouse lines from the Col2a1-hIL8-WPRE transgenics could be established, since no Col10a1-hIL8-WPRE founders could be obtained. No phenotype was seen in any of the four Col2a1-hIL8-WPRE transgenic mouse lines derived from one founder. This could have several reasons. Firstly, there was only one founder that had black eyes suggesting a stronger expression of the transgene. It might be that the level of transgene expression was not high enough to cause a phenotype, because only the eye color has changed from red to black in the founder but the coat color was not changed at all. This indicates that the expression of the transgene was not high enough to change the color of the fur (Fig. 62). Secondly, it might be that IL8 does not play a role in pathogenesis of CHH. At the end of this study a third CHH patient sample became available for total RNA isolation. This third patient together with the first two patients was tested for *IL8* expression level via quantitative Real-Time PCR (Fig. 60). While the first two patients showed an upregulation of *IL8* (consistent with the microarray data) the third patient had normal IL8 RNA level. It still might be that

while the RNA level of this patient was normal, the protein level still could have been elevated.

Fig. 62: Transgenic mice with strong transgene expression using the coat color vector.

Mice (founders) are 7.5 days old. On the left is a Tg with strong transgene expression. The eyes are black and the coat color has almost completely changed. In the middle is a Tg with just black eyes, but no change of the coat color. On the right is a WT FVB/N littermate with red eyes. Tg: transgenic mouse
Picture provided by Dipl. Biol. Bettina Keller.

The second gene of interest was a putative lymphocyte G_0/G_1 switch gene (*G0S2*). The immune defect of CHH patients primarily affects the T-cell system. Mäkitie et al., reported a more generalized hematopoietic impairment. In their studies, there was defective *in vitro* colony formation in all myeloid lineages, including erythroie, granulocyte-macrophage, and megakaryocyte colony formation. This suggested a common cell proliferation defect in CHH. Further *in vitro* studies of T-cells isolated from CHH patients suggested a defect of the transition of the G0 to the G1 phase of the cell cycle (Fig. 63). Therefore the mouse orthologe, *G0s2*, was cloned under the control of the *Col2a1* and *Col10a1* promoter respectively to study the effect of overexpression of *G0s2* on bone formation and growth.

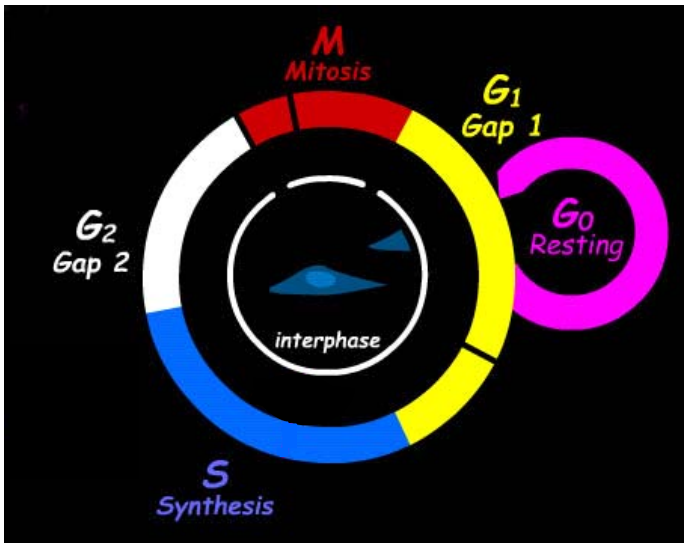

Fig. 63: Schematic of the cell cycle.

Different stages of the cell cycle are shown. The black interruptions of the circle indicate cell cycle check points. The first one is the intra-G_1 check point. The 2nd checkpoint is just before starting the mitosis and the 3rd is the intra-mitosis checkpoint.

From:
http://www.cellsalive.com/index.htm

Unfortunately, none of the transgenic founders showed a change of neither the coat nor the eye color. Two founders of each transgene (Col2a1-G0s2-lacZ and Col10a1-G0s2-lacZ, respectively) were randomly chosen to establish transgenic mouse lines. None of the transgenic lines showed any phenotype. It might very well be that the level of transgene expression was not high enough to cause any phenotype. It has been reported that lacZ expression might inhibit the transgene expression (Dr. Guang Zhou, personal communication). So, at this point *G0S2* cannot totally be excluded as a downstream target of *RMRP*.

To further evaluate a putative role of an overexpression of *G0S2* in CHH it might be useful to change the transgenic construct. The lacZ reporter gene could be replaced by the WPRE element to enhance the transgene expression (Mian et al., 2005). To distinguish the endogenous *G0S2* from the transgene a V5 tag could be added in frame at the N-terminus of the transgene. But before starting the transgenic mouse studies it might be of interest to verify the upregulation of *G0S2* in the third CHH patient that is now available. If *G0S2* is upregulated consistently in all three patients it suggests that overexpression of *G0S2* might play a role in the pathogenesis of CHH. When examining the *Rmrp* expression pattern in the in situ hybridization (Fig. 25) the *Col1a1* might be a very interesting promoter for the transgenic mouse studies as well.

4.8 Yeast Studies

Since *RMRP* is not translated into a protein it is very hard to predict how a mutation in this gene might alter its function. Because *RMRP* is highly conserved among a variety of species mutations that have been found in CHH patients and that were conserved between human and yeast were introduced into the yeast ortholog *NME1*. At the time the yeast experiments were started five mutations were identified that were conserved from human to yeast. Four of those were introduced into the yeast ortholgoue *NME1* (Tab. 14). Although the position of the fifth mutation, a 154G>T base pair substitution (Ridanpää et al., 2002), was highly conserved from human to yeast it was not introduced into the yeast orthologue *NME1*, because this region has been deleted in yeast without any detectable phenotype (Mark Schmitt personal communication).

Studies in yeast have attributed multiple functions to the Ribonuclease Mitochondrial RNA Processing ribonuclease (RNase MRP) complex (Fig. 64). In mitochondria it plays a role during mitochondrial DNA replication. A short RNA primer forming a DNA-RNA hybrid initiates this replication. RNase MRP cleaves this primer so that the DNA polymerase can complete the replication process. Loss of RNase MRP function might therefore result in a mitochondrial depletion. The mutations studied here do not seem to alter proper mitochondrial function as shown in mitochondrial depletion tests in yeast as well as in one CHH fibroblast cell line. Maybe there are other RNases that compensate for RNase MRP in mitochondria like RNase HI (Cerritelli and Crouch, 1998).

In yeast RNase MRP plays a role in pre-ribosomal RNA processing. It cleaves at the A_3-site that in turn leads to the maturation of the 5.8S rRNA. It converts the long form of the 5.8S rRNA (5.8S_L rRNA) to the short and active form of the 5.8S rRNA (5.8S_S rRNA) that is incorporated into the ribosome. Two of the five *nme1*^{mutant} strains show an alteration in the normal ratio of the 5.8S_L rRNA versus the 5.8S_S rRNA. 70A>G is just outside of the P3 domain. This position is highly conserved among a variety of species. In yeast it can form a 9 bp duplex with the 5.8S rRNA (Clayton, 1994). This mutation might therefore affect the maturation of the 5.8S rRNA that could be seen in the change of the ratio of the long versus the short form of the 5.8S rRNA in yeast (Fig. 49).

When cells were depleted of RNase MRP RNA, there was failure to cleave at the B1b processing site; however, if the B1a endonuclease could still produce its cleavage product, the observed change in the ratio of the two species would occur. The B1a endonuclease maybe normally present in limiting amounts so that most of the RNA is cleaved by the B1b (RNase MRP?) enzyme to produce the final 1:10 ratio of the long: short form of the 5.8S rRNA normally seen (Rubin, 1974). With the depletion of the B1b endonuclease, 5.8Sb rRNA would become predominantly a substrate for the B1a endonuclease such that more 5.8Sa rRNA would be produced. However, with limiting amounts of the B1a endonuclease, all of the pre-5.8S rRNA may not be efficiently cleaved and the aberrant 305-nt 5.8Sb rRNA is thereby produced (Schmitt and Clayton 1993). This might delay rRNA processing, ribosome biogenesis, translation of proteins in general or change the stability of ribosomal RNA. The study of ribosomal RNA processing in CHH patients is still pending, but it might be that a putative ribosomal RNA processing defect might be compensated by other enzymes like the DEAD-box protein 3 (DBP3) (Weaver et al., 1997).

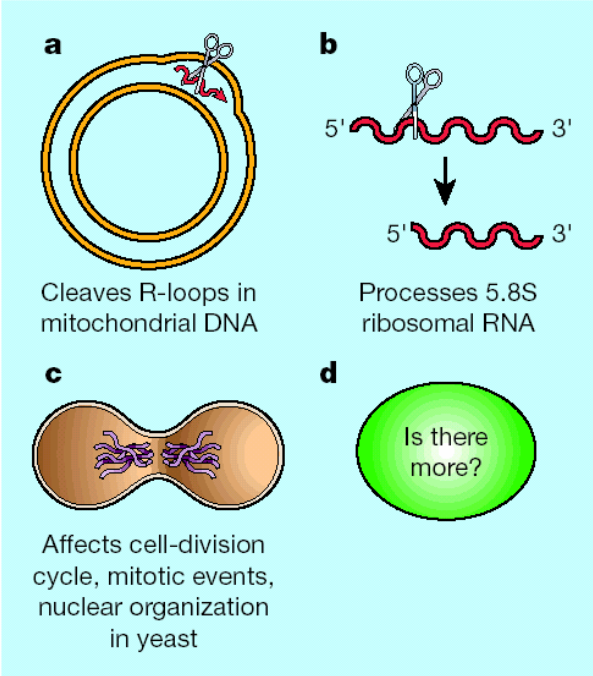

Fig. 64: Summary of RNase MRP functions.

Studies in yeast have attributed multiple functions to the RNase MRP ribonucleotide complex.
a: Schematic of mitochondrial DNA as double ring. An RNA primer (red arrow) primes mitochondrial DNA replication. This primer is cleaved by RNase MRP (scissors).
b: RNase MRP is involved in a late step of ribosomal rRNA processing. It cleaves (scissors) a rRNA precursor that leads to the maturation of the 5.8S rRNA.
c: RNase MRP plays a role in the cell cycle progression at the end of mitosis.
d: There might be an as yet unidentified function of RNase MRP.
From: Cai et al., 2001.

Mutations in protein components of RNase MRP result in a cell cycle delay in yeast. These mutants have an exit-from-mitosis defect (Cai et al., 2002). This defect is caused by an increase in CLB2 (B-cyclin) levels caused by an increase in *CLB2* mRNA stability. Normally *CLB2* mRNA levels decrease rapidly when the cell completes the mitosis. RNase MRP cleaves the 5' UTR of *CLB2* that results in a rapid degradation of the mRNA by the Xrn1 nuclease (5'→3' exoribonuclease) and not by exosomes that are usually responsible for mRNA degradation (Gill et al., 2004). In this study no cell cycle phenotype could be observed in the $nme1^{mutant}$ strains. There was no detectable change in the cell cycle progression under normal growth conditions or after stress induction through γ-irradiation. γ-irradiation induces DNA double strand breaks. So the double strand break repair mechanism does not seem to be affected by the *nme1* point mutations. Other stress responses were not tested like UV or oxidative stress that affects base pair modifications or treatment with mitomycin C that results in strand crosslinking. The latter two stress responses will activate different 'repair cascades' than the repair of DNA double strand breaks.

The studies in yeast suggest that there might be yet another function of RNase MRP. It might act as a site-specific ribonuclease similar to its function of cleaving *CLB2* in mRNA degradation (Gill et al., 2004), but in the microarray studies performed here, *CLB2* is not affected. While the DNA sequence might be conserved among different species the function might not be. If the function would be conserved from human to yeast, an up-regulation of

the *CLB2* gene in the microarray study would have been expected. In addition two protein subunits that are specific for RNase MRP Smn1p and RNP1 have been identified in yeast, but there are no human orthologs found yet. On the other hand Rpp38 is part of the human RNase MRP complex, but there is no ortholgous gene in yeast identified so far (Tab. 18).

Table 18: Species comparison of homologies of RNase MRP protein and RNA components

MRP subunit	*S. cerevisiae*	*S. pombe*	*C. elegans*	*D. melanogaster*	*M. musculus*	*H. sapiens*	shared by RNase P
RNA	NME1	NME1	not yet identified		MuMRP	RMRP	
protein subunits	Snm1	*T42459	not yet identified				no
	Pop1	*T50203	*C05D11.9	*LD21623	*BAB30296.1	hPop1	yes
	Pop3	not yet identified					yes
	Pop4	*P87120	*C15C6.4	*CG8038	*BAB22410.1	hPop4	yes
	Pop5	*T41635	*T27292	*CG14057	*BAB23935	hPop5	yes
	Pop6	not yet identified		+	not yet identified		yes
	Pop7/Rpp2	not yet identified	+	not yet identified	+	Rpp20	yes
	Pop8	not yet identified			+	not yet identified	yes
	Rpp1	*CAB087492	*T33715	*CG11606	RNaseP2	Rpp30	yes
	not yet identified					Rpp38	
	RMP1					not yet identified	no

* putative ortholgues
\+ alignment results fell below ortholgue designation criteria
modified from Aulds et al., 2002 and Salinas et al., 2005.

In addition, no yeast orthologes have been identified to the human proteins RPP14, RPP25, and RPP40 that are part of the RNase MRP complex (Welting et al., 2004) and also shared by the RNase P complex in humans. Interestingly, the yeast orthologe to human RPP21 is Rpr2p that was postulated to be specific for RNase P, but RPP21 is postulated of being part of the human RNase MRP complex (Welting et al., 2004).

These data suggest, while the DNA sequence might be conserved, the function might not be. The function of the RNase MRP complex might have changed during evolution, since there are no orthologues of RMRP found in *C. elegans* and *D. melanogaster*.

Interestingly, there is some clinical overlap of Shwachman-Diamond syndrome, Methaphyseal Chondrodysplasia type Schmid and Cartilage Hair Hypoplasia. The SDBS

gene plays a role in RNA metabolism (Boocock et al., 2003) and MCDS results from a functional haploinsufficiency in some cases due to nonsense-mediate decay of mutant *COL10A1* alleles induced by aberrant disulfide bond formation and intracellular retention in the endoplasmatic reticulum (Wilson et al., 2005). There maybe some analogies between these conditions and CHH with similar pathogenic mechanisms involved.

Alternatively, *RMRP* could act as a micro RNA in gene regulation. Structurally, *RMRP* can fold to hairpin structures that theoretically could be processed by drosha and dicer (Fig. 65). The pri-miRNA is transcribed by RNA Polymerase I then cleaved by drosha to produce the pre-miRNA. Then dicer processes this pre-miRNA to give rise to the mature miRNA. Bound to the miRNP complex the miRNA when exactly complementary to the target mRNA may lead to mRNA degradation. If the miRNA is partially complementary to the target mRNA this might result in an inhibition of protein translation.

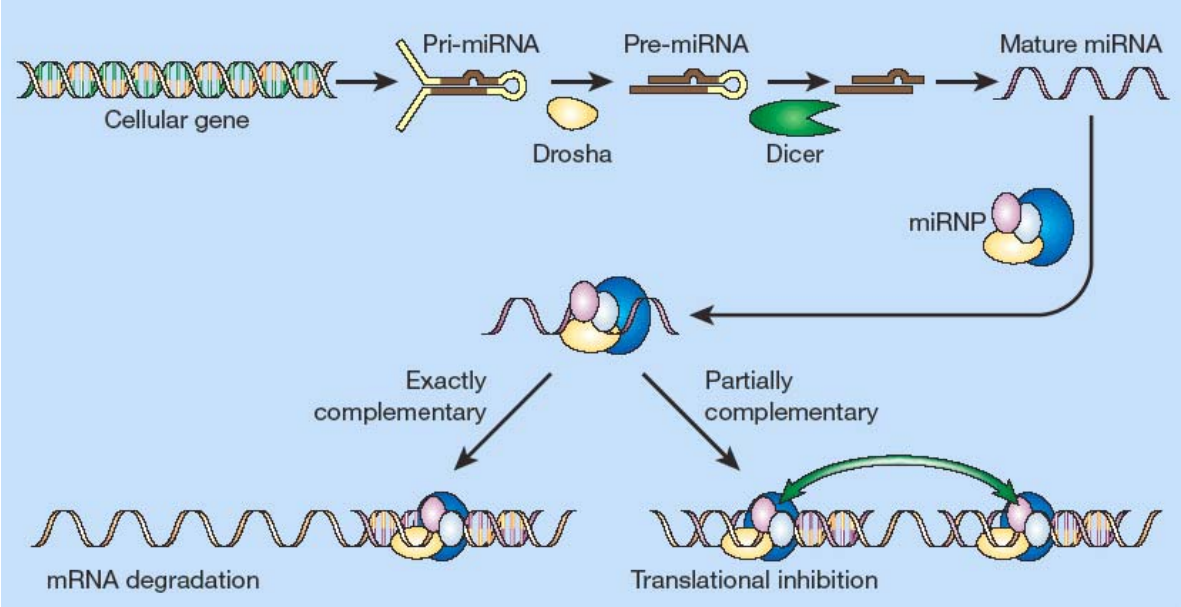

Fig. 65: Schematic of maturation of miRNA.

The Pri-miRNA is transcribed by RNA Polymerase I then cleaved by drosha to produce the pre-miRNA. Then dicer processes this pre-miRNA to give rise to the mature miRNA. Bound to the miRNP complex the miRNA when exactly complementary to the target mRNA may lead to mRNA degradation. If the miRNA is partially complementary to the target mRNA this might result in an inhibition of protein translation. From: Novina and Sharp (2004).

4.9 Conclusions

The radiologic findings of CHH in association with the clinical symptoms of low birth length, subsequent severe growth failure, and abnormal hair correlate with presence of *RMRP* mutations. *RMRP* seems to be highly polymorphic despite of its conservation throughout a variety of different species. Reasons for this might be failure of repair mechanisms, relaxed selective pressure or a local hot spot for a high mutation rate. Whether the polymorphisms in the *RMRP* gene contribute to the pleiotropic and variable phenotype of CHH remains unclear. Abundant mutations in the promoter region were detected. These may cause a hypomorphic state that decreases the level of *RMRP* transcription. The point mutations do not seem to alter the essential functions of the yeast orthologue of *RMRP*. The studies in yeast showed normal mitochondrial function, normal chromosomal stability during mitosis, no delay in cell cycle progression, and normal telomere length, but the point mutations might decrease RNA stability in humans as shown in the quantitative Real-Time PCR analysis.

Two of the five $nme1^{mutant}$ strains ($nme1^{70A>G}$ and $nme1^{2bpdel}$) show an alteration in the ratio of the long versus the short/active form of the 5.8S rRNA. This finding could not be verified in humans yet, but if the adequate human material will become available this can be tested easily, since the method to look at pre-ribosomal processing is very well established. The pre-ribosomal defect might delay rRNA processing, ribosome biogenesis, translation of proteins in general or change the stability of ribosomal RNA.

While the nucleotide position of the mutations is conserved, function may not be, since there are no othologoues *RMRP* genes found in *C. elegans* and *D. melanogaster*. Alternatively, functions evident in *NME1*, the orthologue yeast gene, might have altered during evolution resulting in an yet unknown role of *RMRP*. It might act as a micro RNA in gene regulation. The conditional targeted *Rmrp* allele of the mouse model will help to elucidate the underlying pathogenic mechanism of CHH. The mechanistic defect of bone and hair seen in CHH might be analogue processes, since there are striking similarities for example between the Wnt signaling pathway in bone (reviewed by Westendorf et al., 2004) and hair (reviewed by Schmidt-Ullrich and Paus, 2005) development.

The microarray studies showed upregulation of many cytokines and other genes that are involved in immune responses and cell cycle regulation. This is consistent with the findings of immune response defects in CHH patients that were characterized by isolation and stimulation of T- and B-cells from peripheral blood of CHH patients. The role of cytokines and cell cycle regulatory genes is also very similar in bone (reviewed by Okada and Tanaka, 2004) and hair growth (reviewed by Paus et al., 2005) growth. The analysis of these genes in the mouse model with the conditional targeted *Rmrp* allele will help to dissect these pathogenic mechanisms in CHH.

5 Summary

Cartilage Hair Hypoplasia (CHH) or metaphyseal chondrodysplasia McKusick type (OMIM #250250) is an autosomal recessive multisystemic disease characterized by metaphyseal skeletal involvement with dwarfism and symptoms including fine and sparse hair, deficient cellular immunity and predisposition to malignancy. CHH is one of the few Mendelian diseases caused by mutations in a non-coding RNA gene, *RMRP*. *RMRP* is a nuclear encoded RNA that is the RNA component of the ribonucleoprotein complex RNase MRP that functions as an endonuclease. Yeast studies suggest its involvement in processing of pre-rRNA in the nucleolus, cleavage of mitochondrial RNA priming mitochondrial DNA replication, and progression of the cell cycle at the end of mitosis. Mutation analysis was performed in 32 patients, referred with the clinical diagnosis of probable CHH. *RMRP* mutations were found in 24 cases. The combination of significantly reduced birth length, subsequent severe growth failure and deficient hair growth appeared to be highly correlated with the detection of mutations in the *RMRP* gene. A study of the Pol III *RMRP* promoter suggests that promoter duplications found in CHH patients abolish transcription of the *RMRP* gene, a finding confirmed by quantitative Real-Time-PCR analysis of patient lymphoblasts. This analysis showed a 7-fold down-regulation of the *RMRP* RNA level in three patients. Two patients were compound heterozygous for a base pair substitution and one patient was compound heterozygous for a base pair substitution and a promoter duplication. *In vitro* studies of the mutant promoters also showed a significant reduction of the *RMRP* promoter activity independent of the length of the promoter duplication. *RMRP* mutations introduced into the yeast ortholog *NME1* neither altered mitochondrial function nor affected mitochondrial depletion in a CHH patient fibroblast cell line. Chromosomal segregation and chromosomal stability during mitosis also seems to be unaffected in yeast. Interestingly, the most commonly found mutation 70A>G causes an alteration in ribosomal processing in *Saccharomyces cerevisiae*. The ratio of the short versus the long form of the 5.8S rRNA ($rRNA_S$/5.8S $rRNA_L$) is shifted from a 10:1 ratio to a 2:3 ratio. This might delay rRNA processing, ribosome biogenesis, translation of proteins in general or change the stability of ribosomal RNA. Microarray studies performed with two patients suggest that *RMRP* mutations are associated with significant up-regulation of several cytokine family and cell cycle regulatory genes when compared to normal control individuals. These data suggest that alteration of ribosomal processing leads to altered cytokine signalling and cell cycle

progression in terminally differentiated cell types such as lymphocytic and chondrocytic lineages involved in CHH pathogenesis.

Based on the microarray studies two candidate genes that were significantly upregulated in two CHH patients when compared to two normal controls where further characterized in transgenic mouse studies (*IL8* and *G0s2*). *IL8* was selected, because of its important role in chondrocyte maturation. *G0s2* was a good candidate gene, because it is a putative lymphocyte G0/G1 switch gene. *In vitro* studies of T-cells of CHH patients suggest a defect of the transition from the G0 to the G1 phase of the cell cycle. Both genes were overexpressed in the proliferating and hypertrophic chondrocyte zone of the growth plate, but none of the transgenic mouse lines showed any obvious phenotype. This could be due to the relatively weak transgene expression or these two genes might not play a role in the pathogenesis of CHH.

A mouse model with conditional targeted *Rmrp* allele will help to elucidate the pathogenic mechanisms of CHH. A conventional knockout mouse model of *Rmrp* might be lethal, since *RMRP* is ubiquitously expressed and no deletion of the whole gene has been found in CHH patients.

6 References

Alizadeh AA, Eisen MB, Davis RE, Ma C, Lossos IS, Rosenwald A, Boldrick JC, Sabet H, Tran T, Yu X, Powell JI, Yang L, Marti GE, Moore T, Hudson J Jr, Lu L, Lewis DB, Tibshirani R, Sherlock G, Chan WC, Greiner TC, Weisenburger DD, Armitage JO, Warnke R, Levy R, Wilson W, Grever MR, Byrd JC, Botstein D, Brown PO, Staudt LM (2000): Distinct types of diffuse large B-cell lymphoma identified by gene expression profiling. *Nature* **403**(6769):503-11.

Allison DS, Goh SH, Hall BD (1983): The promoter sequence of a yeast $tRNA^{tyr}$ gene. *Cell* **34**:655-664.

Amizuka N, Warshawsky H, Henderson JE, Goltzman D, Karaplis AC (1994): Parathyroid hormone-related peptide-depleted mice show abnormal epipyseal cartilage development and altered endochondral bone formation. *J Cell Biol* **126**:1611-1623.

Ammann RA, Duppenthaler A, Bux J, Aebi C (2004): Granulocyte Colony-Stimulating Factor-Responsive Chronic Neutropenia in Cartilage-Hair Hypoplasia. *J Pediatr Hematol Oncol* **26**(6): 379-381.

Balling R, Deutsch U, Gruß P (1988): Undulated, a mutation affecting the development of the mouse skeleton, has a point mutation in the paired box of Pax 1. *Cell* **55**:431-435.

Bi W, Deng JM, Yhang Y, Behringer RR, De Crombrugghe B (1999): Sox9 is required for cartilage formation. *Nat Genet* **22**:85-89.

Birnboim HC, and Doly J (1979): A rapid alkaline extraction procedure for screening recombinant plasmid DNA. *Nucleic Acids Res* **7**(6):1513-1523.

Bocca G, Weemaes CM, van der Burget I, Otten BJ (2004): Growth hormone treatment in cartilage-hair hypoplasia: effects on growth and the immune system. *J Pediatr Endocrinol Metab* **17**:47-54.

Boerkoel CF, Takashima H, John J, Yan J, Stankiewicz P, Rosenbarker L, Andre JL, Bogdanovic R, Burguet A, Cockfiled S, Cordeiro I, Fründ S, Illies F, Joseph M, Kaitila I, Lama G, Loirat C, McLeod DR, Milford DV, Petty EM, Rodrigo F, Saraiva JM, Schmidt B, Smith GC, Spranger J, Stein A, Thiele H, Tizard J, Weksberg R, Lupski JR, Stockton DW (2002): Mutant chromatin remodeling protein SMARCAL1 causes Schimke immuno-osseous dysplasia. *Nat Genet* **30**:215-220.

Bogenhagen DF (1985): The intragenic control region of the Xenopus 5 S RNA gene contains two factor A binding domains that must be aligned properly for efficient transcription initiation. *J Biol Chem* **260**:6466-6471.

Bonafé L, Schmitt K, Eich G, Giedion A, Superti-Furga A (2002): RMRP gene sequence analysis confirms a cartilage-hair hypoplasia variant with only skeletal manifestations and reveals a high density of single-nucleotide polymorphisms.*Clin Genet* **61**:146-151.

Boocock GRB, Morrison JA, Popovic M, Richards N, Ellis L, Durie PR, Rommens JM (2003): Mutations in SBDS are associated with Shwachman-Diamond syndrome. *Nat Genet* **33**:97-101.

Brasier AR, Tate JE and Habener JF (1989): Optimized use of the firefly luciferase assay as a reporter gene in mammalian cell lines. *Biotechniques* **7**(10):1116-1122.

Briggs MD, Hoffman SM, King LM, Olsen AS, Mohrenweiser H, Leroy JG, Mortier GR, Rimoin DL, Lachman RS, Gaines ES, Cekleniak JA, Knowlton RG, Cohn DH (1995): Pseudoachondroplasia and multiple epiphyseal dysplasia due to mutations in the cartilage oligomeric matrix protein gene. *Nat Genet* **10**:330-336.

Cadle RG, Dawson T, Hall BD (1996): The prevalence of genetic disorders, birth defects and syndromes in central and eastern Kentucky. *J Ky Med Assoc* **94**:237-241.

Cai T, Reilly TR, Cerio M, Schmitt ME (1999): Mutagenesis of *SNM1*, which encodes a protein component of the yeast RNase MRP, reveals a role for this ribonucleoprotein endoribnuclease in plasmid segregation. *Mol Cell Biol* **19**:7857-7869.

Cai T, Aulds J, Gill T, Cerio M, Schmitt ME (2002): The Saccharomyces cerevisiae RNase mitochondrial RNA processing is critical for cell cycle progression at the end of mitosis. *Genetics* **161** (3):1029-1042.

Castigli E, Irani AM, Geha RS, Chatila T (1995): Defective expression of early activation genes in cartilage-hair hypoplasia (CHH) with severe combined immunodeficiency (SCID). *Clin Exp Immunol* **102**(1):6-10.

Cerritelle SM, Crouch RJ (1998): Cloning, expression, and mapping of ribonucleases H of human and mouse related to bacterial RNase HI. *Genomics* **53**(3):300-307.

Chambers TJ (2000): Regulation of the differentiation and function of osteoclasts. *J Pathol* **192**:4-13.

Chan D, Jacenko O (1998): Phenotypic and biochemical consequences of collagen X mutations in mice and humans. *Matrix Biol* **17**:169-184.

Chang DD, Clayton DA (1987): A novel endoribonuclease cleaves at a priming site of mouse mitochondrial DNA replication. *EMBO J* **6**:409-17.

Chen H, Lun Y, Ovchinnikov D, Kokubo H, Oberg KC, Pepicelli CV, Lee B, Johnson RL (1998): Limb and kidney defects in Lmx1b mutant mice suggest an involvement of LMX1B in human nail patella syndrome. *Nat Genet* **19**:51-55.

Chen J, Kyte C, Chan W, Wetmur JG, Fuchs CS, Giovannucci E (2004): Polymorphism in the thymidylate synthase promoter enhancer region and risk of colorectal adenomas. *Cancer Epidermiol Biomarkers Prev* **13**(12):2247-2250.

Chen Y, Dougherty ER, Bittner ML (1997): Ratio-based decisions and the quantitative analysis of cDNA microarray imgaes. *J Biomed Optics* **2**(4):364-374.

Chen YC, Song C, Luo CQ (2003): Short Hairpin RNAs Induced RNA Interference in Human Cells. *Chinese J Cancer* **22**(6):566-570.

Cheung PK, McCormick C, Crawford BE, Esko JD, Tufaro F, Duncan G (2001): Etiological point mutations in the hereditary multiple exostoses gene EXT1: a functional analysis of heparan sulfate polymerase activity. *Am J Hum Genet* **69**:55-66.

Chiang C, Litingtung Y, Lee E, Young KE, Corden JL, Westphal H, Beachy PA (1996): Cyclopia and defective axial patterning in mice lacking Sonic hedgehog gene function. *Nature* **383**:407-413.

Chiang C, Litingtung Y, Harris MP, Simandl BK, Beachy PA, Fallon JF (2001): Manifestation of the Limb Prepattern: Limb Development in the Absence of Sonic Hedgehog Function. *Dev Biol* **236**(2):421-435

Chon MJ, Tickle C (1996): Limbs: a model for pattern formation within the vertebrate body plan. *TIG* **12**:253-257.

Chu S, Archer RH, Zengel JM, Lindahl L (1994): The RNA of RNase MRP is required for normal processing of ribosomal RNA. *Proc Natl Acad Sci USA* **91**:659-663.

Clayton DA (1994): A nuclear function for RNase MRP. *Proc Natl Acad Sci USA* **91**: 4615-4617.

Colvin JS, Bohne BA, Harding GW, McEwen DG, Ornitz DM (1996): Skeletal overgrwoth and deafness in mice lacking fibroblast growth factor receptor 3. *Nat Genet* **12**:390-397.

Craig DW, Stephan DA (2005): Applications of whole-genome high-density SNP genotping. *Expert Rev Mol Diagn* **5**(2):159-170.

Cristello AD, Heximer SP, Russell L, Fordyke DR (1997): Cyclosporin A inhibits early mRNA expression of G0/G1 switch gene 2 (G0S2) in incultured humanblood mononuclear cells. *DNA Cell Biol* **16**(12):1449-1458.

Cserjesi P, Lilly B, Bryson L, Wang Y, Sassoon DA, Olson EN (1992): Mhox, a mesodermally restricted homeodomain protein that binds an essential site in the muscle creative kinase anhancer. *Development* **115**:1087-1101.

Dacquin R, Starbuck M, Schinke T, Karsenty G (2002): Mouse alpha.1(I)-collagen promoter is the best known promoter to drive efficient Cre recombinase expression in osteoblast. *Dev Dyn* **224**:245-251.

Deng C, Wynshaw-Boris A, Yhou F, Kuo A, Leder P (1996): Fibroblast Growth Factor Receptor 3 Is a Negative Regulator of Bone Growth. *Cell* **84**:911-921.

Dobbin KK, Kawasaki ES, Petersen DW, Simon RM (2005): Characterizing dye bias in microarray experiments. *Bioinformatics* (in press).

Donello JE, Loeb JE, Hope TJ (1998): Woodchuck hepatitis virus contains a tripartite posttranscriptional regulatory element. *J Virol* **72**:5085-5092.

Draptchinskaia N, Gustavsson P, Andersson B, Pettersson M, Willig TN, Dianzani I, Ball S, Tchernia G, Klar J, Matsson H, Tentler D, Mohandas N, Carlsson, B, Dahl N (1999): The gene encoding ribosomal protein S19 is mutated in Diamond-Blackfan anaemia. *Nat Genet* **21**:169-175.

Dreyer SD, Zhou G, Lee B (1998): The long and the short of it: developmental genetics of the skeletal dysplasias. *Clin Genet* **54**(6):464-473.

Dreyer SD, Yhou G, Baldini A, Winterpacht A, Yabel B, Cole W, Hohnson RL, Lee B (1998): Mutations in LMX1B cause abnormal skeletal patterning and renal dysplasia in nail patella syndrome. *Nat Genet* **19**:47-50.

Duboule D (2002): Developmental biology: Making progress with limb models, *Nature* **418**:492-493

Dudley AT, Ros MA, Tabin CJ (2002): A re-examination of proximodistal patterning during vertebrate limb development. *Nature* **418**:539-544.

Duncan GM, McDormick C, Tufaro F (2001): The link between heparan sulfate and hereditary bone disease: finding a function for the EXT family of putative tomor suppressor proteins. *J Clin Invest* **108**:511-516.

Eckel JE, Gennings C, Therneau TM, Burgoon LD, Boverhof DR, Zacharewski TR (2005): Normalization of two-channel microarray experiments: a semiparametric approach. *Bioinformatics* **21**(7):1078-1083.

Elliot AM, Field FM, Rimoin DL, Lachman RS (2005): Hand Involvement in Schmid Meta-physeasl Chondrodysplasia. *Am J Med Genet* **132A**:191-193.

Engebrecht J, Hirsch J, Roeder GS (1990): Meiotic gene conversion and crossing over: their relationship to each other and to chromosome synapsis and segregation. *Cell* **62**:927-937.

Engin, Feyza: The function of *Notch1* during skeletogenesis. Ph.D. thesis at Baylor College of Medicine, in the laboratory of Brendan Lee, MD, Ph.D. in the Department of Molecular and Human Genetics, Houston, TX, USA.

Epstein DJ, Vekemans M, Gros P (1991): Splotch (Sp2H), a mutation affecting development of the mouse neural tube, shows a deletion within the paired homeodomain of Pax-3. *Cell* **67**:767-774.

Ertekin-Taner N, Ronald J, Feuk L, Prince J, Tucker M, Younkin L, Hella M, Jain S, Hackett A, Scanlin L, Kelly J, Kihio-Ehman M, Neltner M, Hersh L, Kindy M, Markesbery W, Hutton M, de Andrade M, Petersen RC, Graff-Radford N, Estus S, Brookes AJ, Younkin SG (2005): Elevated amyloid beta protein (Abeta42) and late onset Alzheimer's disease are associated with single nucleotide polymorphisms in the urokinase-type plasminogen activator gene. *Hum Mol Genet* **14**(3):447-460.

Feinberg AP, and Vogelstein B (1983): A technique for radiolabeling DNA restriction endonuclease fragments to high specific activity. *Anal Biochem* **132**(1):6-13.

Galli G, Hofstetter H, Birnstiel ML (1981): Two conserved sequence blocks within eukaryotic tRNA genes are major promoter elements. *Nature* **294**:626-631.

Gietz RD, Schiestl RH, Willems AR and Woods RA (1995): Studies on the transformation of intact yeast cells by the LiAc/SS-DNA/PEG procedure. *Yeast* **11**(4):355-360.

Gill T, Cai T, Aulds J, Wierzbicki S, Schmitt ME (2004): RNase MRP Cleaves the *CLB2* mRNA To Promote Cell Cycle Progression: Novel Method of mRNA Degradation. *Mol Cell Biol* **24**(3):945-953.

Golub TR, Slonim DK Tamayo P, Huard C, Gaasenbeek M, Mesirov JP, Coller H, Loh ML, Downing JR, Caligiuri MA, Bloomfield CD, Lander ES (1999): Molecular classification of cancer: class discovery and class prediction by gene expression monitoring. *Science* **286**(5439):531-537.

Hästbacka J, De la Chapelle A, Mahtani, MM, Clines G, Reeve-Daly MP, Daly M, Hamilton BA, Kusumi K, Trivedi B, Weaver A (1994): The Diastrophic Dysplasia Gene Encodes a Novel Sulfate Transprorter: Positional Cloning by Fine-structure Linkage Disequilibrium Mapping. *Cell* **78**:1073-1087.

Hall CM (2002): International Nosology and Classification of Constitutional Disorders of Bone (2001). *Am J Med Genet* **113**:65-77.

Han SY, Lee NK, Kim KH, Jang IW, Yim M, Kim JH, Lee WJ, Lee SY (2005): Transcriptional induction of cyclooxygenease-2 in osteoclast precursors is involved in RANKL-induced osteoclastogenesis. *Blood* (in press).

Hanakawa Y, Matsuyoshi N, Stanley JR (2002): Expression of Desmoglein 1 Compensates for Genetic Loss of Desmoglein 3 in Keratinocyte Adhesion. *J Invest Derm* **199**(1):27-31.

Harada D, Yamanaka Y, Ueda K, Shimizu J, Inoue M, Seino Y, Tanaka H (2005): An effective case of growth hormone treatment on cartilage-hair hypoplasia. *Bone* **36**:317-322.

Hecht JT, Nelson LD, Crowder E, Wang Y, Elder FFB, Harrison WR, Francomano CA, Prange CK, Lennon GG, Deere M, Lawler J (1995): Mutations in exon 17B of cartilage oligomeric matrix protein (COMP) gene. *Hum Molec Genet* **8**:123-128.

Hermanns P, Lee B (2002):Transcriptional Dysregulation in skeletal malformation syndromes. *Am J Med Genet* **106**(4):258-271.

Hernandez N, Lucito R (1988): Elements required for transcription initiation of the human U2 snRNA gene coincide with elements required for snRNA 3' end formation. *EMBO J* **7**:3125-3134.

Higuchi R, Krummel B and Saiki RK (1988): A general method of in vitro preparation and specific mutagenesis of DNA fragments: study of protein and DNA interactions. *Nucleic Acids Res* **16**(15):7351-7367.

Hinnen A, Hicks JB and Fink GR (1978): Transformation of yeast. *Proc Natl Acad Sci U S A* **75**(4):1929-1933.

Hirschhorn R (1995): Adenosine deaminase deficiency: molecular basis and recent developments. *Clin Immunol Immunopathol* **76**:S219-S227.

Ho SN, Hunt HD, Horton RM, Pullen JK and Pease LR (1989): Site-directed mutagenesis by overlap extension using the polymerase chain reaction. *Gene* **77**(1):51-59.

Hofstetter H, Kressman A, Birnstiel ML (1981): A split promoter for a eucaryotic tRNA gene *Cell* **24**:573-585.

Horiguchi H, Harada A, Oguma E, Sato M, Homma Y, Kayama F, Fukushima M, Matsushima K (2000): Cadmium-induced acute hepatic injury is exacerbated in human interleukin-8 transgenic mice. *Toxicol Appl Pharmacol* **163**(3):231-239.

Horton WA, Hecht JT (1993): The Chondrodysplasias In: Royce PM, Steinmann B (eds) Connective tissue and its heritable disorders. Molecular, genetic, and medical aspects. Wiley-Loss, New York, 541-675.

Hou WS, Bromme D, Zhao Y, Mehler E, Dushey C, Weinstein H, Miranda CS, Frage C, Greig F, Carey J, Rimoin DL, Desnick RJ, Gelb BD (1999): Chracterization of novel cathepsin K mutations in the pro and mature polypeptide regions causing pycnodysostosis. *J Clin Invest* **103**:731-738.

Hsiao YC, Chang HH, Tsai CY, Jong YJ, Horng LS, Lin SF, Tsai TF (2004): Coat color-tagged green mouse with EGFP expressed from the RNA polymerase II promoter. *Genesis* **39**:122-129.

Hull J, Ackerman H, Isles K, Usen S, Pinder M, Thomson A, Kwiatkowski DP (2001): Unusual haplotypic structure of IL8, a susceptibility locus for a common respiratory virus. *Am J Hum Genet* **69**:413-419.

Hull J, Rowlands K, Lockhart E, Sharland M, Moore C, Hanchard N, Kwiatkowski DP (2004): Haplotype mapping of the bronchiolitis susceptibility locus near *IL8*. *Hum Genet* **114**:272-279.

Ideker T, Thorsson V, Ranish JA, Christmas R, Buhler J, Eng JK, Bumgarner R, Goodlett DR, Aebersold R, Hood L (2001): Integrated genomic and proteomic analyses of a systematically perturbed metabolic network. *Science* **292**(5518):929-934.

Johnson DE, Williams LT (1993): Structural and functional diversity in the FGF receptor multigene family. *Advances in cancer research* **60**:1-41.

Johnson RL, Tabin CJ (1997): Molecular models for vertebrate limb development. *Cell* **90**:979-990.

Karsenty G (1998): Genetics of skeletogenesis. *Dev Genet* **22**:301-313.

Karsenty G (1999): The genetic transformation of bone biology. *Gene Dev* **13**:3037-3051.

Karsenty G (2001): When developmental biology meets human pathology. *Proc Natl Acad Sci USA* **98**:5385-5386

Karsenty G, Wagner EF (2002): Reaching a Genetic and Molecular Understanding of Skeletal Development. *Dev Cell* **2**:389-406.

Kim J-E, Nakashima K, de Crombrugghe B (2004): Transgenic Mice Expressing a Ligand-inducible Cre Recombinase in Osteoblasts and Odontoblasts. *Am J Pathol* **165**(6):1875-1882.

Komori T, Yagi H, Nomura S, Yamaguchi A, Sasaki K, Deguchi K, Shimuzu Y, Bronson RT, Gao YH, Inada M, Sato M, Okamoto R, Kitamura Y, Yoshiki S, Kishimoto T (1997): Targeted disruption of Cbfa1 results in a complete lack of bone formation owing to maturational arrest of osteoblasts. *Cell* **89**:755-764.

Kooijman R, van der Burgt CJ, Weemaes CM, Haraldsson A, Scholtens EJ, Yegers BJ (1997): T cell subsets and T cell function in cartilage-hair hypoplasia. *Scand J Immunol* **46**(2):209-215.

Kraus P, Fraidenraich D, Loomis CA (2001): Some distal limb structures develop in mice lacking Sonic hedgehog signaling. *Mech Dev* **100**(1):45-58

Kronenberg HM (2003): Developmental regulation of the growth plate. *Nature* **423**(6937): 332-336.

Kucharzik T, Williams IR (2002-2003): Neutrophil migration across the intestinal epithelial barrier -- summary of in vitro data and description of a new transgenic mouse model with doxycycline-inducible interleukin-8 expression in intestinal epithelial cells. *Pathobiology* **70**(3):143-149.

Kuijpers TW, Ridanpää M, Peters M, de Boer I, Vossen JMJJ, Pals ST, Kaitila I, Hennekam RCM (2003): Short-limbed dwarfism with bowing, combined immune deficiency, and late onset aplastic anaemia caused by novel mutations in the RMRP gene. *J Med Genet* **40**:761-766.

Kunkel GR, Pederson T (1989): Transcription of a human U6 small nuclear RNA gene invivo withstands deletion of intragenic sequences but not of an upstream TATATA box. *Nucleic Acids Res* **17**:7371-7379.

Lanske B, Karaplis AC, Lee K, Luz A, Vortkamp A, Pirro A, Karperien M, Defize LHK, Ho C, Mulligan RC, Abou-Samra AB, Juppner H, Segre GV, Kronenberg HM (1996): PTH/PTHrP receptor in early development and Indian hedgehog-regulated bone growth. *Science* **273**:663-666.

Laufer E, Nelson CE, Johnson RL, Morgan BA, Tabin C (1994): Sonic hedgehog and Fgf-4 act through a signaling cascade and feedback loop to integrate growth and patterning of the developing limb bud. *Cell* **79**:993-1003.

Lee DY, Clayton DA (1997): RNase mitochondrial RNA processing correctly cleaves a novel R loop at the mitochondrial DNA leading-strand origin of replication. *Genes Dev* **1**(11):582-592.

Lee LG, Connell CR, Woo SL, Cheng RD, McArdle BF, Fuller CW, Halloran ND and Wilson RK (1992): DNA sequencing with dye-labeled terminators and T7 DNA polymerase: effect of dyes and dNTPs on incorporation of dye-terminators and probability analysis of termination fragments. *Nucleic Acids Res* **20**(10):2471-2483.

Lee JE, Choi JH, Lee JH, Lee MG (2005): Gene SNPs and mutations in clinical genetic testing: haplotype-based testing and analysis. *Mutat Res* **573**(1-2):195-204.

Li C, Xia B, Yang Y, Li J, Xia HH (2005): TNF gene polymorphisms and Helicobacter Pylori infection in gastric carcinogenesis in Chinee population. *Am J Gastroenterol* **100**(2):290-294.

Li K, Smagula CS, Parsons WJ, Richardson JA, Gonzalez M, Hagler HK, Williams RS (1994): Subcellular partitioning of MRP RNA assessed by ultrastructural and biochemical analysis. *J Cell Biol* **124**:871-882.

Lobo S, Hernandez N (1989): A 7 bp mutation converts a human RNA polymerase II snRNA promoter into an RNA polymerase III promoter. *Cell* **58**:55-67.

Lobo SM, Hernandez N (1989): A 7 bp mutation converts a human RNA polymerase II snRNA promoter into an RNA polymerase III promoter. *Cell* **58**:55-67.

Logan M, Martin JF, Ngy A, Lobe C, Olson EN, Tabin CJ (2002): Expression of Cre Recombinase in the Developing Mouse Limb Bud Driven by a *Prx1* Enhancer. *genesis* **33**:77-80.

Lohnes D, Kastner P, Dierich A, Mark M, LeMeur M, Chambon P (1993): Function of retinoic acid receptor gamma in the mouse. *Cell* **73**:643-658.

Loomis CA, Harris E, Michaud J, Wurst W, Hanks M, Joyner AL (1996): The mouse engrailed-1 gene and ventral limb patterning. *Nature* **382**:360-363.

Lu MF, Cheng HT, Lacy AR, Kern MJ, Argao EA, Potter SS, Olson EN, Martin JF (1999): Paired-related homeobox genes cooperate in handplate and hind limb zeugopod morphogenesis. *Dev Biol* **205**:145-157.

Luo G, D'Souza R, Hogue D, Karsenty G (1995): The matrix Gla protein gene is a marker of the chondrogenesis cell lineage during mouse development. *J Bone Miner Res* **10**:325-334.

Luo Y, Xu H, Li Y, Han ZY, Qiu MY, Chen Q, Liu SZ, Ni S, Xie Y, Mao YM (2003): Validation of cDNA microarray technology. *Yi Chuan Xue Bao* **30**(7):611-618.

Lygerou Y, Allmang C, Tollervey D, Séraphin B (1996): Accurate Processing of a Eukaryotic Precursor Ribosomal RNA by Ribonuclease MRP in Vitro. *Science* **272**:268-270.

Ma B, Hernandez N (2002): Redundant cooperative interactions for assembly of a human U6 transcription initiation complex. *Mol Cell Biol* **22**(22):8067-8078.*:*

Mäkitie O, Marttinen E, Kaitila I (1992): Skeletal growth in carilage-hair hypoplasia. A radiological study of 82 patients. *Pediatr Radiol* **22**:434-439.

Mäkitie O, Kaitila I (1993): Cartilage-hair hypoplasia: clinical manifestations in 108 Finnish patients. *Eur J Pediatr* **152**:211-217.

Mäkitie O, Sulisalo T, de la Chapelle A, Kaitila I (1995): Cartilage-hair hypoplasia. *J Med Genet* **32**:39-43.

Mäkitie O, Kaitila I, Savilahti E (1998): Susceptibility to infections and in vitro immune functions in cartilage-hair hypoplasia. *Eur J Pediatr* **157**:816-820.

Mäkitie O, Juvonen E, Dunkel L, Kaitila I, Siimes MA (2000): Anemia in children with cartilage-hair hypoplasia is related to body growth and to the insulin-like growth factor system. *J Clin Endocrinol Metab* **85**(2):563-568.

Mäkitie O, Kaitila I, Pukkala E, Teppo L, Savilahti E (2000a): The role of immune deficiency in cartilage-hair hypoplasia. *Duodecim* **116**(12):1299-1305.

Mäkitie O, Kaitila I, Savilahti E (2000b): Deficiency of humoral immunity in cartilage-hair hypoplasia. *J Pediatr* **137**(4):487-492.

Mäkitie O, Kaitila I, Rintala R (2001). Hirschsprung disease associated with severe cartilage-hair hypoplasia. *J Pediatr* **138**(6):929-931.

Marigo V, Johnson RL, Vortkamp A, Tabin C (1996): Sonic hedgehog differentially regulates expression of GLI and GLI3 during limb development. *Dev Biol* **180**:273-283.

Matsson H, Davey EJ, Draptchinskaia N, Hamaguchi I, Ooka A, Leveen P, Forsberg E, Karlsson S, Dahl N (2004): Targeted disruption of the ribosomal protein S19 gene is lethal prior to implantation. *Mol Cell Biol* **24**:4032-4037.

Mattaj IW, Dathan NA, Parry HW, Carbon P, Krol A (1988): Changing the RNA polymerase specificity of U snRNA gene promoters. *Cell* **55**:435-442.

McKusick VA, Eldridge R, Hostetler JA, Egeland JA, Ruangwit U (1965): Dwarfism in the Amish. II. Cartilage-hair hypoplasia. *Bull Johns Hopkins Hosp* **116**:285-326.

Merritt AJ, Berika MY, Zhai W, Kirk SE, Ji B, Hardman MJ, Garrod DR (2002): Suprabasal Desmoglein 3 Expression in the Epidermis of Transgenic Mice Results in Hyperproliferation and Abnormal Differentiation. *Mol Cell Biol* **22**(16):5846-5858.

Merz D, Liu R, Johnson K, Terkeltaub R (2003): IL-8/CXCL8 and Growth-Related Oncogene α/CXCL1 Induce Chondrocyte Hypertrophic Differentiation. *J Immun* **171**:4406-4415.

Mian A,Guenther M, Finegold M, Ng P, Rodgers J, Lee B (2005): Toxicity and adaptive immune response to intracellular transgenes delivered by helper-dependent vs. first generation adenoviral vectors. *Mol Genet Metab* **84**(3):278-288.

Mittal V, Ma B, Hernandez N (1999): $SNAP_C$: A core promoter factor with a built-in DNA-binding damper that is deactivated by the Oct-1 POU domain. *Genes Dev* **13**:1807-1821.

Morcuende JA, Weinstein SL (2003): Developmental Skeletal Anomalies. *Birth Defects Research* (Part C) **69**:197-207.

Motykova G, Weilbächer KN, Horstmann M, Rieman DJ, Fisher DZ, Fisher DE (2001): Linking osteopetrosis and pycnodysostosis: Regulation of cathepsin K expression by the microphthalmia transcription factor family. *Proc Natl Acad Sci USA* **98**:5798-5803.

Mundlos S (1994): Expression patterns of matrix genes during human skeletal development. Gustav Fischer Verlag, Stuttgart. Vol **28** No. 3.

Muragaki Y, Mundlos S, Upton J, Olson BR (1996): Altered growth and branching patterns in synpolydactyly caused by mutations in HOXD13. *Science* **272**:548-551.

Nadon R, Shoemaker J (2002): Statistical issues with microarrays: processing and analysis. *Trends Genet* **18**(5):265-271.

Nakashima E, Mabuchi A, Kashimada K, Onishi T, Zhang J, Ohashi H, Nishimura G, Ikegawa S. (2003): RMRP mutations in Japanese patients with cartilage-hair hypoplasia. *Am J Med Genet* **123A**:253-256.

Nakashima E, Mabuchi A, Makita Y, Masuno M, Ohashi H, Nishimura G, Ikegawa S (2004): Novel SBDS mutations caused by gene conversion in Japanese patients with Shwachman-Diamand syndrome. *Hum Genet* **114**:345-348.

Nilssen EA, Synnes M, Kleckner N, Grallert B, Boye E (2003): Intra-G_1 arrest in response to UV irradiation in fission yeast. *Proc Natl Acad Sci USA* **100**(19):10758-10763.

Niswander L, Jeffrey S, Martin GR, Tickle C (1994): A positive feedback loop coordinates growth and patterning in the vertebrate limb. *Nature* **371**:609-612.

Novina CD, Sharp PA (2004): The RNAi revolution. *Nature* **430**(6996):161-164.

Oberg KC, Greer LF, Naruse T (2004): Embryology of the Upper Limb: The Molecular Orchestration of Morphogenesis. *Handchir Mikrochir Plast Chir* **36**:98-107.

Okada Y, Tanaka Y (2004): Immune signals in the context of secondary osteoporosis. *Histol Histopathol* **19**(3):863-866.

Ornitz DM, Marie PJ (2002): FGF signalling pathways in endochondral and intramembranous bone development and human genetic disease. *Gene Dev* **16**:1446-1465.

Otto F, Thornell AP, Crompton T, Denzel, A, Gilmour KC, Rosewell, IR, Stamp GW, Beddington RS, Mundlos S, Olsen BR, Selby PB, Owen MJ (1997): Cbfa1, a candidate gene for cleidocranial dysplasia syndrome, is essential for osteoblast differentiation and bone development. *Cell* **89**:765-771.

Pan W (2002): A Comparative Review of Statistical Methods for Discovering Differentially Expressed Genes in Replicated Microarray Experiments. *Bioinformatics* **12**:546-554.

Parr BA, McMahon AP (1995): Dorsalizing signal Vnt-7a required for normal polarity of D-V and A-P axes of mouse limb. *Nature* **374**:350-353.

Paule MR, White RJ (2000): Survey and summary: transcription by RNA polymerase I and III. *Nucleic Acids Res* **28**(6):1283-1298.

Paus R, Nickoloff BJ, Ito T (2005): A 'hairy' privilege. *TRENDS in Immunology* **26**(1):32-40.

Reimer G, Raska L, Scheer V, Tran EM (1988): Immunolocalization of 7-2 ribonucleoprotein in the granular component of the nucleolus. *Exp Cell Res* **176**:117-128.

Ridanpää M, van Eenennaam H, Pelin K, Chadwick R, Johnson C, Yuan B, vanVenrooij W, Pruijn G, Salmela R, Rockas S, Mäkitie O, Kaitila I, de la Chapelle A (2001): Mutations in the RNA component of RNase MRP cause a pleitropic human disease, cartilage-hair hypoplasia. *Cell* **104**:195-203.

Ridanpää M, Sistonen P, Rockas S, Rimoin DL, Mäkitie O, Kaitila I (2002): Worldwide mutation spectrum in cartilage-hair hypoplasia: ancient founder origin of the major 70A→G mutation of the untranslated RMRP. *Eur J Hum Genet* **10**:439-447.

Ridanpää M, Ward LM, Rockas S, Särkioja M, Mäkelä H, Susic M, Glorieux FH, Cole WG, Mäkitie O (2005): Genetic changes in the RNA compnents of RNase MRP and RNase P in Schmid metaphyseal chondrodysplasia. *J Med Genet* **40**:741-746.

Riddle RD, Johnson RL, Laufer E, Tabin C (1993): Sonic Hedgehog Mediates the Polarizing Activity of the ZPA. *Cell* **75**:1401-1416.

Riddle RD, Ensini M, Nelson C, Tsuchida T, Jessell TM, Tabin C (1995): Induction of the LIM homeobox gene Lmx1 by WNT7a establishes dorsoventral pattern in the vertebrate limb. *Cell* **83**:631-640.

Rijli FM, Chambon P (1997): Genetic interactions of Hox genes in limb development: learning from compound mutants. *Curr Opin Genet Dev* **7**:481-487.

Riley PA (1994): *Int J Radiat Biol* **65**:27-33.

Rocke DM, Durbin B (2001): A model for measurement error for gene expression arrays. *J Comput Biol* **8**(6):557-569.

Rossert J, Eberspaecher H, de Crombrugghe B (1995): Separate cis-acting DANN elements of the mouse pro-alpha-1(I) collagen promoter direct expression of reporter genes to different type I collagen-producing cells in transgenic mice. *J Cell Biol* **129**:1421-1432.

Rubin GM (1974): Three forms of the 5.8S ribosomal RNA species in *Saccharomyces cerevisiae*. *Eur. J. Biochem*. **41**(1):197-202.

Saiki RK, Gelfand DH, Stoffel S, Scharf SJ, Higuchi R, Horn GT, Mullis KB and Erlich HA (1988): Primer-directed enzymatic amplification of DNA with a thermostable DNA polymerase. *Science* **239**(4839):487-491.

Sakou T (1998): Bone morphogenetic proteins: from basic studies to clinical approaches. *Bone* **22**:591-603.

Salinas K, Wierzbicki S, Zhou L, Schmitt ME (2005): Characterization and Purification of *Saccharomyces cerevisiae* RNase MRP Reveals a New Unique Protein Component. *J Biol Chem* **12**:11352-11360.

Sanger F, Nicklen S and Coulson AR (1977): DNA sequencing with chain-terminating inhibitors. *Proc Natl Acad Sci U S A* **74**(12):5463-5467.

Saunders JW (1948): The proximo-distal sequence of origin of the parts of the chick wing and the role of the ectoderm. *J Exp Zool* **108**:363-403.

Saunders JW, Gasseling M (1968): Ectodermal-mesenchymal interaction inthe origin of the limb. In: Epithelial-mesenchymal interaction; Fleischmayer; Billingham, R.E (eds.). Williams and Wilkins, Baltimore: 78-97.

Schipani E, Langman CB, Parfitt AM, Jensen GS, Kikuchi S, Kooh SW, Cole WG, Jüppner H (1996): Constitutively activated receptors for parathyroid hormone and parathyroid hormone-related peptide in Jansen's metaphyseal chondrodysplasia. *J Med* **335**:708-714.

Schmidt-Ullrich R, Paus R (2005): Molecular principles of hair follicle induction and morphogenesis. *BioEssays* **27**:247-261.

Schmitt ME, Brown TA and Trumpower BL (1990): A rapid and simple method for preparation of RNA from Saccharomyces cerevisiae. *Nucleic Acids Res* **18**(10):3091-3092.

Schmitt ME, Clayton DA (1992): Yeast site-specific ribonucleoprotein endoribonuclease MRP contains an RNA component homologous to mammalian RNase MRP RNA and essential fo cell viability. *Genes Dev* **6**:1975-1985.

Schmitt ME, Bennett JL, Dairaghi DJ, Clayton DA (1993): Secondary structure of RNase MRP RNA as predicted by phylogenetic domparison. *FASEB J* **7**:208-213.

Schmitt ME, Clayton DA (1994): Isolation of a unique protein component of the yeast RNase MRP: an RNA-binding protein with a zinc-cluster domain. *Genes Dev* **8**:2617-2628.

Schramm L, Hernandez N (2002): Recruitment of RNA polymerase III to its target promoters. *Genes Dev* **16**:2593-2620.

Schwabe JWR, Rodriguez-Esteban C, Belmonte JCI (1998): Limbs are moving, where are they going? *TIG* **14**:229-235.

Schwabe GC, Mundlos S (2004): Genetics of Congenital Hand Anomalies. *Handchir Mikrochir Plast Chir* **36**:85-97.

Shadel GS, Buckenmeyer GA, Clayton DA, Schmitt ME (2000): Mutational analysis of the RNA component of Saccharomyces cerevisiae RNase MRP reveals distinct nuclear phenotypes. *Gene* **245**:175-184.

Sharp S, DeFranco D, Dingermann T, Farrell P, Soll D (1981): Internal control regions for transcription of eukaryotic tRNA genes. *Proc Natl Acad Sci USA* **78**:6657-6661.

Silengo M, Valanzise M, Sorasio L, Ferrero GB (2002): Hair as a diagnostic tool in dysmorphology. *Clin Genet* **62**:270-272.

Simonet WS, Huges TM, Nguyen HQ, Trebasky LD, Danilenko DM, Medlock ES (1994): Long-term impaired neutrophil migrtion in mice overexpressing human interleukin-8. *J Clin Invest* **94**(3):1310-1319.

SØrlie T, Perou CM, Tibshirani R, Aas T, Geisler S, Johnsen H, Hastie T, Eisen MB, van de Rijn M, Jeffrey SS, Thorsen T, Quist H, Matese JC, Brown PO, Botstein D, Eystein Lonning P, Borresen-Dale AL (2001): Gene expression patterns of breast carcinomas distinguish tomor subclasses with clinical implications. *Proc Natl Acad Sci USA* **98**(19):10869-10874.

Southern EM (1975): Detection of specific sequences among DNA fragments separated by gel electrophoresis. *J Mol Biol* **98**:503-517.

Spranger J, Winterpacht A, Zabel B (1994): The type II collagenopathies: a spectrum of chondrodysplasias. *Eur J Pediatr* **153**:56-65.

Spranger J (1997): Irrtümer der Skelettentwicklung. *Monatsschr Kinderheilk* **145**:334-341.

Spranger JW, Brill PW, Poznanski A (2002): Bone dysplasias. An atlas of genetic disorders of skeletal development. Oxford Univ Pres, 2nd Edition, Oxford.

Stevens DA, Williams GR (1999): Hormone regulation of chondrocyte differentiation and endochondral bone formation. *Mol Cell Endocrinol* **151**:195-204.

Storm EE, Huynh TV, Copeland NG, Jenkins NA, Kingley DM, Lee S-J (1994): Limb alterations in brachypodism mice due to mutations in a new member of the TGFβ-superfamily. *Nature* **368**:639-643.

Sulisalo T, Mäkitie O, Sistonen P, Ridanpää M, El-Rifai W, Ruuskanen O, de la Chapell A, Kaitila I (1997): Uniparental disomy in cartilage-hair hypoplasia. *Eur J Hum Genet* **5**:35-42.

Summerbell D (1974): A quantitative analysis of the effect of excision of the AER from the chick limb-bud. *J Embryol Exp Morph* **32**: 651-660

Sun X, Lewandoski M, Meyers EN, Liu Y, Maxon RE Jr, Martin GR (2000): Conditional inactivation of Fgf4 reveals complexity of signalling during limb bud development. *Nat Gen* **25**(1):83-86.

Sun X, Mariani FV, Martin GR (2002): Functions of FGF signalling from the apical ectodermal ridge in limb development. *Nature* **418**:501-508.

Superti-Furga A, Bonafé L, Rimoin DL (2001): Molecular-Pathogenetic Classification of Genetic Disorders of the Skeleton. *Am J Med Genet* **106**:282-293.

Tarca AL, Cooke JEK, Mackay J (2005): A robust neural networks approach for spatial and intensity dependent normalization of cDNA microarray data. *Bioinformatics* (in press)

Teitelbaum SL (2000): Bone Resorption of Osteoclasts. *Science* **289**:1504-1508.

Thomas JT, Lin K, Nandedkar M, Camargo M, Cervenka J, Luyten FP (1996): A human chondrodys-plasia due to a mutation in a TGF-beta superfamily member. *Nat Genet* **12**:315-317.

Topper JN, Clayton DA (1990): Characterization of human MRP/Th RNA and its nuclear gene: Full length MRP/Th RNA is an active endoribonuclease when assembled as an RNP. *Nucleic Acids Res* **18**:793-799.

Tu I-P, Schaqner M, Diehn M, Sikic BI, Brown PO, Botstein D, Fero MJ (2004): A method for detecting and correcting feature misidentification on expression microarrays. *BMC Genomics* **5**:64 - doi:10.1186/1471-2164-5-64

van't Veer LJ, Dai H, van de Vijver MJ, He YD, Hart AA, Mao M, Peterse HL, van der Kooy K, Marton MJ, Witteveen AT, Schreiber GJ, Kerkhoven RM, Roberts C, Linsley PS, Bernards R, Friend SH (2002): Gene expression profiling predicts clinical outcome of breast cancer. *Nature* **415**(6871):530-536.

Vortkamp A, Lee K, Lanske B, Segre GV, Kronenberg HM, Tabin CJ (1996): Regulation of rate of cartilage differentiation by Indian hedgehog and PTH-related protein. *Science* **273**:613-622.

Vulliamy T, Marrone A, Goldman F, Dearlove A, Bessler M, Mason PJ, Dokal I (2001): The RNA component of telomerase is mutated in autosomal dominant dyskeratosis congenita. *Nature* **413**:432-435.

Walker SC, Avis JM (2004): A Conserved Element in the Yeast RNase MRP RNA Subunit can Participate in a Long-range Base-pairing Interaction. *J Mol Biol* **341**:375-388.

Wang S, Eithier S (2004): A generalized likelihood ratio test to identify differentially expressed genes from microarray data. *Bioinformatics* **20**(1):100-104.

Wang Y, Middleton F, Horton JA, Reichel L, Farnum CE, Damron TA (2004): Microarray analysis of proliferative and hypertrophic growth plate zones identifies differentiation markers and signal pathways. *Bone* **35**:1273-1293.

Welting TJM, vn Venrooij WJ, Purijn GJM (2004): Mutual interactions between subunits of the human RNase MRP ribonucleoportein complex. *Nucleic Acids Res* **32**(7):2138-2146.

Wen X, Wu GD (2001): Evidence for epigenetic mechanisms that silence both basal and immune-stimulated transcription of the IL-8 gene. *J Immunol* **166**(12):7290-7299.

Westendorf JJ, Kahler RA, Schroeder TM (2004): Wnt signaling in osteoblasts and bone diseases. *Gene* **341**:19-39.

Williams MS, Ettinger RS, Hermanns P, Lee B, Taskinen M, Mäkitie O (2005): The natural history of severe anemia in cartilage-hair hypoplasia. *Am J Med Genet* (in press)

Willig TN, Draptchinskaia N, Dianzani I, Ball S, Niemeyer C, Ramenghi U, Orfali K, Gustavsson P, Garelli E, Brusco A, Tiemann C, Perignon JL, Bouchier C, Cicchiello L, Dahl N, Mohandas N, Tchernia G (1999): Mutations in ribosomal protein S19 gene and Diamond Blackfan anemia: wide variations in phenotypick expression. *Blood* **94**:4294-4306.

Wilson R, Freddi S, Chan D, Cheah KSE, Bateman JF (2005): MISFOLDING OF COLLAGEN X CHAINS HARBORING SCHMID METAPHYSEASL CHONDRODYSPLASIA MUTATIONS RESULTS IN APERRANT DISULFIDE BOND FORMATION; INTRACELLULAR RETENTION AND ACTIVATION OF THE UNFOLDED PROTEIN RESPONSE. *J Biol Chem* in press

Wood W, Kao M, Gordon D and Ridgway E (1989): Thyroid hormone regulates the mouse thyrotropin beta-subunit gene promoter in transfected primary thyrotropes. *J Biol Chem* **264**(25):14840-14847.

Yel L, Aggarwal S, Gupta S (1999): Cartilage-hair hypoplasia syndrome: increased apoptosis of T lymphocytes is associated with altered expression of Fas (CD95), FasL (CD95L), IAP, Bax, and Bcl2. *J Clin Immunol* **19**(6):428-434.

Zabel BU, Winterpacht A (2000): Osteochondrodysplasien - genetisch bedingte Störungen der Skelettentwicklung. In: Ganten, D und Ruckpaul K (Hrsg) Handbuch der molekularen Medizin, Band 7: Monogen bedingte Erbrankheiten, Teil 2. Springer Verlag Berlin, Heidelberg, New York 249-279.

Zhang P, Jobert AS, Couvinea A, Silve C (1998): A homozygous inactivating mutation in the parathyroid hormone/parathyroid hormone-related peptide receptor causing Blomstrand chondrodysplasia. *J Clin Endocrinol Metab* **83**:3365-3368.

Zhao X, Pendergrast OS, Hernandez N (2001): A positioned nucleosome on the human U6 promoter allows recruitment of $SNAP_C$ by the Oct-1 POU domain. *Mol Cell* **7**:539-549.

Zheng Q, Zhou G, Morello R, Chen Y, Garcia-Rojas X, Lee B (2003): Type X collagen gene regulation by Runx2 contributes directly to its hypertrophic chondrocyte-specific expression in vivo. *J Cell Biol* **162**:833-842.

Zhou G, Lefebvre V, Zhang Z, Eberspaecher H, de Crombrugghe B (1998): Three high mobility group-like sequences within a 48-base pair enhancer of the Col2a1 gene are required for cartilage-specific expression in vivo. *J Biol Chem* **273**:14989-14997.

Zufferey R, Donello JE, Trono D, Hope TJ (1999) Woodchuck hepatitis virus posttranscriptional regulatory element enhances expression of transgenes delivered by retroviral vectors. *J Virol* **73**:2886-2892.

8 Appendix

8.1 Abbreviations

#	number
A	Adenin
abs	absolute
Ac	acetate
AER	apical ectodermal ridge
bp	base pair
BSA	bovine serum albumin
C	cytosine
ºC	degree Celsius
cDNA	complementary DNA
CEN	centromere on episomal plasmid
CHH	Cartilage Hair Hypoplasia
Ci	Curie
dATP	deoxyadenosine triphosphate
dCTP	deoxycytidine triphosphate
dGTP	deoxyguanosine triphosphate
dNTPs	deoxynucleotide triphosphates
	(a mixture of dATP, dTTP, dCTP, dGTP 1:1:1:1)
Δ	delta – deletion of endogenous yeast gene
DBA	Diamond-Blackfan Anemia
DEPC	diethyl-pyrocarbonate
DMEM	MEM with high concentration of D-glucose
DNA	deoxynucleic acid
Dpc	days post conception
DSE	distal sequence element
DTT	dithiothritol
dTTP	deoxytymidine triphosphate
E	embryonic day (of embryonic mouse development)
EBV	Ebstein-Barr virus

E. coli	*Escherichia coli*
EDTA	ethylenediamine tetracetic acid
e.g.	exempli gratia (for example)
EL-buffer	Erythorocyte Lysis-buffer
EMBL	European Molecular Biology Laboratory
ES	embryonic stem cells
EtOH	ethanol
FACS	Fluorescence-Activated Cell Sorting
FGF	*Fibroblast Growth Factor*
Fig.	Figure
5-FOA	5-fluoroorotic acid
FTT	failure to thrive
g	acceleration of gravity
G	guanine
G0S2	*Cell cycle switch gene from G0 to S phase*
h	hour
H & E	Hematoxylin and Eosin
HIS	histidine gene on episomal plasmid as selection marker
hrs	hours
hTR	*human telomerase RNA*
IL8	*Interleukine 8*
IPTG	isopropyl-β-D-thio-galactopyranoside
ko	knockout
LB-medium	Luria-Bertani medium
LEU2	leucine gene on episomal plasmid as selection marker
Lmx1b	*LIM homeobox gene 1 b*
µ	micro
M	molar
MCDS	Metaphyseal Chondrodysplasia type Schmid
MEM	minimal essential medium
min	minute(s)
miRNA	micro RNA
ml	mililiter
MTN	multiple tissue Northern Blot

n	nano
NCBI	National Center for Biotechnology Information
NME1	*nuclear mitochondrial endonuclease 1*
NTE	sodium-tris-EDTA buffer
OCD	osteochondrodysplasia
OD	optical density
OMIM	Online Mendelian Inheritance in Man
OPTI-MEM	optimized MEM for transfections
ORF	open reading frame
PAA	poly-acrylamide
PBS	phosphate buffered saline
PCR	polymerase chain reaction
PEG	poly ethylene glycol
PFA	paraformaldehyde
PI	Propidium Iodide
PNK	polynucleotide kinase
PSE	proximal sequence element
PZ	progress zone
RANKL	*receptor activator of NF-κB ligand*
RMRP	*RNase Mitochondrial RNA Processing*
RNA	ribonucleic acid
rpm	revolutions per minute
RPMI	cell culture medium developed at Roswell Park Memorial Insitute by Moore et al.,1966
RT	room temperature
RT-PCR	reverse transcriptase polymerase chain reaction
Runx2	*Runt homoebox gene 2*
s	second(s)
SBDS	Schwachman-Bodian-Diamond Syndrome
SD	standard deviation
SDS	sodium dodecyl sulfate
Shh	*Sonic hedgehog*
shRNA	short hairpin RNA
siRNA	short interfering RNA
$SNAP_C$	small nuclear RNA activating protein complex

SNP	single nucleotide polymorphism
snRNA	small nuclear RNA
SSC	standard-saline-citrate buffer
T	thymine
Tab	Table
TAE	tris-acetic-EDTA buffer
Taq	Thermophilus aquaticus DNA polymerase I
TBE	tris-borate-EDTA buffer
TBP	TATA binding protein
TE	tris-EDTA buffer
TEMED	N,N,N',N'-tetramethylethylendiamine
Tris	Tris(hydoxymethyle)aminomethane
Trp	tryptophan gene on episomal plasmid as selection marker
U	units
UPD	uniparental disomy
URA3	uracil gene on episomal plasmid as selection marker
USA	United States of America
UTP	uracil triphosphate
UTR	untranslated region
vs.	versus
wt	wild type
X-gal	5-bromo-4-chloro-indolyl-β-D-galactoside
YPD	Yeast-Peptone-Dextrose rich medium
ZPA	zone of polarizing activity

8.2 CHH Patient Questionnare

Parent's Name:

_____

Date Contacted Parent: ____ / ____ / _____ **Interviewed by**: _____
(month) (day) (year)

Questionnaire for CHH Patients

I. **Identification Data**:

A. **NAME**:

_____
(LAST) (FIRST) (MIDDLE)

B. **DATE OF BIRTH**: ___/ ___ / ____ **CURRENT AGE**: ____
(month) (day) (year)

C. **GENDER**: ☐ Female ☐ Male

D. **ETHNIC EXTRACTION**:
- ☐ Asian or Pacific Islander
- ☐ African-American
- ☐ Caucasian
- ☐ Hispanic
- ☐ Other (specify): _____

E. **PRESENT DAY LOCATION OF PATIENT**:
1. Country:
   _____
2. State/Province:
   _____
3. County:
   _____
4. City/Town:
   _____

II. **Family History**:

A. **PARENTS**: [***** Establish paternity of child.] Child is or is not adopted?

1. Does your family have any new children that were born since the last medical contact? ☐ Y ☐ N

B. **OTHER RELATIVES**:
1. Do you know of any relatives that are noticeably shorter in height compared to the rest of the family? ("For example, less than 5 feet if every one else is 5'5'?") ☐ Y ☐ N

   If yes, provide relationship to patient._____

2. Do you know of any relatives that have birth defects, especially involving the bones? ☐ Y ☐ N

   If yes, did this person (or these persons) have any other health problems?

   _____
   _____
   _____
   _____

3. Do you know of any relatives that attended special education classes or experienced any learning problems in grade school? ☐ Y ☐ N

   a. If yes, how far in class level did they go in school?

   _____
   _____
   _____

   b. If already grown-up, are they able to live independently?

   _____
   _____
   _____

III. **Patient History**:

A. **BIRTH HISTORY**: [* Obtain APGAR score if possible.] APGAR= ___

1. Did you have any problems during pregnancy with the patient? ☐ Y ☐ N

   Specify:_____
   _____
   _____

2. Did your child have any medical problems immediately after childbirth? ☐ Y ☐ N

   Specify:_____
   _____
   _____

3. What was the term of your pregnancy?
   Months: _____ *OR* Weeks: _____

4. Did the baby show any problems by ultrasound examination during your pregnancy? ☐ Y ☐ N

If yes, provide some description

_____
_____

5. How much did your baby weigh at birth?
   a. Circle one: by memory _____ pounds _____ounces
      by record (or _____ Kg)
6. What was the length of your baby?
   a. Circle one: by memory _____ inches
      by record (or _____ cm)

7. What was your baby's head size?
   b. Circle one: by memory _____ inches
      by record (or _____ cm)

8. Do you have information on your child's height starting from the age of one year until the present? ☐ Y ☐ N

   If yes, what measurement(s) at what ages are available?

   _____
   _____
   _____

B. **PHENOTYPIC CHARACTERISTICS**:

1. HAIR GROWTH:
   a. Do you know of any problems with your child's hair growth?
      ☐ Y ☐ N

      If yes, describe it.

      _____
      _____
      _____
      _____

   b. Do you consider the growth rate of your child's scalp hair to be:
      ☐ normal
      ☐ slow

   c. How would you describe the condition of your child's scalp hair at present?

      _____
      _____
      _____
      _____

d. How often does your child need to have the hair cut? [Give change in age.]
☐ about every six weeks
☐ about every six months
☐ about every year
☐ other: _____

2. HEIGHT:
Is your child much shorter than his/her classmates?
☐ Y ☐ N

Can you attempt any description of his/her body proportion?
☐ length of arms and legs in proportion to body size or stature, or
☐ considerably shorter than proportionate to body size

Is your child's stature and/or body size similar to that of his/her classmates?
☐ Y ☐ N

Is your child's description of head size in proportion to body size?
☐ Y ☐ N

Is the head size ☐ larger in proportion to body size?
or ☐ smaller

3. JOINT MOVEMENT:
a. Do you notice any problems of your child regarding his/her moving of arms and legs? ☐ Y ☐ N

If yes, describe it.
_____
_____
_____

b. Have you or anybody else noticed any abnormality of any joint mobility or gait?
☐ Y ☐ N

If yes, is it characterized as ☐ restricted mobility, or
☐ excessive bone mobility

c. Can you point out the specific joint(s) involved?
_____
_____
_____

d. Would you describe the mobility in the elbows as:
☐ restricted (not being able to move them completely), or
☐ excessive (being able to move them too much)

e. Does your child have any problems with moving the elbows?
☐ Y ☐ N

If yes, describe it.
_____
_____
_____

f. Are you sure that the child's shoulders and wrists have normal mobility?
☐ Y ☐ N

If no, describe it.
_____
_____
_____

g. Does your child have any motion problems in the knees?
☐ Y ☐ N

h. Do your child's legs look straight? ☐ Y ☐ N

i. Has there been a description of the knees in the medical record?
☐ Y ☐ N

If yes, are they:
☐ bow-legged (far apart) or
☐ knock-knees (knees touching)
☐ other: (provide description)
_____
_____
_____
_____

j. Do you have medical records/documents/x-rays stating that your child's hands, fingers, feet and toes are abnormally short?
☐ Y ☐ N
1. Are the small joints in the hands, fingers, feet and toes abnormally loose?
☐ Y ☐ N
2. Is the skin thought to be excessive? ☐ Y ☐ N
3. Are skin and joints loose enough to allow finger segments to be impacted into one another?
☐ Y ☐ N

4. IMMUNE FUNCTION:
   a. Has your child ever been described as having had more than the average number of infections a year? ☐ Y ☐ N

      If yes, what information was given in regard to your child's history of general infections, and lung infections?

      _____
      _____
      _____

      1. How many colds a year did your child have during:
         a. infancy (less than one year)? _____
         b. early childhood (1 to 5 years)? _____
         c. late childhood (5 to 10 years)? _____
         d. adolescence (after 10 years)? _____
      2. How many times a year has your child had a flu-like illness during:
         a. infancy (less than one year)? _____
         b. early childhood (1 to 5 years)? _____
         c. late childhood (5 to 10 years)? _____
         d. adolescence (after 10 years)? _____

   b. Has your child ever been admitted to the hospital because of infection(s) over the years? ☐ Y ☐ N

   c. Did your child receive antibiotic treatment(s) on such occasions? ☐ Y ☐ N

   d. How often did such serious infections recur?

      _____

   e. If infections were recorded in the growing child, were they occurring
      ☐ less frequently
      ☐ equally frequent
      ☐ more frequently as the child grew older?

   f. Has the word "anemia" ever been used in the description of blood quality?
      ☐ Y ☐ N

   g. What was the number of white blood cells shown to be?
      ☐ low
      ☐ normal
      ☐ high

h. Has your child undergone any medical tests concerning the immune system?
☐ Y ☐ N

If yes, please mention the type(s) of tests performed and where performed?

_____
_____
_____
_____
_____

i. Do you permit releasing the patient's record? ☐ Y ☐ N

5. GASTROINTESTINAL FUNCTION:

a. Has your child had bowel movement problems, such as diarrhea? ☐ Y ☐ N

b. Has your child ever been described as having "failure to thrive"? ☐ Y ☐ N

c. Did your child have problems with constipation (regularity)?
☐ Y ☐ N

d. On average, how often a day did your child have bowel movements:

1. as an infant (<1 year)
_____
2. as a child (<10 years)
_____
3. How often now?
_____

e. Has the term "Hirschsprung disease" ever been used to describe your child's bowel movement problem?
☐ Y ☐ N

f. Has the term "Malabsorbtion" ever been used to describe the deficiency of bowel function? ☐ Y ☐ N

g. Compared to other children, did you ever think that your child often had a full or bloated belly? ☐ Y ☐ N

C. ***EDUCATION HISTORY:***

1. Has your child been able to follow regular classes in school?
   ☐ Y ☐ N

D. ***OTHER RELEVANT QUESTIONS:***

1. Have you any remaining comments on your child's problem with growth, stature or on any other health problem(s) he or she is still facing?

   _____
   _____
   _____
   _____

2. Are you and your spouse blood-related? ☐ Y ☐ N

   If yes, can you be more specific about the type or degree of family-relationship?
   (first cousins; second cousins; other)

   _____
   _____
   _____
   _____

8.4 Publications

Williams MS, Ettinger RS, Hermanns P, Lee B, Taskinen M, Mäkitie O (2005): The natural history of severe anemia in cartilage-hair hypoplasia. *Am J Med Genet* (in press)

Mendoza-Londono R, Lammer E, Watson R, Harper J, Hatamochi A, Hatamochi-Hayashi S, Napierala D, Hermanns P, Collins S, Roa BB, Hedge MR, Wakui K, Nguyen D, Stockton DW, Lee B (2005): Characterization of a new syndrome associating craniosynostosis, delayed fontanel closure, parietal foramina, imperforate anus and skin eruption – CDAGS. *Am J Hum Genet* July 2005 (in press).

John F. Bateman, Susanna Freddi, Robyn McNeil, Elizabeth Thompson, Pia Hermanns, Ravi Savarirayan, and Shireen R. Lamande (2004): Identification of four novel *COL10A1* missense mutations in Schmid Metaphyseal Chondrodysplasia: Further evidence that collagen X NC1 mutations impair trimer assembly. *Hum Mutat* **23**(4):396-402.

Stacey M Curry, Aline G. Daou, Pia Hermanns, Andrea Molinari, Richard Alan Lewis, Bassem A. Bejjani (2004): Cytochrome P4501B1 mutations cause only part of primary congenital glaucoma in Ecuador. *Ophtalmic Genetics* **25**(1):3-9.

P. Hermanns, B. Lee (2002):Transcriptional Dysregulation in skeletal malformation syndromes. *Am J Med Genet* **106**(4):258-271.

8.5 Talks

Pia Hermanns, J. G. Leroy, A. Bertuch, T. Bertin, B. Dawson, A. Tran, M. Schmitt, B. Zabel, B. Lee: Cartilage Hair Hypoplasia - New Pathogenetic Aspects. 54th Annual Meeting of the American Society of Human Genetics, October 26th – 30th 2004, Toronto, Canada.

Pia Hermanns, Alison Bertuch, Mark Schmitt, Berhard Zabel, Brendan Lee: Functional Studies of the RMRP gene in Cartilage Hair Hypoplasia. 5th Mouse Molecular Genetics Meeting, September 3rd – 7th, 2003, EMBL, Heidelberg, Germany

Pia Hermanns, Alison Bertuch, Elda Munivez, Asad Mian, Vicky Lundblad, Annette Queisser-Luft, Jules Leroy, Juergen Spranger, Bernhard Zabel and Brendan Lee: RNASE MRP (RMRP) AND CARTILAGE HAIR HYPOPLASIA (CHH). 23rd annual workshop on malformations and morphogenesis, David-Smith-Meeting. August 7th – 11th, 2002, Furman University, Greenville, South Carolina, USA.

8.6 Poster presentations

P. Hermanns, J. G. Leroy, A. Bertuch, T. Bertin, B. Dawson, A. Tran, M. Schmitt, B. Zabel, B. Lee: Pathogenesis of Cartilage Hair Hupoplasia. Annual Retreat of the Department of Molecular and Human Genetics. January, 13th – 14th 2005 in the Galvez Hotel, Galveston, Texas, USA.

Pia Hermanns, Alison Bertuch, Elda Munivez and Brendan Lee: Functional studies of the RNA component of RMRP in Cartilage Hair Hypoplasia. Annual Retreat of the Department of Molecular and Human Genetics. January, 15th – 16th 2004 in the Galvez Hotel, Galveston, Texas, USA.

P. Hermanns, A. Bertuch, M. Schmitt, B. Zabel, B. Lee: Functional studies of the RNA component of RMRP in Cartilage Hair Hypoplasia. 53rd Annual Meeting of the American Society of Human Genetics, November 4th – 8th 2003, Los Angeles, Carlifornia, USA. Am. J. Hum. Genetics, Vol 73 (5), p.556.

Pia Hermanns, Alison Bertuch, Elda Munivez and Brendan Lee: Functional Studies of Mutations in an RNase (RMRP) in Cartilage Hair Hypoplasia Patients. Annual Retreat of the Department of Molecular and Human Genetics. January, 16th – 17th 2003 in the Galvez Hotel, Galveston, Texas, USA.

P. Hermanns, A. Bertuch, E. Minivez, A. Mian, V. Lundblad, J. Leroy, B. Zabel and B. Lee: Cartilage Hair Hypoplasia (CHH) and the RNase MRP (RMRP) gene. 52st Annual Meeting of the American Society of Human Genetics, October 15-19, 2002, Baltimore, Maryland, USA. Am. J. Hum. Genetics, Vol 71 (4), p. 543.

Pia Hermanns, Alison Bertuch, Asad Mian, Elda Munivez, Bernhard Zabel, Vicky Lundblad, Brendan Lee: RNase MRP RMRP) and Cartilage Hair Hypoplasia (CHH). Annual Retreat of the Department of Molecular and Human Genetics, January 17th – 18th 2002 in the Galvez Hotel. Galveston, Texas, USA.

Pia Hermanns, Alison Bertuch, Asad Mian, Bernhard Zabel, Carlos Bacino, Vicky Lundblad, Brendan Lee: Analysis of RNase MRP (RMRP) function in cartilage hair hypoplasia (CHH). 51st Annual Meeting of the American Society of Human Genetics, October 12-16, 2001, San Diego, California, USA. Am. J. Hum. Genetics, Vol 69 (4), p.

Pia Hermanns, David Wheeler, Chirstopher Johnson, Maria Lee, Christiane Stelzer, Bernhard Zabel, Andreas Winterpacht, Richard Gibbs, Brendan Lee: Developing an automated tool for characterizing EST sequences from a human cartilage-specific cDNA library. 51st Annual Meeting of the American Society of Human Genetics, October 12-16, 2001, San Diego, California, USA. Am. J. Hum. Genetics, Vol 69 (4), p. 451.

Pia Hermanns, David Wheeler, Chris Johnson, Maria Lee, Richard Gibbs, and Brendan Lee: Developing an automated tool for characterization of EST Sequences from a human cartilage-specific cDNA library. Annual Retreat of the Department of Molecular and Human Genetics, January 11-12, 2001 in the Galvez Hotel, Galveston, Texas, USA.

8.7 Other oral and poster presentations

Roberto Mendoza-Londono, Pia Hermanns, Dobrawa Napierala, Keiko Wakui, Diep Nguyen, Eduard Lammer, Rosemarie Watson, Atsushi Hatamochi, David W. Stockton, Brendan Lee: Clinical Characterization of atypical Cleidocranial Dysplasia with parietal foramina, imperforate anus and porokeratosis mapping to chromosome 22q. Annual Retreat of the Department of Molecular and Human Genetics. January, 13th – 14th 2005 in the Galvez Hotel, Galveston, Texas, USA.

G. Zhou, P. Fonseca, P. Hermanns, E. Munivez, R. Morello, Y. Q. Chen, Q. P. Zheng, B. Lee: Role of a novel repressor, RUNX2-interacting protein, in skeletogenesis. Annual Retreat of the Department of Molecular and Human Genetics. January, 13th – 14th 2005 in the Galvez Hotel, Galveston, Texas, USA.

Roy Morello, Terry Bertin, Silke Schlaubitz, Kevin Preuss, Pia Hermanns, Yuqing Chen, Brendan Lee: Brachydactyly caused by loss of function of sFrp2 signaling. Annual Retreat of the Department of Molecular and Human Genetics. January, 13th – 14th 2005 in the Galvez Hotel, Galveston, Texas, USA.

G. Zhou, P. Hermanns, E. Munivez, R. Morello, Y. Chen, Q. Zheng, M. Carette, H. Kingston, M. Tassabehji, B. Lee: Upregulation of a novel repressor, RUNX2-interacting protein, in patients with 8q22 rearrangements phenocopies cleidocranial dysplasia. 54th Annual Meeting of the American Society of Human Genetics, October 26th – 30th 2004, Toronto, Canada.

M.S. Williams, R.S. Ettinger, P. Hermanns, B. Lee, M. Taskinen, O. Mäkitie: The Natural History of Severe Anemia in Cartilage-Hair Hypoplasia. 54th Annual Meeting of the American Society of Human Genetics, October 26th – 30th 2004, Toronto, Canada.

R. Morello, T. Bertin, K. Preuss, P. Hermanns, Y. Chen, B. Lee: Brachydactyly caused by loss of function of sFrp2 signaling. 54th Annual Meeting of the American Society of Human Genetics, October 26th – 30th 2004, Toronto, Canada.

R. Mendoza-Londono, E. Lammer, R. Watson, A. Hatamochi, P. Hermanns, D. Napierala, K. Wakui, X. Carter, D. Nguyen, D.W. Stockton, B. Lee: Clinical characterization of atypical cleidocranial dysplasia with parietal foramina, imperforate anus and porokeratosis mapping to chromosome 22q. 54th Annual Meeting of the American Society of Human Genetics, October 26th – 30th 2004, Toronto, Canada.

G. Zhou, P. Hermanns, E. Munivez, R. Morello, Y. Chen, Q. Zheng, B. Lee: Regulation of Runx2 Action during Osteoblast Development by a Novel Runx2-interacting Protein. 26th Annual Meeting of the American Society for Bone and Mineral Research. October, 1st – 4th 2004, Seattle, Washington, USA. JBMR Vol 19, Suppl 1, p.S36.

Marc S Williams, Pia Hermanns, Brendan Lee, Mervi Taskinen, Outi Mäkitie: The Natural History of Severe Anemia in Cartilage-Hair Hypoplasia. David-Smith Meeting, August 2004 in Salt Lake City, Utah, USA.

Guang Zhou, Pia Hermanns, Elda Munivez, Roy Morello, Yuqing Chen, Qiping Zheng and Brendan Lee: Regulation of RUNX2/CBFA1 action during osteoblast development by a potential RUNX2-interacting protein. Annual Retreat of the Department of Molecular and Human Genetics. January, 15th – 16th 2004 in the Galvez Hotel, Galveston, Texas, USA

S. Schlaubitz, C. Steltzer, P. Hermanns, A. Winterpacht, T. Hankeln, E.R. Schmitt, F. Jakob, B. Lee, B.U. Zabel: Molecular identification of novel genes, especially transcription factors, from a human fetal growth plate cartilage library. 53rd Annual Meeting of the American Society of Human Genetics, November 4th – 8th 2003, Los Angeles, Carlifornia, USA. Am. J. Hum. Genetics, Vol 73 (5), p. 346.

Roy Morello, Pia Hermanns, Terry Bertin, Yuqing Chen and Brendan Lee: Function of sFrp2 during limb development. Annual Retreat of the Department of Molecular and Human Genetics. January, 16th – 17th 2003 in the Galvez Hotel, Galveston, Texas, USA.

Guang Zhou, Pia Hermanns, Elda Munivez, Yuqing Chen, and Brendan Lee: Regulation of Runx2/Cbfa1 action during osteoblast development by a potential Runx2-interacting protein, RIP. Annual Retreat of the Department of Molecular and Human Genetics. January, 16th – 17th 2003 in the Galvez Hotel, Galveston, Texas, USA.

Zabel Bernhard, Schlaubitz, S., Stelzer, C., Luft, F., Schmidt, E.R., Hankeln, T., Hermanns, P., Lee, B., Jakob, F., Noeth, U., Mohrmann, G., Tagariello, A., Winterpacht, A.: Molecualar identification of genes and pathways involved in skeletogeneis by EST sequence analysis and microarray expression profiling of human mesenchymal stem cell differentiation. 13 th Annual Meeting of the German Society of Human Genetics together with the Austrian Society of Human Genetics and the Swiss Society of Medicak Genetics and the German Human Genome Project (DHGP), September 29th – Oktober 2nd 2002, Leipzig, Germany.

S. Schlaubitz, C. Stelzer, P. Hermanns, G. Mohrmann, A. Tagariello, F. Luft, B. Lee, A. Winterpacht, T. Hankeln, E. Schmidt and B. Zabel: A Cartilage EST-Sequencing Project As Source For Genes Involved In Skeletal Physiology And Pathology. Frontiers of Skeletal Biology, Ninth Workshop of Cell Biology of Bone and Cartilage in Health and Disease, March 16th – 19th 2002 in Davos, Switzerland. Bone, Vol. 30 (3S), p. 31S.

Guang Zhou, Pia Hermanns, Yuqing Chen, Brendan Lee: Regulation of Cbfa1/Rnunx2 action during osteoblast development by a cbfa1-interacting protein, Cip. 51st Annual Meeting of the American Society of Human Genetics, October 12-16, 2001, San Diego, California, USA. Am. J. Hum. Genetics, Vol 69 (4), p. 347.

Winterpacht A, Mohrmann G, Schlaubitz S, Stelzer C, Hermanns P, Muehlbauer C, Lee B, Hankeln T, Zabel B, Schmitdt ER: Molecular identification of genes and pathways involved in skeletogenesis – potential candidates for human disorders. 10th International Congress of Human Genetics, May 15th – 19th 2001, Vienna, Austria. European J. Hum. Genetics, Vol. 9 (1S), p.252.

Guang Zhou, Pia Hermanns, Yuqing Chen, and Brendan Lee: Characterization of a potential CBFA1 interacting protein, CIP. Annual Retreat of the Department of Molecular and Human Genetics, January 11-12, 2001 in the Galvez Hotel, Galveston, Texas, USA.

David Wheeler, Christopher Johnsen, Paula E. Burch, Pia Hermanns, Brendan Lee and Weimin Wu: WEB-Based Trace Viewer That Displays and Trims DNA Sequences from ABI Sequencers. Annual Retreat of the Department of Molecular and Human Genetics, January 11-12, 2001 in the Galvez Hotel. Galveston, Texas, USA.

Zabel B, Stlezer C, Hermanns P, Schlaubitz S, Mohrmann G, Friedl H, Muehlbauer C, Lee B, Hankeln T, Winterpacht A, Schmidt ER: Molecular identification of genes and pathways involved in skeletogenesis by EST generation, full length cDNA isolation and expression profiling. German Human Genome Meeting 2000, November 30th – December 1st 2000, Heidelberg, Germany.

Christopher M. Johnson, Pia Hermanns, Brendan Lee. and David A. Wheeler: Optimization of extraction of high-quality sequence from ABI Sequencer reads. Keck 2000 Symposium, October 16-17, 2000, Baylor College of Medicine and Rice University, Houston, Texas, USA.

Guang Zhou, Pia Hermanns, Yuqing Chen, and Brendan Lee: Characterization of a potential CBFA1 interacting protein, CIP. Annual Retreat of the Department of Molecular and Human Genetics, February 3-4, 2000 at Columbia Lakes Resort, West Columbia, Texas, USA.

Winterpacht A, Endele S, Fuhry M, Hermanns P, Zabel B: Molecular dissection of the Wolf-Hirschhorn syndrome - Isolation and characterization of novel candidate genes in man and mouse. Gordon Research Conference Human Molecular Genetics, Newport, 8.-13.8.1999.

Winterpacht A, Endele S, Fuhry M, Hermanns P, Zabel B: The Wolf-Hirschhorn syndrome: Towards the molecular dissection of a complex phenotype- XX Dawid W. Smith Workshop on Malformations and Morphogenesis, Schlangenbad, 3.8.-9.8.1999.

Endele S., Fuhry M, Pak S-J, Hermanns P, Maringer M, Zabel B, Winterpacht A: Molecular dissection of the Wolf Hirschhorn syndrome - isolation and characterization of novel candidate genes. Jahrestagung der Gesellschaft für Humangenetik, Nürnberg, 24.-27.3.1999 Med Genetik 11:134,1999.

Endele S, Pak S-J, Fuhry M, Hermanns P, Maringer M, Tinschert S, Zabel B, Winterpacht A: LETM1 - a novel Ca^{2+}-binding protein deleted in Wolf-Hirschhorn syndrome. 48th Annual Meeting of the American Society of Human Genetics, Denver, 27.10.-31.10.1998, Am J Hum Genet 63:A9,1998.

Winterpacht A, Endele S, Maringer M, Hermanns P, Fuhry M, Zabel B: Das Wolf-Hirschhorn-Syndrom - Ansätze zur molekulargenetischen Aufklärung eines „contigous gene"-Syndroms. 94. Jahrestagung der Deutschen Gesellschaft für Kinderheilkunde und Jugendmedizin, Dresden, 2.-5.10.1998. Monatsschr Kinderheilkd 146:S142,1998.

Endele S, Maringer M, Hermanns P, Fuhry M, Zabel B, Winterpacht A: Detailed analysis of novel human and corresponding murine genes located in the Wolf-Hirschhorn-syndrome critical region. 10. Jahrestagung der Gesellschaft für Humangenetik, Jena, 25.-28.3.1998, Med Genetik 10:170,1998.

Prawitt D, Rodriguez P, Higgins M, Landers J, Hermanns P, Morgenbesser S, Munroe D, Housman D, Pelletier J, Winterpacht A, Zabel B: Characterization of transcripts in a subregion of 11p15.5 linked to the Beckwith-Wiedemann syndrome and Wilms' tumor formation. 9. Jahrestagung der Gesellschaft für Humangenetik, Innsbruck, 16.-19.4.1997, Med Genetik 9:52,1997.

Prawitt D, Munroe D J, Pelletier J, Loebert R, Bric E, Hermanns P, Housman D E, Winterpacht A, Zabel B U: Identification of a NAP related gene in the Wilm's tumor candidate region at 11p15.5. Am J Hum Genet 59 (4): No. 419, 1996.

Ross, R.,Kleinz, R., Gillitzer, C., Hermanns, P., Frosch, S., Schwing, J., Kleinert, H., Foerstermann, U. and Reske-Kunz, A.B. (1994): Expression of the inducible Nitric Oxide synthase (iNOS) in murine epidermal keratinocytes and Langerhans cells XXV. Tagung der Gesellschaft fuer Immunologie, Konstanz Congress-Abstract p. 272.

Ross, R., Gillitzer, C., Kleinz, R., Hermanns, P., Frosch, S., Schwing, J., Kleinert, H., Foerstermann, U. and Reske-Kunz, A.B. (1994): Expression of the inducible Nitric Oxide synthase (iNOS) in murine epidermal Langerhans cells and keratinocytes is enhanced by contact-allergen. XXII. Jahrestagung der Arbeitsgemeinschaft dermatologische Forschung, Wuerzburg Congress-Abstract p. 189